Analysis of Mitigating Concrete Cracks with Bacteria

Prepared by:

Lisa Burris
Natalie Hull
Zeynep Basaran Bundur
Cansu Acarturk
Judith Straathof
Yijing Liu
Ilgin Sandalci

Prepared for:

Ohio's Research Initiative for Locals
The Ohio Department of Transportation,
Office of Statewide Planning & Research

Project ID Number 112683

December 2022

Final Report

Technical Report Documentation Page

1. Report No.	2. Government Accession No.	3. Recipient's Catalog No.
FHWA/OH-2022-29		

4. Title and Subtitle	5. Report Date
Analysis of Mitigating Concrete Cracks with Bacteria	**December 2022**
	6. Performing Organization Code

7. Author(s)	8. Performing Organization Report No.
Lisa Burris, Natalie Hull, Zeynep Basaran Bundur, Cansu Acarturk, Judith Straathof, Yijing Liu, Ilgin Sandalci	

9. Performing Organization Name and Address	10. Work Unit No. (TRAIS)
Ohio State University **2036 Neil Ave** **Columbus, OH 43210**	
	11. Contract or Grant No.
	34877

12. Sponsoring Agency Name and Address	13. Type of Report and Period Covered
Ohio Department of Transportation **1980 West Broad Street** **Columbus, Ohio 43223**	**Final Report**
	14. Sponsoring Agency Code

15. Supplementary Notes

16. Abstract

Incorporating bacteria into concrete has been proposed as a method of mitigating the negative impacts of concrete cracking, and may also lead to increased strength and durability through calcium carbonate precipitation and porosity reductions by the bacteria. This study aimed to increase understanding of the use of microorganisms in concrete by investigating: performance of axenic and environmentally-derived bacteria cultures to increase resiliency of bacteria for use in upscaled use in concrete systems; effects of curing method and exposure to hot and cold temperatures and salts; and performance of bacteria in a pilot scale pavement application.

In this work, *B. subtilis* was used as an axenic strain and a non-axenic bacterial system was produced from Columbus, Ohio soil. The effects of pH, growth time, incubation temperature, and nutrient solution concentration were compared with their effectiveness in generating dense bacterial cultures capable of biomineralization. Changes in compressive strength, electrical resistivity, sorptivity, and drying shrinkage in paste, mortar, and concrete samples incorporating bacteria were compared to controls. Varying curing regimes (ponding of the samples and daily spraying) were evaluated for their ability to induce biomineralization and crack healing. The effect of environmental factors including cold and hot weather temperatures, and exposure to deicing salt solution were evaluated. Numbers of living bacterial cells were tracked across all samples to link numbers of cells with changes in performance.

The results demonstrate that bacteria are capable of healing cracks <0.3mm in width, and non-axenic bacterial cultures can be used to promote biomineralization and crack healing. Existing concrete mixture designs using portland cement and fly ash can be used with bacterial solutions. Calcium sulfoaluminate (CSA) cement can also be used, and provided a better environment for preserving living bacterial cells within the paste over time. CSA showed slightly better improvements to microstructure and crack healing over time compared to OPC mixtures. A lightweight aggregate must be incorporated into mortar and concrete mixtures, replacing a portion (~10%) of the fine aggregate, in order to protect the bacteria during the initial mixing process. Nutrient solution provided to the bacteria to induce biomineralization and heal cracks should be applied through spraying in order to generate the best crack healing potential. Exposure to hot and cold temperatures and salt solutions resulted in bacterial cell death and reduced the crack healing potential of the bacteria. Finally, simple life-cycle evaluations indicated only minor improvements in service life, although the evaluation method used could not account for cracking healing effects. Production and use of bacteria approximately doubled the cost of concrete during the initial construction period.

17. Keywords	18. Distribution Statement
Concrete, Cement, Cracking, Bacteria, Durability, Biomineralization	**No restrictions. This document is available to the public through the National Technical Information Service, Springfield, Virginia 22161**

19. Security Classification (of this report)	20. Security Classification (of this page)	21. No. of Pages	22. Price
Unclassified	**Unclassified**	**170**	

Form DOT F 1700.7 (8-72) **Reproduction of completed pages authorized**

Credits and Acknowledgments Page

Prepared in cooperation with the Ohio Department of Transportation and the U.S. Department of Transportation, Federal Highway Administration

The authors acknowledge the people who ensured the successful completion of this project, including Richard Lease, Ohio State Biochemistry Lab Supervisor, Abby Spengler, Ravi Patel, Megan Nicholson, and Timothy Huang, Undergraduate Research Assistants, and all of the Ohio State University Structures Group graduate research assistants and postdocs who helped with the installation of sidewalk section: Erin Stewartson, Garrett Tatum, Ramzi Abduallah, Yujia Min, and Madiha Ammari. Significant contribution to the outcomes of this project were also provided by the ORIL panel members: Daniel Miller, Mark Eicher, David Flood, and Jeremiah Upp, who provided frequent feedback on results and guidance regarding some of the testing decisions.

Table of Contents

List of Figures

List of Tables

1 Problem Statement

Concrete is typically used by villages, cities, and counties in Ohio for the construction of bridges. Throughout its life, concrete often develops cracks in the surface due to drying shrinkage, flexural strain, or scaling of the concrete surface. These cracks allow water to permeate the concrete and accelerate deterioration due to the natural winter freezing and thawing cycles. In order for a freezing event, and the accompanying expansion of pore water that leads to cracking to damage concrete, the concrete must have reached a critical saturation point, typically >86% relative internal humidity. For concrete that has reached this level of saturation, during a freezing event the water freezes and expands, resulting in pressurized movement of water through the cementitious microstructure, and damage to hydrated phases, such as C-S-H. In addition, water in cracks on the surface of the concrete can expand, resulting in generation of stress in the concrete surface that can scale away surface concrete. Together these two mechanisms can result in exacerbated cyclical damage, leading to local failure occurring in the concrete, which can result in costly repairs.

Incorporating bacteria into the concrete mixture has been proposed as a method of preventing or mitigating the negative impacts of concrete cracking, as well as leading to increased strength and durability through porosity reductions. When the bacteria is exposed to air, as a result of a crack, the bacteria precipitates a filler mineral, typically a form of calcite, into the concrete. This bio-mineral fills the cracks, and additionally, has been shown to densify concrete microstructure, mitigating the negative impacts of concrete cracking, and leading to increased (tensile and compressive) strengths, reduced permeability and diffusivity, and through these mechanisms, increased concrete service life. If this method is successful and cost-effective, this could provide local public agencies with an opportunity to reduce maintenance and repair activities and the associated costs (Van Tittelboom and De Belie 2013; De Muynck, De Belie, and Verstraete 2010; Achal, Mukherjee, and Reddy 2010).

2 Research Background

Despite encouraging findings surrounding use of bacteria to improve concrete quality, there are many unknowns and challenges regarding bacterial concrete systems. To date few studies have investigated use of bacterial concrete at scales larger than laboratory mortar bars or 2” cubes. In addition, many of the factors that could impact bacterial biomineralization ability in-situ, including impacts of temperature and application of salts, are at best, poorly understood. Further, although several effective strains of bio-mineralizing bacteria have been identified, growth of ‘pure’ (known as “axenic”) bacterial strains requires clean, sterilized laboratories, specialized (and often expensive) equipment, and staff trained in biological growth processes. Use of non-axenic bacterial cultures from the local environment has been investigated only once, and showed significant reductions in cost and increases in performance (Da Silva 2015).

Previous studies have shown that bio-mineralization can be effectively used to increase concrete mixture strength and durability, especially resistance to freezing and thawing. Thus, the primary goal of this research is **to understand the requirements for upscaling bacterial concrete, and assess the feasibility and impact of incorporating bacteria into concrete mixtures used on the local Ohio roadway system for extending service life, specifically with regards to early age crack reductions and densification of concrete microstructure to reduce permeability and**

damage to concrete from freezing and thawing. Specific project objectives include:

- Determine the best bacteria and growth media for use in local applications, and the most efficient nutrient solutions available to grow bacteria for use in concrete.

- Determine the availability of bacteria for local applications and requirements for generating sources large enough to produce adequate concrete volumes.

- Determine the effect of the bacterial systems on concrete strength across a range of common concrete mixture designs used in Ohio, utilizing SCMs, local admixtures, and fibers, as well as one specialty rapid repair cement mixture (using calcium sulfoaluminate cement).

- Determine the effect of curing and environment on bacterial concrete viability.

- Determine the effectiveness of the bacteria at stopping or reducing hairline cracks in the concrete and the length of time over which crack reduction through bio-mineralization can be expected to remain effective.

- Evaluate the impact the incorporation of bacteria has on overall production and lifecycle costs of the concrete.

To address the limitations in knowledge associated with use of bacteria in concrete to prevent cracking, this project investigated the influence of a variety of bacterial systems, including ones produced using local Ohio waste materials, mixture designs, curing and exposure conditions, to determine bacterial system efficiency over time, and optimum growth conditions. In addition, in order to prove the ability of the systems to be upscaled to more realistic production sizes, and realistically examine many of the factors affecting in-situ placements, concrete pavement mixtures (in the form of a sidewalk) were cast, exposed to the Ohio environment, and tracked over the second year of the project, to establish viability of the system when exposed to real-world environmental conditions.

2.1 Tasks

In order to assess the feasibility of implementing effective bacterial concrete systems for use in crack remediation in Ohio concrete, the testing was be conducted in five tasks:

- Task 1: Microorganism selection and growth

- Task 2: Laboratory mortar and concrete testing

- Task 3: Placement and monitoring of in-situ concrete

- Task 4: Life cycle analysis and cost evaluation, and

- Task 5: Production of a final report and fact sheet writing.

2.1.1 Task 1: Microorganism selection and growth

To begin, from the literature a promising bacterial strain, along with several non-axenic cultures

created from biological waste products or environmental samples, were selected. Available nutrient sources were evaluated based on demonstrated efficiency in past research trials and availability in the local Ohio region.

Bacteria (both axenic and non-axenic) were cultured using pH-controlled systems under aerobic conditions to maximize production of vegetative cells and then to maximize sporulation before use in concrete. Multiple pH solutions, nutrient solutions, flask shapes, temperatures, and sporulation methods were tested to evaluate conditions capable of optimizing bacterial sample numbers in terms of time and cost relative to the bacterial sample generated. Bacterial growth and sporulation curves were measured spectrophotometrically and through culture and pasteurization methods. *B. subtilis* axenic bacteria cultures were selected for use in the project based on past successful use and familiarity of the research team. Non-axenic cultures originating from Ohio-local sources were cultured from three sources: 1) a spent food digestate utilized for electricity production in eastern Ohio; 2) wastewater from a whisky production process, obtained from a Columbus, Ohio distillery; and 3) soil from a residence located in Columbus, Ohio, near the Scioto River.

Task 1 deliverables:

- Sources for obtaining bacterial samples, nutrient growth solutions, and equipment required for bacterial propagation and quality control of samples (to be provided in the life cycle cost report).

- Step-by-step overview of the processes and required nutrient solutions required to grow bacteria from the axenic and non-axenic bacteria sources.

- Evaluation of each of the bacterial sources for growth capacity and required process time.

2.1.2 Task 2: Laboratory mortar and concrete testing

The goal of Task 2 was to gain understanding of the impacts of a large number of variables influencing bacterial growth and concrete properties on the performance of the bacterial concrete. In order to maximize the number of variables that can be tested, samples were primarily created using mortar, which requires overall lower quantities of bacteria compared to larger-volume concrete mixtures, while allowing for determination of mixtures with the highest likelihood of success. Following selection and growth of the bacterial strains, mortars were cast to evaluate the impacts of: mixture design parameters (fly ash and lightweight aggregate, OPC, and calcium sulfoaluminate cement[1]); curing length and curing method; curing temperature (high temperature of 80-90 °F (~30 °C), simulating summer placement, low temperature of ~45 °F (~5-10 °C),

[1] CSA cement is theorized, as a result of it's inherently lower pore solution pH (typically ~12.5, compared to the 13.5-14 in OPC concrete), to provide a less severe, and thus better, growth environment for bacteria, enabling bacteria to maintain viability and benefits to the concrete over longer periods of time, or with greater efficiency, potentially resulting in larger decreases in permeability, larger increases in strength, or the ability to fill larger width cracks. Although use of CSA cement will not be the primary focus of this research, simple testing of this facet in conjunction with primary study work will allow for determination of benefit/cost ratio associated with use of CSA cement in conjunction with bacterial concrete. This investigation will also provide some indication on the viability and transferability of the two primary bacterial systems (axenic and non-axenic) to use in alternative concrete mixtures, such as those that might be employed in rapid repair situations.

simulating fall concrete placement); and environmental stressors (application of salt).

For each mixture, the test program to determine the impact of the bacteria and nutrient solution, mixture components (SCMs, etc), curing scheme, and salt application on mortar properties included assessment of: hydration kinetics and setting time, to determine anticipated shifts in setting time and development of mechanical properties, and evaluate the overall impact of the bacteria and nutrient solutions on overall system hydration during the first 7 days after casting; strength development; crack remediation/filling potential of each of the mixtures was tracked using pre-cracked fiber-reinforced mortar bars[2], inspected visually and using thermogravimetric analysis to attempt to quantify calcium carbonate precipitation. Scanning electron microscopy (SEM) was also utilized to identify the presence of the bacteria in crack-healed samples; sorptivity was used to assess changes in pore structure and permeability in the mortars; and viability of bacteria in initial cultures and over time, assessed using a Most Probable Number (MPN) bacterial regrowth method.

A smaller subset of the successful mortar mixtures was upscaled to concrete meeting the ODOT QC1 mixture requirements in order to track drying shrinkage, changes in porosity (based on resistivity), mechanical property development, and viability of the bacteria in concrete.

Task 2 deliverables:

- Evaluation of the impacts of SCMs, lightweight aggregate, and CSA cement on the hydration kinetics, strength development and crack-remediation potential of the bacterial concrete mixtures.

- Understanding of the curing requirements for supporting bacterial system life in concrete infrastructure construction.

- Evaluation of the effect of temperature and environmental stressors, specifically salt, on bacterial system life and changes to strength development, porosity, and shrinkage over the life of a mixture.

- Suggested specification requirements for optimizing design and construction of bacterial concrete within Ohio.

2.1.3 Task 3: Placement and monitoring of in-situ concrete

The goal of Task 3 was to determine the viability of bacterial concrete mixtures for reducing cracking in in-situ concrete placements and to track changes in the durability and determine

[2] Please note: use of fiber reinforcement is provided in these bars, not to test the use of fibers in conjunction with bacteria, but simply to enable pre-cracking of the sections. Without fibers, crack widths would likely be so high as to preclude filling of cracks by bacterial precipitate. It can be assumed from past research work, that fibers will greatly increase the efficiency of the bacteria's ability to close and fill cracks by closing crack widths following removal of the cracking force.

Comparison between crack mitigation and repair abilities in fiber vs. non-fiber reinforced bacterial concrete mixtures may be conducted using the in-situ pavement sections. However, selection of the specific mixtures for testing in the larger pavement sections will be done at a later date, after lab-scale results have been determined.

expected life of the bio-mineralizing bacteria. In order to accomplish this, four concrete test pads were placed, fresh properties measured, and monitored over the course of 12 months, for cracking. Pads were subject to both freezing and thawing conditions (as the weather allows) and application of salts. Monitoring consisted of visual observations of the appearance, number, and width of cracks, and changes in concrete resistivity over the course of the monitoring period. In addition, periodic coring of the pads was conducted in order to determine the state of the bacteria within the pads. A set of smaller companion concrete samples (4x8" cylinders, and small beams) were cast and located with the pads for initial curing to facilitate tracking of pad concrete characteristics, including strength development, shrinkage, and changes in resistivity over time. Additional concrete beams were cast using pad concrete mixture proportions were subjected to cyclical freeze-thaw testing in the ASTM C666 compliant chamber.

Task 3 deliverables:

- Quantification several bacterial concrete formulations crack reduction ability in an in-situ concrete pavement section and demonstrated up-scale-ability of the bacterial concrete mixtures and understanding of correlations between mixture properties (strength, porosity) and freeze-thaw durability.

- Assessment of bulk resistivity and MPN measurements as quality control/quality assurance tests for ensuring viability of bacterial concrete installations.

2.1.4 Task 4: Life cycle analysis and cost evaluation

The goal of Task 4 was to evaluate the financial implications of the use of bacterial concrete in Ohio. Costs associated with the production of the bacterial concrete included: purchase of new required equipment, bacterial samples and nutrient solutions (and their associated transportation), and manpower required to grow and manage the strains, which will be tracked to determine the expected increase in production costs associated with use of this specialty concrete.

Performance improvements expected to be gained from use of bacterial concrete mixtures were proposed to be evaluated using the Life365 life cycle analysis tool, which models increased time to corrosion based on diffusivity/permeability of the concrete mixtures, but significant changes in sorption/permeability were not observed in bacterial samples, so this analysis was not conducted.

Task 4 deliverables:

- Anticipated costs for bacterial sample purchase and growth, including required equipment, nutrient solutions, and manpower.

- Estimated impacts on durability, service life, and maintenance of bacterial concrete systems, compared with that of a more traditional concrete mixture.

2.1.5 Task 5: Production of a final report and fact sheet writing

In Task 5, results were detailed in a final report document for review by the project panel. A summary fact sheet was also created to provide an overview of the most significant findings of the work.

2.2 Literature Overview

Bacterial concrete is concrete in which bacterial spores capable of producing calcium carbonate (a reaction known as "bio-mineralization") have been embedded in order to increase the durability of the concrete through healing of cracks or decreases in ion transport (permeability and diffusivity). The most commonly investigated strains of bacteria used in cementitious mixtures are shown in Table 2.1. These bacteria types can tolerate highly alkaline conditions, form spores, produce urease enzyme and precipitate calcium carbonate. Past work has shown that *Sporoscarina pasteurii*, *Bacillus cereus*, *Bacillus sphaericus*, *Bacillus alkalinitrilicus*, and *Bacillus subtilis* strains are all effective in filling cracks up to 0.97 mm in width (Amiri and Bundur 2018; Wang et al. 2014; Wiktor and Jonkers 2011; Basaran Bundur, Kirisits, and Ferron 2015), and restoring the majority of flexural strength. Bacterial precipitant has additionally been shown to increase durability of concrete through densification of the microstructure, reducing permeability, and thus chloride transport and carbonation, within the concrete (Wang et al. 2014; Achal and Pan 2011). Bacteria has been shown to continue to improve concrete for up to 1 year following casting, (although the vast majority of studies have tested only as far as 28-90 days after casting).

Little work has been done to assess the effectiveness of 'impure' (non-axenic) bacteria for concrete, although De Silva (2015) found that bacteria produced from a potato-derived spent digestate lowered cost and increased embedded bacteria resiliency and effectiveness.

One key question associated asked by this research is, "What are the optimal growth conditions to create bacterial cultures for use in concrete?" In order for sufficient bacteria cells to survive in concrete and result in significant paste improvements, a high initial cell count is required, usually 10^7 – 10^9 CFU/mL (Anbu et al. 2016). Many variables are known to affect bacterial growth including pH, temperature, and nutrient solution composition and concentration, making assessment of the many variables essential for enabling optimization of growth processes. Only a small amount of research has been done to investigate the impact of culturing environment variables on the growth of *B. subtilis* and non-axenic cultures for their use in concrete. Gauvry et al. (2019) grew *B. subtilis* cells in a solution of peptone and yeast extract combination and and incubated at 27, 40 and 49 °C temperatures. 40 °C was determined to be the optimal temperature to obtain spores, at 27 °C, the growth rate was 35% less than at 40 °C and at 49 °C growth rate was faster than at 27 °C but the sporulation was inhibited (Gauvry et al. 2019). A work with *B. sphaericus*, another bacteria used in concrete biomineralization, indicated that optimal pH for growth is between 7 and 9 and calcite precipitation ability increases from 10 °C to 37 °C (Wang et al. 2017).

Table 2.1 - Commonly used bacterial cultures, their effect, and anticipated costs when used in cementitious mixtures.

Bacteria type	Effects	Cost	References
S. pasteurii	Successful at internal crack remediation, survived in mortar up to 11 months when incorporated with growth medium.	$319	Amiri and Basaran (2018), Basaran et al. (2015)
B. sphaericus	High urease activity and high carbonate productivity, translating to nearly 60% increase in compressive strength.	$320	Wang et al. (2010)

B. megaterium	Was able to survive up to 28 days when directly added to mortar, improved compressive strength.	$320	Achal et al. (2011)
B. subtilis	Can survive in wide temperature range, precipitates dense insoluble calcite crystals.	$341	Manikandan and Padmavathi (2015), Seshagiri et al. (2013)
B. cereus	Grows well at lower pH, excellent crack bridging and permeability decreases.	$341	Wu et al. (2019)
B. alkalinitrilicus	Alkali resistant soil bacterium capable of long life: bacteria remained viable up to 100 days in concrete	N.A.	Wiktor and Jonkers (2011)

Bacteria have been successfully used in cementitious mixtures in conjunction with a variety of SCMs including fly ash (Annamalai, Arunachalam, and Sathyanarayanan 2012; Achal, Pan, and Özyurt 2011; Chahal, Siddique, and Rajor 2012a), silica fume (Siddique et al. 2016; Farmani, Bonakdarpour, and Ramezanianpour 2015, Siddique, and Rajor 2012b), and slag (Palin et al. 2013, Siddique et al. 2016), suggesting that they would also be effective when used in typical concrete mixtures used in Ohio, such as the QC1 and QC2 mixtures. In these systems, bio-mineralization resulted in increases in strength and reductions in water permeability or durability in all mixtures, in excess of the improvements gained from use of SCMs. Several studies highlighted significant improvements in bacteria survivability when using a 'protectant' media, such as natural minerals, such as clay or natural zeolites, or lightweight aggregate (Wiktor and Jonkers 2011; J. Y. Wang, De Belie, and Verstraete 2012; Erşan et al. 2015). Immobilizing microorganisms on porous minerals provides a natural protection system to preserve bacteria from the harsh environment of the concrete by stabilizing cells on a carrier (Tezer and Bundur 2021). Lightweight aggregates have also shown promising improvements in bacteria viability and healing of cracks (Sandalci, Tezer, and Basaran Bundur 2021; Wiktor and Jonkers 2011).

Thus, existing research knowledge indicates that:

- A wide variety of bacteria can be used to provide biomineralization in concrete mixtures.
- Optimum growth conditions likely occur at slightly elevated incubation temperatures and in slightly alkaline solutions between pH 7 – 9.
- Concrete mixtures meeting the current requirements of Ohio's QC1 and QC2 mixtures, and utilizing standard SCMs, including slag, silica fume, and fly ash can be utilized without compromising bacterial viability, and
- Use of a protectant media, such as lightweight aggregate, will increase the likelihood of preserving bacteria within the bacterial concrete system.

Additional, more detailed review of the scientific literature regarding bacterial concrete research can be found in Appendix A of this report. Further testing was performed in Task 1 to determine optimum growth conditions for the selected bacteria samples, and testing in Task 2 determined the effect of other mixture variables on bacterial survival.

3 Research Approach

3.1 Bacterial Growth Methods

Laboratory testing was conducted in Task 1 to assess bacterial systems, growth solutions and culturing processes. Four types of systems capable of providing bacteria meeting the requirements for use in concrete were investigated: *B. subtilis* (axenic/pure) bacteria, obtained from the Ohio State University Bacillus Genetic Stock Center (BGSC); spent digestate from an anaerobic digestion power station in Eastern Ohio; whisky distillation wastewater, from a small distillery in Columbus, Ohio; and soil from a residence in Columbus, Ohio, just West of the Scioto River. Bacterial samples were created by growing bacteria from the original sources, dividing the bacterial solution into pellets (called 'aliquots, and storing them in the freezer until they are needed. 1 mL aliquots were then used to start bacterial solutions and were injected into 500 mL nutrient solution in flasks and incubated and shaken at 180 rpm until time of testing.

Figure 3.1 shows the overall process for growth of bacteria, which consisted of three stages. In stage 1, a variety of growth conditions were studied to determine optimum growth conditions for axenic (*B. subtilis)* and non-axenic (soil) cultures. The effect of two different pH values (7 and 9), several growing temperatures to represent hot and cold weather conditions as might be experienced in unconditioned lab spaces (as many concrete producer labs are) and standard room temperature and different nutrient media types and concentrations (nutrient broth and tryptic soy broth solution (TSB), nutrient broth at half, normal and double concentration) were tracked up to 4 days of incubation, tracking numbers of cells present in vegetative (active) and spore (protected, inactive) forms in the samples. Vegetative (active) bacteria die very easily under non-ideal conditions, requiring that spores (protected cells), rather than vegetative cells, be inoculated into the concrete mixture to enable bacteria to survive in the concrete. In stage 2, sporulation efficiency, or numbers of spores in a bacterial sample converted from the vegetative cell sample relative to original sample size, was investigated using two methods: a chemical method (using 2xSG sporulation solution (Leighton 1971); and heat treatment method (40 °C), to maximize the number of spores available for incorporation into the concrete mixture. In stage 3, the biomineralization ability of the bacterial cultures was confirmed and the optimum production conditions (growth time, solution composition, concentration, and pH, incubation temperature and sporulation approach) were determined to establish consistent future production conditions.

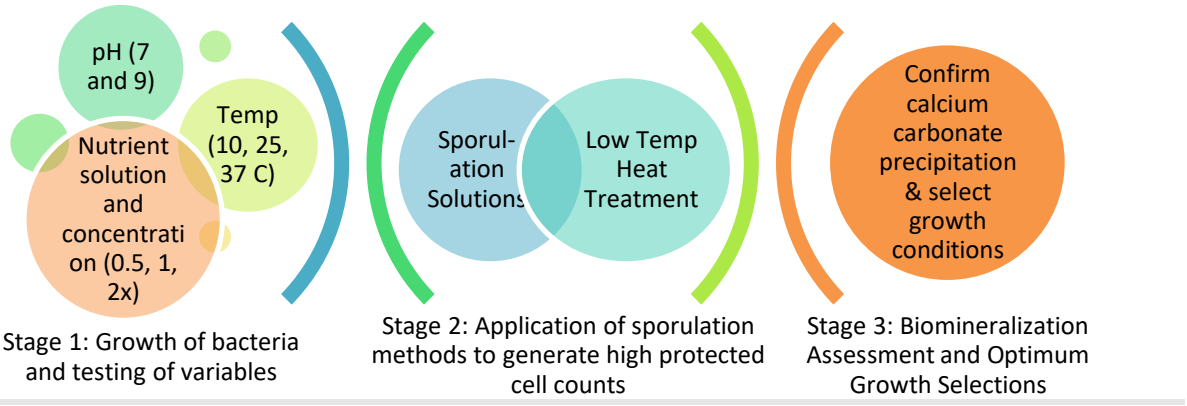

Figure 3.1 - Overall process for bacteria growth, sporulation, and biomineralization.

A significant portion of this project focused on determining the most successful, reliable, and efficient methods of tracking properties associated with the bacteria and bacteria-cement samples, for use in further testing. Multiple methods of assessing bacterial growth were evaluated during the course of the project, including standard spot plating methods, use of optical density measurements (Beal et al. 2020), and most probable number (MPN) culturing methods (Sanders 2012, Beal et al. 2020, Oblinger and Koburger 1975). Specifics regarding the conditions used for each method are provided in the appendix methods section. Best repeatability was obtained from use of spot-plating methods for bacterial counts associated with bacteria prior to inoculation into cementitious media, and MPN methods for bacterial counts associated with samples from pastes, mortars, and concrete.

Multiple methods of assessing the biomineralization-ability of the bacteria were also explored, using x-ray diffraction (XRD), thermogravimetric analysis (TGA), conductivity changes in urea-bearing solutions, and in cement paste and mortar samples, scanning electron microscopy imaging, and crack-filling of fiber-reinforced cracked beams (Wei et al. 2015). No method was found to be successful in quantifying biomineralization for all samples and so instead biomineralization was assessed qualitatively using multiple approaches to confirm biomineralization ability of the bacterial strains. Further details regarding testing utilized in this study can be found in Appendix B.

3.2 Microbial Community Analysis

To further investigate microorganisms involved in concrete systems to prevent and/or heal cracking, axenic (*Bacillus subtilis*) and non-axenic (soil bacteria) cultures were sequenced under a variety of conditions using 16S rRNA gene sequencing on our hand-held nanopore MinION sequencer to identify the types of bacteria present in these samples. A graphic of the process is shown in Figure 3.2. The effects of various factors including storage life, sporulation media, and nutrient media types and concentrations on the microbial community structure and the most dominant bacteria in the samples was investigated. For soil samples which contained bacteria other than *Bacillus subtilis*, typical properties of dominant bacteria found were cataloged to determine potential association with surviving in concrete or contributing to crack prevention or healing. More detail regarding this process is provided in Section 8.2.

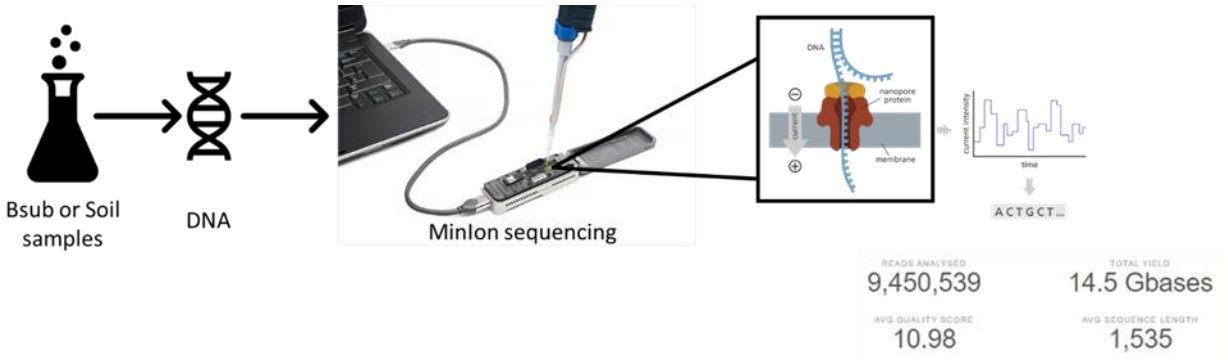

Figure 3.2 - After preparation of samples, *B. subtilis* or soil bacteria samples were subjected to DNA extraction and quantification before MinION sequencing, which passes DNA through protein nanopores to detect electrical signals which are converted into DNA sequences. Sequences are aligned to the 16S rRNA gene and classified taxonomically using Oxford Nanopore Technologies. For this study, more than 9 million sequences were analyzed (totalling more than 14.5 Gbases) with an average sequence length of 1,535 nucleotides (as expected based on our primers) and average quality of 10.98 (which is above average for MinIon sequencing).

3.3 Laboratory Paste and Mortar Production and Testing Methods

In Task 3 a series of pastes and mortars with and without the *B. subtilis* and soil bacteria were cast to evaluate the effect of various concrete mixture components and curing variables on the viability of the bacteria and on the performance of the mixtures. Pastes and mortars were cast using portland and calcium sulfoaluminate cements, with substitutions of a class F fly ash, lightweight aggregate, and phosphate buffer solution (PBS) for a portion of the cement, fine aggregate, or mixing water, respectively. Varying curing methods were used including ponding the samples in a solution with nutrients designed to feed the bacteria (the typical curing method proposed in previous studies) or spraying the nutrient solution on the surface of the samples, and the effect of exposure of the samples to hot and cold temperatures and salt was assessed. The effect of incorporating bacteria in the mixtures was tracked using isothermal calorimetry, compressive strengths, electrical resistivity, and sorptivity of the mixtures. The numbers of bacteria present in the samples were determined using a series of dilutions and the Most Probable Number (MPN) method. Each mixture was also assessed for its ability to heal small (~0.4 mm) cracks, which were evaluated visually and with a non-destructive Ultrasonic Pulse Velocity method. More specific details regarding the materials and testing performed are provided in Section 8.3.

3.4 In-situ Concrete Production and Testing Methods

In Task 4 concrete slabs were cast to evaluate the performance of the bacterial mixtures in a more realistic in-situ environment, as well as to assess scalability of the system. Four approximately 9 ft^3 (6’ x 3’ x 6”) slabs were cast using a rotating drum mixer and the mixture design shown in Table 3.1. The four slabs included: (2) control concrete mixtures without bacteria, (1) slab incorporating *B. subtilis* bacteria, and (1) slab incorporating soil bacteria.

Table 3.1- Concrete Mixture Design.

	Component Mass	
	lbs/yd^3	kg/m^3
Water	305	181
Cement	508	302
Fly Ash	169	101
Coarse Aggregate	1236	733
Fine Aggregate	1243	738
Lightweight Aggregate	123	73

4 in. by 8 in. cylinders and 3 in. x 3 in. x 11.25 in. shrinkage beams were cast simultaneously with the slabs and allowed to cure under the same exposure conditions for 24 hours before demolding. Beam for testing resistance to freezing and thawing were cast at a later time utilizing the same mixtures and casting procedures.

To cure the slabs one of the control slabs and both bacterial slabs, beams, and cylinders were sprayed daily with a nutrient broth, urea, and calcium acetate (NBUC) curing solution from days 1 to 28, until all surfaces of samples were covered with the solution. The other set of control samples were not cured to differentiate between changes in the control resulting from additional curing with the nutrient solution, and those resulting from the bacteria.

Compressive strengths, electrical resistivity, and shrinkage of the concrete mixtures were tracked for 90 days following casting. The number of bacteria in each slab was assessed in 1" core samples obtained from the site and quantified using the MPN method. Change in dynamic modulus after exposure to freezing and thawing conditions was tracked up to 500 cycles. Each slab was inspected for crack development daily for the first week, and weekly up to 90 days, then every three months up to 1 year post placement.

3.5 Lifecycle and Cost Analysis Methods

In Task 4 a comparison of the costs and performance of the bacterial and non-bacterial slabs was performed. The cost of producing bacteria dosages in the concrete mixing water of 10^6 CFU/mL were determined for a variety of nutrient solutions and nutrient solution concentrations, incubation temperatures, and incubation times, based on the projected dried spore count in the mixtures obtained through experimental testing. Materials costs were obtained from commercial laboratory chemical suppliers.

The cost of producing concrete mixtures with or without lightweight aggregate and fly ash, utilizing portland cement or calcium sulfoaluminate cement, and incorporating a water dechlorinating chemical were determined and overall concrete mixture costs with or without bacteria were calculated.

Water absorption values obtained from experimental testing of mortar cubes and an empirical relationship between sorptivity and apparent diffusion coefficient (Siad et al. 2014) were used to estimate 28-d diffusivity. The diffusivity values were then input into a Life 365 model (Bentz and Thomas 2018) of a slab located in Columbus, OH in order to assess the impact of microstructural

refinement resulting from biomineralization on service life and total cost of construction and maintenance of a slab using the bacterial and non-bacterial mixtures over a 100-year service life.

4 Research Findings and Conclusions

Appendices B and C present a detailed report of the testing methodology and the findings of all testing performed for the study, respectively. The primary conclusions are as follows:

For Task 1 - Bacterial Growth work:

For the axenic, *B. subtilis* bacteria:

- *B. subtilis* bacteria provided a relatively resilient bacteria source that is capable of forming protective spores to enable inoculation of the media into concrete, and also provides biomineralization ability without the requirement of an additional urea source.

- *B. subtilis* bacteria was significantly affected by the pH of its growth solution, with reductions in sample bacteria numbers at 24 hours. If incubated for 48 hours the high pH sample could recover and grow to higher numbers than the original sample.

- *B. subtilis* bacterial growth was inhibited by use of incubation temperatures colder than room temperature (10 °C). Growth of vegetative cells was not significantly different for room temperature (25 °C) and high temperature (37 °C) grown samples, but approximately 4x as many spores were formed in the 37 °C sample.

- Very little difference in the growth rate or total cell count was observed for *B. subtilis* based on type of nutrient solution (tryptic soy broth (TSB) or nutrient broth (NB)). Use of nutrient solutions should be confirmed for each bacterial sample, but either TSP or NB can be used to obtain adequate cell counts, based on availability and cost.

- Little difference in *B. subtilis* growth was observed based on nutrient solution concentration (Figure 4.1). To minimize cost, nutrient solutions diluted to half of the original solution concentration are suggested for use without impact on total cell growth capabilities.

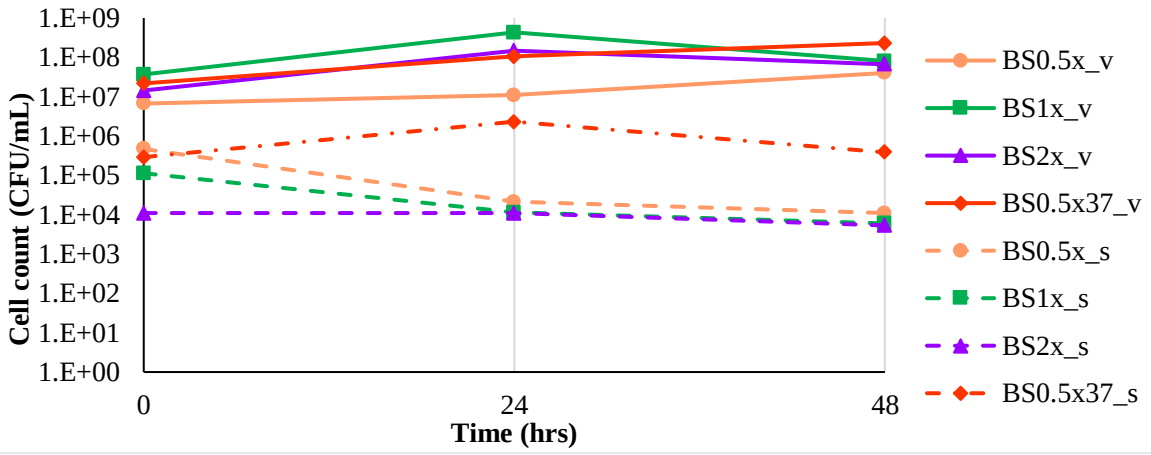

Figure 4.1 - Growth curve evolution of *B. subtilis* from 0 to 48hrs in different solution concentrations at pH 7 and 25 and 37 °C. Error bars represent standard deviation of three replicates. Use of the BS0.5x37 growth condition was selected to maximize spore counts and minimize nutrient solution cost.

- *B. subtilis* samples achieved maximum vegetative cell concentrations after 24 hours, without significant further growth up to 96 hours of incubation. Therefore, it is not necessary to incubate and grow bacterial sample solutions for more than 24 hours.

- Use of low temperature heat treatment as the sporulation method led to 2 orders of magnitude increase in *B. subtilis* spore counts when compared to use of a sporulation chemical (Figure 4.2).

- *B. subtilis* bacteria biomineralization was confirmed through XRD and TGA measurements but was found to occur through a mechanism other than ureolytic activity.

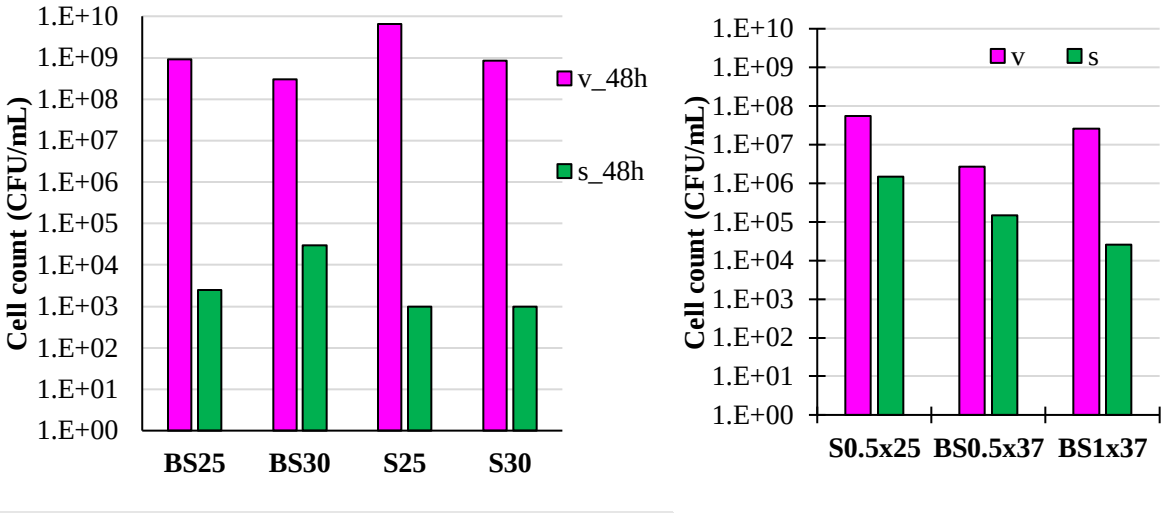

Figure 4.2 - Influence of the sporulation media (left) and low temperature heat treatment (right) on vegetative cell and spore growth for *B. subtilis* and soil under different temperatures (25 °C and 30 °C).

For the non-axenic bacteria:

- Spent digestate and whiskey distillation wastewater sources did not produce bacteria meeting the requirements for use in concrete – either failing to grow in a neutral or high pH growth solutions (pH 7 or 9), or not capable of sporulation. These wastewater sources should not be used to produce bacteria for concrete.

- A simple soil sample obtained from a Columbus, OH residence near the Scioto River was able to produce bacteria capable of forming spores and biomineralizing (Figure 4.3).

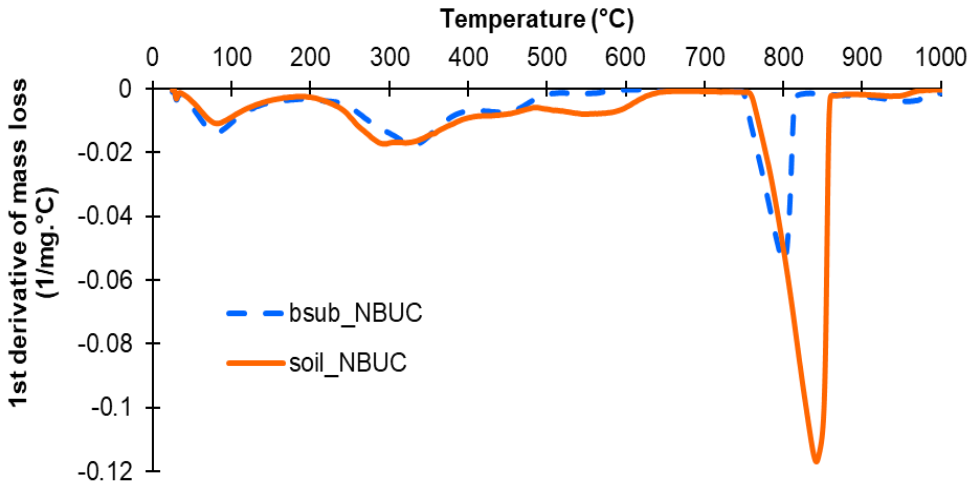

Figure 4.3 - TGA confirmation of soil bacteria biomineralization capacity.

- Soil bacteria achieved maximum concentrations of vegetative cells after 24 hours, without significant further growth up to 96 hours of incubation. Spore concentrations, however, increased by two orders of magnitude (from 10^4 to 10^6 CFU/ mL) from 24 to 48 hrs, suggesting that it may be beneficial to incubate soil growth solutions for additional time, compared to the *B. subtilis* samples.

- The soil bacteria vegetative cell growth was not affected by growth temperatures when grown at room temperature or 37 C. Lower temperature (10 °C) conditions slowed growth, but less significantly than in the *B. subtilis* sample. Spore counts were positively correlated with temperature – with greater temperatures resulting in greater orders of magnitude spore counts.

- Growth solution pH (of 7 or 9) had no effect on vegetative or spore growth of soil bacterial samples.

- Nutrient solution concentration had no effect on soil sample vegetative cell growth but use of the half concentration solution lead to higher sporulation. Therefore, half concentration solution use is recommended to both reduce production costs and obtain greater spore counts (Figure 4.4).

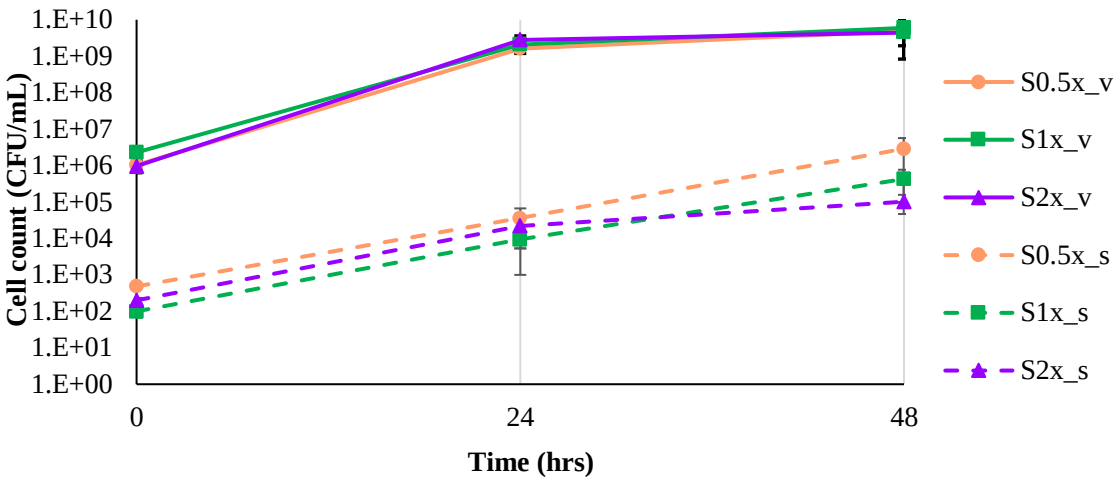

Figure 4.4 - Growth curve evolution of soil from 0 to 48hrs in different solution concentrations at pH 7 and 25 °C. Error bars represent standard deviation of three replicates.

- The bacterial sample produced from soil was more resilient than the axenic *B. subtilis* sample during the growth phase, showing less impact on growth under varying temperature, pH, and nutrient solution conditions, and generating similar or higher cell counts.

- Similar to with the *B. subtilis* bacteria, sporulation using low temperature heat treatment was more effective than use of sporulation solutions for the soil bacterial samples, resulting in 1 or 3 orders of magnitude increases in spore counts using growth solutions incubated for 24 and 48 hours of cell growth, respectively (Figure 4.2).

- Soil bacteria successfully biomineralized calcium carbonate through ureolysis and precipitated higher calcium carbonate quantities than *B. subtilis* samples (Figure 4.4).

For Task 2 – Concrete biomineralization microbial community analysis

- In the *Bacillus subtilis* samples, 99% of sequences were classified to the *Bacillus* genus and 97.4% were classified to the *Bacillus subtilis* species group. This was expected and validates our sequencing and classification approach.

- The non-axenic soil bacteria samples had a more diverse microbial community with more types of bacteria present. Genera typical of soil microbiomes were identified, with some of the most dominant genera including *Acinetobacter, Citrobacter,* and *Aeromonas.* In soil samples, the *Bacillus* genus was present, but at low relative abundance. *Citrobacter* are previously known to be associated with biocementation, and *Acinetobacter* and *Aeromonas* have been used previously in heavy metal bioremediation where they survive harsh conditions.

- Sporulation media had no impact on axenic *B. subtilis* classification. The impact of sporulation media on soil microbiomes was not tested.

- Storage time in dried samples prepared for incorporation into concrete or mortar cubes had no discernable impact on *B. subtilis* microbiomes at day 1, 7, or 14. Storage time had very little

impact on microbiomes in soil samples: after a decrease in *Aeromonas* from day 1, the microbial community was more stable over days 7, 14, and 28 where the most dominant genera remained present but at slightly different relative abundances.

- In soil samples, a lower concentration of nutrient broth (to save costs and encourage sporulation) increased relative abundance of *Aeromonas* while higher concentration of nutrient broth resulted in higher relative abundances of *Acinetobacter* and *Citrobacter*. In soil samples, adding urea to nutrient broth (to increase urease activity and therefore biomineralization potential) increased the abundance of *Raoultella, Stenotrophomonas,* and *Serratia,* as was previously observed for *Raoultella* and *Stenotrophomonas.*

For Task 2 – Laboratory Mortar Testing:

- In general, very little effect was seen in the compressive strength and resistivity of mixtures using bacteria or incorporating fly ash, LWA, or PBS compared to the control OPC mixture. However, use of bacteria and fly ash both resulted in reductions in sorptivity, evidencing greater hydration or refinement of pores through biomineralization (in bacterial samples) and pozzolanic reaction (in the fly ash samples). Evidence of biomineralization was also confirmed through scanning electron microscope (SEM) imaging and thermogravimetric analysis (TGA).

- The effect of bacteria on hydration rates varied depending on cement type and presence of fly ash. OPC cement pastes and mortars were retarded by use of bacterial LWA, with this effect observed in both isothermal calorimetry measurements and in changes in initial and final setting time. However, initial set was accelerated through use of LWA and bacteria in OPC-FA mixtures. Bacteria slightly decreased initial set in CSA mixtures, while retarding final set.

- In general, spray-curing was much more effective at stimulating improvements in crack-healing than was ponding, and also resulted in greater viability of bacteria in samples over time (Figure 4.5).

- Use of LWA as a method of integrating bacteria into the concrete resulted in considerable improvements in bacterial survivability when compared to samples without LWA. LWA represents additional concrete mixture cost, but is essential for protecting bacteria and ensuring extended crack-healing ability (Figure 4.5).

- Use of PBS in lieu of mixing water did not result in higher bacteria viability in mortar samples when compared to samples with dechlorinated tap water. Use of dechlorinated tap water is sufficient production of bacterial concrete mixtures (Figure 4.5).

- The highest bacteria survivability was observed in samples prepared with CSA cement (Figure 4.5).

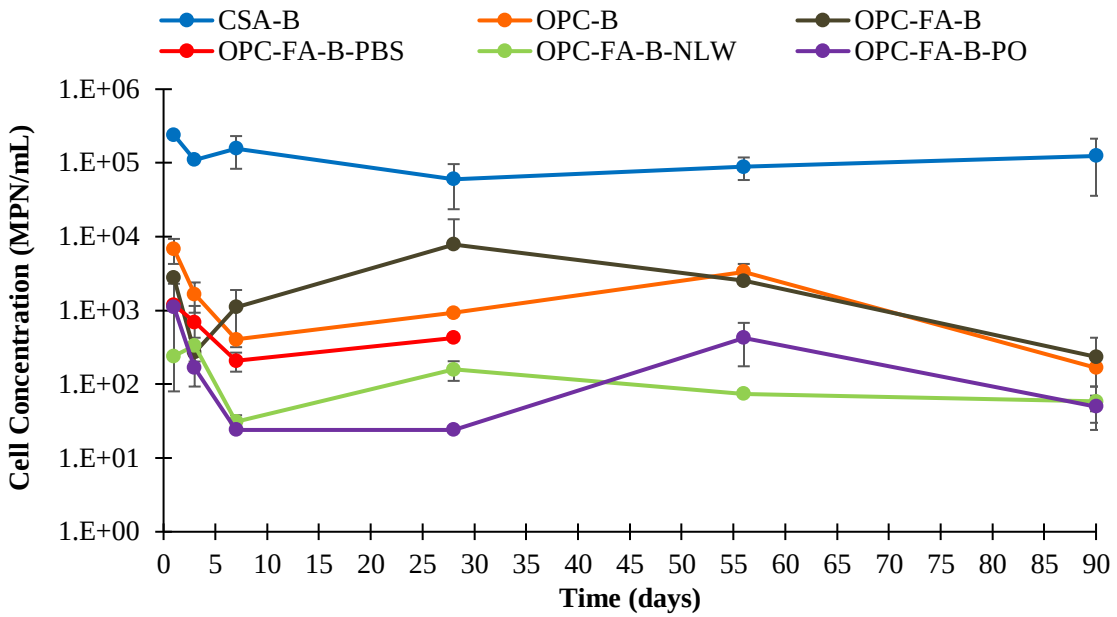

Figure 4.5 - Viability of B. subtilis bacteria in mortar cubes over 90 days. Legend nomenclature is as follows: PO indicates the sample was cured by ponding in nutrient solution, PBS indicates use of phosphate buffer solution in place of mixing water, NLW indicates that lightweight aggregate was not used.

- Partial crack healing occurred in bacterial OPC beams using both *B. subtilis* and soil bacteria. Crack healing was accompanied by increases in UPV, lower water absorption, and greater calcium carbonate precipitate levels compared to the control samples indicating internal crack healing.

- Fly ash did not affect the viability of bacteria in mortar samples up to 90 days following casting. Use of *B. subtilis* with the OPC-fly ash binder resulted in almost full crack closure and the most significant improvement in UPV values and water absorption out of the tested mortar mixtures. Use of the OPC-fly ash binder with soil bacteria led to the greatest densification in the (uncracked mortar) microstructure. However, full crack closure was not observed with these samples, which may suggest that use of soil bacteria with OPC-fly mixtures ash resulted in remediation of internal cracks and pores rather than the crack mouth.

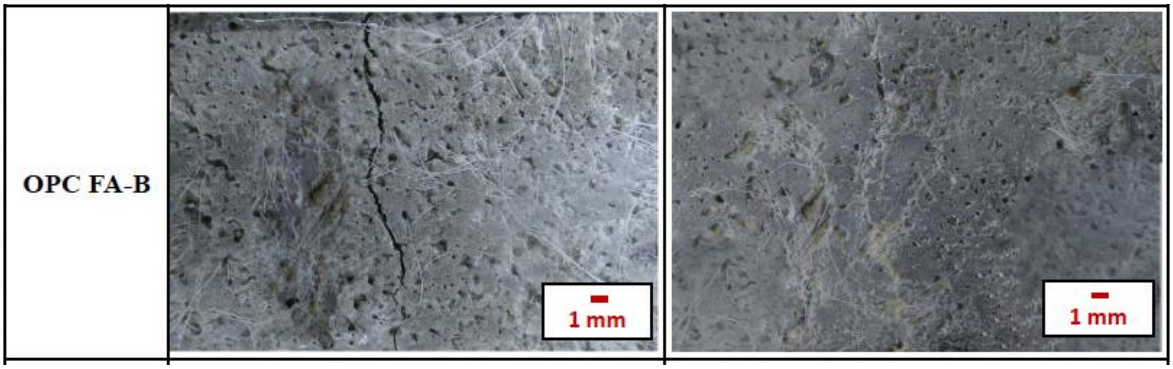

Figure 4.6 - Crack images of a healed crack in a OPC-FA *B. subtilis* sample. Image on the right shows the sample immediately after cracking and left after 6 weeks of spray curing.

- The highest *B. subtilis* and soil bacteria viability was obtained through use of CSA cement and may enable greater later age crack healing potential than mixtures using portland cement. Complete crack healing was observed in bacterial CSA cement samples, with accompanying improvements in UPV results, water absorption, and calcium carbonate contents. However, CSA crack healing required more time (8 weeks vs. 6 weeks) and more application of nutrient solution, compared to the OPC mixtures.

- The effect of exposure of bacterial mortars to non-standard (high and low) temperatures is unclear. Both low and high temperature curing resulted in a decrease in the bacterial viability compared to room temperature samples, very little difference was observed in compressive strengths among the samples, and no visual evidence of crack healing occurred. However, slight increases (suggesting further microstructural densification or crack healing) were measured using UPV in HT-cured samples and water absorption was reduced in both high- and low-temperature cured samples relative to control samples. More testing is needed to fully understand the effect of environmental temperatures on bacterial concrete and mortar performance.

- Exposure of samples to salt resulted in a reduction in the number of living bacteria in the sample and significantly reduced the compressive strength of the *B. subtilis* samples. Although the exposure to salt did not negatively affect strength development in the soil bacteria sample, and resulted in improvements (reductions) in initial and secondary sorptivity relative to the non-salt-exposed soil bacteria samples, no evidence of crack healing was obtained from visual observations, UPV measurements, or cracked-region sorptivity measurements. Exposure to salt appeared to have negated the crack-healing ability of the bacterial mortars.

For Task 3 – In-situ Concrete Testing:

- No cracking occurred on any of the slabs, including both the cured and uncured controls, and the bacterial concrete mixtures, through the first year of the placement of the concrete. LWA is known to provide internal curing and reduce the prevalence of shrinkage cracks, and may have contributed to prevention of shrinkage cracking in the concrete slabs.

- All bacterial and control samples resulted in similar compressive strengths development across the testing period. Similarly, no significant difference in the resistivity was found between the bacterial and the control samples and bacteria did not appear to have a significant effect on drying shrinkage.

- Soil bacteria resulted in the largest reduction in dynamic modulus among the samples exposed to freezing and thawing. However, the soil bacteria sample merely decreased to 95% of its initial value after 500 cycles, which is well above the minimum limit of 70% of the initial sample dynamic modulus. The *B. subtilis* and control samples did not demonstrate any loss in the dynamic modulus through the end of 500 cycles.

For Task 4 – Lifecycle and Cost Analysis:

- Benefits associated with production and use of bacterial concrete come at a significant cost. Altered concrete mixture designs to utilize lightweight aggregate and dechlorinated water

resulted in increases in concrete costs of approximately 7-8%, but bacterial production methods pushed concrete costs to at least 100% of non-bacterial concrete mixtures. Cost increases were primarily driven by the large volumes of bacterial growth solution required to achieve adequate concentrations of bacterial spores.

- Although bacterial mortars and concrete generally outperformed or performed similarly to their non-bacterial counterparts in terms of absorption, compressive strength development, ultrasonic pulse velocity changes, crack healing ability, and resistance to freezing and thawing, these improvements did not lead to significant increases in service life, at least according to the approximate methods utilized in this study.

- Further work is needed to more precisely assess changes in durability over time in bacterial samples from a more wholistic perspective, and to further assess the ability of the bacteria to heal cracks and prevent water intrusion relative to the associated increases in cost to produce these mixtures.

5 Recommendations for Implementation

Both axenic *B. subtilis* and soil-produced bacteria were able to be grown, and to produce spores to sufficient quantities, in reasonable timeframes (24 or 48 hours), and in solutions with varying pH, temperature, and nutrient solution conditions. Choice of bacteria for future bacterial solution production, based on growth and sporulation phase results, indicate that both types of bacteria are suitable for use in concrete systems. In the growth and sporulation phases the soil bacteria were more resilient to changes in environment and were able to be grown and transformed to sporulated samples at slightly higher rates than the *B. subtilis* bacteria. However, although mortars with both types of bacteria demonstrated evidence of biomineralization and crack healing, after incorporation in cementitious pastes, mortars, and concrete, the axenic *B. subtilis* bacteria demonstrated greater survivability, biomineralization capacity, microstructural refinement (based on sorption reductions) and crack healing performance. Based on this, **use of an axenic culture, in this case *B. subtilis* bacteria, is recommended over production of a culture from the local environment**. Both sources can be propagated and regrown in new nutrient solutions to enable harvesting of bacteria for months or years from the same bacteria source solution through aliquoting procedures.

Optimized growth conditions for *B. subtilis* bacteria were selected as 0.5xNB, pH 7, and 37 °C over 24 hours, and 0.5xNB, pH 7 and 25 °C, over 48 hours for soil bacteria cultures. **It does not appear that consistent conditions, specifically temperature and required time, for optimized growth can be applied to different types of bacteria, and should be determined individually for specific sample types in order to minimize the volumes of growth solution required to produce concentrations of 10^6 CFU/mL of concrete mixing water.** This concentration (10^6 CFU/mL mixing water) of spores in the mixing water solution represents the minimum concentration that should be used. 10^6 CFU/mL was sufficient in facilitating up to 90-day life of cells in laboratory conditions, but less evidence of biomineralization occurred in the exterior concrete. Initially greater cell numbers will likely result in greater numbers of bacteria preserved in the concrete over longer time periods, supporting higher crack healing potential. **More work**

should be conducted to determine the minimum cell concentration needed to ensure crack healing.

Results suggest that existing concrete mixtures utilizing portland cement, calcium sulfoaluminate cement (more typical in rapid repair products) and fly ash will not hinder bacterial viability, but lightweight aggregate MUST be incorporated into those mixtures (in this study this was accomplished through substitution of 10% of the fine aggregate with bacteria filled lightweight sand) in order to protect bacteria from initial harsh mixing conditions. Ideally bacterial mixes would be placed in spring or fall, so as to avoid high or low temperatures which were shown to result in greater cell death and reduced crack healing potential. Bacteria were not found to harm strength development or resistance to freezing and thawing of concrete in which they were incorporated.

Successful crack healing and reductions in water sorption were observed in all bacterial mortar mixes utilizing spray-curing and not exposed to salts, suggesting that incorporation of bacteria into concrete mixtures may provide potential for crack remediation in infrastructure. Application of the (sprayed on) nutrient-curing solution over a 6-8 week period was required to induce crack healing. Potential crack healing is likely limited to only early age cracking that occurs prior to the first winter following casting of the concrete, as viable bacteria cells declined over time, and samples exposed to salt solutions were unable to heal cracks. Further, costs associated with production of bacterial concrete mixtures were nearly double that of producing conventional concrete mixtures.

Incorporation of bacteria in concrete may be a feasible approach to reducing early age plastic shrinkage cracking in concrete flatwork. **Strong evidence of crack healing and reduction in water infiltration into cracks was provided in this study. However, additional work is needed to understand minimum cell concentrations required to ensure crack healing ability in in-situ installations and to refine and scale bacterial solution production (perhaps utilizing a large-scale solution reactor as is used in enzymatic energy production processes), the major controller of system costs.**

6 Bibliography

Abbas, Amina Aicha, Stella Planchon, Michel Jobin, and Philippe Schmitt. 2014. "Absence of Oxygen Affects the Capacity to Sporulate and the Spore Properties of Bacillus Cereus." Food Micfrobiology 42: 122–31. https://doi.org/10.1016/j.fm.2014.03.004.

Abdel-Aleem, H., Dishisha, T., Saafan, A., Aboukhadra, A.A., Gaber, Y., 2019. Biocementation of soil by calcite/aragonite precipitation using: Pseudomonas azotoformans and Citrobacter freundii derived enzymes. RSC Adv. 9, 17601–17611. https://doi.org/10.1039/c9ra02247c

Achal, Varenyam, Abhijit Mukherjee, Deepika Kumari, and Qiuzhuo Zhang. 2015. "Biomineralization for Sustainable Construction - A Review of Processes and Applications." Earth-Science Reviews 148: 1–17. https://doi.org/10.1016/j.earscirev.2015.05.008.

Achal, Varenyam, Abhijit Mukherjee, and M. Sudhakara Reddy. 2010. “Biocalcification by Sporosarcina Pasteurii Using Corn Steep Liquor as the Nutrient Source.” Industrial Biotechnology 6 (3): 170–74. https://doi.org/10.1089/ind.2010.6.170.

Achal, Varenyam, and Xiangliang Pan. 2011. “Characterization of Urease and Carbonic Anhydrase Producing Bacteria and Their Role in Calcite Precipitation.” Current Microbiology 62 (3): 894–902. https://doi.org/10.1007/s00284-010-9801-4.

Achal, Varenyam, and Xiangliang Pan. 2014. “Influence of Calcium Sources on Microbially Induced Calcium Carbonate Precipitation by Bacillus Sp. CR2.” Applied Biochemistry and Biotechnology 173 (1): 307–17. https://doi.org/10.1007/s12010-014-0842-1.

Achal, Varenyam, Xiangliang Pan, and Nilüfer Özyurt. 2011. “Improved Strength and Durability of Fly Ash-Amended Concrete by Microbial Calcite Precipitation.” Ecological Engineering 37 (4): 554–59. https://doi.org/10.1016/j.ecoleng.2010.11.009.

Adewoyin, M.A., Okoh, A.I., 2018. The natural environment as a reservoir of pathogenic and non-pathogenic Acinetobacter species 33, 265–272.

Amiri, Ali, and Zeynep Başaran Bundur. 2018. “Use of Corn-Steep Liquor as an Alternative Carbon Source for Biomineralization in Cement-Based Materials and Its Impact on Performance.” Construction and Building Materials 165: 655–62. https://doi.org/10.1016/j.conbuildmat.2018.01.070.

Anbu, Periasamy, Chang Ho Kang, Yu Jin Shin, and Jae Seong So. 2016. “Formations of Calcium Carbonate Minerals by Bacteria and Its Multiple Applications.” SpringerPlus 5 (1): 1–26. https://doi.org/10.1186/s40064-016-1869-2.

Annamalai, Sathesh Kumar, Kantha D. Arunachalam, and K. S. Sathyanarayanan. 2012. “Production and Characterization of Bio Caulk by Bacillus Pasteurii and Its Remediation Properties with Carbon Nano Tubes on Concrete Fractures and Fissures.” Materials Research Bulletin 47 (11): 3362–68. https://doi.org/10.1016/j.materresbull.2012.07.024.

ASTM C109: Standard test method for compressive strength of hydraulic cement mortars (using 2-in. or [50-mm] cube specimens. 2016. ASTM International.

ASTM C128: Standard test method for density, relative density (specific gravity) and absorption of fine aggregate. 2015. ASTM International.

ASTM C157: Standard test method for length change of hardened hydraulic cement mortar and concrete. 2014. ASTM International.

ASTM C305: Standard practice for mechanical mixing of hydraulic cement pastes and mortars. 2016. ASTM International.

ASTM C597: Standard test method for pulse velocity through concrete. 2016. ASTM International.

ASTM C666: Standard Test Method for Resistance of Concrete to Rapid Freezing and Thawing. 2015. ASTM International.

ASTM C778: Standard specification for standard sand. 2021. ASTM International.

ASTM C1585: Standard test method for measurement of rate of absorption of water by hydraulic-cement concretes. 2020. ASTM International.

ASTM C1679: Standard practice for measuring the hydration kinetics of hydraulic cementitious mixtures using isothermal calorimetry. 2014. ASTM International.

ASTM C1761: Standard specification for lightweight aggregate for internal curing of concrete. 2017. ASTM International.

Azarsa, G. and Gupta, R. 2017. "Electrical resistivity of concrete for durability evaluation: a review." Advances in Materials Science and Engineering 2017.

Bang, S., Lippert, J., Yerra, U., Mulukutla, S., Bang, S. S. 2010. "Microbial calcite, a bio-based smart nanomaterial in concrete remediation." International Journal of Smart and Nano Materials 1: 28-39.

Basaran, Zeynep. 2013. "Biomineralization in cement based materials: inoculation of vegetative cells." University of Texas at Austin.

Basaran Bundur, Zeynep, Mary Jo Kirisits, and Raissa Douglas Ferron. 2015. "Biomineralized Cement-Based Materials: Impact of Inoculating Vegetative Bacterial Cells on Hydration and Strength." Cement and Concrete Research 67: 237–45. https://doi.org/10.1016/j.cemconres.2014.10.002.

Bastos, R., Pessoa, G., Oliveira, W.F. De, Santa, D., Marques, C., Tereza, M., Verônica, E., Maciel, M., Cassandra, L., Barroso, B., 2019. Microbial Pathogenesis The genus Aeromonas: A general approach 130, 81–94. https://doi.org/10.1016/j.micpath.2019.02.036

Beal, Jacob, Natalie G. Farny, Traci Haddock-Angelli, Vinoo Selvarajah, Geoff S. Baldwin, Russell Buckley-Taylor, Markus Gershater et al. "Robust estimation of bacterial cell count from optical density." Communications biology 3, no. 1 (2020): 1-29.

Bentz, E. C., and Thomas, M. D. A., "Life-365 Service Life Prediction Model, Version 2.2.3," 2018, http://www.life-365.org/ (last accessed July 29, 2022).

Bundur, Zeynep Başaran, Sungwoo Bae, Mary Jo Kirisits, and Raissa Douglas Ferron. 2017. "Biomineralization in Self-Healing Cement-Based Materials: Investigating the Temporal Evolution of Microbial Metabolic State and Material Porosity." Journal of Materials in Civil Engineering 29 (8): 1–8. https://doi.org/10.1061/(ASCE)MT.1943-5533.0001838.

Burris, L. E., and Kurtis, K. E. 2018. "Influence of set retarding admixtures on calcium sulfoaluminate cement hydration and property development," Cement and Concrete Research, 104: 105–113.

Chahal, Navneet, Rafat Siddique, and Anita Rajor. 2012. “Influence of Bacteria on the Compressive Strength, Water Absorption and Rapid Chloride Permeability of Fly Ash Concrete.” Construction and Building Materials 28 (1): 351–56. https://doi.org/10.1016/j.conbuildmat.2011.07.042.

Choi, J.Y., Kim, Y., Ko, E.A., Park, Y.K., Jheong, W.H., Ko, G.P., Ko, K.S., 2012. Acinetobacter species isolates from a range of environments: Species survey and observations of antimicrobial resistance. Diagn. Microbiol. Infect. Dis. 74, 177–180. https://doi.org/10.1016/j.diagmicrobio.2012.06.023

Dupraz, Christophe, R. Pamela Reid, Olivier Braissant, Alan W. Decho, R. Sean Norman, and Pieter T. Visscher. 2009. “Processes of Carbonate Precipitation in Modern Microbial Mats.” Earth-Science Reviews 96 (3): 141–62. https://doi.org/10.1016/j.earscirev.2008.10.005.

Eltarahony, M., Kamal, A., Zaki, S., Abd-El-Haleem, D., 2021. Heavy metals bioremediation and water softening using ureolytic strains Metschnikowia pulcherrima and Raoultella planticola. J. Chem. Technol. Biotechnol. 96, 3152–3165. https://doi.org/10.1002/jctb.6868

Erşan, Yusuf Çağatay, Emma Hernandez-Sanabria, Nico Boon, and Nele De Belie. 2016. “Enhanced Crack Closure Performance of Microbial Mortar through Nitrate Reduction.” Cement and Concrete Composites 70: 159–70. https://doi.org/10.1016/j.cemconcomp.2016.04.001.

Erşan, Yusuf Çałatay, Filipe Bravo Da Silva, Nico Boon, Willy Verstraete, and Nele De Belie. 2015. “Screening of Bacteria and Concrete Compatible Protection Materials.” Construction and Building Materials 88: 196–203. https://doi.org/10.1016/j.conbuildmat.2015.04.027.

Fakhar, A., Gul, B., Gurmani, A.R., Khan, S.M., Sultan, T., Chaudhary, H.J., Rafique, M., 2022. Technology Heavy metal remediation and resistance mechanism of Aeromonas, Bacillus, and Pseudomonas: A review. Crit. Rev. Environ. Sci. Technol. 52, 1868–1914. https://doi.org/10.1080/10643389.2020.1863112

Farmani, Farshad, Babak Bonakdarpour, and Ali Akbar Ramezanianpour. 2015. “PH Reduction through Amendment of Cement Mortar with Silica Fume Enhances Its Biological Treatment Using Bacterial Carbonate Precipitation.” Materials and Structures/Materiaux et Constructions 48 (10): 3205–15. https://doi.org/10.1617/s11527-014-0391-7.

Fern, A., Jos, M., 2020. An Update on the Genus Aeromonas: Taxonomy, Epidemiology, and Pathogenicity.

Gao, Z., Wang, L., and Yang, H. 2021. “Investigation of the residual mechanical and porosity properties of cement mortar under axial stress during heating.” Materials 14: 1944. https://doi.org/10.3390/ma14081944

Gauvry, Emilie, Anne Gabrielle Mathot, Olivier Couvert, Ivan Leguérinel, and Louis Coroller. 2021. “Effects of Temperature, PH and Water Activity on the Growth and the Sporulation Abilities of Bacillus Subtilis BSB1.” International Journal of Food Microbiology 337

(October 2020). https://doi.org/10.1016/j.ijfoodmicro.2020.108915.

Gauvry, Emilie, Anne Gabrielle Mathot, Olivier Couvert, Ivan Leguérinel, Matthieu Jules, and Louis Coroller. 2019. “Differentiation of Vegetative Cells into Spores: A Kinetic Model Applied to Bacillus Subtilis.” Applied and Environmental Microbiology 85 (10): 1–13. https://doi.org/10.1128/AEM.00322-19.

Gorospe, Choco Michael, Sang Hyun Han, Seong Geun Kim, Joo Young Park, Chang Ho Kang, Jin Hoon Jeong, and Jae Seong So. 2013. “Effects of Different Calcium Salts on Calcium Carbonate Crystal Formation by Sporosarcina Pasteurii KCTC 3558.” Biotechnology and Bioprocess Engineering 18 (5): 903–8. https://doi.org/10.1007/s12257-013-0030-0.

Hossain, S., Wimalasena, S.H.M.P., De Zoysa, M., Heo, G.J., 2017. Prevalence of Citrobacter spp. From Pet Turtles and Their Environment. J. Exot. Pet Med. 26, 7–12. https://doi.org/10.1053/j.jepm.2016.10.004

Hull, N. M., Reens, A. L., Robertson, C. E., Stanish, L. F., Harris, J. K., Stevens, M. J., Frank, D. N., Kotter, C., & Pace, N. R. (2015). Molecular analysis of single room humidifier bacteriology. Water Research, 69, 318–327. https://doi.org/10.1016/j.watres.2014.11.024.

Jakubovskis, R., Ivaske, A., Malaiskine, J., and Urbonavicius, J. 2022. Impact of portland cement type on bacterial viability in biological concrete.” Cement and Concrete Composites 127: 104413. doi.org/10.1016/j.cemconcomp.2022.104413.

Jiang, Lu, Guanhua Jia, Yongzhen Wang, and Zhu Li. 2020. “Optimization of Sporulation and Germination Conditions of Functional Bacteria for Concrete Crack-Healing and Evaluation of Their Repair Capacity.” ACS Applied Materials and Interfaces 12 (9): 10938–48. https://doi.org/10.1021/acsami.9b21465.

Jonkers, Henk M., Arjan Thijssen, Gerard Muyzer, Oguzhan Copuroglu, and Erik Schlangen. 2010. “Application of Bacteria as Self-Healing Agent for the Development of Sustainable Concrete.” Ecological Engineering 36 (2): 230–35. https://doi.org/10.1016/j.ecoleng.2008.12.036.

Keilman, G. R., K. Burtis, B. Tanimoto, and R. H. Doi. 1976. “Effect of Netropsin on the Derepression of Enzymes during Growth and Sporulation of Bacillus Subtilis.” Journal of Bacteriology 128 (1): 80–85. https://doi.org/10.1128/jb.128.1.80-85.1976.

Kurtulus, C., Irmak, T. S., and Sertcelik, I. 2010. “Physical and mechanical properties of gokceada: Imbros (ne aegean sea) island andesites.” Bulletin of Engineering Geology and the Environment 69: 321-324.

Lee, H, R D Cody, a M Cody, and P G Spry. 2000. “Effects of Various Deicing Chemicals on Pavement Concrete Deterioration.” Proceedings of Mid-Continent Transportation Symposium, 151–55.

Legg Jr, F. E. 1956. "Freeze-thaw durability of Michigan concrete coarse aggregates." Highway Research Board Bulletin 143.

Leighton, T. J., and Roy H. Doi. "The stability of messenger ribonucleic acid during sporulation in Bacillus subtilis." Journal of Biological Chemistry 246, no. 10 (1971): 3189-3195.

Li, Q., You, P., Hu, Q., Leng, B., Wang, J., Chen, J., Wan, S., Wang, B., Yuan, C., Zhou, R., Ouyang, K., 2020. Effects of co-contamination of heavy metals and total petroleum hydrocarbons on soil bacterial community and function network reconstitution. Ecotoxicol. Environ. Saf. 204. https://doi.org/10.1016/j.ecoenv.2020.111083

Liao, C. H., Shollenberger, L. 2003. "Survivability and long-term preservation of bacteria in water and in phosphate-buffered saline." Letters in applied microbiology 37: 45-50.

Luo, Mian, and Chunxiang Qian. 2016. "Influences of Bacteria-Based Self-Healing Agents on Cementitious Materials Hydration Kinetics and Compressive Strength." Construction and Building Materials 121: 659–63. https://doi.org/10.1016/j.conbuildmat.2016.06.075.

Madika, Abubakar, J.B. Ameh, and D.A. Machido. 2017. "Isolation and Screening of Bacillus Subtilis from Soil for Amylase Production." Ujmr 2 (2): 82–86.

Manikandan, A. T., and A. Padmavathi. 2015. "An Experimental Investigation on Improvement of Concrete Serviceability by Using Bacterial Mineral Precipitation." RSI International II: 46–49.

Muynck, Willem De. 2009. "Microbial Interactions with Mineral Building Materials." Ghent University.

Muynck, Willem De, Nele De Belie, and Willy Verstraete. 2010. "Microbial Carbonate Precipitation in Construction Materials: A Review." Ecological Engineering 36 (2): 118–36. https://doi.org/10.1016/j.ecoleng.2009.02.006.

Muynck, Willem De, Kim Verbeken, Nele De Belie, and Willy Verstraete. 2013. "Influence of Temperature on the Effectiveness of a Biogenic Carbonate Surface Treatment for Limestone Conservation." Applied Microbiology and Biotechnology 97 (3): 1335–47. https://doi.org/10.1007/s00253-012-3997-0.

Muynck, W. De, Cox, K., De Belie, N., and Verstraete, W. 2008. "Bacterial carbonate precipitation as an alternative surface treatment for concrete." Construction and Building Materials 22: 875–885.

Neale, E. K., and G. B. Chapman. 1970. "Effect of Low Temperature on the Growth and Fine Structure of Bacillus Subtilis." Journal of Bacteriology 104 (1): 518–28. https://doi.org/10.1128/jb.104.1.518-528.1970.

Neville, A. M., and Brooks, J. J. 1987. "Concrete Technology." Longman Scientific and Technical England.

Nguyen, Thanh Ha, Elhem Ghorbel, Hanaa Fares, and Annelise Cousture. 2019. "Bacterial Self-Healing of Concrete and Durability Assessment." Cement and Concrete Composites 104 (June). https://doi.org/10.1016/j.cemconcomp.2019.103340.

Nosouhian, Farzaneh, Davood Mostofinejad, and Hasti Hasheminejad. 2016. “Concrete Durability Improvement in a Sulfate Environment Using Bacteria.” Journal of Materials in Civil Engineering 28 (1): 04015064. https://doi.org/10.1061/(asce)mt.1943-5533.0001337.

Oblinger, J. L., and J. A. Koburger. "Understanding and teaching the most probable number technique." Journal of Milk and Food technology 38, no. 9 (1975): 540-545.

Othman, R., Naher, U.A., Yusoff, S.Z., 2013. Effect of urea-N on growth and indoleacetic acid production of Stenotrophomonas maltophilia (Sb16) isolated from rice growing soils in Malaysia. Chil. J. Agric. Res. 73, 187–192. https://doi.org/10.4067/S0718-58392013000200016

Palin, D., Wiktor, V., Jonkers, H.M. 2013. “Bacteria-based self-healing concrete for application in the marine environment,” In Proceedings of the 4th International Conference on Self-Healing Materials, ICSHM2013, Ghent, Belgium, 16-20 June 2013.

Perez, Hector, and Monica Garcia. 2020. “Bioprecipitation of Calcium Carbonate by Bacillus Subtilis and Its Potential to Self-Healing in Cement-Based Materials.” Journal of Applied Research and Technology 18: 245–58.

Ramachandran, S. K., Ramakrishnan, V., Bang, S. S. 2001. “Remediation of concrete using micro-organisms,” ACI Materials Journal-American Concrete Institute 98: 3-9.

Rao, M. V.Seshagiri, V. Srinivasa Reddy, and Ch Sasikala. 2017. “Performance of Microbial Concrete Developed Using Bacillus Subtilus JC3.” Journal of The Institution of Engineers (India): Series A 98 (4): 501–10. https://doi.org/10.1007/s40030-017-0227-x.

Rao, M V Seshagiri, V Srinivasa Reddy, M Hafsa, P Veena, and P Anusha. 2013. “Bioengineered Concrete - A Sustainable Self-Healing Construction Material.” Research Journal of Engineering Sciences 2 (6): 45–51.

Reeksting, Bianca J., Timothy D. Hoffmann, Linzhen Tan, Kevin Paine, and Susanne Gebhard. 2020. “In-Depth Profiling of Calcite Precipitation by Environmental Bacteria Reveals Fundamental Mechanistic Differences with Relevance to Application.” Applied and Environmental Microbiology 86 (7): 1–16. https://doi.org/10.1128/AEM.02739-19.

Siad, H., Mesbah, H. A., Mouli, M., Escadeillas, G., & Khelafi, H. (2014). Influence of mineral admixtures on the permeation properties of self-compacting concrete at different ages. *Arabian Journal for Science and Engineering*, *39*(5), 3641-3649.

Sandalci, Ilgin, Mustafa Mert Tezer, and Zeynep Basaran Bundur. 2021. “Immobilization of Bacterial Cells on Natural Minerals for Self-Healing Cement-Based Materials.” Frontiers in Built Environment 7 (April): 1–15. https://doi.org/10.3389/fbuil.2021.655935.

Sanders, Erin R. “Aseptic laboratory techniques: plating methods.” Journal of visualized experiments : JoVE ,63 e3064. 11 May. 2012, doi:10.3791/3064

Sandler, Stanley R., Wolf Karo, Jo-Anne Bonesteel, and Eli M. Pearce. 2007. “Thermogravimetric

Analysis." Polymer Synthesis and Characterization, 108–19. https://doi.org/10.1016/b978-012618240-8/50022-8.

Sarkar, Manas, Dibyendu Adak, Abiral Tamang, Brajadulal Chattopadhyay, and Saroj Mandal. 2015. "Genetically-Enriched Microbe-Facilitated Self-Healing Concrete-a Sustainable Material for a New Generation of Construction Technology." RSC Advances 5 (127): 105363–71. https://doi.org/10.1039/c5ra20858k.

Senol, E., 2004. Stenotrophomonas maltophilia: The significance and role as a nosocomial pathogen. J. Hosp. Infect. 57, 1–7. https://doi.org/10.1016/j.jhin.2004.01.033.

Sengul, O., 2014. "Use of electrical resistivity as an indicator for durability," Construction and Building Materials 73: 434-441.

Shen, J., & Xu, Q. 2019. "Effect of elevated temperatures on compressive strength of concrete." Construction and Building Materials 229: 116846. doi.org/10.1016/j.conbuildmat.2019.116846

Siddique, Rafat, Karambir Singh, Pau Kunal, Malkit Singh, Valeria Corinaldesi, and Anita Rajor. 2016. "Properties of Bacterial Rice Husk Ash Concrete." Construction and Building Materials 121: 112–19. https://doi.org/10.1016/j.conbuildmat.2016.05.146.

Silva, Filipe Bravo Da. 2015. "Up-Scaling the Production of Bacteria for Self-Healing Concrete Application." Ghent University.

Skevi, L., Reeksting, J., Hoffmann, T. D., Gebhard, S. and Paine K. 2021. "Incorporation of bacteria in concrete: The case against MICP as a means for strength improvement." Cement and Concrete Composites 120: 104056.

Snellings, R. 2016. "X-ray powder diffraction applied to cement." A practical guide to microstructural analysis of cementitious materials 107.

Spangler, L.C., Lu, L., Kiely, C.J., Berger, B.W., McIntosh, S., 2016. Biomineralization of PbS and PbS-CdS core-shell nanocrystals and their application in quantum dot sensitized solar cells. J. Mater. Chem. A 4, 6107–6115. https://doi.org/10.1039/c5ta10534j

Tittelboom, Kim Van, and Nele De Belie. 2013. Self-Healing in Cementitious Materials-a Review. Materials. Vol. 6. https://doi.org/10.3390/ma6062182.

Tziviloglou, E., Wiktor, V., Jonkers, H.M. and Schlangen, E. 2016. "Bacteria-based self-healing concrete to increase liquid tightness of cracks." Construction and Building Materials, 122, 118-125.

US EPA. "Most probable number (MPN) calculator." https://mostprobablenumbercalculator.epa.gov/mpnForm. Last accessed on 15 June 2022.

Wang, J. Y., N. De Belie, and W. Verstraete. 2012. "Diatomaceous Earth as a Protective Vehicle for Bacteria Applied for Self-Healing Concrete." Journal of Industrial Microbiology and

Biotechnology 39 (4): 567–77. https://doi.org/10.1007/s10295-011-1037-1.

Wang, J. Y., D. Snoeck, S. Van Vlierberghe, W. Verstraete, and N. De Belie. 2014. "Application of Hydrogel Encapsulated Carbonate Precipitating Bacteria for Approaching a Realistic Self-Healing in Concrete." Construction and Building Materials 68: 110–19. https://doi.org/10.1016/j.conbuildmat.2014.06.018.

Wang, J. Y., H. Soens, W. Verstraete, and N. De Belie. 2014. "Self-Healing Concrete by Use of Microencapsulated Bacterial Spores." Cement and Concrete Research 56: 139–52. https://doi.org/10.1016/j.cemconres.2013.11.009.

Wang, Jianyun, Henk M. Jonkers, Nico Boon, and Nele De Belie. 2017. "Bacillus Sphaericus LMG 22257 Is Physiologically Suitable for Self-Healing Concrete." Applied Microbiology and Biotechnology 101 (12): 5101–14. https://doi.org/10.1007/s00253-017-8260-2.

Wei, Shiping et al. "Biomineralization processes of calcite induced by bacteria isolated from marine sediments." Brazilian journal of microbiology : [publication of the Brazilian Society for Microbiology] vol. 46,2 455-64. 1 Jun. 2015, doi:10.1590/S1517-838246220140533

Weiss, Jason, Dale Bentz, Anton Schindler, and Pietro Lura. "Internal curing." *Structure* 12 (2012).

Whiffin, Victoria S. 2004. "Microbial CaCO3 Precipitation for the Production of Biocement." Murdoch University.

Wiktor, Virginie, and Henk M. Jonkers. 2011. "Quantification of Crack-Healing in Novel Bacteria-Based Self-Healing Concrete." Cement and Concrete Composites 33 (7): 763–70. https://doi.org/10.1016/j.cemconcomp.2011.03.012.

Wilks, Jessica C., Ryan D. Kitko, Sarah H. Cleeton, Grace E. Lee, Chinagozi S. Ugwu, Brian D. Jones, Sandra S. Bondurant, and Joan L. Slonczewski. 2009. "Acid and Base Stress and Transcriptomic Responses in Bacillus Subtilis." Applied and Environmental Microbiology 75 (4): 981–90. https://doi.org/10.1128/AEM.01652-08.

Wu, Mingyue, Xiangming Hu, Qian Zhang, Di Xue, and Yanyun Zhao. 2019. "Growth Environment Optimization for Inducing Bacterial Mineralization and Its Application in Concrete Healing." Construction and Building Materials 209: 631–43. https://doi.org/10.1016/j.conbuildmat.2019.03.181.

Xu. J., and Wang. X. 2018. Self-healing of concrete cracks by use of bacteria containing low alkali cementitious material." Construction and Building Materials 167: 1–14.

Zhang, P., and Panesar, D. K. 2018. Water absorption of carbonated reactive MgO concrete and its correlation with the pore structure," Journal of CO2 Utilization 24: 350–360.

7 Appendix A – Literature Review

Bacterial concrete is concrete in which bacterial spores capable of producing calcium carbonate (a reaction known as "bio-mineralization") have been embedded in concrete to increase the durability of the concrete through healing of cracks or decreases in ion transport (permeability and diffusivity). Use of bacteria has been shown capable of improving both concrete strength and durability through its crack healing ability, as well as its densification of the existing concrete microstructure, similar to the process occurring with pozzolanic materials such as fly ash. In order to successfully induce this reaction, several very specific conditions need to be met:

- The bacterial strains used should be resistant to high pH systems.

- The bacteria must be capable of survival over long periods of time without nutrients by forming endospores. Endospores are dormant, metabolically inactive, protective structures that bacteria turn into when they undergo stress. When suitable conditions are provided, bacteria can regenerate themselves becoming metabolically active and reacting to precipitate calcium carbonate minerals, filling cracks and restoring impermeability.

- Upon 'regenerating,' the bacteria must have a food source (such as nitrogen and carbon) available to fuel the bio-mineralization reaction. Although need for a nitrogen and carbon source is agreed upon, the best method of application of nutrients to the concrete system is still being investigated.

The most commonly investigated strains of bacteria used in cementitious mixtures are shown in Table 7.2. These bacteria types can tolerate highly alkaline conditions, form spores, produce urease enzyme and precipitate calcium carbonate. Past work has shown that *Sporoscarina pasteurii*, *Bacillus cereus*, *Bacillus sphaericus*, *Bacillus alkalinitrilicus*, and *Bacillus subtilis* strains are all effective in filling cracks up to 0.97 mm in width (Amiri and Bundur 2018; Wang et al. 2014; Wiktor and Jonkers 2011; Basaran Bundur, Kirisits, and Ferron 2015), and restoring the majority of flexural strength. Bacterial precipitant has additionally been shown to increase durability of concrete through densification of the microstructure, reducing permeability, and thus chloride transport and carbonation, within the concrete (Wang et al. 2014; Achal and Pan 2011). Bacteria has been shown to continue to improve concrete for up to 1 year following casting, (although the vast majority of studies have tested only as far as 28-90 days after casting).

Table 7.1 - Commonly used bacterial cultures, their effect, and anticipated costs when used in cementitious mixtures.

Bacteria type	Effects	Cost	References
S. pasteurii	Successful at internal crack remediation, survived in mortar up to 11 months when incorporated with growth medium.	$319	Amiri and Basaran (2018), Basaran et al. (2015)
B. sphaericus	High urease activity and high carbonate productivity, translating to nearly 60% increase in compressive strength.	$320	Wang et al. (2010)
B. megaterium	Was able to survive up to 28 days when directly added to mortar, improved compressive strength.	$320	Achal et al. (2011)

B. subtilis	Can survive in wide temperature range, precipitates dense insoluble calcite crystals.	$341	Manikandan and Padmavathi (2015), Seshagiri et al. (2013)
B. cereus	Grows well at lower pH, excellent crack bridging and permeability decreases.	$341	Wu et al. (2019)
B. alkalinitrilicus	Alkali resistant soil bacterium capable of long life: bacteria remained viable up to 100 days in concrete	-	Wiktor and Jonkers (2011)

Bacteria have been successfully used in cementitious mixtures in conjunction with a variety of SCMs including fly ash (Annamalai, Arunachalam, and Sathyanarayanan 2012; Achal, Pan, and Özyurt 2011; Chahal, Siddique, and Rajor 2012a), silica fume (Siddique et al. 2016; Farmani, Bonakdarpour, and Ramezanianpour 2015, Siddique, and Rajor 2012b), and slag (Palin et al. 2013, Siddique et al. 2016), suggesting that they would also be effective when used in typical concrete mixtures used in Ohio, such as the QC1 and QC2 mixtures. In these systems, bio-mineralization resulted in increases in strength and reductions in water permeability or durability in all mixtures, in excess of the improvements gained from use of SCMs. Several studies highlighted significant improvements in bacteria survivability when using a 'protectant' media, such as natural minerals, such as clay or natural zeolites, or lightweight aggregate (Wiktor and Jonkers 2011; J. Y. Wang, De Belie, and Verstraete 2012; Erşan et al. 2015). Immobilizing microorganisms on porous minerals provides a natural protection system to preserve bacteria from the harsh environment of the concrete by stabilizing cells on a carrier (Tezer and Bundur 2021). Lightweight aggregates and perlite have also shown to provide promising improvements in bacteria viability and healing of cracks (Sandalci, Tezer, and Basaran Bundur 2021; Wiktor and Jonkers 2011, Jiang et al. 2020).

Although the strains of bio-mineralizing bacteria shown in Table 7.2 have been proven effective for improving the properties and performance of cementitious systems, growth of 'pure' (known as "axenic") bacterial strains is not trivial. The typical bacterial sample growth process requires clean, sterilized laboratories, specialized (and sometimes expensive) equipment including autoclaves, incubators, and centrifuges, as well as staff trained in biological growth processes. Cultivation of non-axenic bacteria for concrete may result in simplified procedures and increased resiliency bacteria, produced at lower cost and through consumption of current local waste materials. These 'impure' strains of bacteria have been only preliminarily explored, and present significant opportunities for use of these systems in Ohio concrete. One study (De Silva 2015), which utilized a non-axenic bacterial system produced from sludge from a "potato treatment plant" saw **costs reduced by a factor of 10-20x** compared to those of the 'pure' strain systems used in the same study (from an increase in the cost of concrete from \$920-2000/yd^3 concrete for the axenic bacteria system to ~\$100/yd^3 concrete for the impure system). The same potato-sludge bacterial system was able to obtain a bacterial activity 1.6x higher than that of the pure bacterial strain systems, and generated some of the highest compressive strengths, out of the 11 systems investigated. This suggests that not only are pure strains of bacteria not necessary for obtaining the improvements to concrete performance, but ignoring the opportunity to produce and use this type of impure bacterial system would be irresponsible from a financial standpoint. Still, research and testing are essential in order to ascertain the processes required and viability of non-axenic bacterial systems for use in concrete, especially on the local scale (as this study was conducted in Belgium).

In addition to choosing an effective bacterial source, nutrient solutions are required to grow

bacteria and induce microbial precipitation of calcium carbonate. Nitrogen and carbon are required within these solutions to ensure bacterial viability, with an additional calcium source needed for microbial induced calcium carbonate precipitation. Urea is used as the main nitrogen source for the cells in many growth solutions. The type of nutrient solution can have significant impacts on the numbers of bacteria grown and their ability to densify the concrete and prevent cracking. The most efficient nutrient solutions for bacteria growth are shown in Table 7.3. In addition to supporting bacterial culture growth, however, nutrient solutions can also affect cement hydration, significantly increasing setting times and slowing development of mechanical properties and durability. Therefore, choice of nutrient solution can be as important to the success of the concrete system as is choice of bacterial strain and the effects of each solution should be understood before they can be applied on a large scale.

Table 7.2 - Growth media for bacterial solutions.

Nutrient solution	Effect	Reference
Urea-Yeast extract (YE)	Improves calcium carbonate precipitation but retards the hydration therefore may decrease strength, especially at early ages.	Zhang et al. (2017), Basaran et al. (2015)
Urea-Corn steep liquor (CSL)	Improves urease activity and calcite production, decreases the retardation effect of the bacteria, is cheaper than YE but since it is waste product of corn industry, but subject to batch to batch variability.	Amiri and Basaran (2018)
Urea-peptone	Alkaline medium can be used to increase sporulation.	Jonkers et al. (2010), Qiu et al. (2014)
Urea-calcium lactate	No negative effects on the strength but effect on the setting time is unclear.	Wiktor and Jonkers (2011), Jonkers et al. (2010), Luo and Qian (2016), Paine (2016)
Urea-calcium nitrate	Accelerates hydration and decreases setting time.	Luo and Qian (2016)
Urea-calcium chloride	More effective than calcium nitrate at inducing biomineralization but a concern for corrosion in concrete.	Whiffin (2004)
Urea-lactose mother liquor (LML)	By-product of dairy industry, better performance than YE.	Achal et al. (2009)

Despite the progress that has been made in use of bacterial concrete to improve cementitious materials' durability, many aspects specifically regarding the upscaling and use of bacterial mixtures from laboratory- to in-situ concrete remain poorly understood. Several challenges exist with regards to upscaling:

- Lack of understanding of bacterial growth protocols and translation of (and hopefully, simplification of) these methods for use in ready-mix plants,

- Limited quantification of the effects of concrete mixture formulations on bacteria's life and efficiency, including use of local Ohio materials and SCMs, to determine optimum mixture formulation protocols,

- Poor understanding of requirements for curing to maintain and preserve bacterial activity,

- Lack of information regarding the effects of environmental conditions on bacterial growth and precipitation activity, including placement and curing temperatures (will bacteria survive Ohio's winter and summer conditions, can bacterial concrete be successfully placed in late fall), and the impact of the use of deicing salts on bacterial condition and life.

- Uncertainty regarding the length of time over which crack healing can be expected to continue throughout the life of the structure.

Without understanding the effects of these factors on the efficacy of the bacterial-concrete system, it will be difficult to ensure the design and construction of efficient and cost-effective systems incorporating this technology.

In addition, few studies, even those including "Bacterial Concrete" in the title have tested larger than mortar samples, and even fewer discussed the processes required for upscaling production of their bacterial samples for use in concrete. However, one study (De Silva 2015) *was* able to successfully perform a small scale upscale their bacterial system from a laboratory size mortars to a scale more realistic to production of systems for concrete. They scaled bacterial solutions from 150 mL to 5L successfully, without decreasing bacterial activity, calcium carbonate precipitation ability of the samples, nor inducing compressive strength decreases in the samples they tested. While these initial results are promising and suggest that upscaling of bacterial concrete production processes is possible, knowledge required for successful upscaling of bacteria required for producing this type of concrete, and additionally, the effects of placing, curing, and using the concrete outside of controlled laboratory conditions remains extremely limited.

7.1 Biomineralization Ability

In order to successfully heal cracks, bacteria cells should be able to biomineralize, in other words, microbes (bacteria) should be able to precipitate calcium carbonate. If the microorganism is a ureolytic bacteria, it can decompose urea into ammonia and carbon dioxide by producing urease enzyme, resulting in an increase in the pH of the environment (Achal et al. 2015). When in the presence of calcium, the pH increase activates calcium carbonate precipitation, as shown in Eqs. 1 and 2.

$$CO(NH_2)_2 + H_2O \leftrightarrow {CO_3}^{2-} + 2{NH_4}^{+} + 2H_2O \quad (1)$$

$${Ca}^{2+} + {CO_3}^{2-} \leftrightarrow CaCO_3(s) \quad (2)$$

Biomineralization ability of the bacteria can be quantified based on bacterial ureolytic activity. Conductivity measurements are used to track urea consumption (De Muynck et al. 2013) since one mole urea produces 2 mol NH_4^+ and 1 mol CO_3^{2-}, ion production from urea consumption increases solution conductivity proportionally (Eq. 1). Thus, higher urea consumption tends to higher conductivity of urea solution (J. Wang et al. 2017). Consumption of urea shows the ureolytic

activity of bacteria and therefore its calcite precipitation efficiency. High bacterial urease activity usually indicates a high and fast carbonate production and higher calcium carbonate precipitation.

Calcium carbonate precipitation in bacterial concrete samples can be tracked using X-ray diffraction, thermogravimetric analysis (TGA), scanning electron microscopy (SEM) and Fourier transform infrared spectroscopy (FTIR). In order to obtain the clearest understanding of the presence and quantity of varying calcium carbonate phases in biomineralized samples the application of multiple techniques is necessary. Although the TGA and FTIR methods have similar sample preparation processes and utilize similar sample amounts for analysis, TGA is capable only of providing only the total calcium carbonate quantity and unable to differentiate between phases due to the presence of overlapping decarbonation temperatures among the $CaCO_3$ phases. FTIR, on the other hand, is able to identify different polymorphs of calcium carbonate using reference infrared bands of different phases but quantification using FTIR is difficult. XRD is capable of determining and quantifying different phases of calcium carbonate. It needs larger amount of sample than both TGA and FTIR, resulting in more representative data. However, it has the most difficult sample preparation process among other methods. SEM imaging requires more experience to get high quality images and to analyze morphologies visually. However, in addition to obtaining different phases of calcium carbonate, SEM images can show indications of bacteria present within the biomineralized mineral microstructure.

Ersan et al. (2016) and Tezer and Bundur (2021) tested the precipitation in mortar samples using SEM and FTIR. They obtained samples from the cracked location and used an approximately 1 cm^3 sample area for SEM imaging and 10 mg powders for FTIR. From SEM imaging Tezer and Bundur (2021) observed two polymorphs of calcium carbonate (calcite and vaterite) and indications of rod-shaped bacteria. From FTIR analysis they identified calcite as the most dominant precipitated material, with a small amount of aragonite and vaterite also present in some samples. Ersan et al. (2016) confirmed that, from both FTIR and SEM analysis, the precipitated minerals inside the cracks were mainly calcite and aragonite.

Similar to FTIR, XRD and TGA can be used to track calcium carbonate precipitation by determining phase contents in the powdered cement samples and evaluating decomposition temperature of calcium carbonate, respectively. Basaran et al. (2015) determined precipitated calcium carbonate quantities present in bacterial and non-bacterial cement pastes using both XRD and TGA. For the sample preparation, they ground hardened cement pastes to powder and they used approximately 20 mg samples for TGA and 2 g for XRD. From XRD results, they determined that the precipitated calcium carbonate was calcite, with the bacterial paste having higher calcite content, shown through higher intensity calcite phase peaks (Basaran et al. 2015). Their TGA results were consistent with XRD results, bacterial paste resulting in higher amounts of calcium carbonate, with amounts further increased using nutrient medium in the place of mixing water (Basaran et al. 2015).

7.2 Factors Affecting Biomineralization

In order for sufficient bacteria cells to survive in concrete and result in significant paste improvements, a high initial cell count is required, usually $10^7 – 10^9$ CFU/mL (Anbu et al. 2016). Many variables are known to affect bacterial growth including pH, temperature, and nutrient solution concentration. The type of nutrient solution can have significant impacts on the numbers

of bacteria grown and their ability to densify the concrete and heal cracking (Basaran et al. 2015). In addition, bacteria can grow preferentially in specific nutrient solutions depending on the bacteria type. Suggested nutrient medias for *B. subtilis* are peptone, meat extract, tryptic soy broth, yeast extract and/or combination of these food sources (Nosouhian, Mostofinejad, and Hasheminejad 2016; Sarkar et al. 2015; Nguyen et al. 2019). Amount of nutrient source is also important for bacteria to grow. Wang et al. (2017) found out that increasing the concentration of the yeast extract in the solution resulted in faster growth, greater bacterial concentration, and higher quantities of urea decomposed, thus resulting in greater microbial precipitate quantities and crack filling potential.

7.2.1 Temperature and pH

Some work has investigated the impact of culturing environment variables on the growth of *B. subtilis* and non-axenic cultures for their use in concrete. Gauvry et al. (2019) grew *B. subtilis* cells in a solution of peptone and yeast extract combination and incubated at 27, 40 and 49 °C temperatures. Results indicated 40 °C to be the optimal temperature to obtain spores, at 27 °C, the growth rate was 35% less than at 40 °C and at 49 °C growth was faster but the sporulation was inhibited (Gauvry et al. 2019). Another study on the growth and sporulation abilities of *B. subtilis* showed that *B. subtilis* microorganisms were able to grow from 5.5 °C to 55.7 °C, with optimal conditions at 46.9 °C (Gauvry et al. 2021). At 37 °C and pH 7 the maximum sporulation probability was reached much sooner than 25 °C, meanwhile and no spores appeared at 10 °C from 16h to 40h of culturing (Gauvry et al. 2021). Neale and Chapman (1970) studied effects of temperature changes on *B. subtilis*, changing incubation temperatures from 37 °C to 15 °C. They observed increases in the viable cell count after a time indicating a recovery from thermal stress; however, when temperature switched to 12 °C from 37 °C they did not observe an increase in viable counts and recovery, suggesting that cells grown at low temperatures perform poorly when later exposed to higher temperature systems. In addition to that, they suggested that low temperatures induced undesireable structural modifications when cells were grown at 12 and 15 °C when compared to 37 °C (Neale and Chapman 1970). Similar to other enzymatic reactions, the urea hydrolysis and calcium carbonate precipitation are generally increased by increase in temperature from 10 to 37°C. At a lower temperature (10°C), $CaCO_3$ precipitation rate greatly dropped and *B. sphaericus* spores had a slower $CaCO_3$ precipitation than vegetative cells, due to the fact that spores are dormant and take time to first become active, while vegetative cells are always in an active state (Wang et al. 2017; De Muynck et al. 2013). De Muynck et al. also found that the highest and fastest production of $CaCO_3$ was obtained at a high temperature of 37°C, due to the high ureolytic activity at this temperature (De Muynck et al. 2013).

Work with *B. sphaericus*, another bacteria used in concrete biomineralization, indicated that optimal pH for growth is between 7 and 9 and calcite precipitation ability increases from 10 °C to 37 °C (Wang et al. 2017). A study tested growth of *B. subtilis* at low (4.5 to 5) and high (8.9 to 9.3) pH values, with results indicating that B. *subtilis* could successfully grow from pH 4.8 to 9.2 with the optimal pH condition at pH 6.8 (Gauvry et al. 2021). Another study investigated the growth response of *B. subtilis* in acid and base environments, and found that when pH was shifted from 8.5 to 6, there was a short lag in the growth rate; however, for pH shift from 6 to 8.5 and 7.4 to 8.8 longer growth arrests (several hours) were observed (Wilks et al. 2009). They explained the lag time required for growth shift to high pH required greater genetic adaptation at pH 9 than at pH 6 (Wilks et al. 2009). A similar response is expected from bacteria when introduced into the

high pH concrete pore solution. Additionally, the pH of the growth solution affects the dissolution or precipitation of carbonate and precipitation usually occurs in an alkaline environment (when pH>8) (Dupraz et al. 2009). If the pH levels become low, the carbonate will tend to dissolve rather than precipitate (Anbu et al. 2016). Urease enzyme activity is affected by the pH as well, which is optimum when pH is 8 (Gorospe et al. 2013).

7.2.2 Calcium source

In addition to the nutrient source, calcite precipitation depends on the calcium source present with the bacteria. Several studies have used $CaCl_2$ as the calcium source and it was found successful in inducing calcite precipitation (Achal et al. 2011; Whiffin 2004; Ramachandran et al. 2001; Bang et al. 2010). However, $CaCl_2$ can be harmful to reinforced concrete structures since the addition of chloride increases the risk of corrosion (Perez and Garcia 2020; Achal and Pan 2014). Calcium nitrate is also commonly used in order to prevent addition of chloride ions to the concrete. Use of calcium nitrate as the calcium source results in lower total precipitation than through use of calcium chloride (Luo and Qian 2016). Both solutions are well known hydration accelerators, increasing the speed of hydration of the concrete and reducing setting time, a change which may or may not be beneficial or desired, depending on the application (Achal and Pan 2014; Luo and Qian 2016). As an alternative, calcium acetate can also be used since it does not have a known effect on the concrete properties and has similar amount of calcium carbonate precipitation as calcium nitrate (Lee et al. 2000; Achal and Pan 2014).

7.2.3 Oxygen amount

Oxygen is needed for aerobic bacterial growth and sporulation as well as nutrients, as bacteria cells consume oxygen during the growth process. Use of different culturing containers can change the quantities of oxygen introduced into incubating samples, resulting in changes in growth kinetics. For example, use of baffled flasks disrupts circular laminar flow and causes additional turbulence within the flask, leading to increased gas exchange surface area in the liquid, see Figure 7.1.

Figure 7.1 - (a) standard flask; (b) baffled flasks.

Wang et al. (2017) has shown that oxygen was almost completely consumed by growth of vegetative cells and spore germination in the nutrient medium in 20 hours. However, it was found that oxygen had no effect on ureolytic activity of vegetative cells. Similar levels of urease were produced in oxygen limited and oxygen non-limited conditions (Wang et al. 2017; Whiffin 2004). This suggests that although bacteria have a great need for adequate oxygenation in growth solution

samples they are not harmed, with respect to biomineralization ability, by imperfect conditions. However, even though oxygen does not have an effect on the ureolytic activity, a strong decrease in the sporulation rate of *B. cereus* cells in the absence of oxygen has been observed (Abbas et al. 2014).

In addition to effects on the bacterial growth and sporulation, lack of availability of the oxygen in the crack depth is a limiting factor for self-healing of the cracks. If sufficient oxygen is not available within the depth of the cracks, healing may be restricted to the surface only, affecting the sealing efficiency. To overcome this issue and enhance calcite precipitation, it was suggested to apply wet and dry curing cycles to the cracks rather than keeping samples constantly in a wet environment (Wang et al 2014; Tziviloglou et al 2016).

7.3 Methods of sporulation

Due to the inability of bacterial vegetative cells to resist the high pH of the concrete and high-shear forces experienced during concrete mixing, bacteria cells need to be incorporated into concrete in the form of spores. Spores are more resistant to the alkaline environment of the concrete and concrete mixing process, as well as dry environment of hydrated concrete. For bacteria cells to survive for extended time, most studies have focus on embedding bacteria in the form of spores (Wang et al. 2017; Jiang et al. 2020; Da Silva 2015). However, obtaining spores is not trivial and it is necessary to optimize the sporulation conditions and increase the rate of sporulation.

Sporulation typically occurs by exposing the bacterial source to stress, in the form of nutrient deficiencies, or non-ideal conditions such as high or low temperatures, lack of moisture, or non-ideal solution pH. The most common methods of sporulation include long term incubation of the bacterial solutions for 14 – 28 days, use of sporulation media, and drying bacteria cells in 40 °C or 60 °C oven. Wang et al. (2014) incubated *B. sphaericus* cells with shaking conditions at 28 °C for 28 days and applied pasteurization to kill the vegetative cells after the incubation period. They encapsulated the spores in microcapsule and were able to reach 10^9 spores/g microcapsules. Use of sporulation media, instead of long-term incubation, has also been found as an effective method for obtaining spores. Jonkers et al. (2010) cultured *B. pseudofirmus* and *B. cohnii* cells in an alkaline sporulation medium with nutrient broth at pH 10 on a shaker table until desired spore concentration was reached. After that, they centrifuged the culturing solutions and resuspended spore pellets in tap water to use in cement stone test specimens (10^8 spores/cm^3 cement stone). In an environmental bacteria study, Reeksting et al. (2020) collected environmental samples from limestone caves and calcareous soils. For spore production, they inoculated overnight grown and centrifuged cells in a sporulation medium consisting of nutrient broth and various chemicals, then incubated it for at least 48 hours until majority of cells reached endospores.

In order to decrease the culturing time to obtain high spore numbers and increase the efficiency of the sporulation media, these methods can also be performed together. Jiang et al. (2020) cultivated *B. cohnii* cells in a sporulation media containing sodium, potassium, phosphate, sulphate, and magnesium for 4 days, reaching 10^9 CFU/mL, followed by immobilization of the cells into expanded perlite, which was then dried at 40 °C. Similarly, Ersan et al. (2015) applied low temperature heat treatment at 60 °C to granulated nitrate reducing bacteria to induce sporulation prior to use in mortar samples.

8 Appendix B: Research Approach

8.1 Task 1 Experimental Materials and Methods

8.1.1 Bacterial Growth Optimization

For this study, *B. subtilis* was selected as an axenic culture since it can survive in wide temperature range and precipitate dense insoluble calcite crystals. Soil, obtained from a Columbus, Ohio residence (Figure 8.1), was used to produce a non-axenic (impure, multi-organism) bacterial system. Soil was selected for two reasons: (i) its wide availability as an environmental material and (ii) most common types of bacteria that are able to biomineralize, especially *B. subtilis*, have been shown to live in soil (Seshagiri Rao et al. 2017, Madika et al. 2017). In addition to the soil sample, bacterial growth of spent digestate samples obtained from methane/energy production process, and whiskey wastewater sample obtained from a Columbus, Ohio distillery were also tested.

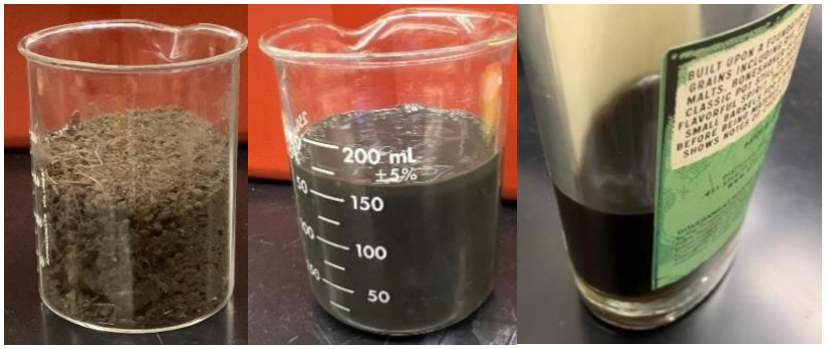

Figure 8.1 - From left to right: Soil sample obtained from a Columbus, OH garden; spent digestate solution; whiskey distillation wastewater.

In addition to choosing an effective bacterial source, nutrient solutions are required to grow bacteria and induce microbial precipitation of calcium carbonate. Nitrogen and carbon are required within these solutions to ensure bacterial viability, with an additional calcium source needed to induce microbial calcium carbonate precipitation (Achal et al. 2015). Tryptic soy broth (TSB) and nutrient broth (NB) were selected as initial nutrient mediums to grow *B. subtilis* cells since they are both suggested nutrient sources for *B. subtilis*. Initial growth results of vegetative cells and spores of *B. subtilis* in NB and TSB at 37 °C are shown in Figure 8.2. The results indicate that TSB led to one order of magnitude higher vegetative cell counts when compared to NB; however, NB led to greater spore count than TSB at a given temperature. While greater cell numbers are initially attractive, spores are desirable for use in concrete mixtures, due to their higher likelihood of survival. Therefore, NB was selected for use in all further experiments. Since *B. subtilis* is a common soil bacterium, and knowledge of the soil sample bacterial type was not yet available, the same nutrient medium, NB, was selected for both axenic and non-axenic cultures.

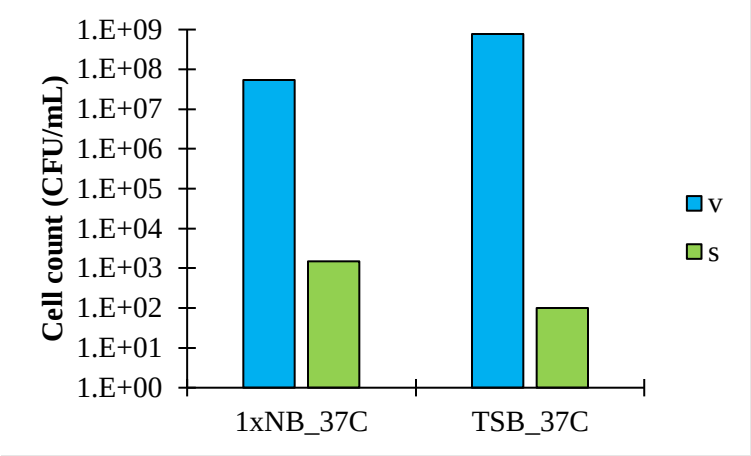

Figure 8.2 - Concentration of *B. subtilis* at 24hr at 37 °C in different nutrient mediums (s: spores, v: vegetative cells).

Figure 8.3 shows the overall process for growth of bacteria, which consisted of two stages. In stage 1, a variety of growth conditions were studied to determine optimum growth conditions for axenic (*B. subtilis*) and non-axenic (soil) cultures. Two different pH values (7 and 9), several growing temperatures to represent hot and cold weather under unconditioned lab conditions (as many concrete producer labs are) and standard room temperature and different nutrient media concentrations (half, normal and double dosages) were tested. After completing stage 1, optimum growth conditions and optimum method for sporulation were determined and biomineralization ability of these two cultures were confirmed for concrete related measurements.

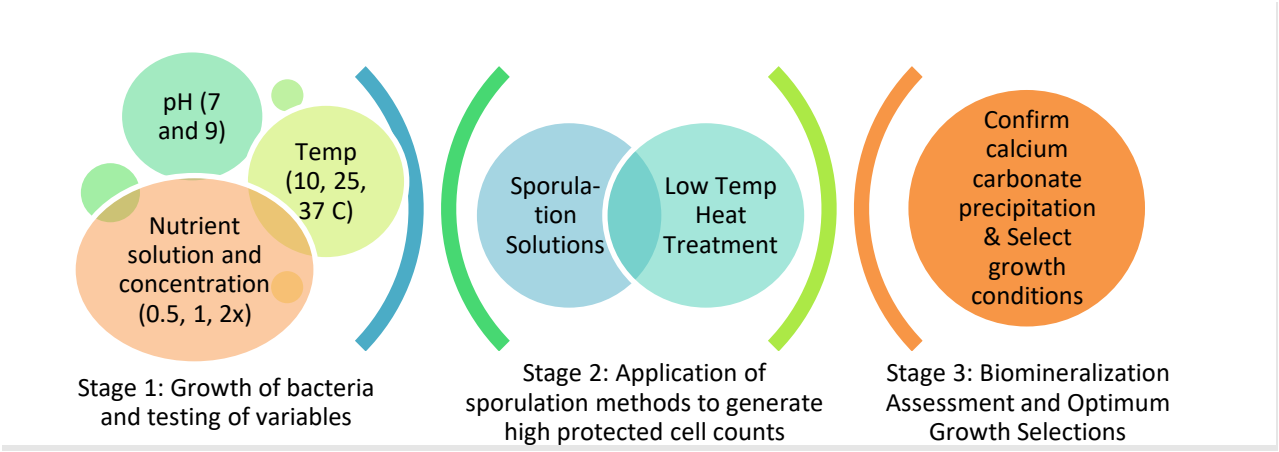

Figure 8.3 - Overall process for bacteria growth, sporulation, and biomineralization.

B. subtilis strain (type 3A1, strain 168) was obtained from Bacillus Genetic Stock Center (BGSC) and 1 mL frozen aliquots were prepared from this strain. To prepare frozen aliquots, obtained bacterial filter disks were placed on a solid media and hydrated with a few drops of a nutrient solution and plates were incubated overnight at 37 °C. A single colony was scraped from the plate, placed in 50 mL nutrient solution, and the bacterial solution was incubated for 24 hours at 37 °C. The solution was centrifuged 24 hours later, the centrifuged pellet was mixed with a nutrient solution and 10% glycerol and the solution was placed in 1 mL tubes and frosted. For soil samples,

2.5 g of soil was added into 50 mL nutrient solution and incubated for 24 hours at 25 °C with 180 rpm shaking conditions. At 24 hours, frozen aliquots were prepared from this solution. To obtain growth curves of *B. subtilis* and soil samples, 1 mL of frozen aliquots were injected into 50 mL nutrient solution. Similar to the process used for the soil sample, for spent digestate and whiskey distillation solution 1 mL of each solution was placed into 50 mL nutrient solution and incubated for 24 hours at 25 °C with 180 rpm shaking conditions.

For this study, nutrient broth (NB) was used as a nutrient source for both cultures. Growth medium (1xNB) consisted of 8 g nutrient broth (NB) per 1 L of deionized (DI) water and its pH was adjusted to 7 using NaOH unless otherwise specified. 15 g of agar was added to 1 L liquid medium if a solid media was required to make agar plates. Agar plates are used to determine the bacterial counts (Figure 8.4, right). After preparation, growth media was autoclaved at 121 °C for 45 minutes for sterilization. After sterilization, solutions were kept at room temperature (23°C) and mixed with bacteria when cool. All bacteria suspensions were inoculated (0.2% volume/volume) in sterile NB solution and cells were grown aerobically at a given temperature and 180 rpm shaking conditions for 48 hours (Figure 8.3, left). One mL of sample was obtained at given time intervals, serially diluted (10^0-10^9) in test tubes containing 1X PBS (phosphate buffer saline) and plated on agar plates. Plates were incubated at 37 °C for 24 hours and after 24 hours viable cell counts were obtained (Fig. 6, right). To obtain spores, another 1 mL sample was pasteurized, killing non-sporulated bacteria, at 70 °C for 15 minutes and the same plating process was performed.

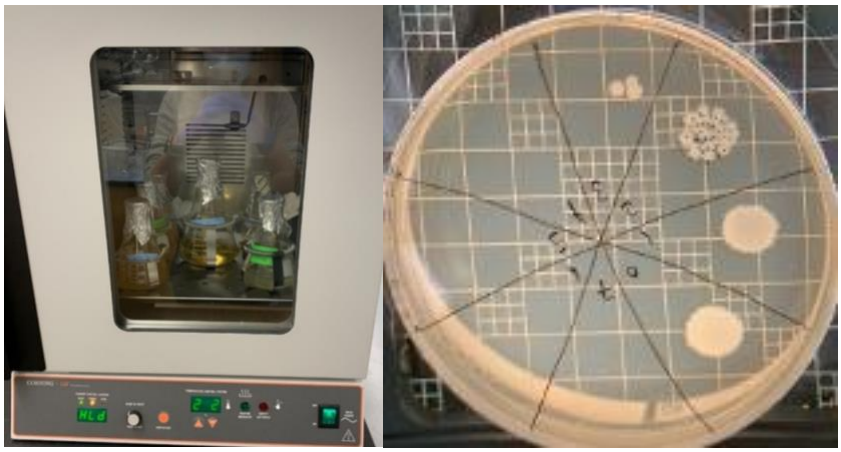

Figure 8.4 – (left) Shaking incubator with bacterial solution flasks, (right) agar plates for determining the bacterial counts.

8.1.2 Sporulation methods

In order to ease the sporulation process and reduce the required sporulation time with the long-term culturing, sporulation efficiency was investigated using two methods – through introduction of a sporulation solution for 48 hours, and through heat treatment. In the first sporulation method, bacterial cultures were grown in a media called 2xSG which consists of 16 g of nutrient broth, 2 g KCl, 0.5g $MgSO_4.7H_2O$, 1 mL 1 M $Ca(NO_3)_2$, 1 mL 0.1 M $MNCl_2.H_2O$, 1 mL 1 mM $FeSO_4$ and 2 mL filter sterilized glucose (50% weight/volume) per liter of DI water. First, nutrient broth, KCl and $MgSO_4.7H_2O$ were added to DI water and the mixture was autoclaved after adjusting the pH to 7 with addition of 1 M NaOH to kill any bacteria present in the solutions or flask. Other solutions

were autoclaved separately (except glucose) and after solutions were cooled to 55 °C, everything was combined. Bacteria cells were inoculated into the solutions, incubated at 25 and 30 °C temperatures, and plated at 24 and 48 hours.

In the second sporulation method bacterial cells were heat treated at low temperature. After growing bacteria in nutrient solutions for 24 or 48 hours, solutions were centrifuged, washed with sterile saline, and the centrifuged pellet was gently dried at 40 °C for 2-3 hours, until reaching the surface-dry condition, to induce sporulation. Following this process, dried pellets were stored in a 4 °C refrigerator until the time of use. Our study showed that cells can stay viable for at least 2-3 weeks in the refrigerator. At the time of use, the dried pellet is resuspended in fresh nutrient solution in order to utilize the dried cells. In both methods the number of spores was determined by pasteurizing the sample at 70 °C for 15 min to kill cells remaining in the vegetative state, then performing a serial dilution and count of cells after the standard 24-hour incubation period.

8.1.3 Determining the Biomineralization Ability of Bacteria Cells

A calibration curve was developed using known amounts of urea and urease to track the relationship between hydrolyzed urea and changes in conductivity utilizing the method described in Whiffin (2004) and DeMuynck (2008) (Figure 8.5). For the standard curve generation, 0.1, 0.2, 0.3, 0.35M urea stock solutions were prepared to get the complete hydrolysis of different concentrations of urea. 25 mL of each solution was transferred to 50 mL centrifuge tubes and 5 g of urease (Type IX urease from Jack Beans, Sigma-Aldrich) was added to each tube. After 24 hours of incubation at 37°C on a shaker at 120 rpm, conductivity of the samples was measured.

From the calibration curve a multiplication factor was determined from the inverse slope of the regression fitted to observations from the calibration study, and used to determine the quantity of urea hydrolyzed in samples based on solution conductivity changes over time (Eq. 3). Two replicates were performed and their average was calculated to determine the multiplication factor.

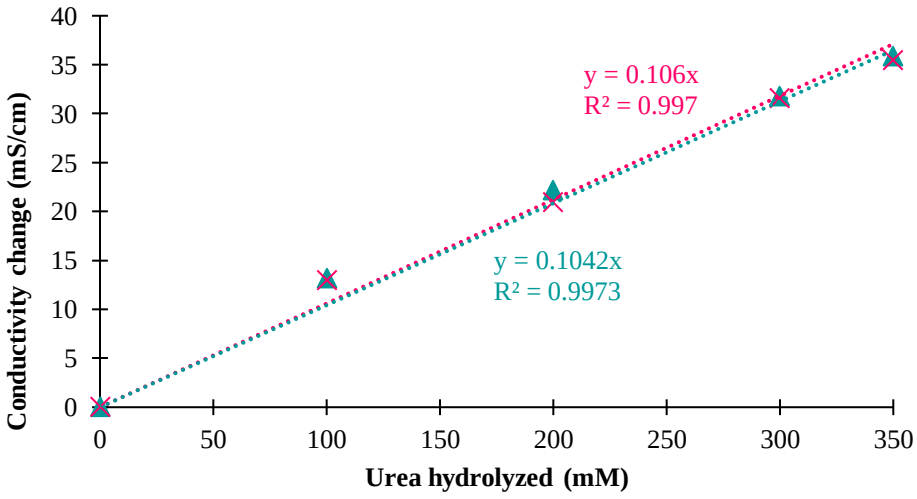

Figure 8.5 - Conductivity calibration curve, change in conductivity as a function of urea hydrolyzed.

$$Urea\ hydrolyzed\ (mM) = 9.50 \times\ conductivity\ change\ (mS/cm) \quad (3)$$

In order to obtain the ureolytic activity of the *B. subtilis* and soil bacteria, bacterial cells were grown in 0.5xNB nutrient solution, the solution was centrifuged, the centrifuge media was washed twice with sterile saline, and then the centrifuged cells were dried to induce sporulation. Dried cells were reinjected in NBUC solution containing 8 g nutrient broth, 10 g urea, 15 g calcium acetate per liter of DI water, and were re-grown for 48 hours to mimic the state of the bacteria just prior to inoculation into the concrete. After 48 hours, the solution was centrifuged and washed with sterile PBS, and centrifuged cells were injected in 50 mL urea + NaCl solution (urea 20 g/L and NaCl 8.5 g/L). The tubes were stored at 25 °C room temperature until the measurement time. At specific times, 15 mL of the solution was transferred into a tube and conductivity readings were taken at 0, 24 and 48 hours using a conductivity meter (Orion STAR A210).

To understand the calcium carbonate precipitation ability of the bacterial cultures, thermogravimetric analysis (TGA) and phase content analysis were conducted. For TGA testing, after growing centrifuged cells in NBUC solution, the solution was centrifuged, cells were dried at 40 °C, and thermal analysis of the samples was conducted using a Mettler-Toledo DSC/TGA. Approximately 30 mg samples were heated in 70 uL alumina crucible at 10 °C/min from 25 °C to 1000 °C in nitrogen. The quantity of calcium carbonate present in the samples was determined from the mass loss between 750 °C and 850 °C which is a known decomposition temperature of calcium carbonate.

X-ray diffraction (XRD) was utilized to determine the phase content of the bacterial samples. *B. subtilis* and soil aliquots were injected in urea and NB solutions separately and incubated for 24 hours with shaking conditions at 180 rpm. After 24 hours of incubation, calcium acetate was added to the solutions to induce biomineralization and the solutions were incubated for an additional 24 hours. Then, solutions were centrifuged, and cells were dried at 40 °C. Dried samples were placed in the XRD sample container and scanned with a BRUKER D8 XRD in flat plate reflection Johannsson mode, using a copper X-ray source producing CuKα radiation. The diffractometer was operated at 40 kV and 40 mA and scans were run from 20 to 60 degrees of 2θ with a step size of 0.02°. XRD scan mineralogy was assessed using Profex Open Source XRD and Rietveld Refinement software (Döbelin and Kleeberg 2015).

8.2 Task 2: DNA Sequencing Materials and Methods

8.2.1 Sample collection and growth, and study overview

Axenic (*B. subtilis*, type 3A1, strain 168) bacteria were obtained from the Ohio State University Bacillus Genetic Stock Center (BGSC); non-axenic soil cultures were collected from a residence in Columbus, Ohio.

For this study, *B. subtilis* cells were grown in Tryptic soy broth (TSB) and/or nutrient broth (NB) while soil bacteria were grown in nutrient broth (NB) and nutrient broth. Concentrations for nutrient broth included 1X manufacturer recommended strength or at half strength (0.5xNB). 1

mL frozen aliquots for *B. subtilis* and soil bacteria were prepared according to methods for aliquots preparation documented section 8.1.1 of this report. For the original soil aliquot, 2.5 g of soil was added into 50 mL NB solution and incubated for 24 hours at 25 °C with 180 rpm shaking.

For the storage life experiment, *B. subtilis* and soil bacteria were grown in TSB and 0.5x NB solutions for 24 hours, respectively. Then, the solutions were centrifuged and washed with 1x phosphate buffered saline (PBS). The centrifuged pellets were dried in a 40 °C oven. Then, dried pellets were reinjected to solutions on specific days (1,7 and 14 days for *B. subtilis*, or at 7 14 and 28 days for soil). After the storage time, samples were incubated for 24 hours (at 37 °C for *B. subtilis*, 25 °C for soil).

For the sporulation experiment, bacterial cultures were firstly grown in TSB for 24 hours and then suspended in 2xSG sporulation media for 24 hours.

Some samples were used to detect ureolytic activity of the *B. subtilis* and soil bacteria. For these samples, the bacterial cells were grown in 0.5xNB nutrient solution, the solution was centrifuged, the centrifuge media was washed twice with sterile saline, and then the centrifuged cells were dried to induce sporulation. Dried cells were reinjected in NBUC solution containing 8 g nutrient broth, 10 g urea, 15 g calcium acetate per liter of DI water, and were re-grown for 48 hours.

A summary of conditions for each sample analyzed by DNA sequencing to determine microbial communities is shown in Table 8.1.

Table 8.1 - Summarized information regarding growth conditions, DNA concentration and sequence reads for each B. subtilis and soil bacteria sample.

Barcode	Culture Type	Experiment	Media	Incubation time (days)	Incubation temp (°C)	Inoculum	DNA Concentration (ng/μL)	Sequence Reads
BC1	Axenic *B. subtilis*	Storage life	TSB	1	37	Dry	450	783875
BC2	Axenic *B. subtilis*	Storage life	TSB	7	37	Dry	387	618630
BC3	Axenic *B. subtilis*	Storage life	TSB	14	37	Dry	50	742745
BC5	Axenic *B. subtilis*	Sporulation	TSB	1-->2	37	Frozen aliquots	682	641225
BC6	Axenic *B. subtilis*	Nutrients	TSB	1	37	Frozen aliquots	524	819168
BC11a*	Axenic *B. subtilis*	Nutrients	0.5xNB	1	25	Frozen aliquots	511	658785
BC13b*	Axenic *B. subtilis*	Nutrients	0.5xNB	1	25	Frozen aliquots	37	11

BC4	Non-axenic Soil bacteria	Storage life	0.5xNB	7	25	Dry	587	781628
BC7	Non-axenic Soil bacteria	Storage life	0.5xNB	14	25	Dry	617	678716
BC8	Non-axenic Soil bacteria	Storage life	0.5xNB	28	25	Dry	825	192329
BC9a*	Non-axenic Soil bacteria	Nutrients	NB	1	25	Original soil aliquots	4500	583960
BC16b*	Non-axenic Soil bacteria	Nutrients	NB	1	25	Original soil aliquots	389	28
BC10a*	Non-axenic Soil bacteria	Nutrients	0.5xNB	1	25	Frozen aliquots	732	195594
BC12b*	Non-axenic Soil bacteria	Nutrients	0.5xNB	1	25	Frozen aliquots	623	610594
BC14	Non-axenic Soil bacteria	Urea test	NBUC solution	2	25	Dry	7000	807869
BC15	Non-axenic Soil bacteria	Urea test	NB	2	25	Dry	427	769324

* a and b represent replicates of an experiment condition.

The overall workflow for the microbial community analysis of B. sub and soil samples from sample preparation through DNA preparation, MinION sequencing through protein nanopores to detect electrical signals which are converted into DNA sequences and classified taxonomically using Oxford Technologies is depicted in Figure 8.6. Each step is described in more detail below.

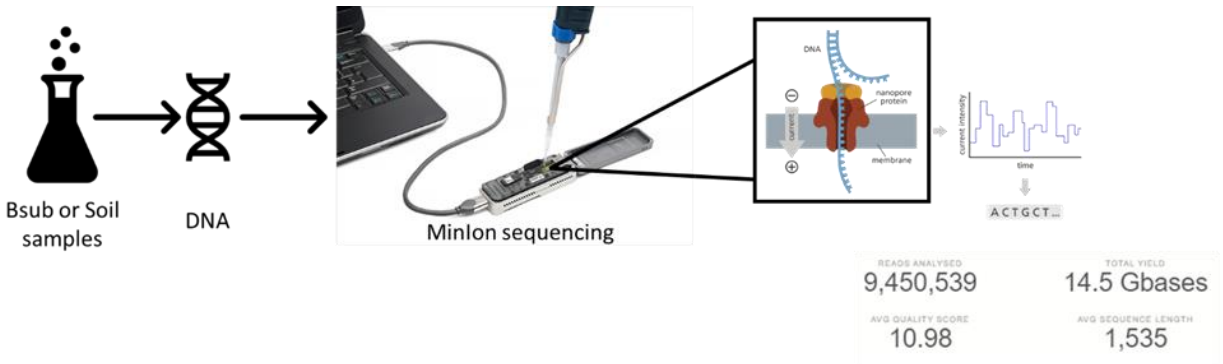

Figure 8.6 - After preparation of samples, *B. subtilis* or soil bacteria samples were subjected to DNA extraction and quantification before MinION sequencing, which passes DNA through protein nanopores to detect electrical signals which are converted into DNA sequences. Sequences are aligned to the 16S rRNA gene and classified taxonomically using Oxford Nanopore Technologies. For this study, more than 9 million sequences were analyzed (totalling more than 14.5 Gbases) with an average sequence length of 1,535 nucleotides (as expected based on our primers) and average quality of 10.98 (which is above average for MinIon sequencing).

8.2.2 DNA extraction and quantification

DNA from *B. subtilis* and soil bacteria under different growth conditions were extracted by phenol:chloroform:isoamyl alcohol reagents. DNA extraction tubes are made by 2X Buffer B reagent (5M sodium chloride (NaCl), 100X Tris-EDTA buffer (TE), 20% sodium dodecyl sulphate (SDS)), nuclease-free water, 0.1mm silica/zirconium beads and phenol:chloroform:isoamyl alcohol which was described by Hull et al. (2015), previously. DNA extraction tubes are stored at -80°C until needed. 500 µl liquid from samples were transferred to DNA extraction tubes and homogenized by bead beating for 2 minutes (BioSpec, Mini-Beadbeater-96). Following bead beating, tubes were centrifuged at 16,000 × g for 5 minutes to separate the solution into a phenol:chloroform:isoamyl alcohol phase, interphase, and upper aqueous phase. 450 µl aqueous supernatant was transferred to a 1.5 mL screw-cap tube. 10 µg glycogen, 200 µL 7.5M ammonium acetate, and 650 µL Isopropanol were added to tubes and mixed by vortex. Tubes were centrifuged at 16,000 × g for 30 minutes. Then supernatants were discarded, and pellets were formed at the bottom of the tubes. Pellets were resuspended in 800 µl 75% ethanol and centrifuged at 16,000 × g for 5 minutes. Supernatants were discarded and pellets were air dried for at least 2 hours at room temperature and then suspended in 200 µL filter sterilized 1X TE (10mM Tris, 1mM EDTA). DNA were stored at -80°C freezer for further quantification and sequencing. Qubit Fluorometer with 1X dsDNA High Sensitivity (HS) Assay kits were used to quantify the DNA concentration. 10 µl of standard 1 and standard 2 were mixed with 190 µl working solution buffer, then the Qubit Fluorometer was calibrated with the two standards. To quantify the sample concentration, 1µl sample was mixed with 199 µl working solution and then tested. Information of growth conditions and DNA concentration for *B. subtilis* and soil bacteria samples were listed in Table 8.1.

8.2.3 Full length 16S rRNA sequencing

For library preparation, DNA extracts were mixed with LongAmp Hot Start Taq 2X Matere Mix and 16 desired barcodes (16S Barcoding Kit 1- 24: SQK-16S024) and amplified by PCR using specific 16S primers (27F and 1492R) using the cycling conditions in Table 8.2. Then the prepared library was loaded into the flow cell (FLO-MIN106D) for sequencing in the device of MinION

Mk 1C according to the manufacturer's protocol. We did a hardware check first then we passed the flow cell check with 1300 available pores. Then we set different parameters to start sequence. We set the run length as 48 hours at -180 mV bias voltage. We selected fast basecalling and enabled barcoding. For quality control, we set the threshold of Qscore as 7 and all the fastq files with a score over 7 went to a pass folder which were used for downstream analysis.

Table 8.2 - Cycling conditions for 16s rRNA sequencing library preparation.

Stage	Time	Temperature	Cycle number
Initial denaturation	1 min	95 °C	1
Denaturation	20 secs	95 °C	25
Annealing	30 secs	55 °C	25
Extension	2 mins	65 °C	25
Final extension	5 mins	65 °C	1
Hold		4 °C	

8.2.4 Sequence analysis

Reads per sample after sequencing are shown in Table 8.1. Two samples (replicate of *B. subtilis* in 0.5xNB and replicate of original soil aliquot in NB) had very low sample coverage. The FASTQ 16S workflow in EPI2ME platform was used to analyze the nanopore data from the 16S rRNA sequencing to provide phylogenetic classification of bacterial groups in samples. The password-protected report is available here:https://epi2me.nanoporetech.com/report-293654. After the EPI2ME processing, 8885138 reads were classified with an 91% average accuracy. Also, the EPI2ME 16S output provided a summary table of the phylogenetic information. A lineage information for the abundance of bacteria at different taxa (genus and species) level was analyzed by following the tutorial (https://labs.epi2me.io/notebooks/Analysis_of_EPI2ME_16S_CSV_Output.html) and were visualized to bar plots in R with ggplot. Alpha diversity in different growth conditions were calculated by Shannon metrics and visualized in R with ggplot. The Shannon index takes into account the number of species living in a community (richness) and their relative abundance (evenness). The index indicates how diverse number and distribution of particular species are in a given sample. The higher the index, the more diverse the species are in the community. R scripts used for all analyses and figures are available at the end of Appendix D.

8.3 Task 2: Laboratory Paste and Mortar Experimental Materials and Methods

8.3.1 Materials

Calcium sulfoaluminate (CSA) cement sourced from Buzzi Unicem, ordinary portland cement (OPC) sourced from Lehigh Cement and fly ash sourced from a power plant in Conesville, Ohio

were used for all paste and mortar mixtures. Oxide contents of OPC and CSA cement and phase compositions of OPC, CSA cement and fly ash are shown in Table 8.3 and Table 8.4, respectively. Oxide and phase compositions were determined through Rietveld analysis of quantitative X-ray diffraction (QXRD) utilizing a rutile (Alfa Aesar, 99.9%) internal standard for OPC and CSA cement and zincite (Fisher, 99%) for fly ash. Deionized water (18 kOhm) was used for all paste mixtures and dechlorinated Columbus tap water was used for all mortar mixtures except when otherwise stated. Phosphate buffer saline (PBS) was used in one mix as a mixing solution in lieu of water. Dechlorinated water was obtained by leaving tap water in a beaker for at least 24 hours to allow for off-gassing of the chlorine.

Table 8.3 - Oxide compositions for CSA cement and OPC.

Oxides	CSA (wt%)	OPC (wt%)
SiO_2	7.99	20.3
Al_2O_3	26.64	4.97
Fe_2O_3	1.22	4.04
CaO	44.4	63.55
MgO	0.78	2.21
SO_3	14.43	2.97
K_2O	-	0.69
Na_2O	-	0.11
CO_2	1.55	1.49

Table 8.4 - Phase compositions for CSA cement, OPC and Fly ash.

Phases	CSA (wt%)	OPC (wt%)	Fly Ash (wt%)
Alite (C_3S)	-	54.61	-
Belite (C_2S)	21.09	17.35	-
Brownmillerite (C_4AF)	7.03	12.41	-
Aluminate (C_3A)	6.69	6.38	1.43
Calcite	2.49	-	-
Anhydrite	14.97	1.54	0.21
Hemihydrate	-	4.04	-
Gypsum	-	0.83	-
Ye'elimite	45.46	-	-
Quartz	0.23	-	7.69
Mullite	-	-	10.23
Periclase (MgO)	-	-	0.28
Maghemite	-	-	3.98
Amorphous	-	-	75.95

ASTM C109 (2016) graded Ottawa sand, certified to meet the ASTM C778 (2021) graded sand standard, was used as fine aggregate for all mortar cubes in this work. For incorporating bacteria

cells into the concrete, lightweight aggregate (LWA, from ARCOSA, Indiana) was used. 48-hour absorption capacity and specific gravity were calculated according to ASTM C1761 (2017) and C128 (2015), and determined as 15% and 1.42, respectively. Fineness modulus of LWA was calculated as 3.38. The particle size distributions of the sand and LWA are shown in Figure 8.7.

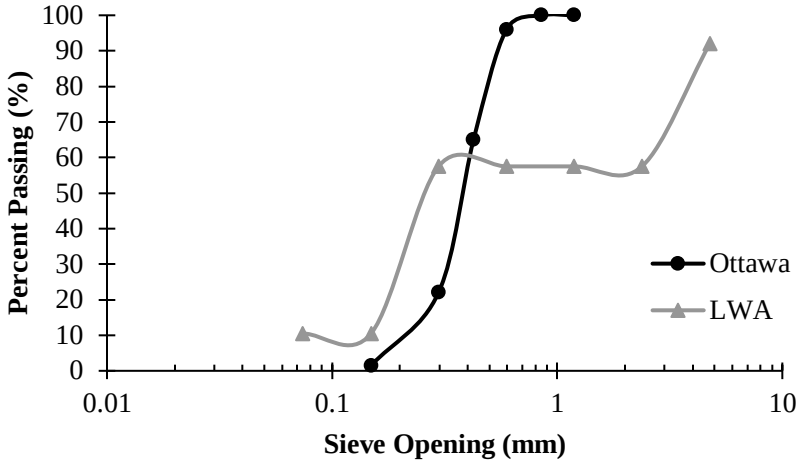

Figure 8.7 - Particle size distributions of sand and LWA.

Hydration kinetics, compressive strength development and crack remediation potential of bacterial and non-bacterial samples were tested to investigate the performance of bacteria in cement paste and mortars. All cement pastes and mortars were prepared at a w/c by mass of 0.45. In order to prevent compaction and workability issues for rapid hardening CSA cement, 1% citric acid (Alfa Aesar, 99%) by cement weight was used as a retardant in CSA mix.

8.3.2 Immobilization of Bacteria Cells

For all bacterial pastes and mortars, low temperature heat-treated and dried bacteria samples were immobilized into lightweight aggregate prior to incorporating the LWA and bacteria into mortar and concrete mixtures. To obtain dried bacteria, frozen aliquots of each type of bacteria were grown at specific conditions as determined based on optimal growth conditions. *B. subtilis* cells were grown at 37 ℃, in 0.5xNB solution, at pH 7, for 24 hours and soil bacteria cells were grown at 25 ℃, in 0.5xNB solution, at pH 7, for 48 hours. After the growth period, the solutions were centrifuged, and bacteria pellets were dried in an oven at 40 ℃. The dried bacteria were stored in a 4 ℃ refrigerator until immobilized into the lightweight aggregate for use in the cubes. The amount of bacteria was determined based on in order to have 10^7 CFU/mL spores initially in the mortar mixes.

To immobilize bacteria into the LWA, the dried bacteria pellets were dispersed in 0.5xNB solution and then LWA added to the solution. The solution was incubated for 24 hours, shaking at 180 rpm. After 24 hours, the solution was filtered to remove excess solution from the LWA and the LWA and bacteria were dried in a 40 ℃ oven for 2-3 hours until reaching saturated surface dry condition. For the non-bacterial control cubes, 15% tap water by weight of LWA was mixed with the LWA 48 hours before mixing to bring it saturated surface dry condition.

Before making samples, the bacterial LWA was enumerated to obtain accurate initial cell

concentrations in the cubes. Immobilized LWA was suspended in 0.5NB for 10 minutes, then sonicated for 2 minutes to release bound cells from the LWA into the NB solution, then allowed to settle for 10 minutes. The supernatant was extracted, one mL of sample was serially diluted in test tubes containing 1X PBS and plated on nutrient broth – agar plates. Plates were incubated at 37 °C for 24 hours and after 24 hours viable cell counts were obtained. To obtain spores, another 1 mL sample was pasteurized, killing non-sporulated bacteria, at 70 °C for 15 minutes and the same plating process was performed. For all bacterial paste and mortar samples, initial *B. subtilis* and soil bacteria vegetative cell concentrations were 10^8 CFU/mL and spore concentrations were 10^7 CFU/mL for *B. subtilis* and 10^6 for soil.

8.3.3 Bacterial Cement Pastes

Isothermal calorimetry was used to investigate effects of bacteria on cement hydration kinetics up to 48 hours. Cement pastes for isothermal calorimetry were prepared with a w/c of 0.45 using the procedures outlined in ASTM C1679 (2019). The mixtures tested are shown in Table 8.5. Bacteria cells were immobilized into LWA and LWA was enumerated prior to mixing, as described previously.

Table 8.5 – Mixtures tested for isothermal calorimetry.

	Cement only	LWA	LWA+*B. subtilis* bacteria	LWA+soil bacteria
OPC	x	x	x	x
CSA	x	x	x	x
OPC (80%) Fly Ash (20%)	x	x	x	x

Approximately 25 g pastes were mixed with a 6-speed hand mixer from Hamilton Beach at the lowest speed for 30 s and at the highest speed for 90 s. After mixing, 5g of each paste was placed into a glass ampoule, sealed, and inserted in the calorimeter, with heat evolution tracked in a TAM AIR calorimeter for 48 hours. All samples were placed into the calorimeter within 2-3 minutes of water-cement contact. The temperature was maintained at 25°C throughout the testing and TAM AIR software was used to collect data to a computer. All of the samples were tested in duplicate. Qualitative data analysis was performed by examining how the shape and the time to occurrence of main heat release peak evolved.

8.3.4 Bacterial Mortar Cubes

Bacterial and non-bacterial cement mortar samples were cast to evaluate the effect of fly ash, CSA cement, lightweight aggregate (LWA), mixing solution compositions (tap water and PBS) and different curing methods (ponding and spraying) on the performance of the mortars. Additionally, to evaluate the environmental conditions, one set of samples was cured at high temperature and low temperature and one set was exposed to concentrated salt solution for 7 days. LWA was used as the immobilization source for bacterial samples. Compositions of samples are shown in Table 8.6.

Two-inch mortar cubes with and without bacteria were prepared according to ASTM C305 (2016). The sand to cement ratio was 1:2.75 and LWA was replaced by 10% of sand in specific mixes. In

non-LWA mixture (OPC-FA-NLW), the immobilization procedure was applied to 10% of sand instead of LWA using the same conditioning variables (time, drying temperature, dosing of bacteria relative to sand mass). First, water was mixed with cement with 3-speed Hobart mixer for 30s at the lowest speed. After 30s, sand was added to cement paste and mixed for 30s at the same speed following by mixing 30s at the highest speed. Mixture was rested for 90s and then mixed for 60s. After placing mortars in the molds, molds were cured at between 22-23 °C room temperature, 100% relative humidity (RH) and demolded after 24 hours 1-day samples were tested right after the molds were removed. Curing methods were applied starting from day 1 and spray cured samples were kept in the lab environment, to simulate relevant environmental conditions for larger-scale field samples, at room temperature, until test day. Temperature and relative humidity of the laboratory was not controlled and varied between 40-60% RH and 20-25 °C. Spray curing was used as the regular curing method for five samples and one sample (OPC-FA-PO) was cured by ponding. For spray curing, samples were sprayed daily with nutrient broth, urea, calcium acetate (NBUC) solution until all surfaces of samples were covered with the solution. For ponding, samples were submerged in NBUC solution for 2 days and then followed by air drying for 2 days. Both curing methods were applied for 28 days and then samples were kept in the lab environment, unless otherwise stated.

To assess the effect of varying curing temperatures on the bacteria viability and performance, after demolding the cubes, the low temperature (OPC-FA-LT) samples were stored in a 7 ℃ refrigerator for 14 days. The high temperature samples (OPC-FA-HT) were placed in a 40 ℃ oven for approximately 6 hours each day for the first 14 days after they were made. Both sets of cubes were sprayed with NBUC solution each day for 28 days to continue the curing process. For salt exposure, OPC-FA-SA mixtures were cured for 28 days with spray curing and then the samples were immersed for 7 days into 23% NaCl solution. After 7 days of the exposure, samples were taken out from the salt solution and spray curing was applied through the end of 63 days.

Table 8.6 - Compositions of mortar cube samples.

Samples	Cementitious Materials	Immobilization	Mixing Solution	Curing
OPC-FA	OPC (80%) Fly ash (20%)	LWA (bacterial or non-bacterial)	Tap water	Spraying
OPC	OPC	LWA (bacterial or non-bacterial)	Tap water	Spraying
CSA	CSA	LWA (bacterial or non-bacterial)	Tap water	Spraying
OPC-FA-NLW	OPC (80%) Fly ash (20%)	Sand (bacterial or non-bacterial)	Tap water	Spraying
OPC-FA- PO	OPC (80%) Fly ash (20%)	LWA (bacterial or non-bacterial)	Tap water	2-day ponding, 2-day air drying
OPC-FA-PBS	OPC (80%) Fly ash (20%)	LWA (bacterial or non-bacterial)	PBS	Spraying
OPC-FA-LT	OPC (80%) Fly ash (20%)	LWA (bacterial or non-bacterial)	Tap water	Spraying, samples kept at 7 °C for 14 days

OPC-FA-HT	OPC (80%) Fly ash (20%)	LWA (bacterial or non-bacterial)	Tap water	Spraying, samples kept at 40 °C for 6 hours/day for 14 days
OPC-FA-SA	OPC (80%) Fly ash (20%)	LWA (bacterial or non-bacterial)	Tap water	Spraying, samples exposed to salt solution after 28 days of hydration for 7 days

8.3.5 Mortar Testing

Bulk electrical resistivity test was performed with triplicate 2" mortar cube samples to track porosity evolution in each sample. Electrical resistivity is affected by sample moisture conditions, with more saturated samples having lower resistivity (Sengul 2014). Additionally, pore solution chemistry can also impact the resistivity readings (Azarsa and Gupta 2017). To help normalize saturation levels, prior to resistivity measurements cubes were placed into a room with 100% RH at 72-75 °F for 1 day. For measurement, saturated surface dry mortar cubes were placed between parallel metal plates with moist sponge contacts connected to an electrical resistivity meter (Proceq Resipod). Readings were allowed to stabilize for 10-15 seconds and the measurement was recorded.

Compressive strengths of mortars were conducted with triplicate samples at 1, 3, 7, 28, 56 and 90 days according to the ASTM C109 (2016). The cubes were placed into a Forney compression machine (250,000 lbf capacity) using a 75% break percentage, 75 psi/s ramp rate and a pre-load of 100 lbf.

Viable *B. subtilis* and soil cells were enumerated with duplicate tests via MPN analysis at 1, 3, 7, 28, 56 and 90 days after casting. The MPN method provides an estimate of the number of cells in the vegetative state in the sample. After testing for compressive strength, mortar cube samples were crushed to 3-5 mm particles with a sterile ceramic mortar and pestle. 30 g of crushed sample was then suspended in 45 mL fresh, sterilized (by autoclaving at 121 °C for 45 minutes) 0.5xNB solution at pH 7 for 10 minutes. The suspension was sonicated for 2 minutes to release bound cells from the sample and allowed to settle for 10 minutes. Then the supernatant was extracted, and triplicate serial dilutions were prepared with 0.5NB in test tubes. The tubes were incubated at 37 ℃ for 48 hours and the growth of cells in the test tubes was observed based on the solution turbidity. Turbid samples were recorded as positive tubes and non-turbid samples as negative tubes. The positive number of tubes were entered to the EPA's MPN calculator to determine the bacterial count in the cubes (US EPA, 2022).

Sorptivity testing was conducted according to modified ASTM C1585 (2020). At 7, and 28 days, triplicates of samples were dried in oven at 60 °C until constant mass (approximately for 48 hours). 60 °C was selected in order to prevent microstructural degradation that can occur at higher temperatures. After drying in the oven, 4 sides of a cube were healed with a water-proof polymeric coating (Conheal, CS-1800) to ensure uni-directional water infiltration. The top and bottom sides of the cube were not coated. The top surface of the cube, which was not exposed to water, was covered with plastic wrap to prevent water evaporation. The cubes were then immersed in water with the water level not more than 5 mm from the bottom of the cube. The quantity of water absorbed in specified time intervals per ASTM C1585 (2020) was measured by weighing the specimen using a weighing balance with a precision of 0.1 g. Before weighing samples, excess surface water was removed with a paper towel. The mass of each cube was measured at 1, 5, 10,

20, and 30 minutes, once every hour for 6 hours, and once a day for 7 days. The measurements up to 1 day were indicated as initial absorption and measurements after 1 day were attributed to secondary absorption. The absorption (I) was calculated by dividing the change in sample mass at each time by the product of the cross-sectional area of the sample and the density of the water. Initial water absorption was calculated by finding the slope of the line that is the best fit to I versus square root of time from 1 minutes to 6 hours. Secondary water absorption was calculated using by the same procedure from 1 days to 7 days.

8.3.6 Self-healing Investigation of Bacterial Mortar Beams

To compare the self-healing ability of bacterial and non-bacterial samples, mortar beams were cast using mixtures of OPC and fly ash, OPC, and CSA. Seven sample preparation procedures were used to compare changes in the mortar bars:

1) OPC mixture cured by spray curing;
2) OPC-FA, OPC and fly ash mixture cured by spray curing;
3) CSA mixture cured by spraying;
4) OPC-FA-PO, OPC and fly ash mixture cured by ponding;
5) OPC-FA-LT, OPC and fly ash mixture cured at 7 °C for 14 days;
6) OPC-FA-LT, OPC and fly ash mixture cured at 40 °C for 6 hours/day for 14 days;
7) OPC-FA-SA, OPC and fly ash mixture exposed to salt solution for 7 days after 28 days of hydration.

Each of the mixtures was cast with no bacteria, with *B. Subtilis* or with soil bacteria. For each mixture, with or without bacteria, three cracking and curing regimes were used: CC - cracked at 14 days and cured until the end of healing period; U - uncracked and cured until the end of healing period (to assess changes in UPV due to additional curing and potential precipitation from the curing solution); NC - cracked at 14 days, but without additional curing applied through the end of healing period. The same procedures were performed to grow bacteria cells, immobilize them into LWA and enumerate LWA as discussed previously.

Mortar beams (40 mm x 40 mm x 160 mm) with and without bacteria were prepared in triplicates (total of 9 beams for each mixture and each bacterial condition (no bacteria, *B. Subtilis*, or soil bacteria) – 6 beams were cracked and 3 remained uncracked). Mortars were mixed according to ASTM C305 (2016). Amounts of cement, water, sand, and LWA were held constant across all mixtures, as detailed in the Section 7.2.2.3 but 12-mm micro synthetic fibers were added to the mortar at a rate of 6 g/500 g of cement to provide flexural resistance during crack initiation. After placing mortars in the molds, molds were cured at between 72-75 °F, 100% RH and demolded after 24 hours. Spray curing or pond curing methods were applied starting from day 1.

At 14 days after mixing, the samples were removed from the curing environment and samples were cracked by flexural loading using displacement-controlled machine (0.05 mm/sec). The crack

width of the samples ranged from 0.4 – 0.5 mm. One set of samples (U) from each variable were not cracked to be used as a negative control. After the formation of cracks, one set of cracked samples (C) was cured by spraying or ponding and another set of cracked samples (NC) was not cured through the end of healing period. OPC samples were observed for 6 weeks for crack closure performance since they did not have additional crack healing after 4 weeks, whereas all other samples were observed for 8 weeks due to having slower healing than OPC samples. OPC-FA-PO samples were cast to compare the efficiency of spraying and ponding curing methods on the crack healing capacity of the samples. OPC-FA-PO samples were cured by 2-day ponding and 2-day air drying starting from demolding of the beams. Images of the cracks were taken weekly with a digital camera (Panasonic Lumix, DC-FZ20) starting from right after crack formation and through the end of healing period. Images were taken at Macro Zoom settings by zooming in 3x and using 1 mm spaced ruler for scaling. Lighting conditions were adjusted manually.

In order to evaluate the crack healing performance, ultrasonic pulse velocity (UPV) measurements were conducted according to ASTM C597 (2016). The test was performed by measuring traverse time of an electrical pulse generated by an electro-acoustical transducer across the longest dimension of the mortar beams using a UPV meter (James Instruments, V-meter). Cracks and porosity present in the concrete results in longer traverse time, allowing UPV to indicate the quality of the concrete or mortar samples. It has been suggested that good quality mortar should have ultrasonic pulse velocities greater than 4000 m/s (Neville and Brooks 1987).

UPV measurements were taken weekly on air-dry sample starting from immediately following crack formation through the end of healing period. Prior to the measurements, petroleum jelly was applied onto the transducers to create good contact between the transducer and beam. The frequency of the UPV meter was set to 500 kHz with high voltage. UPV readings were measured by pressing the transducers on each end of the beams and recording the traverse time. After obtaining traverse time readings, pulse velocity was calculated by dividing the length of the beam (in meters) by the traverse time (in seconds). UPV readings of the samples were obtained in triplicates.

Water absorption was measured for the cracked and/or healed area on each beam after the healing processes of the mortar bar samples were completed. Testing was conducted according to modified ASTM C1585 (2020). Triplicate samples were dried in an oven at a temperature of 60 °C to a constant mass (for approximately 48 hours). After drying, a 40 x 40 mm area around the cracked zone was selected and all other surfaces of the beams were sealed with non-absorbent coating to ensure unidirectional water entrance. The beams were immersed in water with the water level in contact, but not more than 5 mm above the cracked surface of the beam. The absorption rate was determined using the same measurement and analysis procedures as detailed previously for the sorptivity test.

After the completion of the absorption test, beam samples were broken into two pieces through the cracked zone of the healed bacterial samples. Pieces smaller than 1 cm^3, were collected from the cracked surface to investigate under scanning electron microscopy (SEM). SEM was used to characterize the precipitated material and to identify microstructural indications of the bacteria cells. Broken crack-healed mortar samples were taped on aluminum studs with carbon tapes, then coated with gold to create a conductive surface and prevent charging. SEM imaging was performed using a scanning electron microscope (FEI Apreo) with low vacuum mode at an accelerating

voltage of 5 kV and working distance of 10±2 mm.

Additional ~40 mg powders were obtained from the surface of the crack zones of the crack-healed mortar bars and thermogravimetric analysis (TGA) was conducted to quantify calcium carbonate is present in the samples using a Mettler-Toledo DSC/TGA, heating samples in 70 µL alumina crucible at 10 ℃/min from 25 ℃ to 1000 ℃ in nitrogen. The quantity of calcium carbonate present in the samples was determined from the mass loss between 600 °C and 800 °C which is a known decomposition temperature of calcium carbonate.

8.4 Task 3 - Concrete Placement Experimental Methods

8.4.1 Materials

OPC (Lehigh Cement) and fly ash (Reclaimed ash, Conesville, Ohio) were used for all concrete mixtures. Oxide contents and phase compositions of OPC and fly ash are shown in the previous section. Dechlorinated Columbus tap water was used for all concrete mixtures by adding 0.2 mL of the 0.1 N sodium thiosulfate solution per 1 L of water for dechlorination.

The concrete sand used was obtained commercially from Columbus Builder's Supply and was used as the fine aggregate in all batches of the concrete. Specific gravity and fineness modulus of sand were determined as 2.5 and 2.56, respectively. An ODOT approved #67 coarse aggregate, specific gravity of 2.67, was supplied by United Aggregates. For incorporating bacteria cells into the concrete lightweight aggregate (LWA) was obtained from ARCOSA (Indiana). 48-hour absorption capacity and specific gravity were calculated according to ASTM C1761 (2017) and C128 (2015), respectively, and determined as 15% and 1.42, respectively. Fineness modulus of LWA was calculated as 3.38.

8.4.2 Slab construction and test methods

The concrete mixture design utilized for all concrete mixtures is shown in Table 8.7. In all concrete mixtures 678 lb/yd^3 of total cementitious materials, 1236 lb/yd^3 of coarse aggregate and 1366 lb/yd^3 of fine aggregate were used (Table 8.7). The water-to-cement ratio was kept at 0.45 but water dosage was adjusted to account for the aggregate absorption capacities and moisture contents. Fly ash was substituted for OPC at a rate of 20% of the cement content and LWA replaced 10% of the fine aggregate. Additions of bacteria were designed to provide 10^6 CFU of bacteria spores/mL of mixing water. Air entraining admixture and superplasticizer were dosed to provide 7±2% air content and 4±1" slump. All mixtures were able to achieve these values.

Table 8.7- Concrete Mixture Design.

	Component Mass	
	lbs/yd^3	kg/m^3
Water	305	181
Cement	508	302
Fly Ash	169	101

Coarse Aggregate	1236	733
Fine Aggregate	1243	738
Lightweight Aggregate	123	73

For growing the bacteria for use in the concrete, frozen aliquots of each type of bacteria were grown at specific conditions as determined based on optimal growth conditions (see Task 1 results). *B. subtilis* cells were grown at 37 ℃, in 0.5xNB solution, at pH 7, for 24 hours and soil bacteria cells were grown at 25 ℃, in 0.5xNB solution, at pH 7, for 48 hours. After the growth period, 1L solutions were centrifuged using high-capacity centrifuge in order to separate the bacteria from the solution, then the bacteria pellets were washed with PBS and dried in an oven at 40 ℃. The dried bacteria were stored in a 4 ℃ refrigerator until immobilization into the lightweight aggregate for use in the concrete.

To immobilize the bacteria into the LWA, the dried *B. subtilis* and soil bacteria pellets were dispersed into dechlorinated tap water. Water volume for the immobilization procedure (15% of the mass of the LWA) was determined based on the 48-hour absorption of the LWA weight in order to ensure full absorption of the bacteria into the LWA. The quantity of bacteria mixed into the LWA was chosen to ensure a quantity of 10^6 CFU would be present in the mixing water of the concrete mixture. The water-bacteria mixtures were allowed to absorb for 48 hours. Before making concrete samples, bacterial LWA was enumerated to obtain the exact amount of initial cell concentration in the cubes as detailed in section 8.3.2. Initial *B. subtilis* and soil bacteria vegetative cell concentrations were 10^8 CFU/mL and spore concentrations were $2x10^6$ CFU/mL for *B. subtilis* and $5x10^5$ CFU/mL for soil bacteria in bacterial mixtures.

Bacterial and non-bacterial, 9 ft^3 concrete slabs (approximate dimensions: 6 ’x 3’ x 6”) were mixed using a 6 ft^3 rotating drum mixer (location is shown in Figure 8.8 and slabs are shown in Figure 8.9). The aggregate (except the LWA) and 10% of the mixing water was added and homogenized for approximately two minutes prior to adding the cement, fly ash, remaining mixing water, and the LWA (with or without bacteria). The mixture was mixed for three minutes, allowed to rest for three minutes, and then mixed for an additional two minutes. Slump and air content of the mixture were checked, and the mixture was remixed for an additional two minutes if adjustments were needed to meet slump and air content targets. 4 in. by 8 in. cylinders and 3 in. x 3 in. x 11.25 in. shrinkage beams were cast simultaneously with the slabs and allowed to cure under the same exposure conditions for 24 hours before demolding. The slabs were placed between 07:00 and 13:00 hours, with temperatures on the day of casting ranging from approximately 75 °F to 85 °F during casting under partly cloudy conditions. The slabs included #10 mesh reinforcement, located at approximately the center of the slab depth. The slabs were consolidated using a vibrator, hand troweled, and broom finished. No curing or protection from sun or wind was applied to the slabs during the first 24 hours in order to encourage cracking resulting from bleed water evaporation and plastic shrinkage (although no plastic shrinkage cracking occurred).

Following demolding, cylinders and beams were moved to lab and kept in the lab at 70-75 °F room temperature and 45-55% relative humidity, to mimic outdoor conditions, until the test day. For curing, one set of control and bacterial slabs, beams, and cylinders were sprayed daily with a nutrient broth, urea, and calcium acetate (NBUC) curing solution from days 1 to 28, until all surfaces of samples were covered with the solution. The other set of control samples were not

cured to differentiate between changes in the control resulting from additional curing with the nutrient solution, and those resulting from the bacteria.

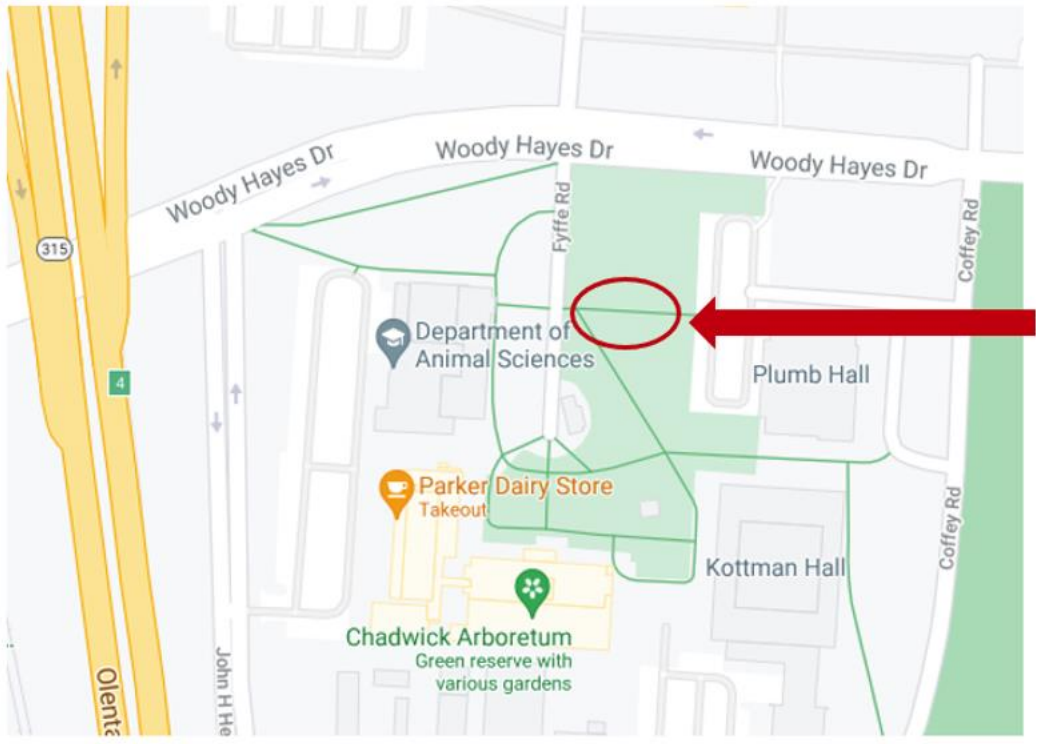

Figure 8.8 - Location of the installed concrete slabs on the Ohio State University campus.

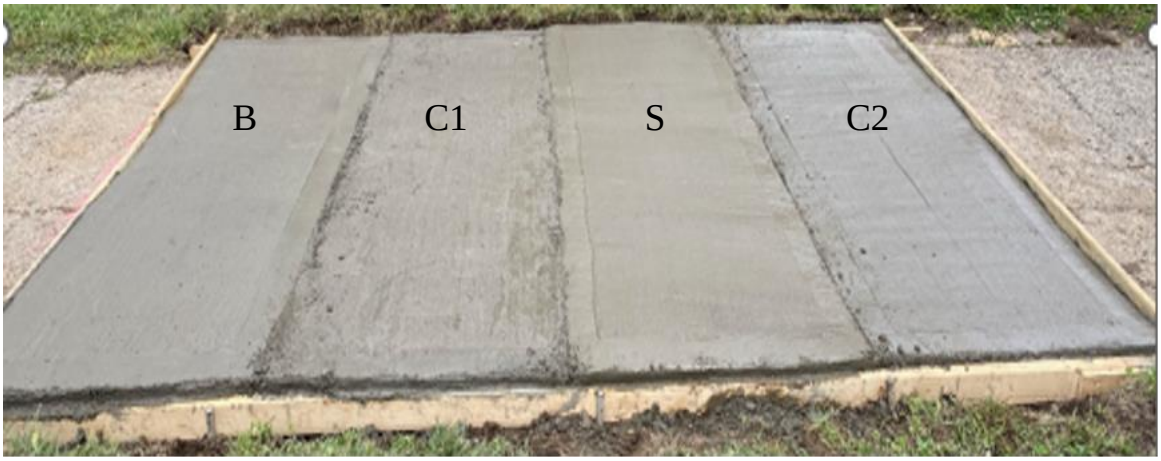

Figure 8.9 - Installed concrete slabs. B: Concrete with *B. subtilis* bacteria, C1: control mixture concrete, cured using the same methods as the bacterial slabs, S: concrete with soil bacteria, C2: control concrete, no curing solution applied.

Electrical resistivity was measured on duplicate samples at 1, 7, 28, 56, 90 and 180 days to investigate the ability of resistivity testing to track changes in the porosity of the sample. Prior to testing, cylinders were placed in a bucket of tap water for 1 hour in order to help normalize sample

saturation levels. Readings were obtained from four sides of saturated surface dry cylinders using a resistivity meter (Resipod proceq, Gilson).

Compressive strengths of cylinders were tested in triplicate samples at 1, 7, 28, 56, 90 and 180 days according to the ASTM C109 (2016). The cylinders were placed into a Forney compression machine (250,000 lbf capacity) using a 75% break percentage, 75 psi/s ramp rate and a pre-load of 100 lbf.

3 in. x 3 in. x 11.25 in. shrinkage beams were prepared to evaluate the length change of the bacterial and control beams. After demolding beams, samples were moved to a room with 50 ± 5% relative humidity. Dimensional change was tracked on triplicate of bars at 1, 4, 7, 28, 56, 90, and 180 days based on ASTM C157 (2014). Length change was calculated by subtracting the initial shrinkage reading from the reading obtained from a sample at any age and dividing this value by the gage length.

In order to analyze durability of the bacterial samples against freeze and thaw, 3 in. x 4 in. x 16 in. freeze-thaw beams were cast. After curing for 35 days, samples were frozen until the time of testing. After thawing and initial testing, samples were weighed and dynamic modulus was tested weekly (36 cycles per week) until reaching 500 cycles (ASTM C666 2015). Percent change of the dynamic modulus with respect to the initial measurements was calculated to determine the loss in the dynamic modulus.

9 Appendix C: Task 1 – Bacterial Source Growth Optimization Research Findings and Conclusions

9.1 Non-axenic Bacterial Source Regrowth

Non-axenic samples were grown at 25 °C in 1xNB solution at pH 7 and pH 9 for 24 hours. Figures 9.1 and 9.2 show growth curves of spent digestate sample (SD), distillery waste-water sample (DW) and soil sample (S) grown at pH 7 and pH 9, respectively. At both pH values, DW sample did not display any cell viability at 0 hours nor 24 hours. SD was able to reach minimum acceptable vegetative cell counts (10^8 CFU/mL), but did not successfully sporulate (a requirement of bacteria for survival in the harsh concrete environment). In addition to poor sporulation, lack of information about bacteria types present, and potential pathogenicity of the spent digestate sample, led to discontinued use of the sample. The bacteria obtained from the soil was the most successful of the non-axenic samples, reaching a vegetative cell concentration of 10^9 CFU/mL at both pH values, and able to form spores. Based on this, soil bacteria were selected as the non-axenic bacteria culture for further testing.

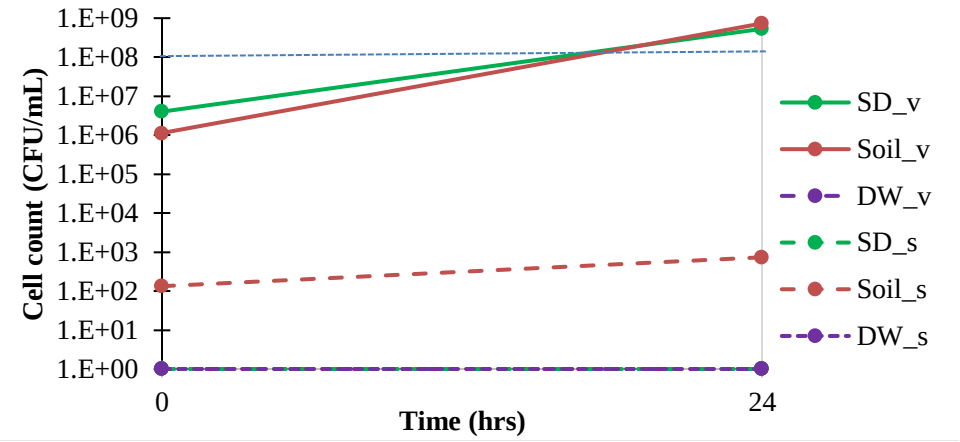

Figure 9.1 - Growth curve evolution of spent digestate (SD), distillery waste-water (DW) and soil samples from 0hr to 24hr in 1xNB at pH 7 (s: spores, v: vegetative cells) (Blue line indicates the minimum acceptable vegetative cell count based on the literature).

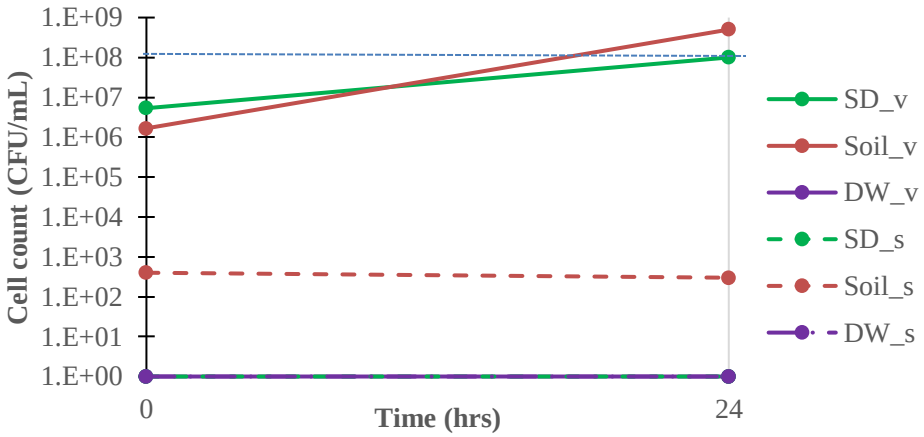

Figure 9.2 - Growth curve evolution of spent digestate (SD), distillery waste-water (DW) and soil samples

from 0hr to 24hr in 1xNB at pH 9 (s: spores, v: vegetative cells) (Blue line indicates the minimum acceptable vegetative cell count based on the literature).

9.2 Long-term growth curves

In order to determine the time required for bacterial samples to reach maximum cell concentrations, growth curves were generated by growing 1 mL bacteria samples in 1xNB solutions for 5 days. 1 mL of sample was obtained at each time interval, serially diluted in test tubes and plated on agar plates. Figure 9.3 shows the growth curves of *B. subtilis* at pH 7 and soil at pH 7. In both the *B. subtilis* and soil bacteria samples cells reached the maximum concentration at or before 48 hours. After 48 hours, a stationary growth period continued up to five days of incubation. Stationary growth occurs when the growth rate of microorganisms drops to zero (the number of cells being generated and number of cells dying is equal).

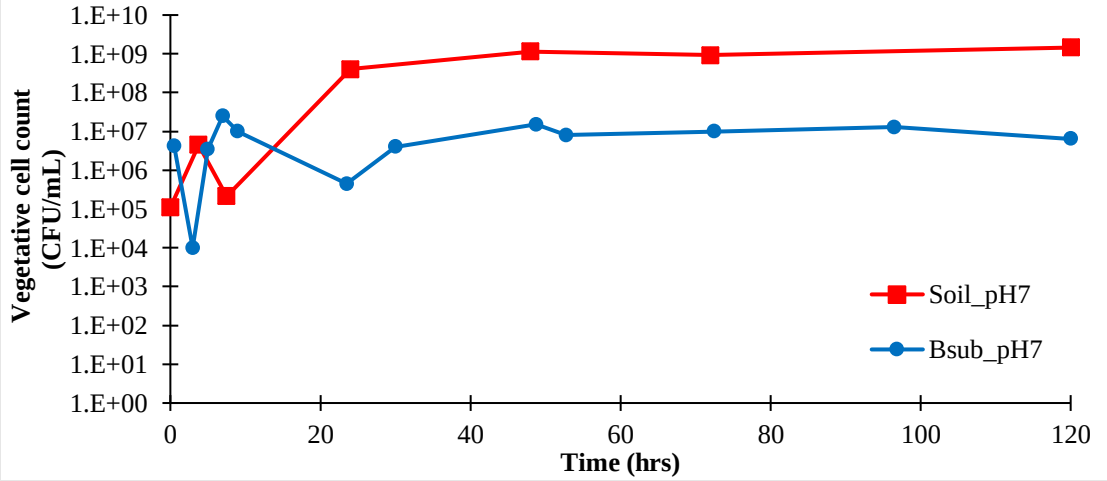

Figure 9.3 - Long term growth of *B. subtilis* and soil samples from 0hr to 120hr in 1xNB.

9.3 Effect of environmental variables on microorganism growth

The influence of temperature on bacterial growth was tracked using solutions incubated at 10, 25 and 37 °C in 1xNB solution at pH 7. Figures 9.4 and 9.5 show growth curves of both vegetative and spore counts of *B. subtilis* and soil, respectively. Samples are abbreviated using the form: xT_v/s, where x is the bacteria type (BS for *B. subtilis* and S for soil), T is the temperature and v/s is indicating vegetative cells (v) or spores (s). Both *B. subtilis* and soil reached 10^8-10^9 CFU/mL vegetative cell counts at 25 °C and 37 °C, with soil bacteria having slightly higher cell count than *B. subtilis*.

Additionally, vegetative soil cells demonstrated ability to grow in cold temperatures (10 °C), while *B. subtilis* cell counts at 10 °C dropped slightly, evidencing higher cell death rates than reproduction rates. *B. subtilis* cells incubated at 10 °C were also unable to form spores. Soil bacteria successfully formed spores at all three temperatures, but generated maximum spore count at 37 °C. From these results, it was concluded that both *B. subtilis* and soil bacteria can be grown either in 25 °C or 37 °C conditions. Use of room temperature conditions, which do not require

incubated environmental chambers, may simplify production of bacterial solutions in unconditioned environments during mild and warm weather (25 °C and 37 °C).

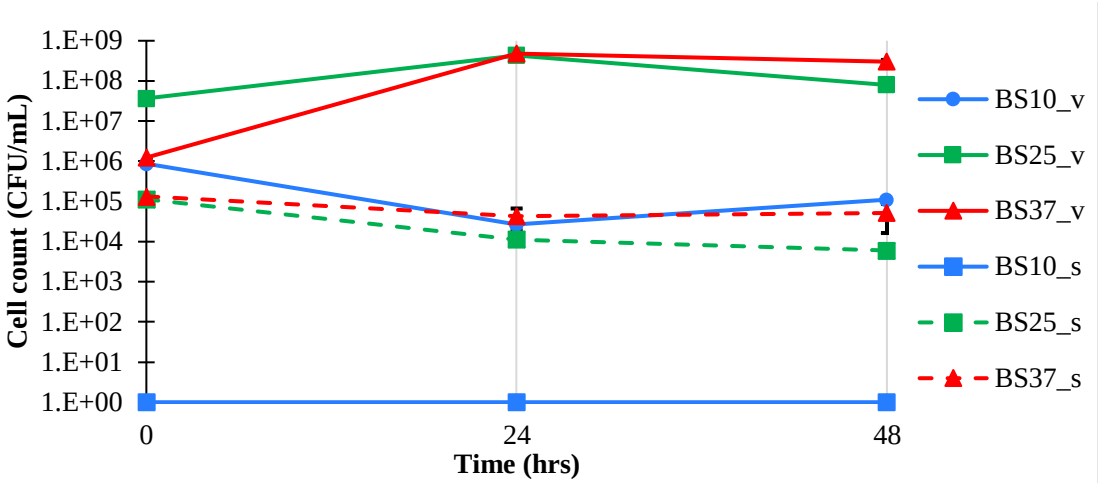

Figure 9.4 - Growth curve evolution of B. subtilis from 0 to 48hr under different temperatures in 1xNB at pH 7. Error bars represent standard deviation of three replicates.

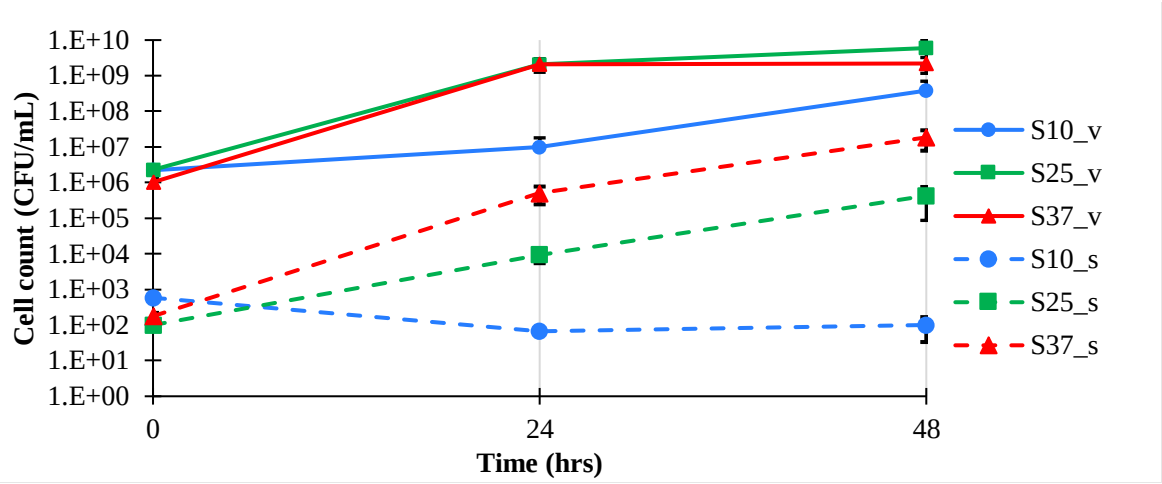

Figure 9.5 - Growth curve evolution of soil from 0hr to 48hr under different temperatures in 1xNB at pH 7. Error bars represent standard deviation of three replicates.

Temperature and nutrient solution concentration were kept consistent at 25 °C and 1xNB, respectively, in order to understand the influence of pH change on the bacterial growth. It was theorized that bacteria cultured in higher pH solutions might better survive in the high pH concrete pore solution. Figures 9.6 and 9.7 display growth curves of both vegetative and spore counts of *B. subtilis* and soil at pH 7 and 9. Samples are abbreviated using the form: xP_v/s, where x is the bacteria type (BS for *B. subtilis* and S for soil), P is the pH and v/s is indicating vegetative cells or spores.

At pH 9 the *B. subtilis* vegetative count was reduced by an order of magnitude compared to initial cell count present in the original solution, and by more than 3 orders of magnitude compared to the sample maintained at pH 7. However, the sample experienced rapid growth between 24 and 48

hours, reaching cell numbers similar to in the pH 7 sample. Soil did not show any significant difference in growth at pH 9 in comparison to pH 7 for both vegetative cells and spores and it reached one order of magnitude higher cell count than *B. subtilis*. Although, both bacteria can survive at higher pH conditions, the growth is initially delayed in the *B. subtilis* samples and pH 9 was not successful at sporulation. Based on this, to minimize the time required to maximize the numbers of cells, it was decided to grow the *B. subtilis* at a neutral pH for 24 hrs.

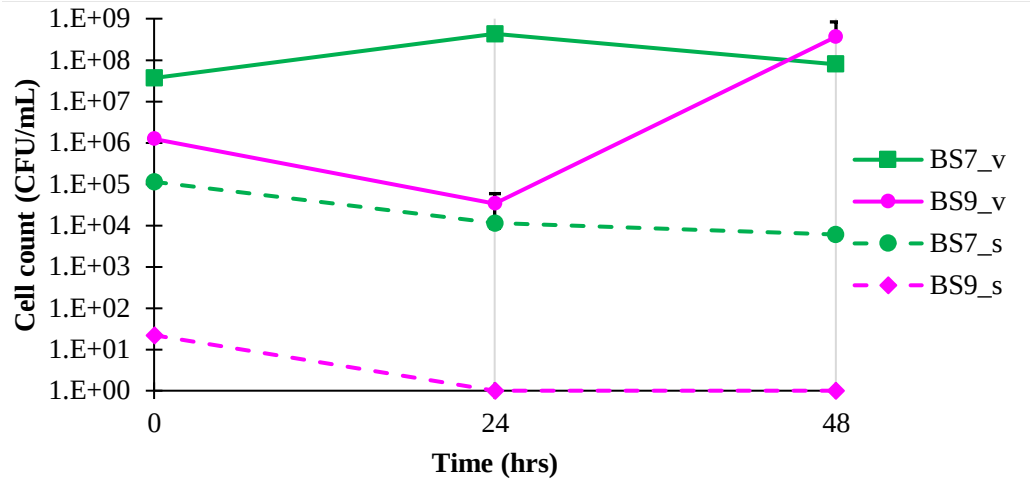

Figure 9.6 - Growth curve evolution of *B. subtilis* from 0hr to 48hr under different pHs in 1xNB at 25 °C. Error bars represent standard deviation of three replicates.

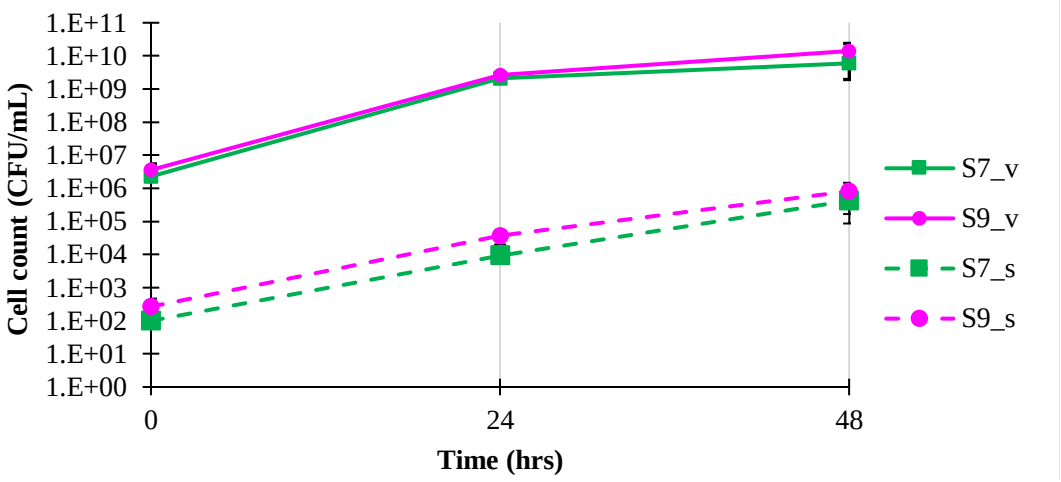

Figure 9.7 - Growth curve evolution of soil from 0hr to 48hr under different pHs in 1xNB at 25 °C. Error bars represent standard deviation of three replicates.

Lastly, different concentrations of nutrient broth solution, 0.5xNB, 1xNB and 2xNB, were tested while keeping temperature (25 °C) and pH (7) constant. The results of bacterial growth for *B. subtilis* and soil are shown in Figures 9.8 and 9.9, respectively. Samples are abbreviated using the form: xCv/s, where x is the bacteria type (BS for *B. subtilis* and S for soil), C is the nutrient solution concentration and v/s is indicating vegetative cells or spores. Using different amounts of nutrients in solution resulted in only small differences for both *B. subtilis* or soil including both vegetative cells and spores.

In addition to these, growth of *B. subtilis* in 0.5xNB concentration at 37 °C was assessed for the ability of higher temperature and lower nutrient solution to simultaneously increase cell counts and sporulation. With this combination, spore counts of *B. subtilis* increased by an additional order of magnitude, however, vegetative cell counts did not change notably.

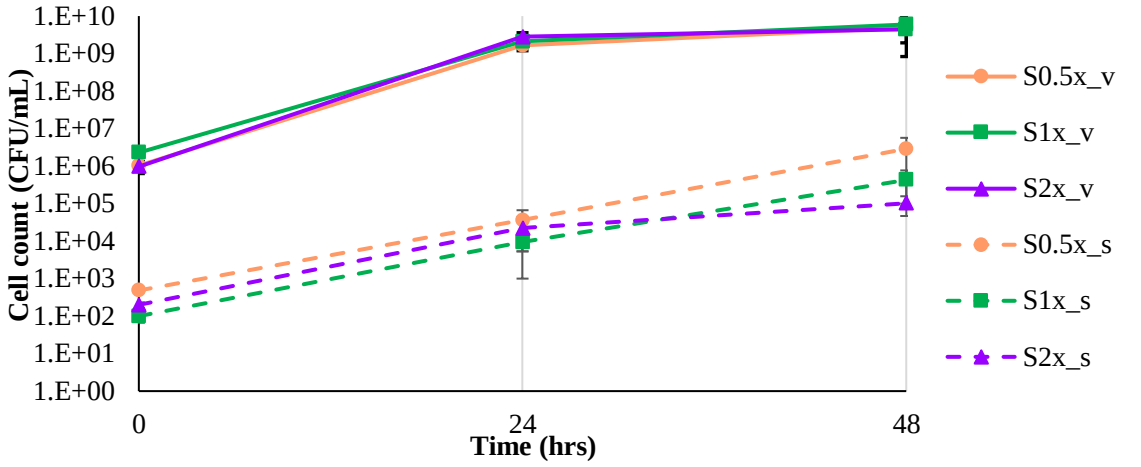

Figure 9.8 - Growth curve evolution of soil from 0 to 48hrs in different solution concentrations at pH 7 and 25 °C. Error bars represent standard deviation of three replicates.

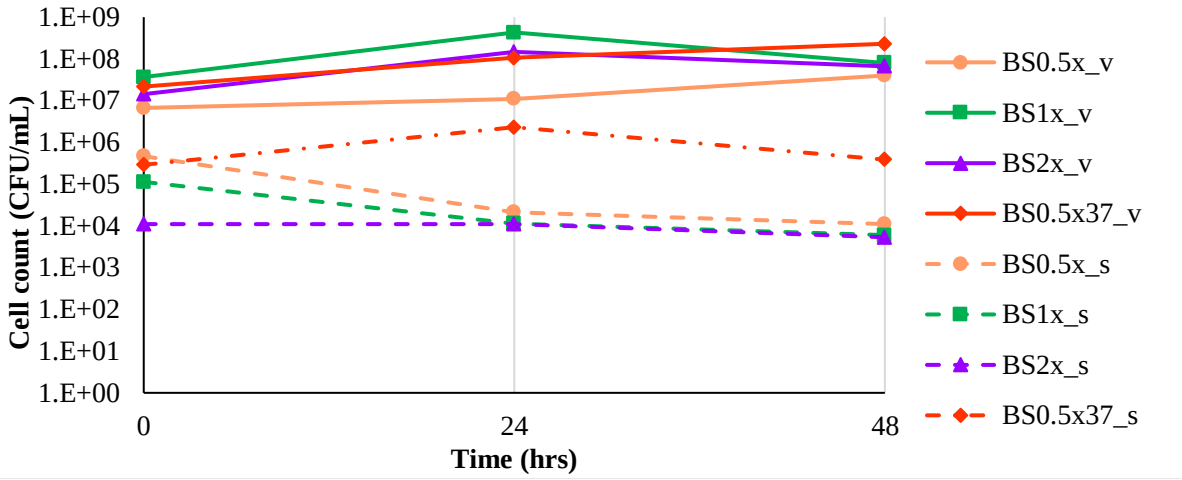

Figure 9.9 - Growth curve evolution of *B. subtilis* from 0 to 48hrs in different solution concentrations at pH 7 and 25 °C. Error bars represent standard deviation of three replicates.

From these results, optimum growth conditions were selected as 0.5xNB, pH 7 and 37 °C for *B. subtilis* and 0.5xNB, pH 7 and 25 °C for soil. Although 37 °C led to slightly better growth for soil than 25 °C, 25 °C was chosen to ease the growth conditions, decrease the equipment use and standardize growth conditions for both bacterial samples.

9.4 Sporulation

After obtaining the growth curves, two different sporulation methods were evaluated over varying incubation times, in order to increase sporulation, including use of mineral-rich sporulation media

and use of low temperature heat treatment. Figure 9.10 shows the impact of the sporulation media on vegetative cell and spore growth for both *B. subtilis* and soil. Samples are abbreviated using the form: xT, where x is the bacteria type (BS for *B. subtilis* and S for soil), T is the temperature and v/s is indicating vegetative cells or spores. This method did not affect vegetative cell count positively or negatively and was not successful in increasing spore numbers even when incubating for a longer time. Spore count remained between 10^3 and 10^5 CFU/mL, nearly the same as the results obtained from not using sporulation media (Figures 9.4 to 9.9).

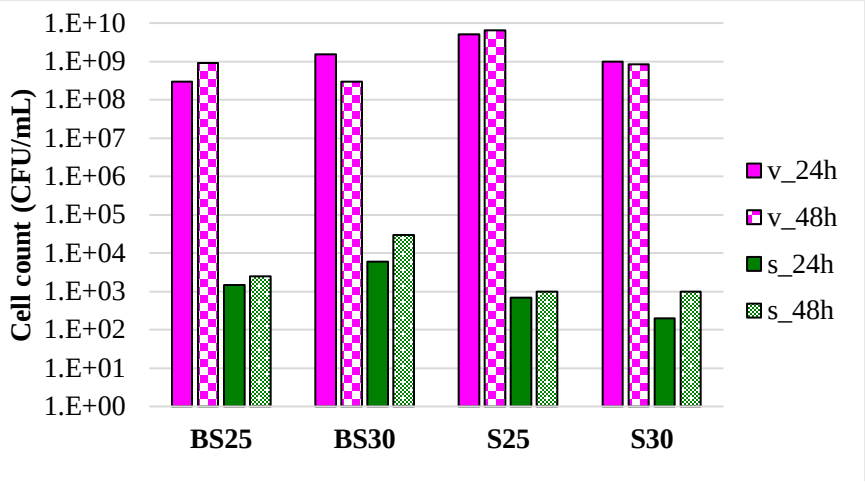

Figure 9.10 - Influence of the sporulation media on vegetative cell and spore growth for *B. subtilis* and soil under different temperatures (25 °C and 30 °C).

Results of the use of low temperature heat treatment for *B. subtilis* and soil are shown in Figure 9.11. Figure 9.11a shows the data for centrifuging and drying after 24 hours of incubation whereas Figure 9.11b shows after 48 hours of incubation. Samples are abbreviated using the form: ACxT, where A is the bacteria type (BS for *B. subtilis* and S for soil), C is the solution concentration, T is the temperature and v/s (legend) indicates vegetative cells or spores. Incubating soil bacterial solution for one additional day increased spore count significantly by two orders of magnitude from 10^4 to 10^6 CFU/mL. However, for *B. subtilis* no explicit changes resulted between incubating for 24 hours and 48 hours or using 0.5xNB and 1xNB solution concentrations. For these reasons, to maximize spore counts soil bacteria should be grown for 48 hours but *B. subtilis* samples do not require more than 24 hours.

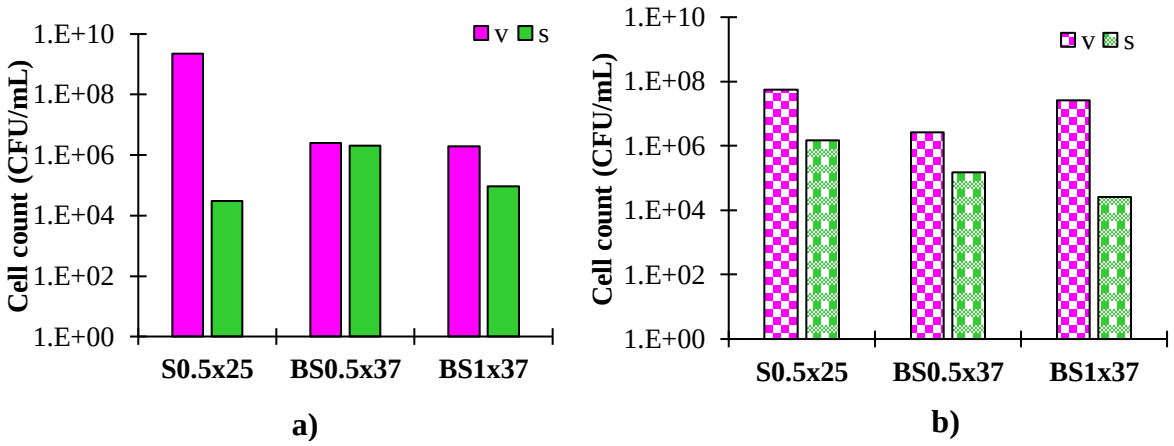

Figure 9.11 - Influence of the low temperature heat treatment for *B. subtilis* and soil in different solution concentrations (0.5xNB and 1xNB) and under different temperatures (25 °C and 37 °C) after a) 24 hours of incubation and b) 48 hours of incubation.

9.5 Biomineralization ability

The results of hydrolyzed urea testing are shown in Figure 9.12, and indicate that soil has a good urea consumption and therefore is an effectively ureolyzing bacteria. *B. subtilis* was not able to decompose urea and it can be concluded that it is a non-ureolytic bacteria.

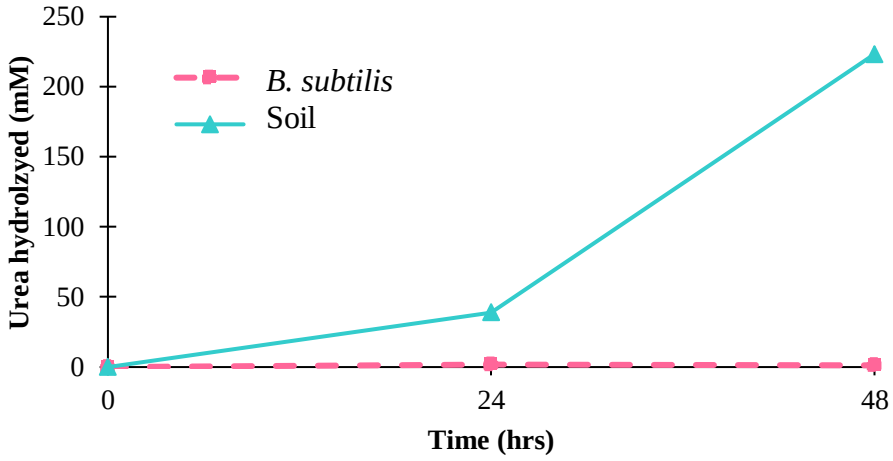

Figure 9.12 - Ureolytic activity of *B. subtilis* and soil.

Although *B. subtilis* is not a ureolytic bacteria, it is still able to promote precipitation by converting environmental CO_2 to carbonate (HCO_3^-) via enzymatic activity in an alkaline environment through the degradation of nitrogen source (Perez and Garcia 2020). In the presence of calcium and carbonate produced from enzymatic hydrolysis, calcium carbonate precipitates in an alkaline system. To verify the biomineralization ability of the *B. subtilis* bacteria before proceeding to utilize it in concrete testing, calcium carbonate content of both bacteria samples and their precipitates was measured using TGA. *B. subtilis* and soil bacteria sample solutions were prepared using a mixture of centrifuged bacterial cells, nutrient solution, urea, and calcium acetate to induce biomineralization. *B. subtilis* and soil bacteria samples were prepared using similar processes in order to allow for comparison of biomineralization capacity. The results shown in Figure 9.13 indicate that, although *B. subtilis* was not able to decompose urea, calcium carbonate precipitate was present in the sample. Calcium carbonate represented 34% of the total sample mass, with the remaining 66% of the sample mass associated with dried bacteria, as all nutrients and dissolved minerals were washed and removed following centrifugation. Soil bacteria also indicated high biomineralization ability, with 62% of the total sample mass associated with calcium carbonate precipitate. The much larger proportion of calcite present in the soil bacteria sample relative to the bacteria mass indicates increased ability for calcium carbonate precipitation in the soil sample relative to *B. subtilis* bacteria when utilizing similar masses of bacteria.

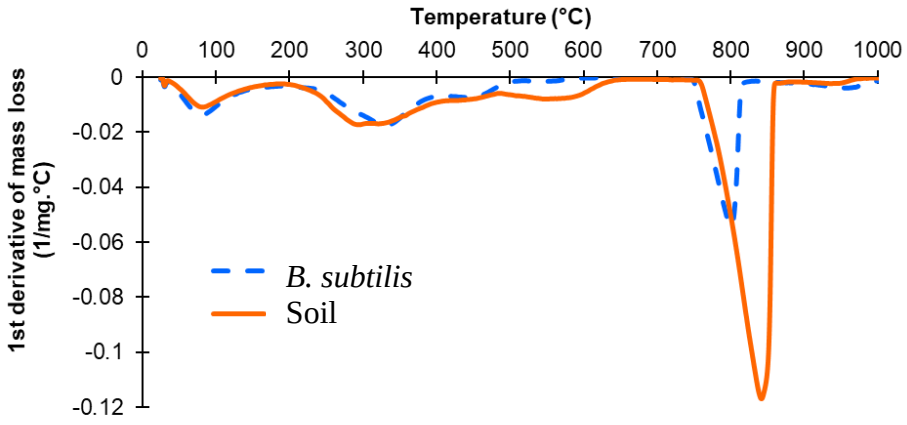

Figure 9.13 - TGA curves of *B. subtilis* and soil.

In addition to TGA testing, calcium carbonate precipitation of bacteria samples was evaluated using phase content analysis using XRD. Results are shown in Figures 9.14 and 9.15 for *B. subtilis* and soil, respectively. Both samples have indications of the presence of two calcium carbonate phases, calcite and vaterite. An increase in Ca^{2+} amount may have resulted in more vaterite precipitation (less stable polymorph with lower solubility) and inhibited the transformation of vaterite to calcite (more stable polymorph with higher solubility) (Amiri and Bundur 2018; Ogino et al. 1987; Bundur et al. 2017). Different types of calcium carbonate may indicate a change in the transition process, but it was observed that the morphology of the calcium carbonate did not affect the sealing on the cracks (Tezer and Bundur 2021).

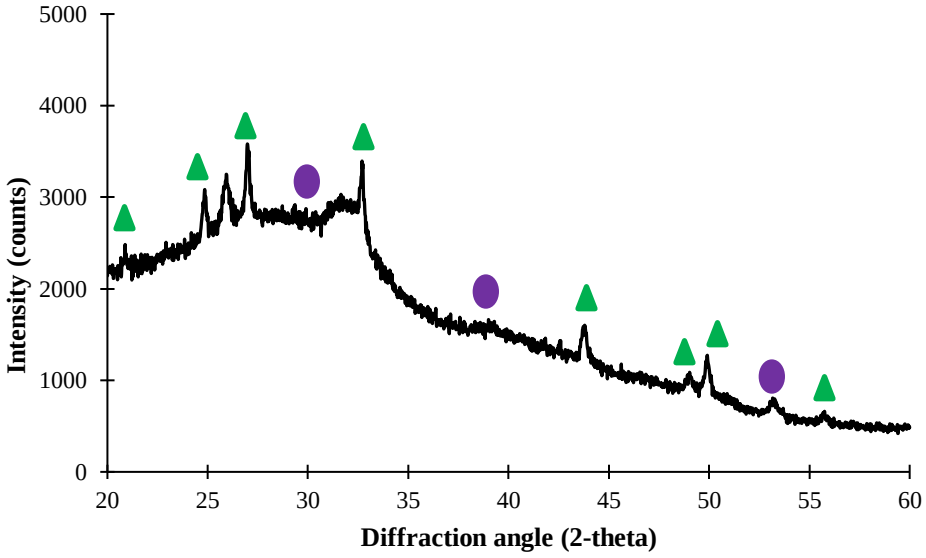

Figure 9.14 - XRD curve of *B. subtilis* from 20° to 60° diffraction angle. Triangle markers indicate calcite crystal structure reflections, circles indicate vaterite crystal structure reflections.

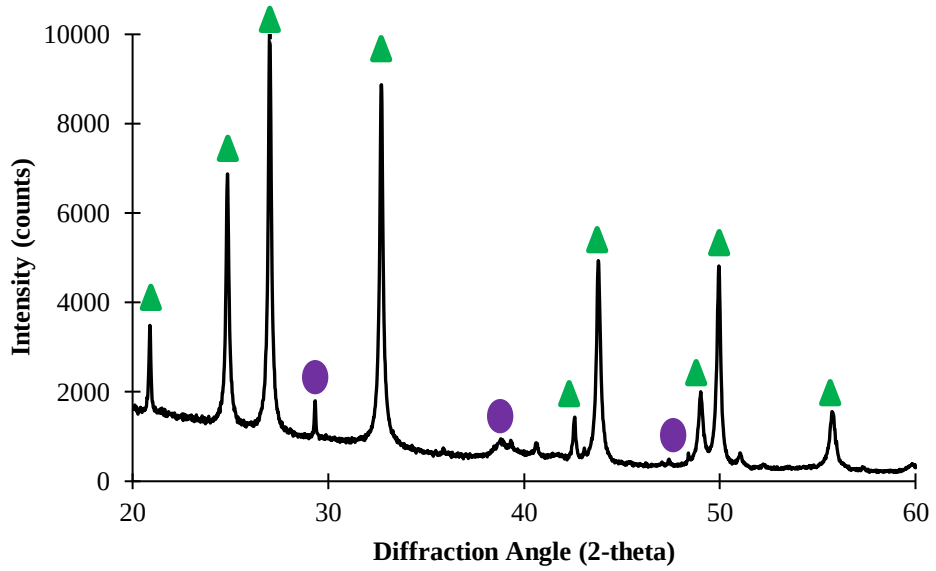

Figure 9.15 - XRD curve of soil from 20° to 60° diffraction angle. Triangle markers indicate calcite crystal structure reflections, circles indicate vaterite crystal structure reflections.

9.6 Conclusions

For the axenic, *B. subtilis* bacteria:

- *B. subtilis* bacteria provided a relatively resilient bacteria source that is capable of forming protective spores to enable inoculation of the media into concrete, and also provides biomineralization ability without the requirement of an additional urea source.

- *B. subtilis* bacteria was significantly affected by the pH of its growth solution, with reductions in sample bacteria numbers at 24 hours. If incubated for 48 hours the high pH sample could recover and grow to higher numbers than the original sample.

- *B. subtilis* bacterial growth was inhibited by use of incubation temperatures colder than room temperature (10 °C). Growth of vegetative cells was not significantly different for room temperature (25 °C) and high temperature (37 °C) grown samples, but approximately 4x as many spores were formed in the 37 °C sample.

- Very little difference in the growth rate or total cell count was observed for *B. subtilis* based on type of nutrient solution (tryptic soy broth (TSB) or nutrient broth (NB)). Use of nutrient solutions should be confirmed for each bacterial sample, but either TSP or NB can be used to obtain adequate cell counts, based on availability and cost.

- Little difference in *B. subtilis* growth was observed based on nutrient solution concentration. To minimize cost, nutrient solutions diluted to half of the original solution concentration are suggested for use without impact on total cell growth capabilities.

- *B. subtilis* samples achieved maximum vegetative cell concentrations after 24 hours, without significant further growth up to 96 hours of incubation. Therefore, it is not necessary to

incubate and grow bacterial sample solutions for more than 24 hours.

- Use of low temperature heat treatment as the sporulation method led to 2 orders of magnitude increase in *B. subtilis* spore counts when compared to use of a sporulation chemical.

- *B. subtilis* bacteria biomineralization was confirmed through XRD and TGA measurements but was found to occur through a mechanism other than ureolytic activity.

For the non-axenic bacteria:

- Spent digestate and whiskey distillation wastewater sources did not produce bacteria meeting the requirements for use in concrete – either failing to grow in a neutral or high pH growth solutions (pH 7 or 9), or not capable of sporulation. These wastewater sources should not be used to produce bacteria for concrete.

- A simple soil sample obtained from a Columbus, OH residence near the Scioto River was able to produce bacteria capable of forming spores and biomineralizing.

- Soil bacteria achieved maximum concentrations of vegetative cells after 24 hours, without significant further growth up to 96 hours of incubation. Spore concentrations, however, increased by two orders of magnitude (from 10^4 to 10^6 CFU/ mL) from 24 to 48 hrs, suggesting that it may be beneficial to incubate soil growth solutions for additional time, compared to the *B. subtilis* samples.

- The soil bacteria vegetative cell growth was not affected by growth temperatures when grown at room temperature or 37 C. Lower temperature (10 °C) conditions slowed growth, but less significantly than in the *B. subtilis* sample. Spore counts were positively correlated with temperature – with greater temperatures resulting in greater orders of magnitude spore counts.

- Growth solution pH (of 7 or 9) had no effect on vegetative or spore growth of soil bacterial samples.

- Nutrient solution concentration had no effect on soil sample vegetative cell growth but use of the half concentration solution lead to higher sporulation. Therefore, half concentration solution use is recommended to both reduce production costs and obtain greater spore counts.

- The bacterial sample produced from soil was more resilient than the axenic *B. subtilis* sample during the growth phase, showing less impact on growth under varying temperature, pH, and nutrient solution conditions, and generating similar or higher cell counts.

- Similar to with the *B. subtilis* bacteria, sporulation using low temperature heat treatment was more effective than use of sporulation solutions for the soil bacterial samples, resulting in 1 or 3 orders of magnitude increases in spore counts using growth solutions incubated for 24 and 48 hours of cell growth, respectively.

- Soil bacteria successfully biomineralized calcium carbonate through ureolysis and precipitated higher calcium carbonate quantities than *B. subtilis* samples.

10 Appendix D: Task 2 Microbial Community Analysis Results and Conclusions

10.1 Growth and Storage Variables Affecting Bacteria in Pre-Concrete Samples

The overall microbial diversity is illustrated with phylogenetic trees which show relationships between microorganisms identified in samples for all the axenic samples and non-axenic samples in Figure 10.1. For all *B. subtilis* samples, *Bacillus* Genus was detected in 4067034 sequences while a subset of 3962796 sequences were classified as *Bacillus subtilis* species. So, 97.4% of sequences from axenic samples belonged to the *Bacillus subtilis* species group, which is consistent with our strain.

A.

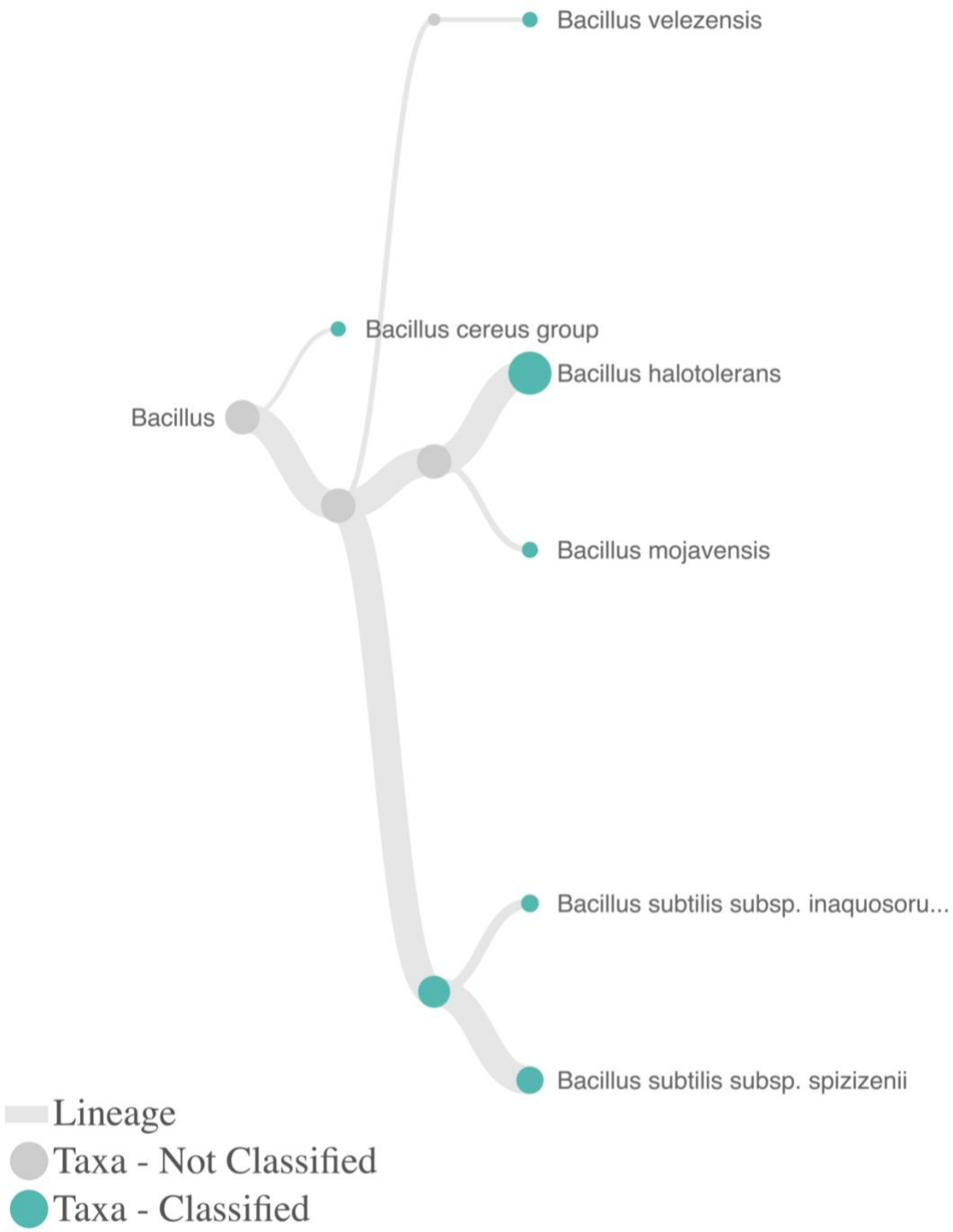
Bacillus velezensis
Bacillus cereus group
Bacillus halotolerans
Bacillus
Bacillus mojavensis
Bacillus subtilis subsp. inaquosoru...
Bacillus subtilis subsp. spizizenii
Lineage
Taxa - Not Classified
Taxa - Classified

B.

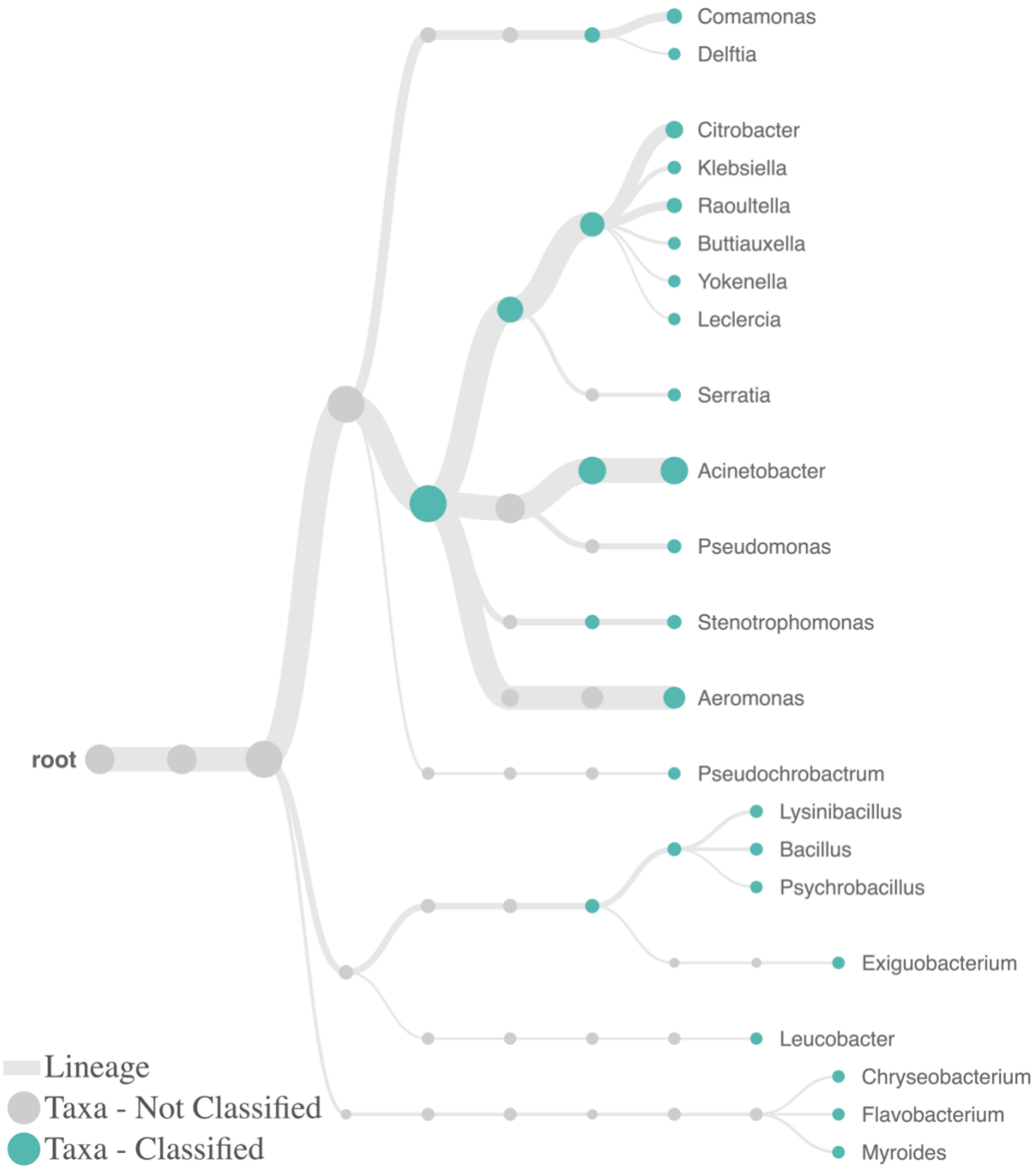

Figure 10.1 - Phylogenetic tree output of 16S workflow in EPI2ME shows the evolutionary relationships among all A. axenic *B.subtilis* samples, shown for all classified sequences at the furthest level of taxonomic resolution, or B. all non-axenic soil samples classified with greater than or equal to 0.1% relative abundance at the (higher and less specific) genus level of taxonomic resolution.

Figure 10.2 indicated that sporulation media had little impact on *B. subtilis* classification. Relative abundances were compared among samples before and after sporulation. Figure 10.3A showed that bacillus made up over 99% of the population in both conditions at genus level, Dominant *B.*

subtilis at species level (Figure 10.3B) also showed no difference on microbiome structure with 60.78% and 58.92% *bacillus halotolerans* and 23.74% and 24.44 % *bacillus spizizenii* before and after sporulation, respectively. Alpha diversity shannon index values before and after sporulation were 0.074 and 0.066.

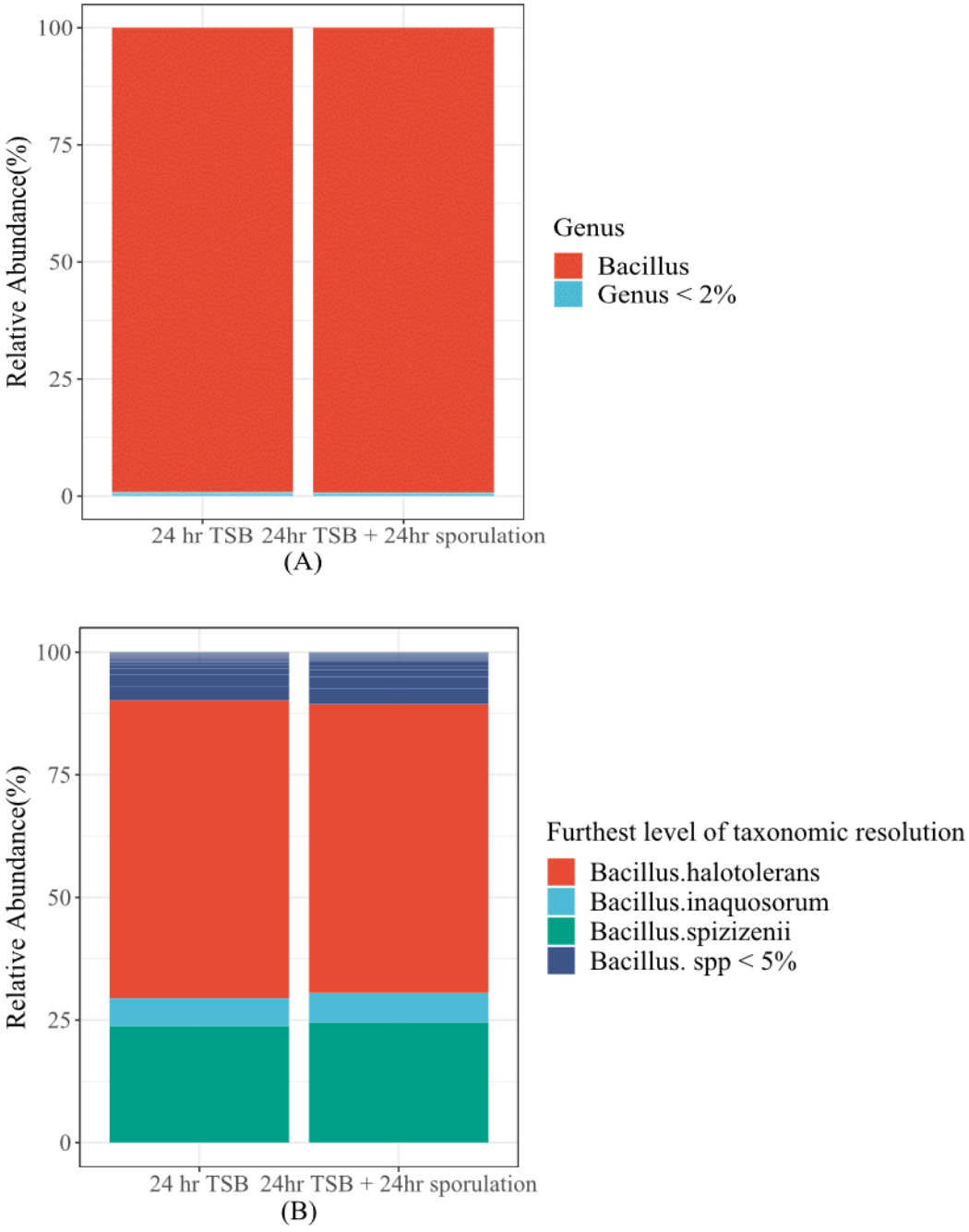

Figure 10.2 - Relative abundance of microbes at Genus level (A) and furthest level of taxonomic resolution (B) in *B. subtilis* aliquot samples that only grew in TSB for 24 hours and *B. subtilis* sample that grew firstly in TSB for 24 hours and then was suspended in 2xSG sporulation media for 24 hours. Less abundant genera that were present at < 2% were aggregated as Genus < 2%. Less abundant species that were present at < 5% were aggregated as *Bacillus.spp* < 5%.

B. subtilis and soil bacteria were grown in the 0.5xNB growth media at 37°C and 25 °C. For *B. subtilis*, almost all the bacteria (99.25% and 100%) belonged to *Bacillus* genus. Figure 10.3B identified three dominant *Bacillus* at the furthest level of taxonomic resolution which were *Bacillus halotolerans* (60.59%), *Bacillus spizizenii* (22.38%) and *Bacillus inaquosorun* (5.93%) in replicate a while classification in replicate b was limited due to low sequence coverage. Compared to the *B. subtilis* sample, soil microbiomes were more diverse as indicated by higher alpha diversity in Figure 10.3C. *Acinetobacter*, *Aeromonas* and *Bacill*us were typical bioremediation microbial genera in soil (Li et al. 2020; Choi et al. 2012; Fakhar et al. 2022) and were identified in our soil samples with a high abundance. At the furthest level of taxonomic resolution, *Aeromonas encheleia* was the most abundant (37.37% and 29.28%).

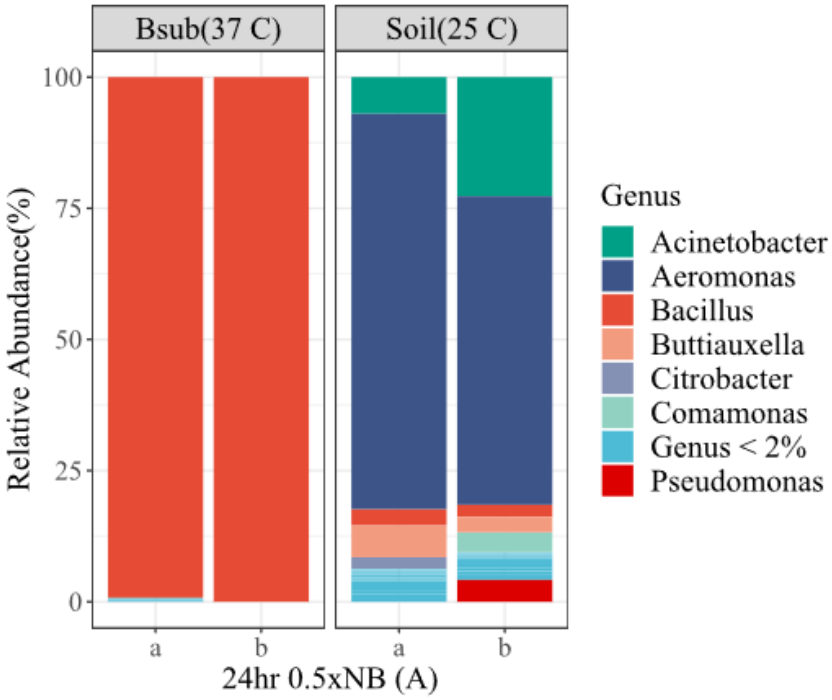

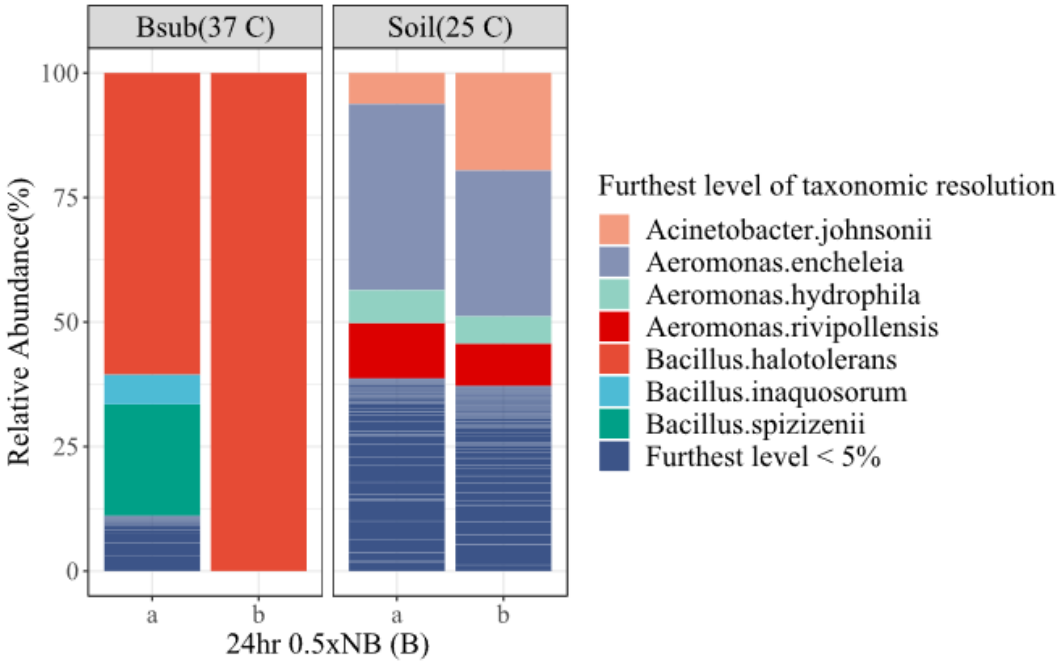

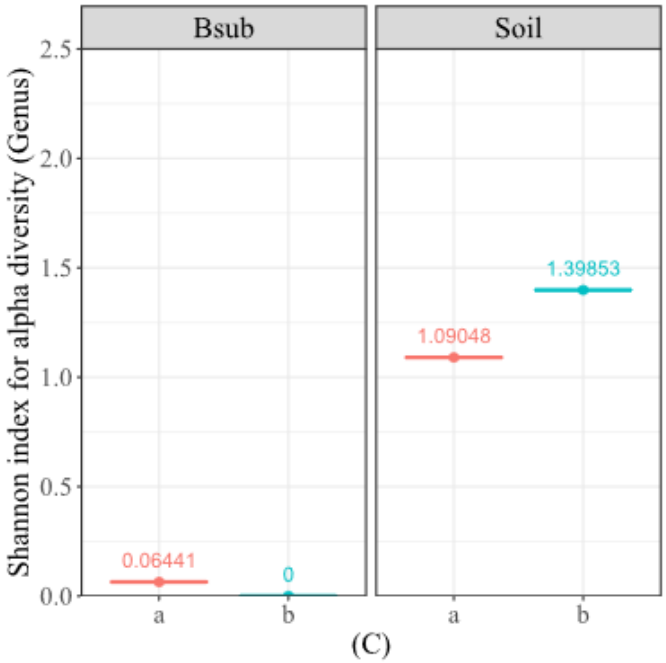

Figure 10.3 - Relative abundance of microbes at Genus level (A) and furthest level of taxonomic resolution (B) in *B. subtilis* and soil bacteria samples that grew in 0.5xNB for 24 hours. Less abundant genera that were present at < 2% were aggregated as Genus < 2%. Less abundant furthest level of taxonomic resolution that were present at < 5% were aggregated as Furthest level < 5%. (C) Alpha diversity that was calculated based on Shannon index.

As shown in Figure 10.4, for *B. subtilis* axenic samples, very little difference in *B. subtilis* sample at genus and the furthest level of taxonomic resolution was observed based on storage time. Abundance of dominant genus (*Bacill*us) and the furthest level of taxonomic resolution (*Bacillus.halotolerans*, *Bacillus spizizenii* and *Bacillus inaquosorun*) and alpha diversity were very close at day 1, day 7 and day 14.

Based on the genus distribution, storage life had little impact on the soil sample microbial community as shown in Figure 10.4. For soil samples, as the storage time increased, the alpha diversity increased in Figure 10.4C which is consistent with the phylogenetic trees increasing number of branches in Figure 10.5. *Acinetobacter* was the most abundant genus across the storage life with three dominant furthest level of taxonomic resolution (*Acinetobacter johnsonii, Acinetobacter oleivorans* and *Acinetobacter pittii*). The next top 5 abundant bacteria in the genera *Citrobacter, Comamonas, Klebsiella, Pseudomonas* and *Raoultella* had only one dominant strain at the furthest level of taxonomic resolution across the storage life. They are *Citrobacter freundii, Comamonas testosteroni, Klebsiella oxytoca*, *Pseudomonas plecoglossicida* and *Raoultella ornithinolytica*. Compared with the original soil aliquot sample in Figure 10.7A, *Bacillus* was rare in dried soil samples.

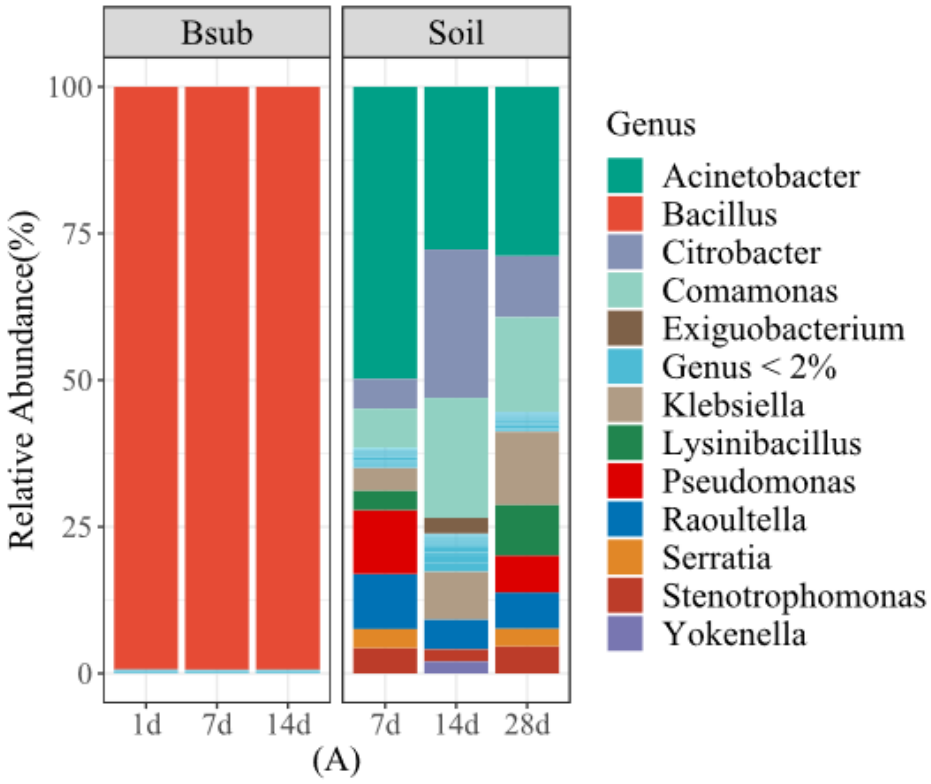

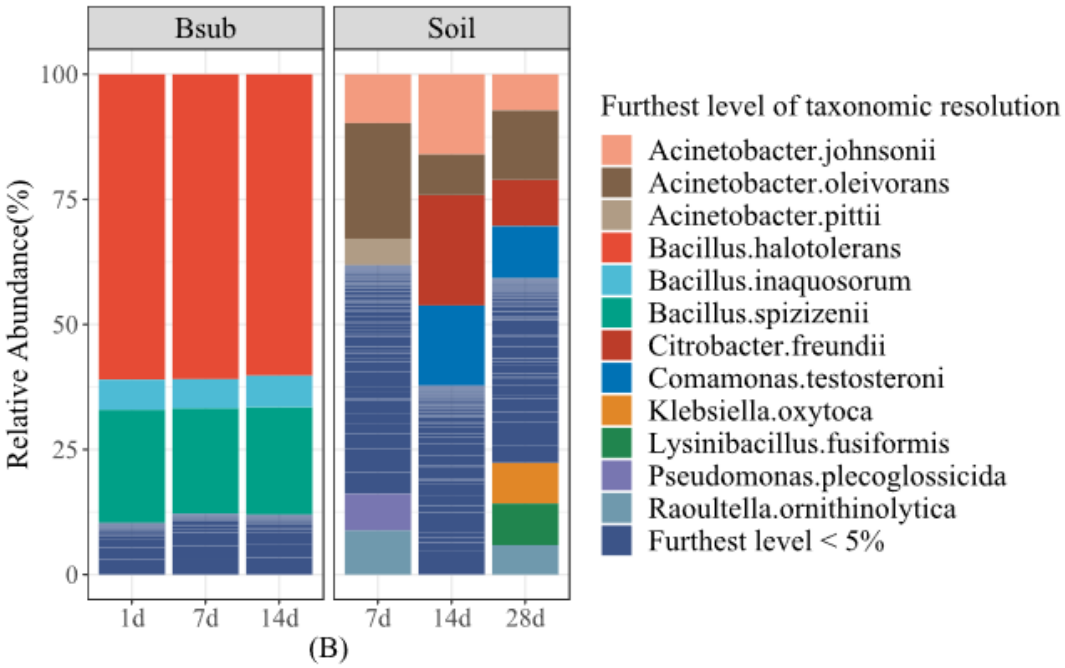

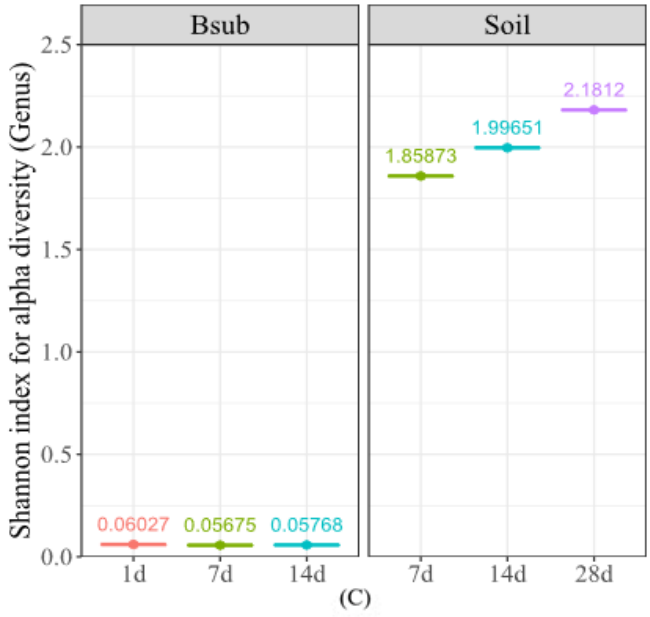

2

Figure 10.4 - Relative abundance of microbes at Genus level (A) and furthest level of taxonomic resolution (B) in dried B. subtilis and soil samples at different storage times. Storage times for dried B. subtilis were 1day, 7 days and 14 days. Storage time for dried soil samples were 7 days, 14 days and 28 days Less abundant genus that were present at <2% were aggregated as Genus < 2%. Less abundant furthest level of taxonomic resolution that were present at < 5% were aggregated as Furthest level < 5%. (C) Alpha diversity that was calculated based on Shannon index.

A.

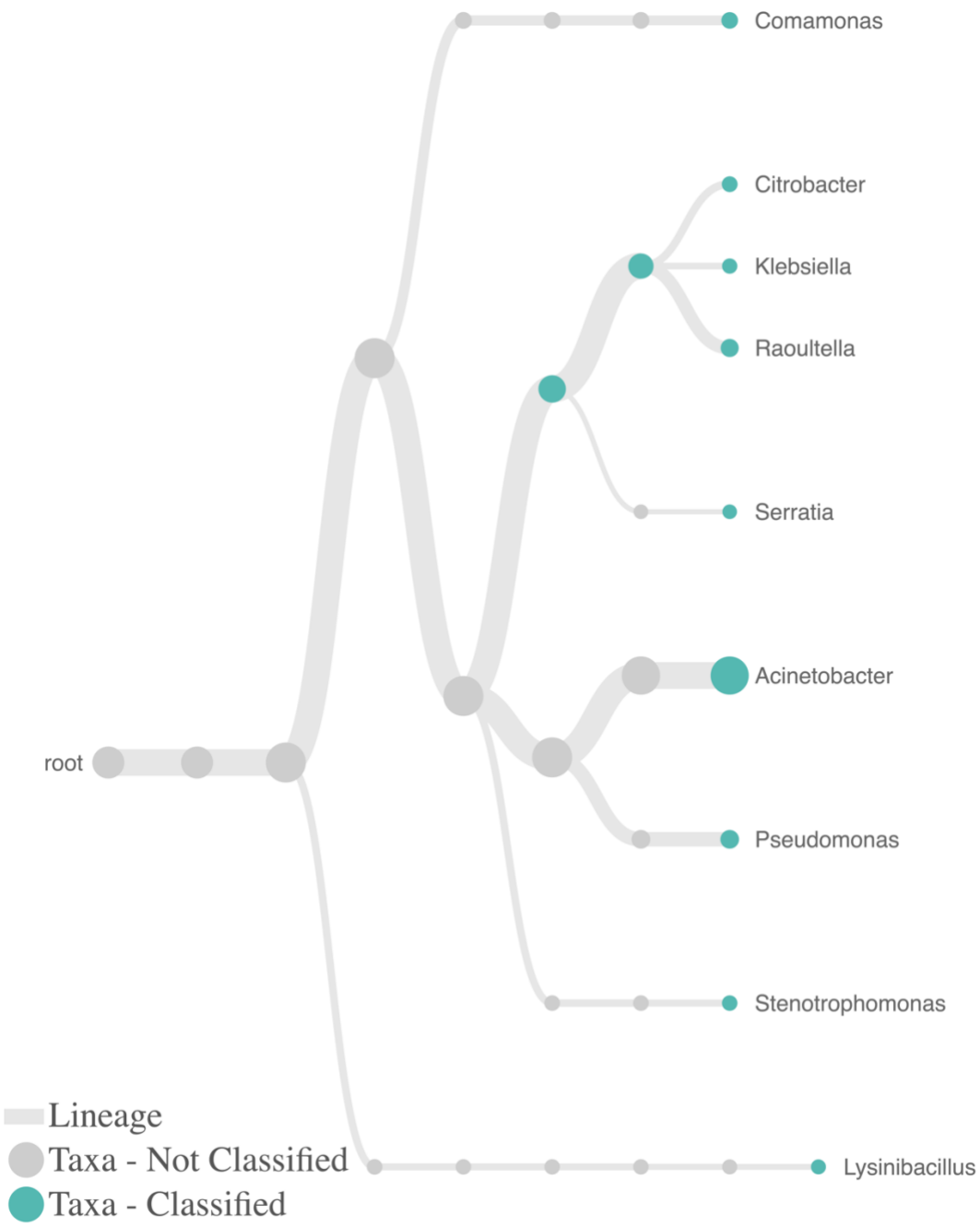
Comamonas
Citrobacter
Klebsiella
Raoultella
Serratia
Acinetobacter
root
Pseudomonas
Stenotrophomonas
Lysinibacillus
Lineage
Taxa - Not Classified
Taxa - Classified

B.

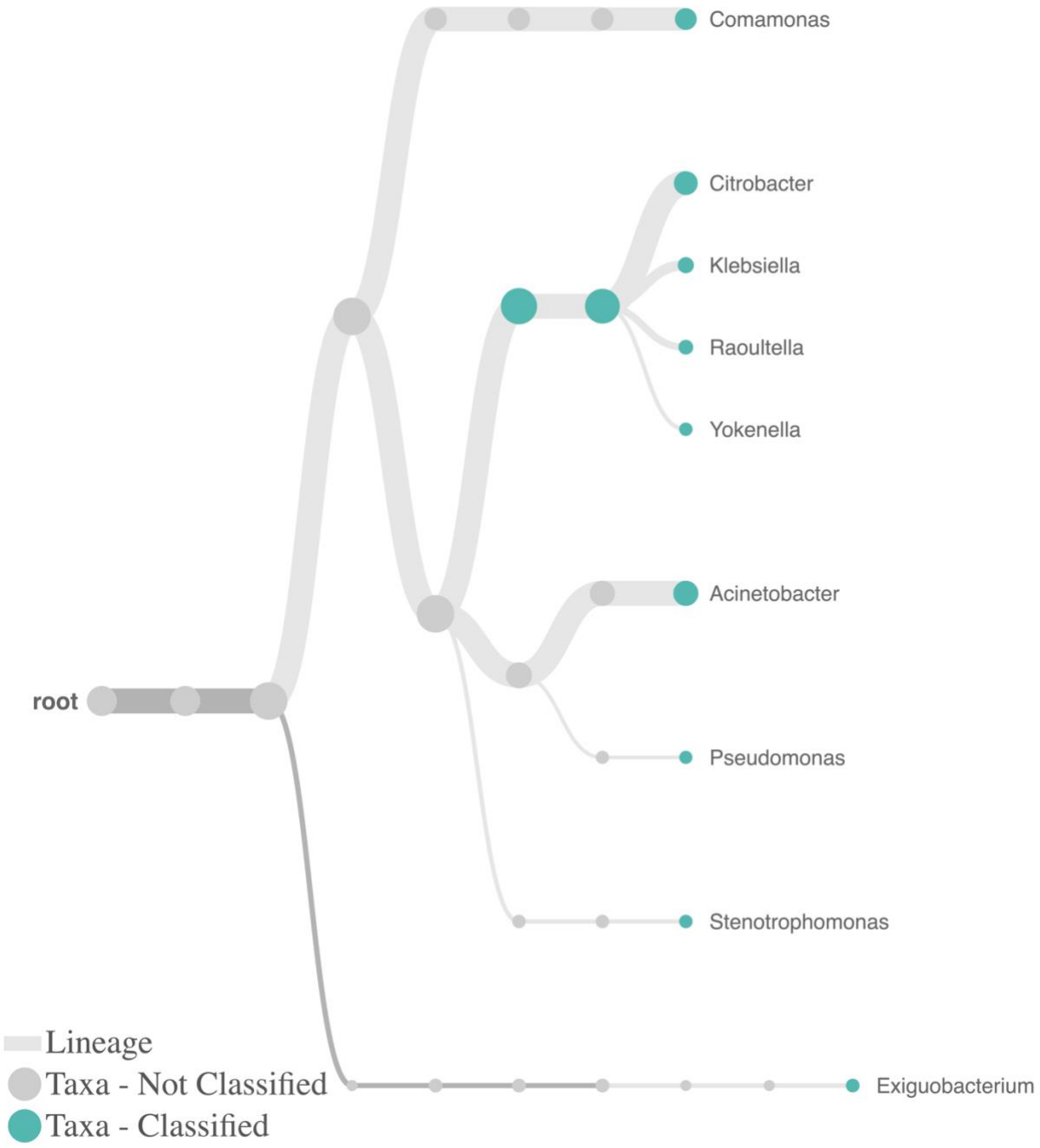
Comamonas
Citrobacter
Klebsiella
Raoultella
Yokenella
Acinetobacter
root
Pseudomonas
Stenotrophomonas
Lineage
Taxa - Not Classified
Taxa - Classified
Exiguobacterium

C.

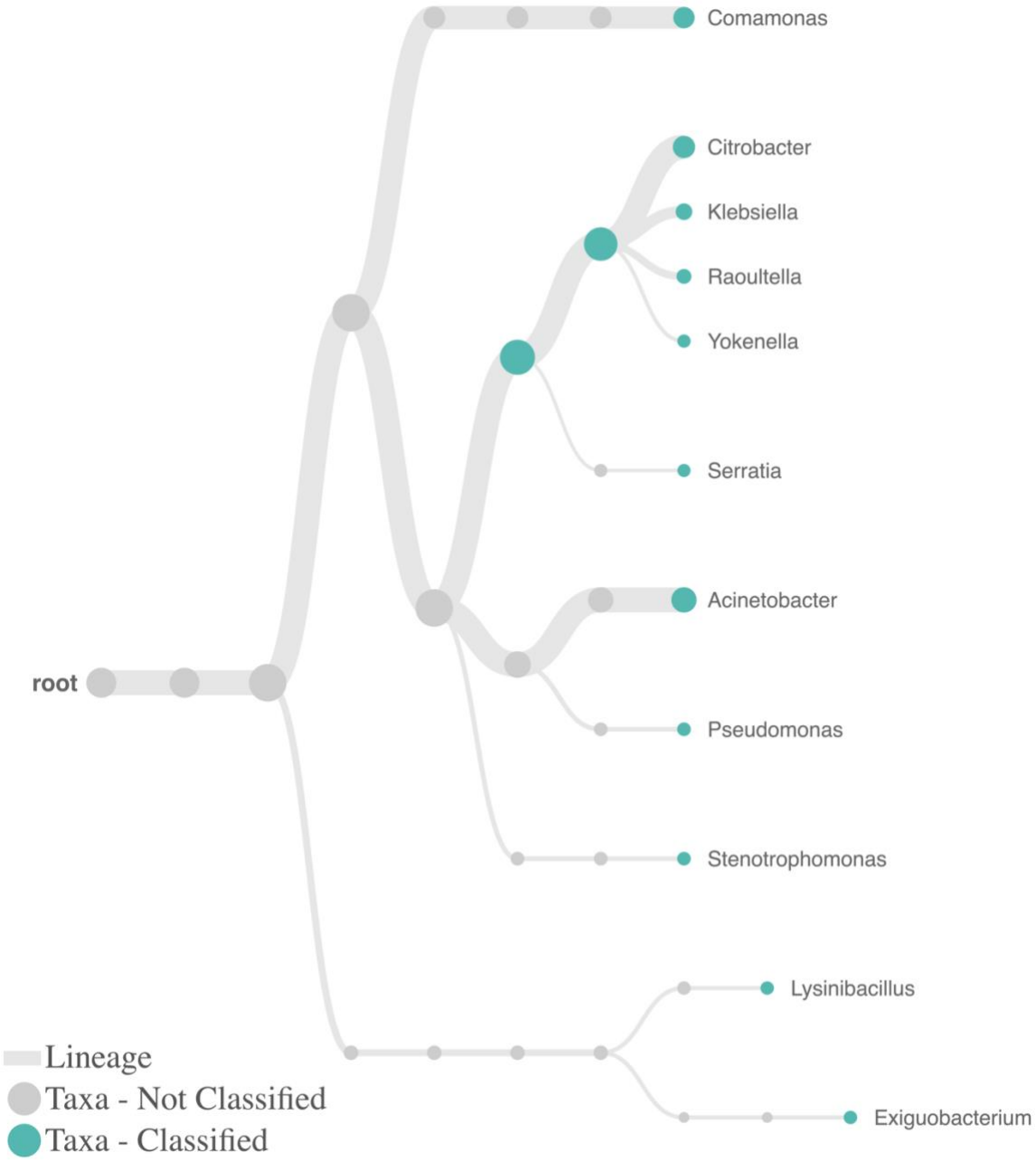

Figure 10.5 - Phylogenetic tree output of 16S workflow in EPI2ME shows the increased diversity at (A.) day 7, (B.) day 14 and (C.) day 28 among non-axenic soil samples with storage experiment, classified with greater than or equal to 1% relative abundance at the (higher and less specific) genus level of taxonomic resolution.

Frozen aliquot soil samples were incubated in 0.5xNB media for 1 day then dried in a 40 °C oven for different days. In Figure 10.6A, 1d a and b represented the microbial community from two replicates of frozen aliquot soil samples while 7d, 14d and 28d were already shown in Figure 10.6A (soil) which represented dried soil samples with increased incubation time after reinjecting to solutions. There was a clear difference between frozen aliquots and dried samples. Frozen aliquots

had more *Aeromonas* more and less alpha diversity (Figure 10.6B), and there was an increase of *Citrobacter* and decrease of *Aeromonas* in dried soil samples.

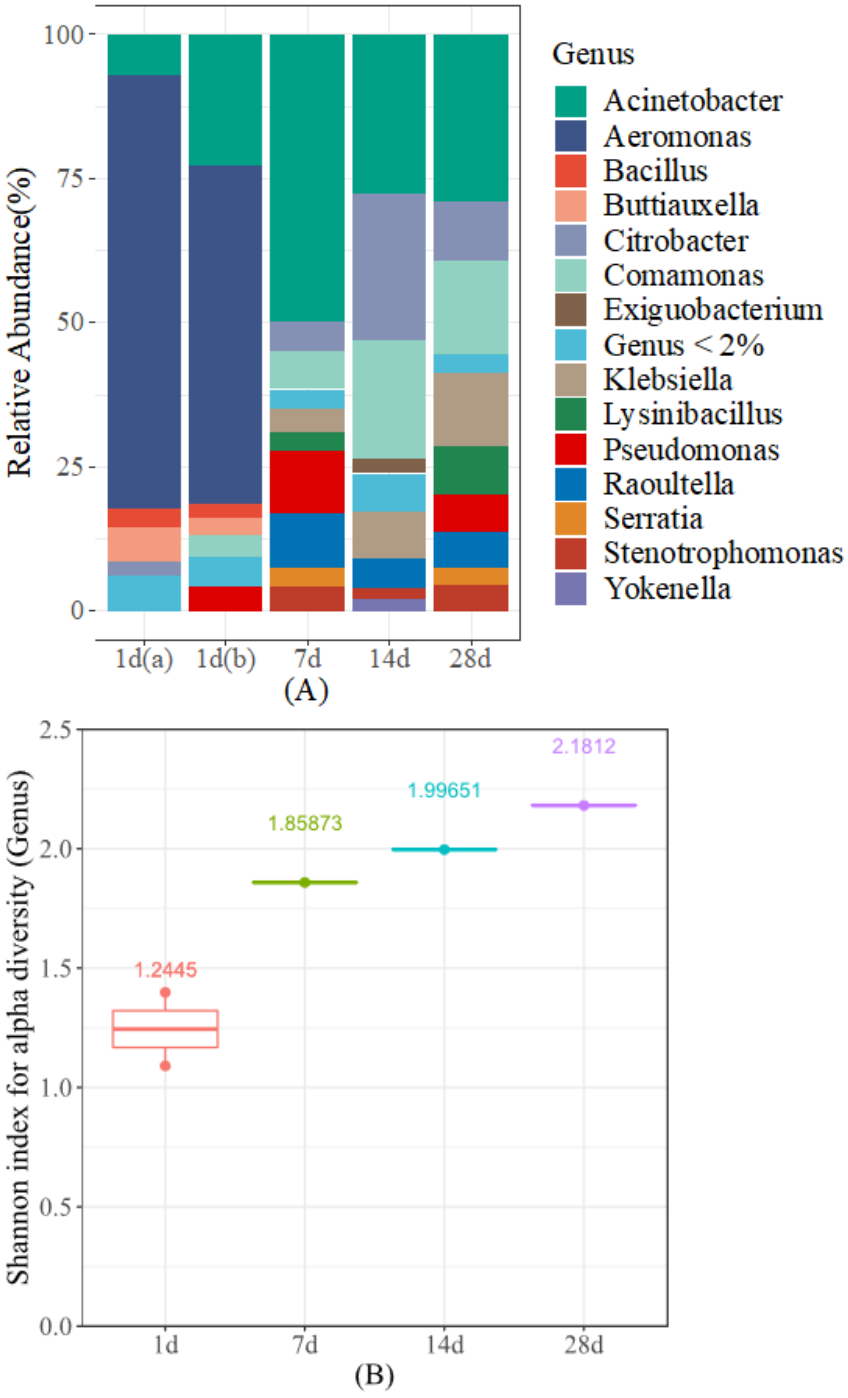

Figure 10.6 - (A) Relative abundance of microbes at Genus level in frozen aliquot (1 day, with replicates a and b) and dried soil samples (7 days, 14 days, and 28 days, same data as Figure 10.5A (soil)). Less abundant genera that were present at < 2% were aggregated as Genus < 2%. (B) Alpha diversity that was calculated based on Shannon index. The alpha diversity value for 1d was the average value from the replicates and the range of the box plot represents the standard deviation of the replicates.

Another experiment determined the impact of sample preparation and urea addition on soil microbiomes. As shown in Figure 10.7, replicate a of the original soil aliquot had more *Aeromonas* (61.95 %) and less *Acinetobacter* (11.48 %) compared to urea test soil samples. Incorporating urea into the growth media slightly increased the alpha diversity and increased relative abundance of *Acinetobacter* (33.99 %) while decreasing relative abundance of *Aeromonas* (7.21 %). Additionally, relative abundance of *Raoultella, Stenotrophomonas, Serratia* increased. Replicate b of the original soil aliquot had a very low sequence coverage (see Table 8.1) so that all of the likely diversity present was not captured and only *Acinetobacter* was observed. Dried soil samples in NB also had less *Aeromonas* (51.3 %) compared to the original aliquot but had a higher relative abundance of *Citrobacter* (34.16 %), and *Bacillus* (3.46 %).

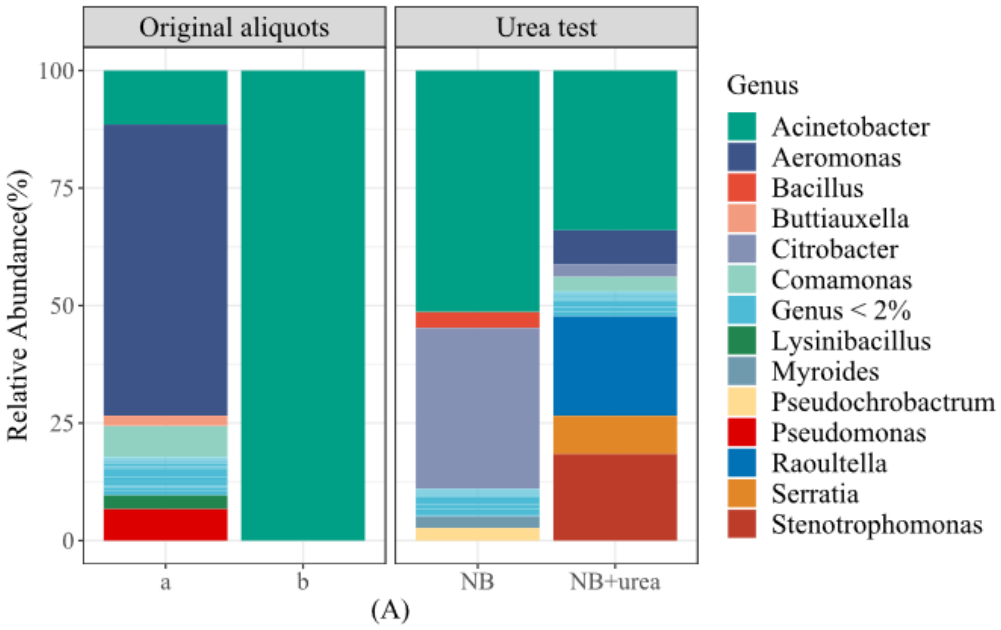

(A)

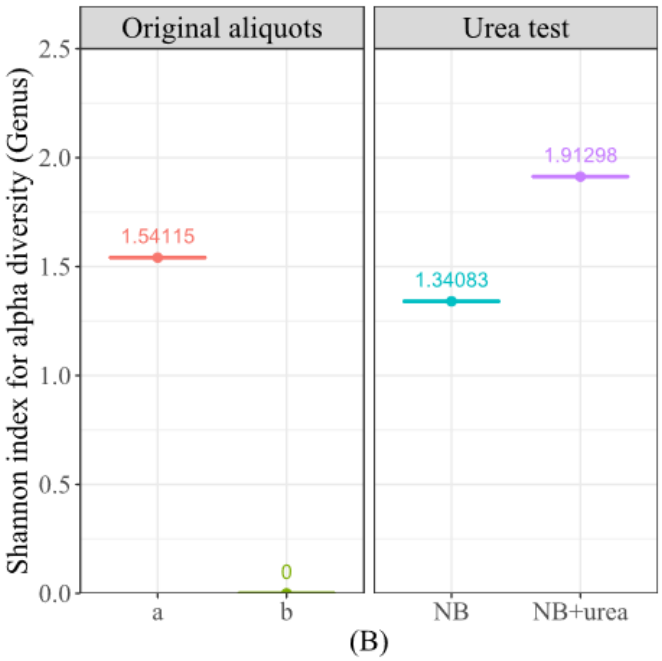

Figure 10.7 - (A) Relative abundance of microbes at Genus level in original soil aliquot in NB, dried soil samples in NB and dried soil samples in NB and urea. Less abundant genus that were present at < 2% were aggregated as Genus < 2%. (B) Alpha diversity that was calculated based on Shannon index.

Difference in microbial community was observed based on nutrient solution concentration, indicating that strength of growth media also impacted microbial communities. As shown in Figure 10.8, 0.5xNB growth media had more *Aeromonas* (75.33 % and 58.78 %) and less *Acinetobacter* (7.00% and 22.72 %) while NB growth media had more *Acinetobacter* (51.31%) and *Citrobacter* (34.16). *Bacillus* were in both conditions with similar relative abundance (3.13%, 2.31% and 3.46%).

Previous studies (Eltarahony et al. 2021; Othman, Naher, and Yusoff 2013) indicated that *Raoultella* and *Stenotrophomonas* were active with the presence of urea. *Raoultella ornithinolytica* can remediate heavy metal polluted soils by biomineralization via urea hydrolysis, and urea can also increase the relative abundance of *Stenotrophomonas maltophilia* through ecological interactions. These factors could explain the increased relative abundance under the urea growth media condition.

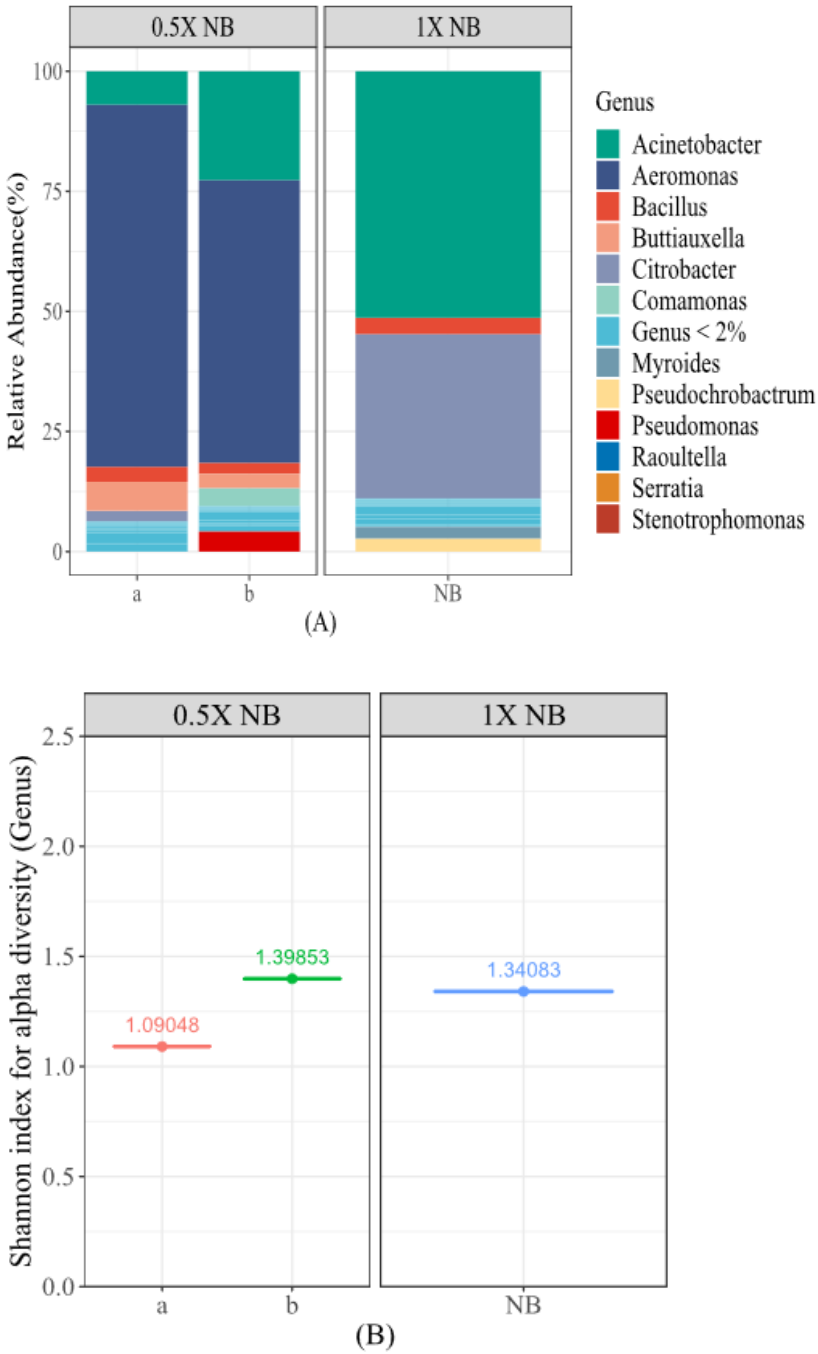

Figure 10.8 - (A) Relative abundance of microbes at Genus level in 0.5xNB and NB dried soil samples. Less abundant genus that were present at < 2% were aggregated as Genus < 2%. (B) Alpha diversity that was calculated based on Shannon index.

10.2 Dominant taxa and their possible functions in soil microbial communities

A summary of the characteristics of the dominant genera of bacteria detected in our samples with a relative abundance greater than 5% is provided in Table 10.1. Note that because some genera

only had one dominant furthest level of taxonomic resolution we focused on that furthest level in particular.

The dominant bacterial genera in soils were *Acinetobacter*, *Aeromonas*, *Citrobacter*, *Comamonas*, *Klebsiella*, *Pseudomonas* and *Raoultella*. *Acinetobacter*, *Aeromonas* and *Pseudomonas* are typical bioremediation microbial genera used to remediate heavy metals in soil, and *Aeromonas* and *Pseudomonas* can tolerate low temperatures. Additionally, *Citrobacter freundii* has previously been utilized to repair cracks in concrete through biocementation, which could partially explain any biomineralization in the concrete or mortar cube results in this study using soil samples.

Although we chose *Bacillus subtilis* for axenic culture studies due to their known biomineralization capabilities (see literature review Table 10.1), B*acillus* genera was not detected in every soil sample but was detected at a low relative abundance in soil samples under the conditions studied.

Table 10.1 - Dominant bacteria in soil samples and their characteristics.

Bacteria	**Characteristics**	**References**
Acinetobacter	• Gram-negative bacteria • Non-motile • Oxidase negative • Nonfermentive • Contribute to the soil fertility • Bioremediation of Cr and Pb polluted soils	(Adewoyin and Okoh 2018; Choi et al. 2012; Li et al. 2020)
Aeromonas	• Gram-negative bacteria • Anaerobic • Opportunistic pathogen and resistant to antibiotics • Can remediate of heavy metal polluted soils by biomineralization and biotransformation • Grow at an optimal temperature of 22–35 °C • Can tolerate pH conditions ranging from 4.5 to 9 • Can tolerate low temperature and increasing concentration of NaCl (0.3%-5%) • Oxidase and catalase positive • Degrading nitrates to nitrites • Glucose fermenters	(Bastos et al. 2019; Fakhar et al. 2022; Fern and Jos 2020)
Citrobacter freundii	• Gram-negative bacteria • Facultative anaerobic • Opportunistic pathogen and resistant to antibiotics • High extracellular urease activities • Repaired cracks and concrete through biocementation	(Hossain et al. 2017; Abdel-Aleem et al. 2019)
Pseudomonas	• Gram-negative bacteria • Aerobic • No spores forming • Can remediate of heavy metal polluted soils by reduce/oxidize transition metals and bioaccumulation • Optimal growth temperature of 37 °C	(Fakhar et al. 2022)

	• Can tolerate temperature of 4 to 42 °C within a pH range of 4 to 8	
Raoultella ornithinolytica	• Gram-negative • Oxidase-negative • Aerobic • Non-motile • Can remediate of heavy metal polluted soils by biomineralization via urea hydrolysis	(Eltarahony et al. 2021)
Stenotrophomonas maltophilia	• Gram-negative • Non-fermentative • Oxidase-negative • Aerobic • Forming biofilms • Biomineralization of metal sulfide nanocrystals • Urea-N can increase its population	(Senol 2004; Spangler et al. 2016; Othman, Naher, and Yusoff 2013)

10.3 Conclusions

To further investigate microorganisms involved in concrete systems to prevent and/or heal cracking, axenic (*Bacillus subtilis*) and non-axenic (soil bacteria) cultures were sequenced under a variety of conditions using 16S rRNA gene sequencing on our hand-held nanopore MinION sequencer to identify the types of bacteria present in these samples. The effects of various factors including storage life, sporulation media, and nutrient media types and concentrations on the microbial community structure and the most dominant bacteria in the samples was investigated. For soil samples which contained bacteria other than *Bacillus subtilis*, typical properties of dominant bacteria found were cataloged to determine potential association with surviving in concrete or contributing to crack prevention or healing. The major findings are:

- In the *Bacillus subtilis* samples, 99% of sequences were classified to the *Bacillus* genus and 97.4% were classified to the *Bacillus subtilis* species group. This was expected and validates our sequencing and classification approach.

- The non-axenic soil bacteria samples had a more diverse microbial community with more types of bacteria present. Genera typical of soil microbiomes were identified, with some of the most dominant genera including *Acinetobacter, Citrobacter,* and *Aeromonas.* In soil samples, the *Bacillus* genus was present, but at low relative abundance. *Citrobacter* are previously known to be associated with biocementation, and *Acinetobacter* and *Aeromonas* have been used previously in heavy metal bioremediation where they survive harsh conditions.

- Sporulation media had no impact on axenic *B. sub* classification. The impact of sporulation media on soil microbiomes was not tested.

- Storage time in dried samples prepared for incorporation into concrete or mortar cubes had no discernable impact on *B. sub* microbiomes at day 1, 7, or 14. Storage time had very little impact on microbiomes in soil samples: after a decrease in *Aeromonas* from day 1, the

microbial community was more stable over days 7, 14, and 28 where the most dominant genera remained present but at slightly different relative abundances.

- In soil samples, a lower concentration of nutrient broth (to save costs and encourage sporulation) increased relative abundance of *Aeromonas* while higher concentration of nutrient broth resulted in higher relative abundances of *Acinetobacter* and *Citrobacter*. In soil samples, adding urea to nutrient broth (to increase urease activity and therefore biomineralization potential) increased the abundance of *Raoultella, Stenotrophomonas*, and *Serratia*, as was previously observed for *Raoultella* and *Stenotrophomonas.*

10.4 Appendix D associated R script for analysis and visualization:

```
setwd("~/R")

# my colors
mypal <- c("#E64B35FF","#4DBBD5FF", "#00A087FF", "#3C5488FF", "#F39B7FFF", "#8491B4FF", "#91D1C2FF", "#DC0000FF",
  "#7E6148FF","#B09C85FF",
        "#BC3C29FF", "#0072B5FF", "#E18727FF", "#20854EFF", "#7876B1FF" ,"#6F99ADFF", "#FFDC91FF", "#EE4C97FF",
  "#4DAAD5FF","#E17960FF",
        "#FFAB18FF","#AAAB18FF")

# View(ord_sample_env_rep) # Notice that every time you run a new series, ord_sample_env_rep should be viewed to check the order
# 1. Abundance plot for Genus
library(ggplot2)
library(readxl)
abun_genus_r <- data.frame(read_xls("abun_genus.xls"))
sample_env <- data.frame(read_xls("aggregated_counts_env.xls"))

# 1) Bsub - sporulation experiment
library(dplyr)
sample_env_specific <- sample_env[c(5,6),]
abun_genus_specific <- abun_genus_r[c(5,6),]
sample_env_rep <-bind_rows(replicate(ncol(abun_genus_specific)-1, sample_env_specific, simplify = FALSE))
ord <- (order(sample_env_rep[,1]))
ord_sample_env_rep<-sample_env_rep[ord,]
rownames(ord_sample_env_rep) <- c(1:nrow(ord_sample_env_rep))
abun_genus_specific1 <- abun_genus_specific[,-1]
abun_matrix <- as.matrix(abun_genus_specific1)
abun_vector <- data.frame(as.vector(t(abun_matrix)))
colnames(abun_vector)<-"Abundance"
abun_genus_specific2 <- data.frame(t(abun_genus_specific))
Genus <- data.frame(rownames(abun_genus_specific2[-1,]))
colnames(Genus)<-"Genus"
Genus_rep <-bind_rows(replicate(nrow(abun_genus_specific), Genus, simplify = FALSE))
rownames(Genus_rep)<-c(1:nrow(Genus_rep))
sample_env_abun <- data.frame(c(ord_sample_env_rep, Genus_rep, abun_vector))
sumlist <- aggregate(sample_env_abun$Abundance, by=list(type=sample_env_abun$barcode),sum) # sum all abundance for each barcode
  (=barplot)
sumlist_rep <- bind_rows(replicate(nrow(Genus), sumlist, simplify = FALSE))
ord <- (order(sumlist_rep[,1]))
sumlist_rep<-sumlist_rep[ord,]
rownames(sumlist_rep) <- c(1:nrow(sumlist_rep))
sumlist_rep<-data.frame(sumlist_rep)
RelativeAbundance <- data.frame(sample_env_abun$Abundance/sumlist_rep$x)
colnames(RelativeAbundance)<-"RelativeAbundance"
sample_env_abun <- data.frame(c(sample_env_abun,RelativeAbundance))
sample_env_abun_simple<-sample_env_abun
sample_env_abun_simple$Genus[sample_env_abun$RelativeAbundance < 0.02] <- "Genus < 2%" #rename Genus with < 2% abundance
# change the color manually
fct<-levels(factor(sample_env_abun_simple$Genus))
fct
colors.set <- c("Bacillus" = mypal[1], "Genus < 2%" = mypal[2])
nrow(data.frame(fct)) == nrow(data.frame(colors.set))
# barplot
p<-ggplot(data=sample_env_abun_simple,aes(x=label,y=RelativeAbundance*100,fill=Genus))+
  geom_bar(aes(),stat="identity",position="stack") +
 scale_fill_manual(values = colors.set,drop=F)
figureF1<- p+ theme_bw() +
  theme(axis.title.x = element_text(size = 16)) +theme(axis.title.y = element_text(size = 16)) + theme(axis.text=element_text(size=14)) +
  theme(legend.title = element_text(size = 16.0)) + theme(legend.text = element_text(size = 16.0)) + theme(strip.text = element_text(size = 16,
  color = "black")) +
  xlab("(A)") + ylab("Relative Abundance(%)")+
  # ggtitle("Bsub - sporulation experiment") +
  theme(plot.title = element_text(hjust = 0.5,size = 16)) + theme(text = element_text("serif"))
svg(file="figureF1.svg", height = 5, width =6 );
figureF1
dev.off()

View(sample_env_abun_simple)
```

```
# 2) 24 hr 0.5xNB experiment - genus level
library(dplyr)
sample_env_specific <- sample_env[c(10:13),]
abun_genus_specific <- abun_genus_r[c(10:13),]
# sample_env_specific <- sample_env[c(11,13,10,12),]
# abun_genus_specific <- abun_genus_r[c(11,13,10,12),]
sample_env_rep <-bind_rows(replicate(ncol(abun_genus_specific)-1, sample_env_specific, simplify = FALSE))
ord <- (order(sample_env_rep[,1]))
ord_sample_env_rep<-sample_env_rep[ord,]
rownames(ord_sample_env_rep) <- c(1:nrow(ord_sample_env_rep))
abun_genus_specific1 <- abun_genus_specific[,-1]
abun_matrix <- as.matrix(abun_genus_specific1)
abun_vector <- data.frame(as.vector(t(abun_matrix)))
colnames(abun_vector)<-"Abundance"
abun_genus_specific2 <- data.frame(t(abun_genus_specific))
Genus <- data.frame(rownames(abun_genus_specific2[-1,]))
colnames(Genus)<-"Genus"
Genus_rep <-bind_rows(replicate(nrow(abun_genus_specific), Genus, simplify = FALSE))
rownames(Genus_rep)<-c(1:nrow(Genus_rep))
sample_env_abun <- data.frame(c(ord_sample_env_rep, Genus_rep, abun_vector))
sumlist <- aggregate(sample_env_abun$Abundance, by=list(type=sample_env_abun$barcode),sum)
sumlist_rep <- bind_rows(replicate(nrow(Genus), sumlist, simplify = FALSE))
ord <- (order(sumlist_rep[,1]))
sumlist_rep<-sumlist_rep[ord,]
rownames(sumlist_rep) <- c(1:nrow(sumlist_rep))
sumlist_rep<-data.frame(sumlist_rep)
RelativeAbundance <- data.frame(sample_env_abun$Abundance/sumlist_rep$x)
colnames(RelativeAbundance)<-"RelativeAbundance"
sample_env_abun <- data.frame(c(sample_env_abun,RelativeAbundance))
sample_env_abun_simple<-sample_env_abun
sample_env_abun_simple$Genus[sample_env_abun$RelativeAbundance < 0.02] <- "Genus < 2%"
fct<-levels(factor(sample_env_abun_simple$Genus))
fct
colors.set <- c("Acinetobacter" = mypal[3], "Aeromonas" = mypal[4],"Bacillus" = mypal[1],
                "Buttiauxella" = mypal[5], "Citrobacter" = mypal[6], "Comamonas" = mypal[7],
                "Genus < 2%" = mypal[2], "Pseudomonas" = mypal[8])
nrow(data.frame(fct)) == nrow(data.frame(colors.set))
sample_env_abun_simple$Microbe.Name <-sample_env_abun_simple$Microbe
sample_env_abun_simple$Microbe.Name[sample_env_abun_simple$Microbe == "Bsub"] <-"Bsud(37 C)"
sample_env_abun_simple$Microbe.Name[sample_env_abun_simple$Microbe == "Soil"] <-"Soil(25 C)"
p<-ggplot(data=sample_env_abun_simple,aes(x=label,y=RelativeAbundance*100,fill=Genus))+
  geom_bar(aes(),stat="identity",position="stack") +
  facet_grid(cols=vars(Microbe.Name),scale="free_x")
p <- p + scale_fill_manual(values = colors.set,drop=F)
figureF2<- p+ theme_bw() +
  theme(axis.title.x = element_text(size = 16)) +theme(axis.title.y = element_text(size = 16)) + theme(axis.text=element_text(size=14)) +
  theme(legend.title = element_text(size = 16.0)) + theme(legend.text = element_text(size = 16.0)) + theme(strip.text = element_text(size = 16,
  color = "black")) +
  xlab("24hr 0.5xNB (A)") + ylab("Relative Abundance(%)")+
  # ggtitle("24 hr 0.5xNB experiment - genus level") +
  theme(plot.title = element_text(hjust = 0.5,size = 16)) + theme(text = element_text("serif"))
svg(file="figureF2.svg", height = 5, width =6 );
figureF2
dev.off()

# 3) Storage life experiment - genus level
library(dplyr)
sample_env_specific <- sample_env[c(1:4,7:8),]
abun_genus_specific <- abun_genus_r[c(1:4,7:8),]
sample_env_rep <-bind_rows(replicate(ncol(abun_genus_specific)-1, sample_env_specific, simplify = FALSE))
ord <- (order(sample_env_rep[,1]))
ord_sample_env_rep<-sample_env_rep[ord,]
rownames(ord_sample_env_rep) <- c(1:nrow(ord_sample_env_rep))
ord_sample_env_rep$label1 <- factor(ord_sample_env_rep$label1,levels = c("1d","7d","14d","28d"))
abun_genus_specific1 <- abun_genus_specific[,-1]
abun_matrix <- as.matrix(abun_genus_specific1)
abun_vector <- data.frame(as.vector(t(abun_matrix)))
colnames(abun_vector)<-"Abundance"
abun_genus_specific2 <- data.frame(t(abun_genus_specific))
```

```
Genus <- data.frame(rownames(abun_genus_specific2[-1,]))
colnames(Genus)<-"Genus"
Genus_rep <-bind_rows(replicate(nrow(abun_genus_specific), Genus, simplify = FALSE))
rownames(Genus_rep)<-c(1:nrow(Genus_rep))
sample_env_abun <- data.frame(c(ord_sample_env_rep, Genus_rep, abun_vector))
sumlist <- aggregate(sample_env_abun$Abundance, by=list(type=sample_env_abun$barcode),sum)
sumlist_rep <- bind_rows(replicate(nrow(Genus), sumlist, simplify = FALSE))
ord <- (order(sumlist_rep[,1]))
sumlist_rep<-sumlist_rep[ord,]
rownames(sumlist_rep) <- c(1:nrow(sumlist_rep))
sumlist_rep<-data.frame(sumlist_rep)
RelativeAbundance <- data.frame(sample_env_abun$Abundance/sumlist_rep$x)
colnames(RelativeAbundance)<-"RelativeAbundance"
sample_env_abun <- data.frame(c(sample_env_abun,RelativeAbundance))
sample_env_abun_simple<-sample_env_abun
sample_env_abun_simple$Genus[sample_env_abun$RelativeAbundance < 0.02] <- "Genus < 2%"
sample_env_abun_simple$label <- factor(sample_env_abun_simple$label,levels = c("1d","7d","14d","28d"))  # change the order of x-axis
fct<-levels(factor(sample_env_abun_simple$Genus))
fct
colors.set <- c("Acinetobacter" = mypal[3], "Bacillus" = mypal[1],
                "Citrobacter" = mypal[6], "Comamonas" = mypal[7], "Exiguobacterium" = mypal[9],
                "Genus < 2%" = mypal[2], "Klebsiella" = mypal[10], "Lysinibacillus" =  mypal[14],
                "Pseudomonas" = mypal[8],
                "Raoultella" =  mypal[12], "Serratia" =  mypal[13], "Stenotrophomonas" =  mypal[11],
                "Yokenella" =  mypal[15])
nrow(data.frame(fct)) == nrow(data.frame(colors.set))
p<-ggplot(data=sample_env_abun_simple,aes(x=label,y=RelativeAbundance*100,fill=Genus))+
  geom_bar(aes(),stat="identity",position="stack") +
  facet_grid(cols=vars(Microbe),scale="free_x") +
scale_fill_manual(values = colors.set,drop=F)
figureF3<- p+ theme_bw() +
  theme(axis.title.x = element_text(size = 16)) +theme(axis.title.y = element_text(size = 16)) + theme(axis.text=element_text(size=14)) +
  theme(legend.title = element_text(size = 16.0)) + theme(legend.text = element_text(size = 16.0)) + theme(strip.text = element_text(size = 16,
  color = "black")) +
  xlab("(A)") + ylab("Relative Abundance(%)")+
  # ggtitle("Storage life experiment - genus level") +
  theme(plot.title = element_text(hjust = 0.5,size = 16)) + theme(text = element_text("serif"))
svg(file="figureF3.svg", height = 5, width =6 );
figureF3
dev.off()

# 4) Storage life experiment - genus level
library(dplyr)
sample_env_specific <- sample_env[c(10,12,4,7:8),]
abun_genus_specific <- abun_genus_r[c(10,12,4,7:8),]
sample_env_rep <-bind_rows(replicate(ncol(abun_genus_specific)-1, sample_env_specific, simplify = FALSE))
ord <- (order(sample_env_rep[,1]))
ord_sample_env_rep<-sample_env_rep[ord,]
rownames(ord_sample_env_rep) <- c(1:nrow(ord_sample_env_rep))
abun_genus_specific1 <- abun_genus_specific[,-1]
abun_matrix <- as.matrix(abun_genus_specific1)
abun_vector <- data.frame(as.vector(t(abun_matrix)))
colnames(abun_vector)<-"Abundance"
abun_genus_specific2 <- data.frame(t(abun_genus_specific))
Genus <- data.frame(rownames(abun_genus_specific2[-1,]))
colnames(Genus)<-"Genus"
Genus_rep <-bind_rows(replicate(nrow(abun_genus_specific), Genus, simplify = FALSE))
rownames(Genus_rep)<-c(1:nrow(Genus_rep))
sample_env_abun <- data.frame(c(ord_sample_env_rep, Genus_rep, abun_vector))
sumlist <- aggregate(sample_env_abun$Abundance, by=list(type=sample_env_abun$barcode),sum)
sumlist_rep <- bind_rows(replicate(nrow(Genus), sumlist, simplify = FALSE))
ord <- (order(sumlist_rep[,1]))
sumlist_rep<-sumlist_rep[ord,]
rownames(sumlist_rep) <- c(1:nrow(sumlist_rep))
sumlist_rep<-data.frame(sumlist_rep)
RelativeAbundance <- data.frame(sample_env_abun$Abundance/sumlist_rep$x)
colnames(RelativeAbundance)<-"RelativeAbundance"
sample_env_abun <- data.frame(c(sample_env_abun,RelativeAbundance))
sample_env_abun_simple<-sample_env_abun
sample_env_abun_simple$Genus[sample_env_abun$RelativeAbundance < 0.02] <- "Genus < 2%"
```

```
sample_env_abun_simple$label2 <- factor(sample_env_abun_simple$label2,levels = c("1d(a)","1d(b)","7d","14d","28d"))
fct<-levels(factor(sample_env_abun_simple$Genus))
fct
colors.set <- c("Acinetobacter" = mypal[3], "Aeromonas" = mypal[4], "Bacillus" = mypal[1],
                "Buttiauxella" = mypal[5], "Citrobacter" = mypal[6], "Comamonas" = mypal[7],
                "Exiguobacterium" = mypal[9], "Genus < 2%" = mypal[2],
                "Klebsiella" = mypal[10], "Lysinibacillus" =  mypal[14], "Pseudomonas" = mypal[8],
                "Raoultella" =  mypal[12], "Serratia" =  mypal[13], "Stenotrophomonas" =  mypal[11],
                "Yokenella" =  mypal[15])
nrow(data.frame(fct)) == nrow(data.frame(colors.set))
p<-ggplot(data=sample_env_abun_simple,aes(x=label2,y=RelativeAbundance*100,fill=Genus))+
  geom_bar(aes(),stat="identity",position="stack")
p<-p+ scale_fill_manual(values = colors.set,drop=F)
figureF4<- p+ theme_bw() +
  theme(axis.title.x = element_text(size = 16)) +theme(axis.title.y = element_text(size = 16)) + theme(axis.text=element_text(size=14)) +
  theme(legend.title = element_text(size = 16.0)) + theme(legend.text = element_text(size = 16.0)) + theme(strip.text = element_text(size = 16,
  color = "black")) +
  xlab("(A)") + ylab("Relative Abundance(%)")+
  # ggtitle("Storage life experiment - genus level") +
  theme(plot.title = element_text(hjust = 0.5,size = 16)) + theme(text = element_text("serif"))
svg(file="figureF4.svg", height = 5, width =6 );
figureF4
dev.off()

# 5) Impact of growth media on soil samples
library(dplyr)
sample_env_specific <- sample_env[c(14:16,9),]
abun_genus_specific <- abun_genus_r[c(14:16,9),]

# sample_env_specific <- sample_env[c(9,16,15,14),]
# rownames(sample_env_specific) <- c(1:4)#
# ns<-data.frame(rownames(sample_env_specific))#
# sample_env_specific <- data.frame(c(ns, sample_env_specific))#
# abun_genus_specific <- abun_genus_r[c(9,16,15,14),]

sample_env_rep <-bind_rows(replicate(ncol(abun_genus_specific)-1, sample_env_specific, simplify = FALSE))
ord <- (order(sample_env_rep[,1]))
ord_sample_env_rep<-sample_env_rep[ord,]
# View(ord_sample_env_rep)
rownames(ord_sample_env_rep) <- c(1:nrow(ord_sample_env_rep))
ord_sample_env_rep$label <- factor(ord_sample_env_rep$label)
ord_sample_env_rep$label2 <- factor(ord_sample_env_rep$label2)
abun_genus_specific1 <- abun_genus_specific[,-1]
abun_matrix <- as.matrix(abun_genus_specific1)
abun_vector <- data.frame(as.vector(t(abun_matrix)))
colnames(abun_vector)<-"Abundance"
abun_genus_specific2 <- data.frame(t(abun_genus_specific))
Genus <- data.frame(rownames(abun_genus_specific2[-1,]))
colnames(Genus)<-"Genus"
Genus_rep <-bind_rows(replicate(nrow(abun_genus_specific), Genus, simplify = FALSE))
rownames(Genus_rep)<-c(1:nrow(Genus_rep))
sample_env_abun <- data.frame(c(ord_sample_env_rep, Genus_rep, abun_vector))
sumlist <- aggregate(sample_env_abun$Abundance, by=list(type=sample_env_abun$barcode),sum)
sumlist_rep <- bind_rows(replicate(nrow(Genus), sumlist, simplify = FALSE))
ord <- (order(sumlist_rep[,1]))
sumlist_rep<-sumlist_rep[ord,]
rownames(sumlist_rep) <- c(1:nrow(sumlist_rep))
sumlist_rep<-data.frame(sumlist_rep)
RelativeAbundance <- data.frame(sample_env_abun$Abundance/sumlist_rep$x)
colnames(RelativeAbundance)<-"RelativeAbundance"
sample_env_abun <- data.frame(c(sample_env_abun,RelativeAbundance))
sample_env_abun_simple<-sample_env_abun
sample_env_abun_simple$Genus[sample_env_abun$RelativeAbundance < 0.02] <- "Genus < 2%"
fct<-levels(factor(sample_env_abun_simple$Genus))
fct
colors.set <- c("Acinetobacter" = mypal[3], "Aeromonas" = mypal[4], "Bacillus" = mypal[1],
                "Buttiauxella" = mypal[5], "Citrobacter" = mypal[6], "Comamonas" = mypal[7],
                "Genus < 2%" = mypal[2],
                # "Klebsiella" = mypal[10],
                "Lysinibacillus" =  mypal[14],
```

```
            "Myroides" = mypal[16], "Pseudochrobactrum" = mypal[17],
            "Pseudomonas" = mypal[8],
            "Raoultella" =  mypal[12], "Serratia" =  mypal[13], "Stenotrophomonas" =  mypal[11])
nrow(data.frame(fct)) == nrow(data.frame(colors.set))
p<-ggplot(data=sample_env_abun_simple,aes(x=label,y=RelativeAbundance*100,fill=Genus))+
  geom_bar(aes(),stat="identity",position="stack")
p<-p+  facet_grid(cols=vars(label2),scale="free_x")
p<-p+  scale_fill_manual(values = colors.set,drop=F)
figureF5<- p+ theme_bw() +
  theme(axis.title.x = element_text(size = 16)) +theme(axis.title.y = element_text(size = 16)) + theme(axis.text=element_text(size=14)) +
  theme(legend.title = element_text(size = 16.0)) + theme(legend.text = element_text(size = 16.0)) + theme(strip.text = element_text(size = 16,
  color = "black")) +
  xlab("(A)") + ylab("Relative Abundance(%)")+
  # ggtitle("Impact of growth media on soil samples") +
  theme(plot.title = element_text(hjust = 0.5,size = 16)) + theme(text = element_text("serif"))
svg(file="figureF5.svg", height = 5, width = 8 );
figureF5
dev.off()


# 6) Storage life experiment - genus level
library(dplyr)
sample_env_specific <- sample_env[c(10,12,15),]
abun_genus_specific <- abun_genus_r[c(10,12,15),]
# sample_env_specific <- sample_env[c(10,12,14,15),]
# abun_genus_specific <- abun_genus_r[c(10,12,14,15),]
sample_env_rep <-bind_rows(replicate(ncol(abun_genus_specific)-1, sample_env_specific, simplify = FALSE))
ord <- (order(sample_env_rep[,1]))
ord_sample_env_rep<-sample_env_rep[ord,]
rownames(ord_sample_env_rep) <- c(1:nrow(ord_sample_env_rep))
ord_sample_env_rep$label <- factor(ord_sample_env_rep$label)
ord_sample_env_rep$label2 <- factor(ord_sample_env_rep$label2)
abun_genus_specific1 <- abun_genus_specific[,-1]
abun_matrix <- as.matrix(abun_genus_specific1)
abun_vector <- data.frame(as.vector(t(abun_matrix)))
colnames(abun_vector)<-"Abundance"
abun_genus_specific2 <- data.frame(t(abun_genus_specific))
Genus <- data.frame(rownames(abun_genus_specific2[-1,]))
colnames(Genus)<-"Genus"
Genus_rep <-bind_rows(replicate(nrow(abun_genus_specific), Genus, simplify = FALSE))
rownames(Genus_rep)<-c(1:nrow(Genus_rep))
sample_env_abun <- data.frame(c(ord_sample_env_rep, Genus_rep, abun_vector))
sumlist <- aggregate(sample_env_abun$Abundance, by=list(type=sample_env_abun$barcode),sum)
sumlist_rep <- bind_rows(replicate(nrow(Genus), sumlist, simplify = FALSE))
ord <- (order(sumlist_rep[,1]))
sumlist_rep<-sumlist_rep[ord,]
rownames(sumlist_rep) <- c(1:nrow(sumlist_rep))
sumlist_rep<-data.frame(sumlist_rep)
RelativeAbundance <- data.frame(sample_env_abun$Abundance/sumlist_rep$x)
colnames(RelativeAbundance)<-"RelativeAbundance"
sample_env_abun <- data.frame(c(sample_env_abun,RelativeAbundance))
sample_env_abun_simple<-sample_env_abun
sample_env_abun_simple$Genus[sample_env_abun$RelativeAbundance < 0.02] <- "Genus < 2%"
fct<-levels(factor(sample_env_abun_simple$Genus))
fct
colors.set <- c("Acinetobacter" = mypal[3], "Aeromonas" = mypal[4], "Bacillus" = mypal[1],
            "Buttiauxella" = mypal[5], "Citrobacter" = mypal[6], "Comamonas" = mypal[7],
            "Genus < 2%" = mypal[2],
            "Myroides" = mypal[16], "Pseudochrobactrum" = mypal[17],
            "Pseudomonas" = mypal[8],
            "Raoultella" =  mypal[12], "Serratia" =  mypal[13], "Stenotrophomonas" =  mypal[11])#,
nrow(data.frame(fct)) == nrow(data.frame(colors.set))
p<-ggplot(data=sample_env_abun_simple,aes(x=label,y=RelativeAbundance*100,fill=Genus))+
  geom_bar(aes(),stat="identity",position="stack")
p<-p+  facet_grid(cols=vars(label3),scale="free_x")
p<-p+  scale_fill_manual(values = colors.set,drop=F)
figureF6<- p+ theme_bw() +
  theme(axis.title.x = element_text(size = 16)) +theme(axis.title.y = element_text(size = 16)) + theme(axis.text=element_text(size=14)) +
  theme(legend.title = element_text(size = 16.0)) + theme(legend.text = element_text(size = 16.0)) + theme(strip.text = element_text(size = 16,
  color = "black")) +
```

```
  xlab("(A)") + ylab("Relative Abundance(%)")+
  # ggtitle("Storage life experiment - genus level") +
  theme(plot.title = element_text(hjust = 0.5,size = 16)) + theme(text = element_text("serif"))
svg(file="figureF6.svg", height = 5, width =8 );
figureF6
dev.off()
```

2. Abundance plot for Phylum

```
# library(ggplot2)
# library(readxl)
# abun_Phylum_r <- data.frame(read_xls("abun_phylum.xls"))
# sample_env <- data.frame(read_xls("aggregated_counts_env.xls"))
#
# # 1) Bsub - sporulation experiment
# library(dplyr)
# sample_env_specific <- sample_env[c(6,5),]
# abun_Phylum_specific <- abun_Phylum_r[c(6,5),]
# sample_env_rep <-bind_rows(replicate(ncol(abun_Phylum_specific)-1, sample_env_specific, simplify = FALSE))
# ord <- (order(sample_env_rep[,1]))
# ord_sample_env_rep<-sample_env_rep[ord,]
# rownames(ord_sample_env_rep) <- c(1:nrow(ord_sample_env_rep))
# abun_Phylum_specific1 <- abun_Phylum_specific[,-1]
# abun_matrix <- as.matrix(abun_Phylum_specific1)
# abun_vector <- data.frame(as.vector(t(abun_matrix)))
# colnames(abun_vector)<-"Abundance"
# abun_Phylum_specific2 <- data.frame(t(abun_Phylum_specific))
# Phylum <- data.frame(rownames(abun_Phylum_specific2[-1,]))
# colnames(Phylum)<-"Phylum"
# Phylum_rep <-bind_rows(replicate(nrow(abun_Phylum_specific), Phylum, simplify = FALSE))
# rownames(Phylum_rep)<-c(1:nrow(Phylum_rep))
# sample_env_abun <- data.frame(c(ord_sample_env_rep, Phylum_rep, abun_vector))
# sumlist <- aggregate(sample_env_abun$Abundance, by=list(type=sample_env_abun$barcode),sum)
# sumlist_rep <- bind_rows(replicate(nrow(Phylum), sumlist, simplify = FALSE))
# ord <- (order(sumlist_rep[,1]))
# sumlist_rep<-sumlist_rep[ord,]
# rownames(sumlist_rep) <- c(1:nrow(sumlist_rep))
# sumlist_rep<-data.frame(sumlist_rep)
# RelativeAbundance <- data.frame(sample_env_abun$Abundance/sumlist_rep$x)
# colnames(RelativeAbundance)<-"RelativeAbundance"
# sample_env_abun <- data.frame(c(sample_env_abun,RelativeAbundance))
# sample_env_abun_simple<-sample_env_abun
# fct<-levels(factor(sample_env_abun_simple$Phylum))
# fct
# colors.set <- c("Actinobacteria" = mypal[1],
#                 "Bacteroidetes"  = mypal[2],
#                 "Balneolaeota"  = mypal[3],
#                 "Chloroflexi"  = mypal[4],
#                 "Firmicutes"  = mypal[5],
#                 "Proteobacteria" = mypal[6])
# nrow(data.frame(fct)) == nrow(data.frame(colors.set))
# p<-ggplot(data=sample_env_abun_simple,aes(x=label,y=RelativeAbundance*100,fill=Phylum))+
#   geom_bar(aes(),stat="identity",position="stack") +
#   scale_fill_manual(values = colors.set,drop=F)
# figureFP1<- p+ theme_bw() +
#   theme(axis.title.x = element_text(size = 16)) +theme(axis.title.y = element_text(size = 16)) + theme(axis.text=element_text(size=12)) +
#   theme(legend.title = element_text(size = 16.0)) + theme(legend.text = element_text(size = 16.0)) + theme(strip.text = element_text(size = 16,
  color = "black")) +
#   xlab("Description") + ylab("Relative Abundance(%)")+
#   # ggtitle("Bsub - sporulation experiment") +
#   theme(plot.title = element_text(hjust = 0.5,size = 16)) + theme(text = element_text("serif"))
# svg(file="figureFP1.svg", height = 5, width =6 );
# figureFP1
# dev.off()
#
# # 2) 24 hr 0.5xNB experiment - Phylum level
# library(dplyr)
# sample_env_specific <- sample_env[c(11,13,10,12),]
# abun_Phylum_specific <- abun_Phylum_r[c(11,13,10,12),]
# sample_env_rep <-bind_rows(replicate(ncol(abun_Phylum_specific)-1, sample_env_specific, simplify = FALSE))
# ord <- (order(sample_env_rep[,1]))
```

```
# ord_sample_env_rep<-sample_env_rep[ord,]
# rownames(ord_sample_env_rep) <- c(1:nrow(ord_sample_env_rep))
# abun_Phylum_specific1 <- abun_Phylum_specific[,-1]
# abun_matrix <- as.matrix(abun_Phylum_specific1)
# abun_vector <- data.frame(as.vector(t(abun_matrix)))
# colnames(abun_vector)<-"Abundance"
# abun_Phylum_specific2 <- data.frame(t(abun_Phylum_specific))
# Phylum <- data.frame(rownames(abun_Phylum_specific2[-1,]))
# colnames(Phylum)<-"Phylum"
# Phylum_rep <-bind_rows(replicate(nrow(abun_Phylum_specific), Phylum, simplify = FALSE))
# rownames(Phylum_rep)<-c(1:nrow(Phylum_rep))
# sample_env_abun <- data.frame(c(ord_sample_env_rep, Phylum_rep, abun_vector))
# sumlist <- aggregate(sample_env_abun$Abundance, by=list(type=sample_env_abun$barcode),sum)
# sumlist_rep <- bind_rows(replicate(nrow(Phylum), sumlist, simplify = FALSE))
# ord <- (order(sumlist_rep[,1]))
# sumlist_rep<-sumlist_rep[ord,]
# rownames(sumlist_rep) <- c(1:nrow(sumlist_rep))
# sumlist_rep<-data.frame(sumlist_rep)
# RelativeAbundance <- data.frame(sample_env_abun$Abundance/sumlist_rep$x)
# colnames(RelativeAbundance)<-"RelativeAbundance"
# sample_env_abun <- data.frame(c(sample_env_abun,RelativeAbundance))
# sample_env_abun_simple<-sample_env_abun
# fct<-levels(factor(sample_env_abun_simple$Phylum))
# fct
# colors.set <- c("Actinobacteria" = mypal[1],
#                 "Bacteroidetes"  = mypal[2],
#                 "Balneolaeota"  = mypal[3],
#                 "Chloroflexi"  = mypal[4],
#                 "Firmicutes"  = mypal[5],
#                 "Proteobacteria" = mypal[6])
# nrow(data.frame(fct)) == nrow(data.frame(colors.set))
# p<-ggplot(data=sample_env_abun_simple,aes(x=label,y=RelativeAbundance*100,fill=Phylum))+
#   geom_bar(aes(),stat="identity",position="stack") +
#   facet_grid(cols=vars(Microbe),scale="free_x")
# p <- p + scale_fill_manual(values = colors.set,drop=F)
# figureFP2<- p+ theme_bw() +
#   theme(axis.title.x = element_text(size = 16)) +theme(axis.title.y = element_text(size = 16)) + theme(axis.text=element_text(size=12)) +
#   theme(legend.title = element_text(size = 16.0)) + theme(legend.text = element_text(size = 16.0)) + theme(strip.text = element_text(size = 16,
  color = "black")) +
#   xlab("Description") + ylab("Relative Abundance(%)")+
#   # ggtitle("24 hr 0.5xNB experiment - Phylum level") +
#   theme(plot.title = element_text(hjust = 0.5,size = 16)) + theme(text = element_text("serif"))
# svg(file="figureFP2.svg", height = 5, width =6 );
# figureFP2
# dev.off()
#
# # 3) Storage life experiment - Phylum level
# library(dplyr)
# sample_env_specific <- sample_env[c(1:4,7:8),]
# abun_Phylum_specific <- abun_Phylum_r[c(1:4,7:8),]
# sample_env_rep <-bind_rows(replicate(ncol(abun_Phylum_specific)-1, sample_env_specific, simplify = FALSE))
# ord <- (order(sample_env_rep[,1]))
# ord_sample_env_rep<-sample_env_rep[ord,]
# rownames(ord_sample_env_rep) <- c(1:nrow(ord_sample_env_rep))
# ord_sample_env_rep$label1 <- factor(ord_sample_env_rep$label1,levels = c("1d","7d","14d","28d"))
# abun_Phylum_specific1 <- abun_Phylum_specific[,-1]
# abun_matrix <- as.matrix(abun_Phylum_specific1)
# abun_vector <- data.frame(as.vector(t(abun_matrix)))
# colnames(abun_vector)<-"Abundance"
# abun_Phylum_specific2 <- data.frame(t(abun_Phylum_specific))
# Phylum <- data.frame(rownames(abun_Phylum_specific2[-1,]))
# colnames(Phylum)<-"Phylum"
# Phylum_rep <-bind_rows(replicate(nrow(abun_Phylum_specific), Phylum, simplify = FALSE))
# rownames(Phylum_rep)<-c(1:nrow(Phylum_rep))
# sample_env_abun <- data.frame(c(ord_sample_env_rep, Phylum_rep, abun_vector))
# sumlist <- aggregate(sample_env_abun$Abundance, by=list(type=sample_env_abun$barcode),sum)
# sumlist_rep <- bind_rows(replicate(nrow(Phylum), sumlist, simplify = FALSE))
# ord <- (order(sumlist_rep[,1]))
# sumlist_rep<-sumlist_rep[ord,]
# rownames(sumlist_rep) <- c(1:nrow(sumlist_rep))
```

```
# sumlist_rep<-data.frame(sumlist_rep)
# RelativeAbundance <- data.frame(sample_env_abun$Abundance/sumlist_rep$x)
# colnames(RelativeAbundance)<-"RelativeAbundance"
# sample_env_abun <- data.frame(c(sample_env_abun,RelativeAbundance))
# sample_env_abun_simple<-sample_env_abun
# sample_env_abun_simple$label <- factor(sample_env_abun_simple$label,levels = c("1d","7d","14d","28d"))
# fct<-levels(factor(sample_env_abun_simple$Phylum))
# fct
# colors.set <- c("Actinobacteria" = mypal[1],
#                 "Bacteroidetes"  = mypal[2],
#                 "Balneolaeota"  = mypal[3],
#                 "Chloroflexi"  = mypal[4],
#                 "Firmicutes"  = mypal[5],
#                 "Proteobacteria" = mypal[6])
# nrow(data.frame(fct)) == nrow(data.frame(colors.set))
# p<-ggplot(data=sample_env_abun_simple,aes(x=label,y=RelativeAbundance*100,fill=Phylum))+
#   geom_bar(aes(),stat="identity",position="stack") +
#   facet_grid(cols=vars(Microbe),scale="free_x") +
#   scale_fill_manual(values = colors.set,drop=F)
# figureFP3<- p+ theme_bw() +
#   theme(axis.title.x = element_text(size = 16)) +theme(axis.title.y = element_text(size = 16)) + theme(axis.text=element_text(size=12)) +
#   theme(legend.title = element_text(size = 16.0)) + theme(legend.text = element_text(size = 16.0)) + theme(strip.text = element_text(size = 16,
  color = "black")) +
#   xlab("Description") + ylab("Relative Abundance(%)")+
#   # ggtitle("Storage life experiment - Phylum level") +
#   theme(plot.title = element_text(hjust = 0.5,size = 16)) + theme(text = element_text("serif"))
# svg(file="figureFP3.svg", height = 5, width =6 );
# figureFP3
# dev.off()
#
# # 4) Storage life experiment - Phylum level
# library(dplyr)
# sample_env_specific <- sample_env[c(10,12,4,7:8),]
# abun_Phylum_specific <- abun_Phylum_r[c(10,12,4,7:8),]
# sample_env_rep <-bind_rows(replicate(ncol(abun_Phylum_specific)-1, sample_env_specific, simplify = FALSE))
# ord <- (order(sample_env_rep[,1]))
# ord_sample_env_rep<-sample_env_rep[ord,]
# rownames(ord_sample_env_rep) <- c(1:nrow(ord_sample_env_rep))
# abun_Phylum_specific1 <- abun_Phylum_specific[,-1]
# abun_matrix <- as.matrix(abun_Phylum_specific1)
# abun_vector <- data.frame(as.vector(t(abun_matrix)))
# colnames(abun_vector)<-"Abundance"
# abun_Phylum_specific2 <- data.frame(t(abun_Phylum_specific))
# Phylum <- data.frame(rownames(abun_Phylum_specific2[-1,]))
# colnames(Phylum)<-"Phylum"
# Phylum_rep <-bind_rows(replicate(nrow(abun_Phylum_specific), Phylum, simplify = FALSE))
# rownames(Phylum_rep)<-c(1:nrow(Phylum_rep))
# sample_env_abun <- data.frame(c(ord_sample_env_rep, Phylum_rep, abun_vector))
# sumlist <- aggregate(sample_env_abun$Abundance, by=list(type=sample_env_abun$barcode),sum)
# sumlist_rep <- bind_rows(replicate(nrow(Phylum), sumlist, simplify = FALSE))
# ord <- (order(sumlist_rep[,1]))
# sumlist_rep<-sumlist_rep[ord,]
# rownames(sumlist_rep) <- c(1:nrow(sumlist_rep))
# sumlist_rep<-data.frame(sumlist_rep)
# RelativeAbundance <- data.frame(sample_env_abun$Abundance/sumlist_rep$x)
# colnames(RelativeAbundance)<-"RelativeAbundance"
# sample_env_abun <- data.frame(c(sample_env_abun,RelativeAbundance))
# sample_env_abun_simple<-sample_env_abun
# sample_env_abun_simple$label2 <- factor(sample_env_abun_simple$label2,levels = c("1d(a)","1d(b)","7d","14d","28d"))
# fct<-levels(factor(sample_env_abun_simple$Phylum))
# fct
# colors.set <- c("Actinobacteria" = mypal[1],
#                 "Bacteroidetes"  = mypal[2],
#                 "Balneolaeota"  = mypal[3],
#                 "Chloroflexi"  = mypal[4],
#                 "Firmicutes"  = mypal[5],
#                 "Proteobacteria" = mypal[6])
# nrow(data.frame(fct)) == nrow(data.frame(colors.set))
# p<-ggplot(data=sample_env_abun_simple,aes(x=label2,y=RelativeAbundance*100,fill=Phylum))+
#   geom_bar(aes(),stat="identity",position="stack")
```

```
# p<-p+ scale_fill_manual(values = colors.set,drop=F)
# figureFP4<- p+ theme_bw() +
#   theme(axis.title.x = element_text(size = 16)) +theme(axis.title.y = element_text(size = 16)) + theme(axis.text=element_text(size=12)) +
#   theme(legend.title = element_text(size = 16.0)) + theme(legend.text = element_text(size = 16.0)) + theme(strip.text = element_text(size = 16,
  color = "black")) +
#   xlab("Description") + ylab("Relative Abundance(%)")+
#   # ggtitle("Storage life experiment - Phylum level") +
#   theme(plot.title = element_text(hjust = 0.5,size = 16)) + theme(text = element_text("serif"))
# svg(file="figureFP4.svg", height = 5, width =6 );
# figureFP4
# dev.off()
#
# # 5) Impact of growth media on soil samples
# library(dplyr)
# sample_env_specific <- sample_env[c(9,16,15,14),]
# abun_Phylum_specific <- abun_Phylum_r[c(9,16,15,14),]
# sample_env_rep <-bind_rows(replicate(ncol(abun_Phylum_specific)-1, sample_env_specific, simplify = FALSE))
# ord <- (order(sample_env_rep[,1]))
# ord_sample_env_rep<-sample_env_rep[ord,]
# rownames(ord_sample_env_rep) <- c(1:nrow(ord_sample_env_rep))
# ord_sample_env_rep$label <- factor(ord_sample_env_rep$label)
# ord_sample_env_rep$label2 <- factor(ord_sample_env_rep$label2)
# abun_Phylum_specific1 <- abun_Phylum_specific[,-1]
# abun_matrix <- as.matrix(abun_Phylum_specific1)
# abun_vector <- data.frame(as.vector(t(abun_matrix)))
# colnames(abun_vector)<-"Abundance"
# abun_Phylum_specific2 <- data.frame(t(abun_Phylum_specific))
# Phylum <- data.frame(rownames(abun_Phylum_specific2[-1,]))
# colnames(Phylum)<-"Phylum"
# Phylum_rep <-bind_rows(replicate(nrow(abun_Phylum_specific), Phylum, simplify = FALSE))
# rownames(Phylum_rep)<-c(1:nrow(Phylum_rep))
# sample_env_abun <- data.frame(c(ord_sample_env_rep, Phylum_rep, abun_vector))
# sumlist <- aggregate(sample_env_abun$Abundance, by=list(type=sample_env_abun$barcode),sum)
# sumlist_rep <- bind_rows(replicate(nrow(Phylum), sumlist, simplify = FALSE))
# ord <- (order(sumlist_rep[,1]))
# sumlist_rep<-sumlist_rep[ord,]
# rownames(sumlist_rep) <- c(1:nrow(sumlist_rep))
# sumlist_rep<-data.frame(sumlist_rep)
# RelativeAbundance <- data.frame(sample_env_abun$Abundance/sumlist_rep$x)
# colnames(RelativeAbundance)<-"RelativeAbundance"
# sample_env_abun <- data.frame(c(sample_env_abun,RelativeAbundance))
# sample_env_abun_simple<-sample_env_abun
# fct<-levels(factor(sample_env_abun_simple$Phylum))
# fct
# colors.set <- c("Actinobacteria" = mypal[1],
#                 "Bacteroidetes"  = mypal[2],
#                 "Balneolaeota"  = mypal[3],
#                 "Chloroflexi"  = mypal[4],
#                 "Firmicutes"  = mypal[5],
#                 "Proteobacteria" = mypal[6])
# nrow(data.frame(fct)) == nrow(data.frame(colors.set))
# p<-ggplot(data=sample_env_abun_simple,aes(x=label,y=RelativeAbundance*100,fill=Phylum))+
#   geom_bar(aes(),stat="identity",position="stack")
# p<-p+  facet_grid(cols=vars(label2),scale="free_x")
# p<-p+  scale_fill_manual(values = colors.set,drop=F)
# figureFP5<- p+ theme_bw() +
#   theme(axis.title.x = element_text(size = 16)) +theme(axis.title.y = element_text(size = 16)) + theme(axis.text=element_text(size=12)) +
#   theme(legend.title = element_text(size = 16.0)) + theme(legend.text = element_text(size = 16.0)) + theme(strip.text = element_text(size = 16,
  color = "black")) +
#   xlab("Description") + ylab("Relative Abundance(%)")+
#   # ggtitle("Impact of growth media on soil samples") +
#   theme(plot.title = element_text(hjust = 0.5,size = 16)) + theme(text = element_text("serif"))
# svg(file="figureFP5.svg", height = 5, width = 8 );
# figureFP5
# dev.off()
#
# # 6) Storage life experiment - Phylum level
# library(dplyr)
# sample_env_specific <- sample_env[c(10,12,15,14),]
# abun_Phylum_specific <- abun_Phylum_r[c(10,12,15,14),]
```

```
# sample_env_rep <-bind_rows(replicate(ncol(abun_Phylum_specific)-1, sample_env_specific, simplify = FALSE))
# ord <- (order(sample_env_rep[,1]))
# ord_sample_env_rep<-sample_env_rep[ord,]
# rownames(ord_sample_env_rep) <- c(1:nrow(ord_sample_env_rep))
# ord_sample_env_rep$label <- factor(ord_sample_env_rep$label)
# ord_sample_env_rep$label2 <- factor(ord_sample_env_rep$label2)
# abun_Phylum_specific1 <- abun_Phylum_specific[,-1]
# abun_matrix <- as.matrix(abun_Phylum_specific1)
# abun_vector <- data.frame(as.vector(t(abun_matrix)))
# colnames(abun_vector)<-"Abundance"
# abun_Phylum_specific2 <- data.frame(t(abun_Phylum_specific))
# Phylum <- data.frame(rownames(abun_Phylum_specific2[-1,]))
# colnames(Phylum)<-"Phylum"
# Phylum_rep <-bind_rows(replicate(nrow(abun_Phylum_specific), Phylum, simplify = FALSE))
# rownames(Phylum_rep)<-c(1:nrow(Phylum_rep))
# sample_env_abun <- data.frame(c(ord_sample_env_rep, Phylum_rep, abun_vector))
# sumlist <- aggregate(sample_env_abun$Abundance, by=list(type=sample_env_abun$barcode),sum)
# sumlist_rep <- bind_rows(replicate(nrow(Phylum), sumlist, simplify = FALSE))
# ord <- (order(sumlist_rep[,1]))
# sumlist_rep<-sumlist_rep[ord,]
# rownames(sumlist_rep) <- c(1:nrow(sumlist_rep))
# sumlist_rep<-data.frame(sumlist_rep)
# RelativeAbundance <- data.frame(sample_env_abun$Abundance/sumlist_rep$x)
# colnames(RelativeAbundance)<-"RelativeAbundance"
# sample_env_abun <- data.frame(c(sample_env_abun,RelativeAbundance))
# sample_env_abun_simple<-sample_env_abun
# fct<-levels(factor(sample_env_abun_simple$Phylum))
# fct
# colors.set <- c("Actinobacteria" = mypal[1],
#                 "Bacteroidetes"  = mypal[2],
#                 "Balneolaeota"  = mypal[3],
#                 "Chloroflexi"  = mypal[4],
#                 "Firmicutes"  = mypal[5],
#                 "Proteobacteria" = mypal[6])
# nrow(data.frame(fct)) == nrow(data.frame(colors.set))
# p<-ggplot(data=sample_env_abun_simple,aes(x=label,y=RelativeAbundance*100,fill=Phylum))+
#   geom_bar(aes(),stat="identity",position="stack")
# p<-p+  facet_grid(cols=vars(label3),scale="free_x") #+
# p<-p+  scale_fill_manual(values = colors.set,drop=F) #+
# figureFP6<- p+ theme_bw() +
#   theme(axis.title.x = element_text(size = 16)) +theme(axis.title.y = element_text(size = 16)) + theme(axis.text=element_text(size=12)) +
#   theme(legend.title = element_text(size = 16.0)) + theme(legend.text = element_text(size = 16.0)) + theme(strip.text = element_text(size = 16,
  color = "black")) +
#   xlab("Description") + ylab("Relative Abundance(%)")+
#   # ggtitle("Storage life experiment - Phylum level") +
#   theme(plot.title = element_text(hjust = 0.5,size = 16)) + theme(text = element_text("serif"))
# svg(file="figureFP6.svg", height = 5, width =8 );
# figureFP6
# dev.off()

# 3. Abundance plot for Species
library(ggplot2)
library(readxl)
abun_Species_r <- data.frame(read_xls("abun_species.xls"))
sample_env <- data.frame(read_xls("aggregated_counts_env.xls"))

# 1) Bsub - sporulation experiment
library(dplyr)
sample_env_specific <- sample_env[c(5,6),]
abun_Species_specific <- abun_Species_r[c(5,6),]
sample_env_rep <-bind_rows(replicate(ncol(abun_Species_specific)-1, sample_env_specific, simplify = FALSE))
ord <- (order(sample_env_rep[,1]))
ord_sample_env_rep<-sample_env_rep[ord,]
rownames(ord_sample_env_rep) <- c(1:nrow(ord_sample_env_rep))
abun_Species_specific1 <- abun_Species_specific[,-1]
abun_matrix <- as.matrix(abun_Species_specific1)
abun_vector <- data.frame(as.vector(t(abun_matrix)))
colnames(abun_vector)<-"Abundance"
abun_Species_specific2 <- data.frame(t(abun_Species_specific))
Species <- data.frame(rownames(abun_Species_specific2[-1,]))
```

```
colnames(Species)<-"Species"
Species_rep <-bind_rows(replicate(nrow(abun_Species_specific), Species, simplify = FALSE))
rownames(Species_rep)<-c(1:nrow(Species_rep))
sample_env_abun <- data.frame(c(ord_sample_env_rep, Species_rep, abun_vector))
sumlist <- aggregate(sample_env_abun$Abundance, by=list(type=sample_env_abun$barcode),sum)
sumlist_rep <- bind_rows(replicate(nrow(Species), sumlist, simplify = FALSE))
ord <- (order(sumlist_rep[,1]))
sumlist_rep<-sumlist_rep[ord,]
rownames(sumlist_rep) <- c(1:nrow(sumlist_rep))
sumlist_rep<-data.frame(sumlist_rep)
RelativeAbundance <- data.frame(sample_env_abun$Abundance/sumlist_rep$x)
colnames(RelativeAbundance)<-"RelativeAbundance"
sample_env_abun <- data.frame(c(sample_env_abun,RelativeAbundance))
sample_env_abun_simple<-sample_env_abun
sample_env_abun_simple$Species[sample_env_abun$RelativeAbundance < 0.05] <- "Species < 5%"
fct<-levels(factor(sample_env_abun_simple$Species))
fct
colors.set <- c("Bacillus.halotolerans" = mypal[1],
                "Bacillus.inaquosorum"  = mypal[2],
                "Bacillus.spizizenii"  = mypal[3],
                "Species < 5%"  = mypal[4])
nrow(data.frame(fct)) == nrow(data.frame(colors.set))
p<-ggplot(data=sample_env_abun_simple,aes(x=label,y=RelativeAbundance*100,fill=Species))+
  geom_bar(aes(),stat="identity",position="stack") +
  scale_fill_manual(values = colors.set,drop=F)
figureFS1<- p+ theme_bw() +
  theme(axis.title.x = element_text(size = 16)) +theme(axis.title.y = element_text(size = 16)) + theme(axis.text=element_text(size=14)) +
  theme(legend.title = element_text(size = 16.0)) + theme(legend.text = element_text(size = 16.0)) + theme(strip.text = element_text(size = 16,
  color = "black")) +
  xlab("(B)") + ylab("Relative Abundance(%)")+
  # ggtitle("Bsub - sporulation experiment") +
  theme(plot.title = element_text(hjust = 0.5,size = 16)) + theme(text = element_text("serif"))
svg(file="figureFS1.svg", height = 5, width =8 );
figureFS1
dev.off()

View(sample_env_abun_simple)

# 2) 24 hr 0.5xNB experiment - Species level
library(dplyr)
sample_env_specific <- sample_env[c(10:13),]
abun_Species_specific <- abun_Species_r[c(10:13),]
sample_env_rep <-bind_rows(replicate(ncol(abun_Species_specific)-1, sample_env_specific, simplify = FALSE))
ord <- (order(sample_env_rep[,1]))
ord_sample_env_rep<-sample_env_rep[ord,]
rownames(ord_sample_env_rep) <- c(1:nrow(ord_sample_env_rep))
abun_Species_specific1 <- abun_Species_specific[,-1]
abun_matrix <- as.matrix(abun_Species_specific1)
abun_vector <- data.frame(as.vector(t(abun_matrix)))
colnames(abun_vector)<-"Abundance"
abun_Species_specific2 <- data.frame(t(abun_Species_specific))
Species <- data.frame(rownames(abun_Species_specific2[-1,]))
colnames(Species)<-"Species"
Species_rep <-bind_rows(replicate(nrow(abun_Species_specific), Species, simplify = FALSE))
rownames(Species_rep)<-c(1:nrow(Species_rep))
sample_env_abun <- data.frame(c(ord_sample_env_rep, Species_rep, abun_vector))
sumlist <- aggregate(sample_env_abun$Abundance, by=list(type=sample_env_abun$barcode),sum)
sumlist_rep <- bind_rows(replicate(nrow(Species), sumlist, simplify = FALSE))
ord <- (order(sumlist_rep[,1]))
sumlist_rep<-sumlist_rep[ord,]
rownames(sumlist_rep) <- c(1:nrow(sumlist_rep))
sumlist_rep<-data.frame(sumlist_rep)
RelativeAbundance <- data.frame(sample_env_abun$Abundance/sumlist_rep$x)
colnames(RelativeAbundance)<-"RelativeAbundance"
sample_env_abun <- data.frame(c(sample_env_abun,RelativeAbundance))
sample_env_abun_simple<-sample_env_abun
sample_env_abun_simple$Species[sample_env_abun$RelativeAbundance < 0.05] <- "Species < 5%"
fct<-levels(factor(sample_env_abun_simple$Species))
fct
colors.set <- c("Acinetobacter.johnsonii"  = mypal[5],
```

```
              "Aeromonas.encheleia"      = mypal[6],
              "Aeromonas.hydrophila"     = mypal[7],
              "Aeromonas.rivipollensis"  = mypal[8],
              "Bacillus.halotolerans"    = mypal[1],
              "Bacillus.inaquosorum"     = mypal[2],
              "Bacillus.spizizenii"      = mypal[3],
              "Species < 5%"             = mypal[4])

nrow(data.frame(fct)) == nrow(data.frame(colors.set))
sample_env_abun_simple$Microbe.Name <-sample_env_abun_simple$Microbe
sample_env_abun_simple$Microbe.Name[sample_env_abun_simple$Microbe == "Bsub"] <-"Bsud(37 C)"
sample_env_abun_simple$Microbe.Name[sample_env_abun_simple$Microbe == "Soil"] <-"Soil(25 C)"
p<-ggplot(data=sample_env_abun_simple,aes(x=label,y=RelativeAbundance*100,fill=Species))+
  geom_bar(aes(),stat="identity",position="stack") +
  facet_grid(cols=vars(Microbe.Name),scale="free_x")
p <- p + scale_fill_manual(values = colors.set,drop=F)
figureFS2<- p+ theme_bw() +
  theme(axis.title.x = element_text(size = 16)) +theme(axis.title.y = element_text(size = 16)) + theme(axis.text=element_text(size=14)) +
  theme(legend.title = element_text(size = 16.0)) + theme(legend.text = element_text(size = 16.0)) + theme(strip.text = element_text(size = 16,
  color = "black")) +
  xlab("24hr 0.5xNB (B)") + ylab("Relative Abundance(%)")+
  # ggtitle("24 hr 0.5xNB experiment - Species level") +
  theme(plot.title = element_text(hjust = 0.5,size = 16)) + theme(text = element_text("serif"))
svg(file="figureFS2.svg", height = 5, width =8 );
figureFS2
dev.off()

# 3) Storage life experiment - Species level
library(dplyr)
sample_env_specific <- sample_env[c(1:4,7:8),]
abun_Species_specific <- abun_Species_r[c(1:4,7:8),]
sample_env_rep <-bind_rows(replicate(ncol(abun_Species_specific)-1, sample_env_specific, simplify = FALSE))
ord <- (order(sample_env_rep[,1]))
ord_sample_env_rep<-sample_env_rep[ord,]
rownames(ord_sample_env_rep) <- c(1:nrow(ord_sample_env_rep))
ord_sample_env_rep$label1 <- factor(ord_sample_env_rep$label1,levels = c("1d","7d","14d","28d"))
abun_Species_specific1 <- abun_Species_specific[,-1]
abun_matrix <- as.matrix(abun_Species_specific1)
abun_vector <- data.frame(as.vector(t(abun_matrix)))
colnames(abun_vector)<-"Abundance"
abun_Species_specific2 <- data.frame(t(abun_Species_specific))
Species <- data.frame(rownames(abun_Species_specific2[-1,]))
colnames(Species)<-"Species"
Species_rep <-bind_rows(replicate(nrow(abun_Species_specific), Species, simplify = FALSE))
rownames(Species_rep)<-c(1:nrow(Species_rep))
sample_env_abun <- data.frame(c(ord_sample_env_rep, Species_rep, abun_vector))
sumlist <- aggregate(sample_env_abun$Abundance, by=list(type=sample_env_abun$barcode),sum)
sumlist_rep <- bind_rows(replicate(nrow(Species), sumlist, simplify = FALSE))
ord <- (order(sumlist_rep[,1]))
sumlist_rep<-sumlist_rep[ord,]
rownames(sumlist_rep) <- c(1:nrow(sumlist_rep))
sumlist_rep<-data.frame(sumlist_rep)
RelativeAbundance <- data.frame(sample_env_abun$Abundance/sumlist_rep$x)
colnames(RelativeAbundance)<-"RelativeAbundance"
sample_env_abun <- data.frame(c(sample_env_abun,RelativeAbundance))
sample_env_abun_simple<-sample_env_abun
sample_env_abun_simple$Species[sample_env_abun$RelativeAbundance < 0.05] <- "Species < 5%"
sample_env_abun_simple$label <- factor(sample_env_abun_simple$label,levels = c("1d","7d","14d","28d"))
fct<-levels(factor(sample_env_abun_simple$Species))
fct
colors.set <- c("Acinetobacter.johnsonii" = mypal[5],
              "Acinetobacter.oleivorans" = mypal[9],
              "Acinetobacter.pittii"     = mypal[10],
              "Bacillus.halotolerans"    = mypal[1],
              "Bacillus.inaquosorum"     = mypal[2],
              "Bacillus.spizizenii"      = mypal[3],
              "Citrobacter.freundii"     = mypal[11],
              "Comamonas.testosteroni"   = mypal[12],
              "Klebsiella.oxytoca"       = mypal[13],
              "Lysinibacillus.fusiformis"  = mypal[14],
```

```
            "Pseudomonas.plecoglossicida" = mypal[15],
            "Raoultella.ornithinolytica" = mypal[16],
            "Species < 5%"  = mypal[4])
nrow(data.frame(fct)) == nrow(data.frame(colors.set))
p<-ggplot(data=sample_env_abun_simple,aes(x=label,y=RelativeAbundance*100,fill=Species))+
  geom_bar(aes(),stat="identity",position="stack") +
  facet_grid(cols=vars(Microbe),scale="free_x") +
  scale_fill_manual(values = colors.set,drop=F)
figureFS3<- p+ theme_bw() +
  theme(axis.title.x = element_text(size = 16)) +theme(axis.title.y = element_text(size = 16)) + theme(axis.text=element_text(size=14)) +
  theme(legend.title = element_text(size = 16.0)) + theme(legend.text = element_text(size = 16.0)) + theme(strip.text = element_text(size = 16,
  color = "black")) +
  xlab("(B)") + ylab("Relative Abundance(%)")+
  # ggtitle("Storage life experiment - Species level") +
  theme(plot.title = element_text(hjust = 0.5,size = 16)) + theme(text = element_text("serif"))
svg(file="figureFS3.svg", height = 5, width =8 );
figureFS3
dev.off()
```

11 Appendix E: Task 2 Laboratory Mortar Testing Research Findings and Conclusions

11.1 SEM Imaging of Bacteria Immobilized LWA

Prior to adding bacterial LWA into the cement pastes or mortars, SEM analysis was conducted to investigate the immobilization procedure using LWA samples. Figure 11.1a shows SEM image of control LWA and b and c show *B. subtilis* and soil immobilized LWAs, respectively. Bacteria were found on bacterial LWA images (shown with red arrows) which have length of 1.5-2 µm, whereas no similar indications were observed from control LWA.

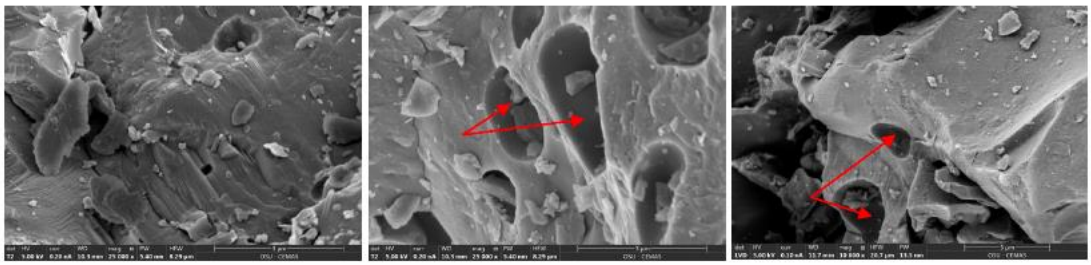

Figure 11.1 - Morphology of a) non-bacterial LWA, b) B. subtilis immobilized LWA, c) soil bacteria immobilized LWA.

11.2 Impact of Bacteria Mixtures on Cement Hydration Kinetics

Hydration kinetics of bacterial and non-bacterial OPC, OPC FA and CSA samples were investigated and Figures 11.2, 11.3 and 11.5 show rate of heat release results of OPC, OPC FA, and CSA samples, respectively. For all samples, use of LWA in addition to the cement paste decreased the amount of heat released. However, LWA did not affect the timing of the hydration reactions. The decrease in the heat release can be attributed to the dilution of the cement system as adding non-reactive LWA to the system led to the reduction in the amount of total reactive component (cement) in the system.

The use of the bacterial LWAs with OPC and OPC FA samples resulted in delays in the start of the acceleration period of the hydration reaction when compared to non-bacterial samples. Main hydration peaks of both B. subtilis (OPC LWA-B, OPC FA LWA-B) and soil (OPC LWA-S, OPC FA LWA-S) samples occurred approximately 3 hours later than in the control sample. The delay can be explained partially by the procedure and materials used for immobilization of bacteria cells with nutrient medium into LWA. Previous studies have shown that use of nutrient media as mixing water in cement pastes caused delays in the hydration reactions due to the nutrient solutions containing sugar and carbohydrates (Basaran 2013; Amiri and Bundur 2018). Sugar and carbohydrates are effective retarders for OPC systems, causing delay in mainly alite (C3S) hydration (main hydration peak in OPC system (Cody et al. 2004; Basaran 2013). However, total delays were greater in bacterial samples than in the samples using nutrient broth without bacteria, suggesting that the bacteria themselves may cause some retarding effect. No significant difference in hydration kinetics was observed when different types of bacteria were used.

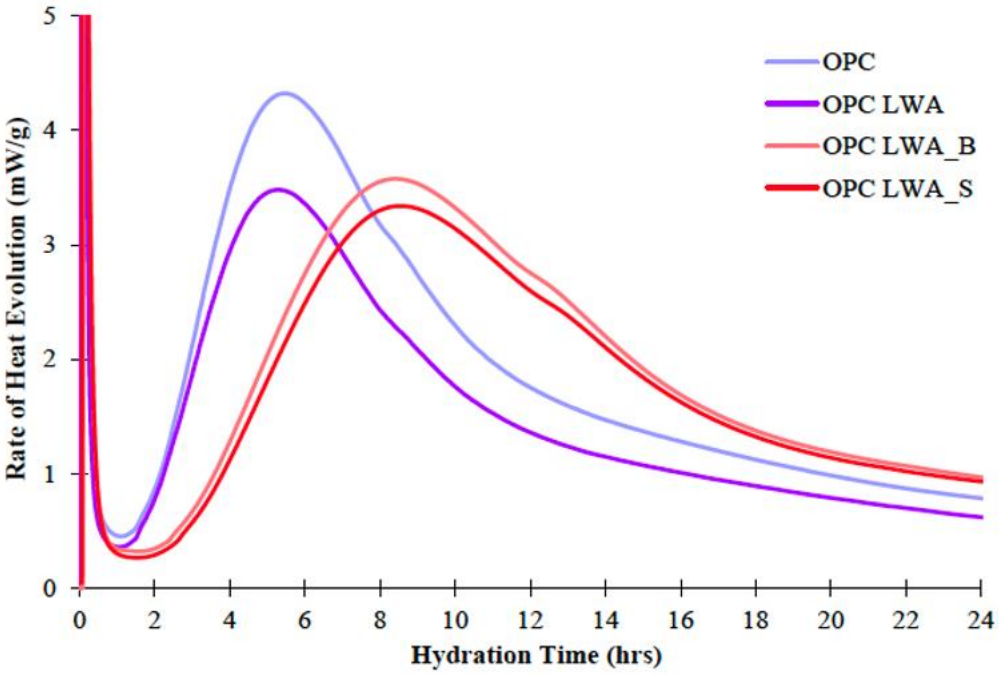

Figure 11.2 - Heat evolution of OPC with bacterial (B. subtilis and soil) and non-bacterial LWAs and without LWA.

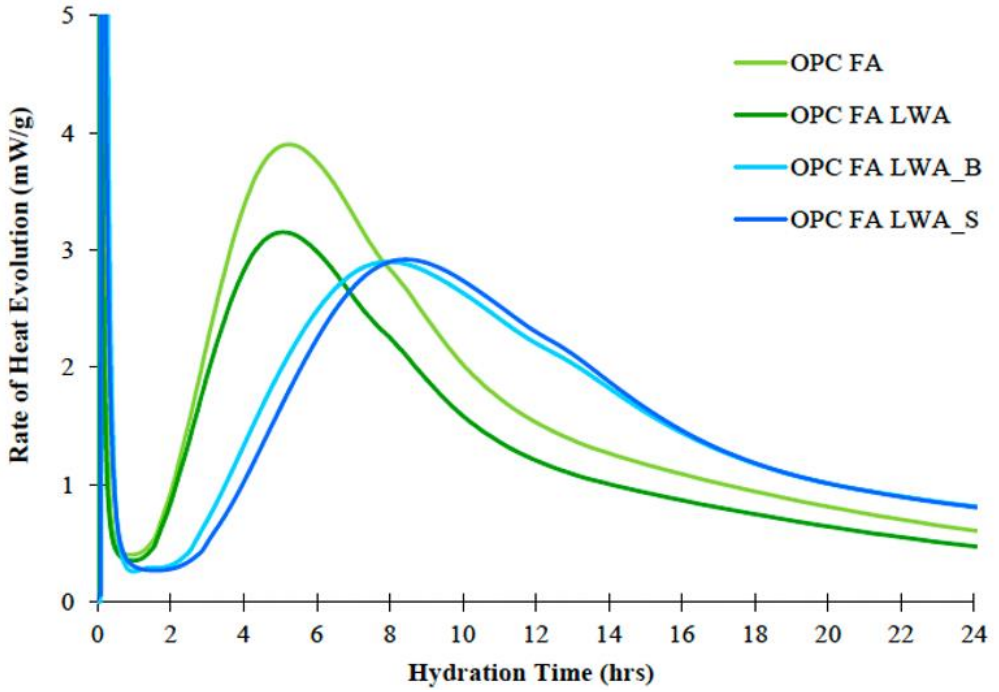

Figure 11.3 - Heat evolution of OPC and fly ash with bacterial (B. subtilis and soil) and non-bacterial LWAs and without LWA.

In order to understand the effect of the nutrient solutions on the hydration kinetics of OPC, OPC cement with addition of full and half dosages of nutrient broth were tested. The results, shown in

Figure 11.4, display hydration reactions were retarded when nutrient broth was used in the place of mixing water. Increasing amounts of nutrient solution also resulted in additional delay in the hydration reactions.

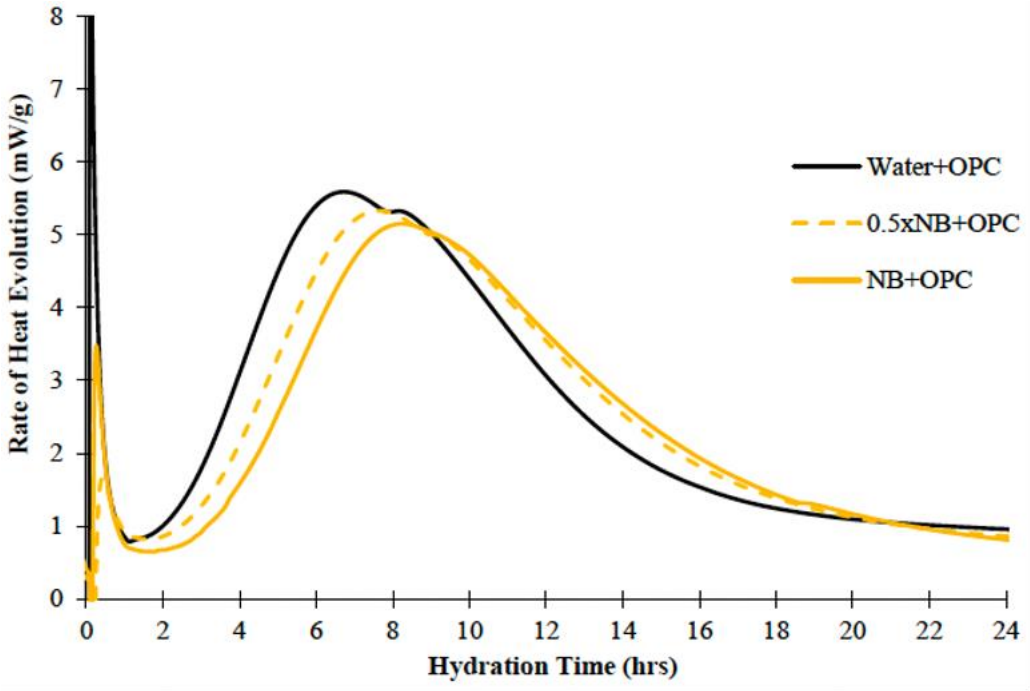

Figure 11.4 - Heat evolution of OPC with the addition of full and half dosages nutrient broth (NB).

When compared to OPC and OPC FA samples, main rate of heat release peaks of CSA samples occurred at approximately 1.5 hours, 3 hours and 6 hours faster than non-bacterial and bacterial samples, respectively, and CSA samples resulted in having much higher rate of heat release (Figure 11.5). Dissimilarly to OPC and OPC FA results, use of bacterial LWA (CSA LWA-B, CSA LWA-S) did not lead to delay in the occurrence of main hydration peak of CSA samples. Unlike the alite (C_3S) phase present in OPC systems, hydration of the predominant cement phase present in CSA (ye'elimite) has not been shown to experience retardation by sugars and carbohydrates as shown in Figure 11.6.

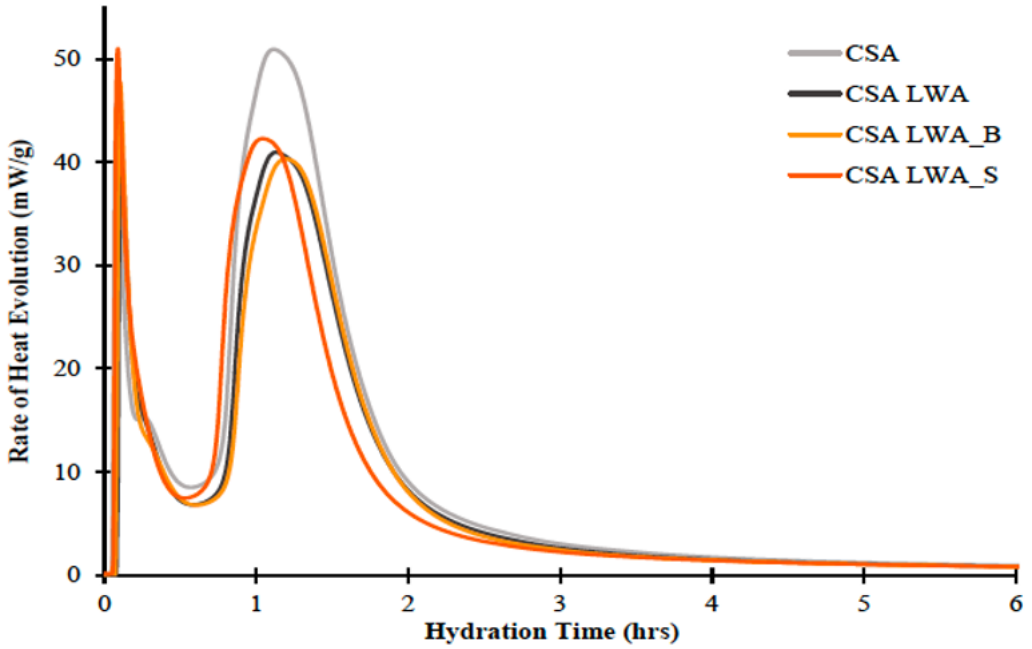

Figure 11.5 - Heat evolution of CSA cement with bacterial (B. subtilis and soil) and non-bacterial LWAs and without LWA.

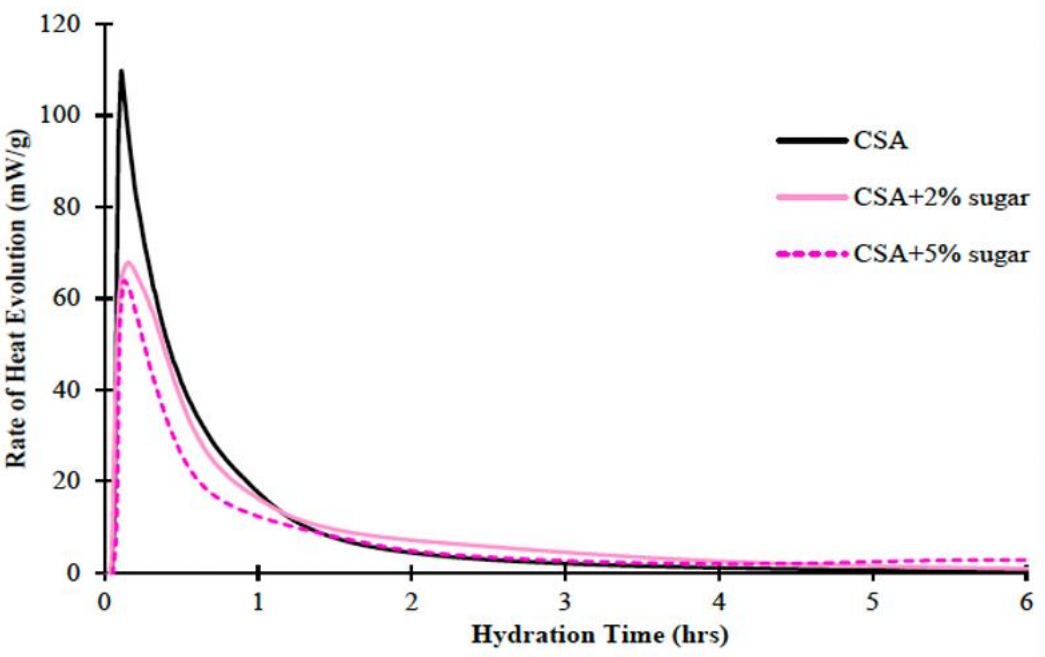

Figure 11.6 - Heat evolution of CSA cement with the addition of dosages varying dosages from 0 to 5%.

Vicat set time testing also evidenced retardation associated with use of bacteria. In OPC mixtures without fly ash incorporation of LWA increased initial setting times by approximately 40 minutes. No further increases in setting time were apparent with addition of bacteria to the LWA, but bacteria lead to an increase in final setting time of 82 and 251 minutes relative to the LWA

mixture for the *B. subtilis* and soil bacteria. An opposite effect was observed in the OPC-FA mixtures. Use of the fly ash significantly increased initial and final setting times relative to the OPC mixture, and incorporation of LWA decreased initial setting time by 108 minutes, but increased final set by 48 minutes. Addition of bacteria reduced initial setting times by 88 and 117 minutes for the *B. subtilis* and soil bacteria, respectively. *B. subtilis* also reduced final setting time by 95 minutes, but no reduction in final setting was observed in the soil bacteria sample. In the CSA samples LWA provided no effect on setting times, while both bacteria samples slightly decreased initial set, and extended final set by 45 minutes.

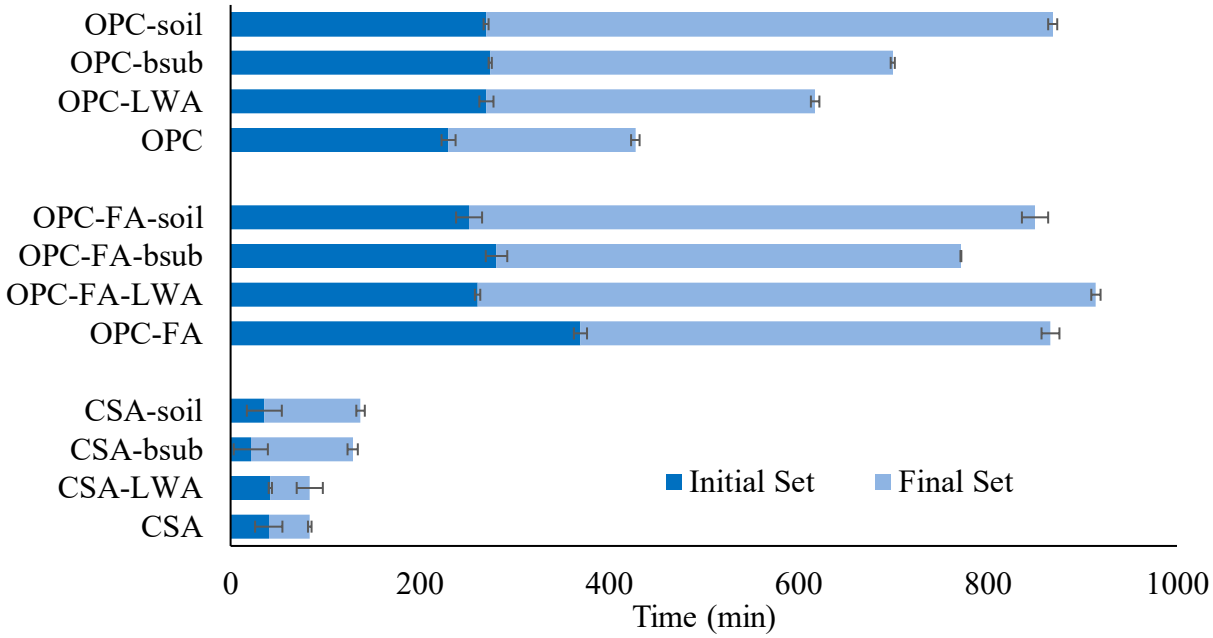

Figure 11.7 - Vicat Setting Time of the OPC, OPC-FA, and CSA mixtures with and without bacteria.

11.3 Impact of Mixture Composition and Curing Method on Mechanical Properties and Durability

11.3.1 Viability of Bacteria

Figure 11.7 shows the bacterial viability of *B. subtilis* cells in mortars with various variables to compare different cementitious binders, curing procedures and mixing compositions. The general trend for all samples shows a decrease in the cell concentration at the beginning (1 to 3 or 7 days) due to the mortality of the surface-attached spores that were in a direct contact with the cement matrix (Jakubovskis et al. 2022) and then it was followed by an increase in the bacteria amount.

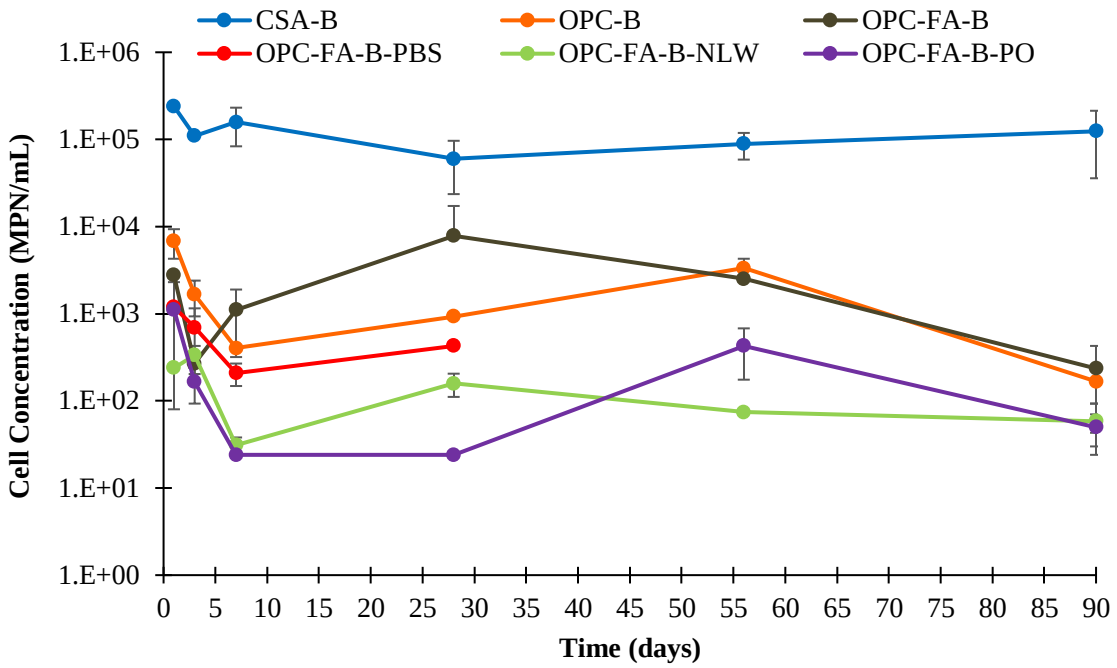

Figure 11.8 - Viability of B. subtilis bacteria in mortar cubes over 90 days. Legend nomenclature is as follows: PO indicates the sample was cured by ponding in nutrient solution, PBS indicates use of phosphate buffer solution in place of mixing water, NLW indicates that lightweight aggregate was not used.

The highest bacteria survivability was observed in samples prepared with CSA cement (CSA-B) which may indicate that lower alkalinity of the CSA cement promotes the bacterial growth by lowering pH. Moreover, bacteria cells were able to remain viable at higher concentrations in the CSA samples (10^5 CFU/mL) even at 90 days of hydration. OPC-FA samples had the second highest viability of bacteria cells up to 28 days but then the rate of survivability decreased dramatically from 28 to 90 days (10^4 MPN/mL to $2x10^2$ MPN/mL). Fly ash is known to react slowly over time, with its pozzolanic reaction typically initiating 28 days or more after initial mixing with cement and water. As fly ash is used to replace a portion of the mixture OPC this results in a reduced reactive material fraction within the mixture at early ages and leads to higher porosity in samples. Greater total porosity and interconnectivity of pores may promote greater infiltration of nutrients into the cement matrix, leading to increased early age bacteria survivability (Achal et al. 2011). OPC samples had similar bacteria viability to OPC-FA samples after 28 days.

Figure 11.8 shows the bacterial viability of soil bacteria cells in mortars. Soil bacteria demonstrated similar trends as were observed for the *B. subtilis* samples, showing a decrease in the cell concentration shortly after sample casting (prior to 7 days) and followed by an increase in the bacteria amount in some samples (OPC- FA, OPC, and OPC-FA-NLW). However, use of soil bacteria in mortar mixtures resulted in lower cell concentrations than *B. subtilis* samples. This may suggest that even though use of soil bacteria led to slightly better initial cell growth and greater cell numbers it had less resilience to the harsh concrete environment.

Similar to *B. subtilis* mixtures, highest soil bacteria survivability was observed in samples prepared with CSA cement (CSA) and in CSA samples bacteria cells were able to remain viable at higher concentrations (10^3 MPN/mL vs $< 10^2$ MPN/mL) after 90 days of hydration when compared to

other soil bacteria samples. Similar to *B. subtilis* mixtures, OPC-FA samples had higher viability of bacteria cells up to 28 days when compared to OPC samples, but their rate of survivability decreased significantly from 28 to 90 days ($4x10^3$ MPN/mL to 10^2 MPN/mL) and the numbers of living cells present at 90 days was approximately the same for the OPC-S and OPC FA-S samples.

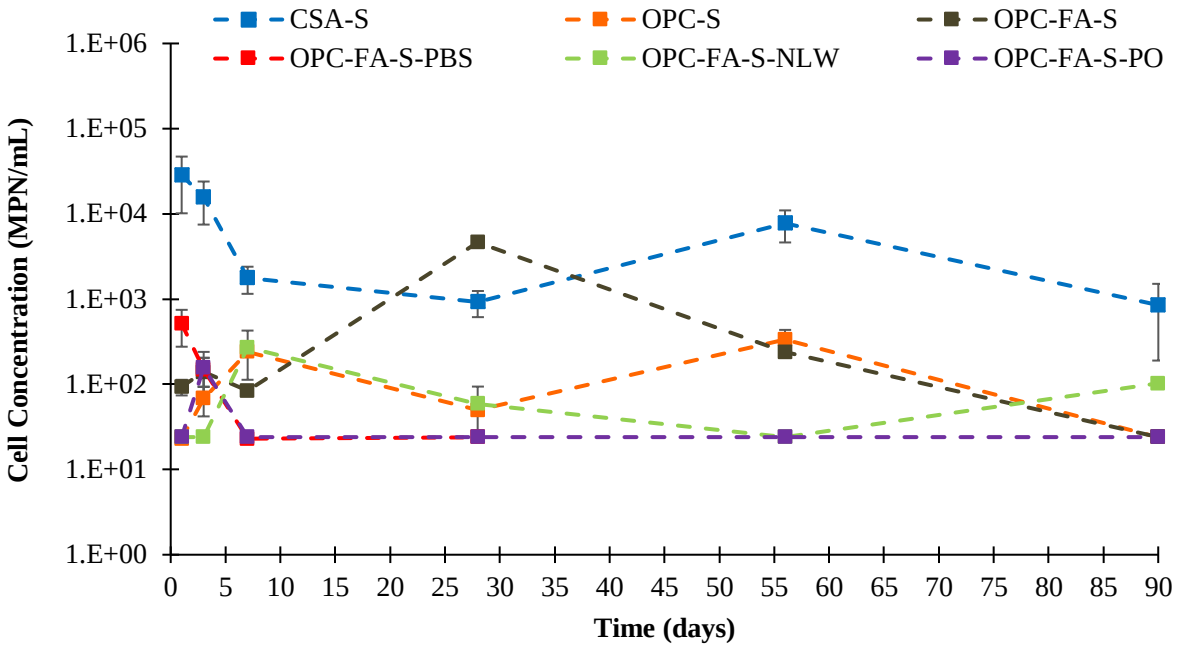

Figure 11.9 - Viability of soil bacteria in mortar cubes over 90 days.

For both bacteria types, use of PBS in mixing water (OPC-FA-PBS) instead of tap water (OPC-FA) resulted in slightly lower bacteria viability between 1 and 28 days, suggesting that use of dechlorinated tap water, does not have a negative effect on the bacteria viability. When LWA was not used in the mixture (OPC-FA-NLW), rate of survivability of both *B. subtilis* and soil cells decreased significantly when compared to mixture with LWA, confirming the cell protection ability of LWA. Use of ponding curing method led to a big decrease in cell viability within *B. subtilis* and soil mortars compared to the spray curing method. Alternating wet and dry curing cycles have been shown to provide greater amounts of oxygen to bacteria than curing methods involving full sample immersion (Wang et al. 2014; Tziviloglou et al. 2016). Thus, spraying may be more beneficial to *B. subtilis* and soil bacteria cells in order to provide sufficient oxygen levels compared to ponding due to the shorter length of wet and dry cycles.

11.3.2 Compressive Strength Development

The compressive strength results of the control, *B. subtilis* and soil mortar cubes with only OPC, OPC and fly ash (OPC-FA) and only CSA cement are shown in Figure 11.9. OPC-FA samples showed slower strength gain through 56 days when compared to OPC samples due to the slower reactivity of the fly ash. After 56 days of hydration, they were able to reach same strength level as OPC samples. Although bacterial OPC-FA samples led to slightly higher strength as compared to non-bacterial sample at some ages (1, 7, 56 days), they were all had the same strength at 90 days. OPC samples had faster strength development than OPC-FA samples, but the presence of the *B.*

subtilis and soil bacteria did not have a significant impact on compressive strengths for OPC mortar samples. Achal et al. (2011) showed increased strength in bacterial samples occurred with the use of fly ash as a result of better nourishment of bacterial cells due to the higher porosity of the fly ash samples at early ages.

CSA samples had greater strength than both OPC and OPC-FA samples for all testing days regardless of their bacteria concentration. CSA bacterial samples had higher strength at 1, 28 and 90 days which may be attributed to the lower alkalinity of CSA cement compared to OPC, leading to higher cell count (as seen from MPN results, Figures 11.7 and 11.8) and thus densified microstructure. Use of soil bacteria in CSA mortars resulted in higher strength compared to use of *B. subtilis* bacteria.

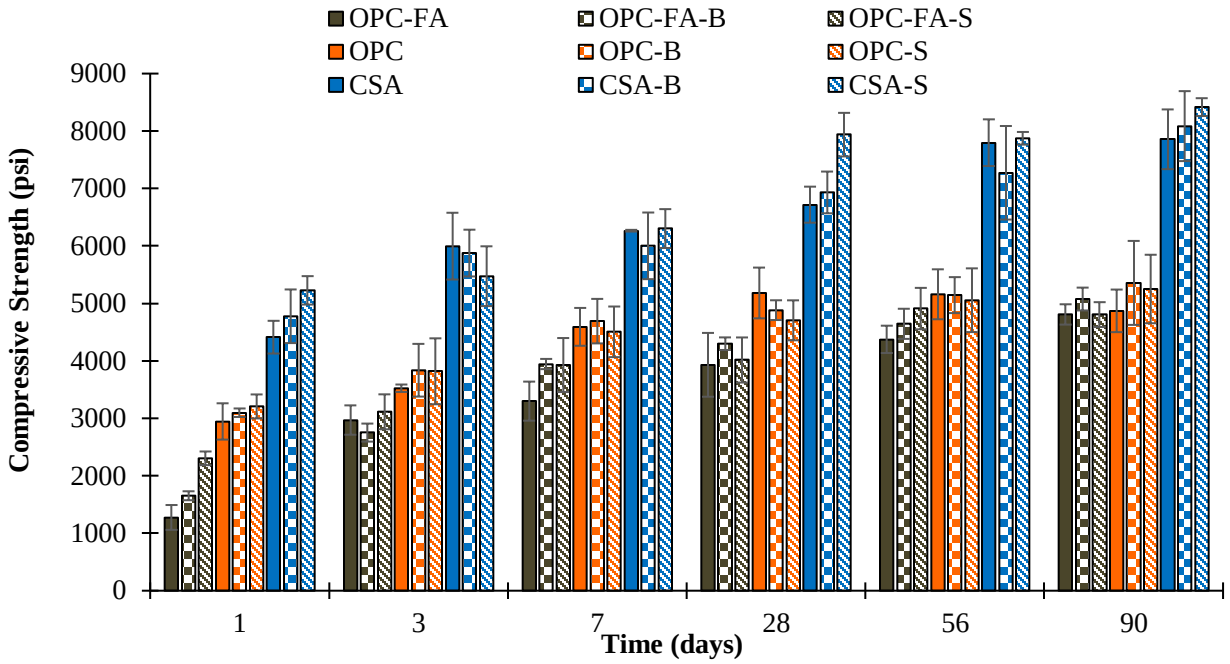

Figure 11.10 - Compressive strengths of bacterial and non-bacterial OPC, OPC FA and CSA mortars.

Figure 11.10 shows the results of compressive strength development of OPC and fly ash samples to compare use of dechlorinated tap water (OPC-FA) and PBS (OPC- FA-PBS) as mixing solution compositions. Use of PBS instead of tap water led to higher strength in both bacterial samples as compared to the control sample. Soil bacteria samples utilizing PBS had higher early strength than *B. subtilis* samples at early ages (1 and 3 days) despite lower bacteria viability (Figure 11.8). This effect is magnified considering that in non-bacteria samples, use of PBS reduced compressive strengths. This may suggest that PBS may have affected strength of control samples negatively and bacteria cells helped to promote the strength, possibly as a result of protecting bacteria from the pH shock (Liao and Shollenberger 2003).

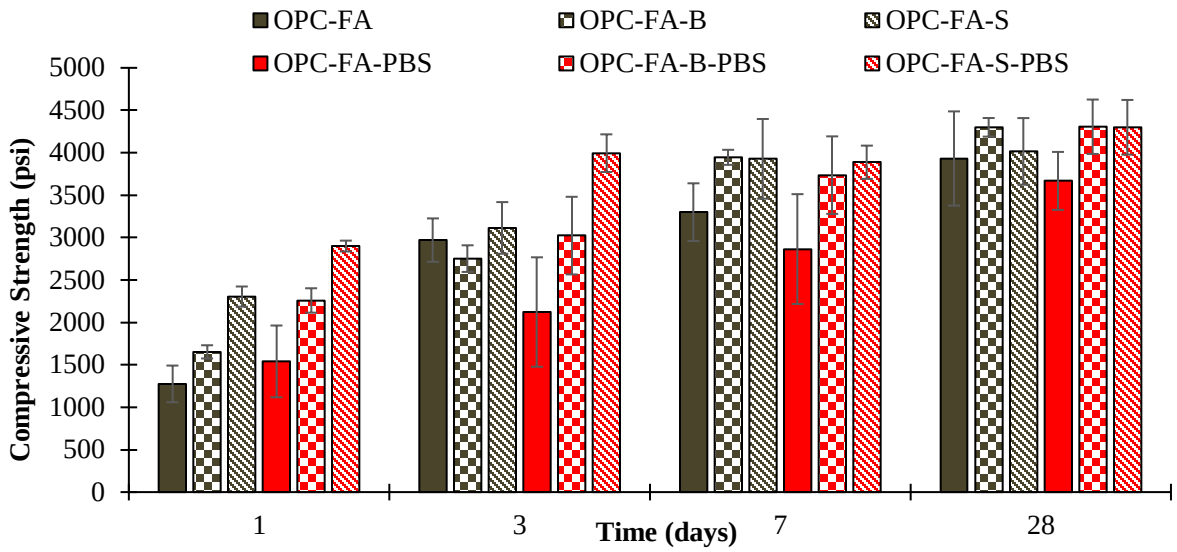

Figure 11.11 - Compressive strengths of bacterial and non-bacterial OPC FA mixtures with dechlorinated tap water (OPC-FA) and PBS (OPC-FA-PBS).

Figure 11.11 shows the results of compressive strength development of control and bacterial OPC and fly ash mixtures with and without LWA (OPC-FA-NLW). Control samples without LWA had higher strength than samples with LWA until 28 days. After 28 days, mixtures without LWA developed higher strengths compared to NLW samples. Bacterial samples without LWA had slightly lower strength up to 28 days of hydration compared to control samples, however, there was a reduction in the strength of the bacterial samples at later ages. At 90 days, the strengths of LWA *B. subtilis* and soil bacteria samples were 19% and 64% were lower than the control sample. These results prove the efficiency of LWA for protecting bacteria cells from the harsh concrete environment and preventing bacteria degradation.

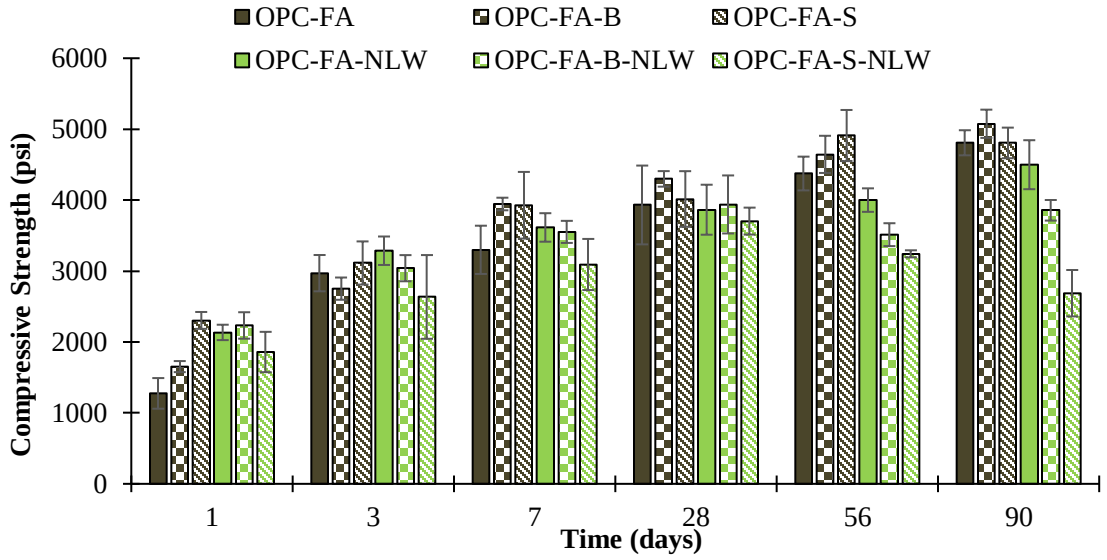

Figure 11.12 - Compressive strengths of bacterial and non-bacterial OPC FA mixtures with (OPC-FA) and without LWA (OPC-FA-LWA).

Lastly, effect of spray and pond curing methods on compressive strength of OPC- FA samples is shown in Figure 11.12. Use of ponding as a curing method did not lead to significant increase or decrease in the strength of control samples in comparison with the spraying (OPC-FA). Similarly, ponded bacterial samples had similar strengths to sprayed bacterial samples. Therefore, since ponding is less suitable for real-life applications, spraying can be considered as the most efficient curing method.

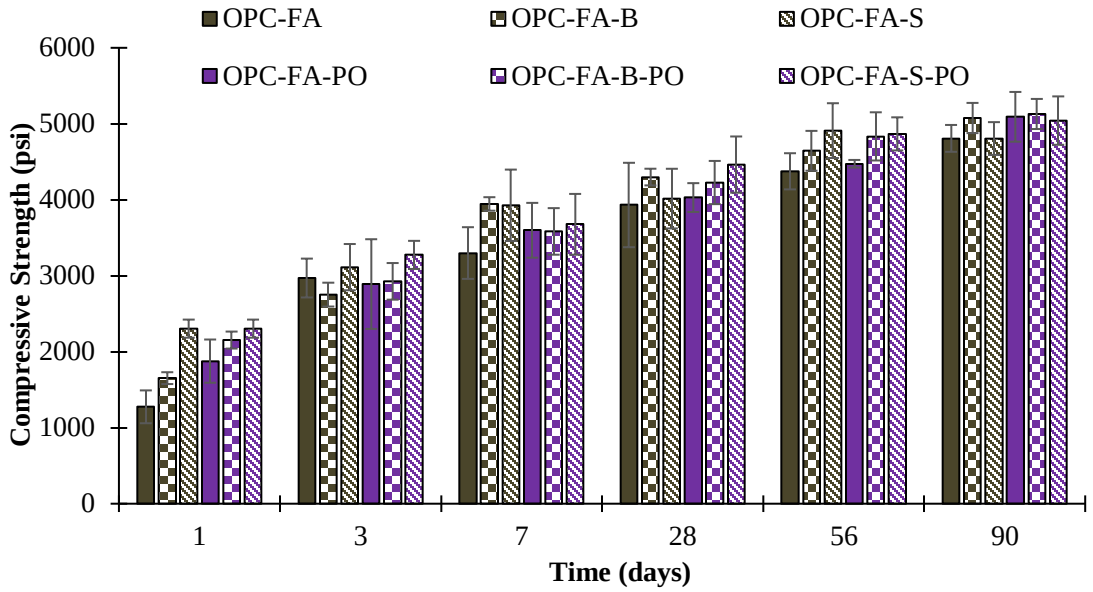

Figure 11.13 - Compressive strengths of bacterial and non-bacterial OPC FA mixtures cured by spraying (OPC-FA) and ponding (OPC-FA-PO).

11.3.3 Electrical Resistivity

Resistivity results of mortars are shown in Figure 11.13. OPC, OPC-FA-PBS and OPC-FA-PO samples had higher resistivity result in the presence of B. subtilis and soil bacteria than control samples at 7 and 28 days. However, at later ages rate of resistivity gain of bacterial samples decreased, resulted in similar or higher resistivity results of control samples. This can be explained by due to the reduction in the porosity of the later age pastes and the increased densification of the pore structure, leading to restricted nutrient access by microorganisms (Ramachandran et al. 2001; Basaran 2013).

Other than OPC and OPC-FA-PBS samples, the effect of bacteria on resistivity was not clear and all variables with both bacteria showed very similar resistivity development as non-bacterial samples. OPC-FA samples had lower resistivity than OPC samples at 7-day, as expected, and higher or very similar resistivity at later ages. Similar to the strength results, samples without LWA resulted in the lowest resistivity among all other samples and decreased resistivity of bacterial samples at 90 days when compared to control samples which can be attributed to the cell death at later ages causing increase in porosity due to creating voids within the matrix. Skevi et al. (2021) showed that dead cells may have been resulted in voids inside the mortar matrix and absence of hydrates.

Ponding samples in NBUC solution caused lower resistivity results than spraying (OPC-FA) due to increased saturation in ponded samples. Electrical resistivity is affected by moisture condition of samples and wetter samples would have lower amount of resistivity. When curing was stopped after 28-days of hydration, resistivity of ponded samples increased, since samples became drier. Consequently, these resistivity results may not be indicative of actual microstructural changes since electrical resistivity measurements are affected by many factors including pore solution chemistry, moisture level of samples, and curing conditions, which were not able to be controlled (Azarsa and Gupta 2017).

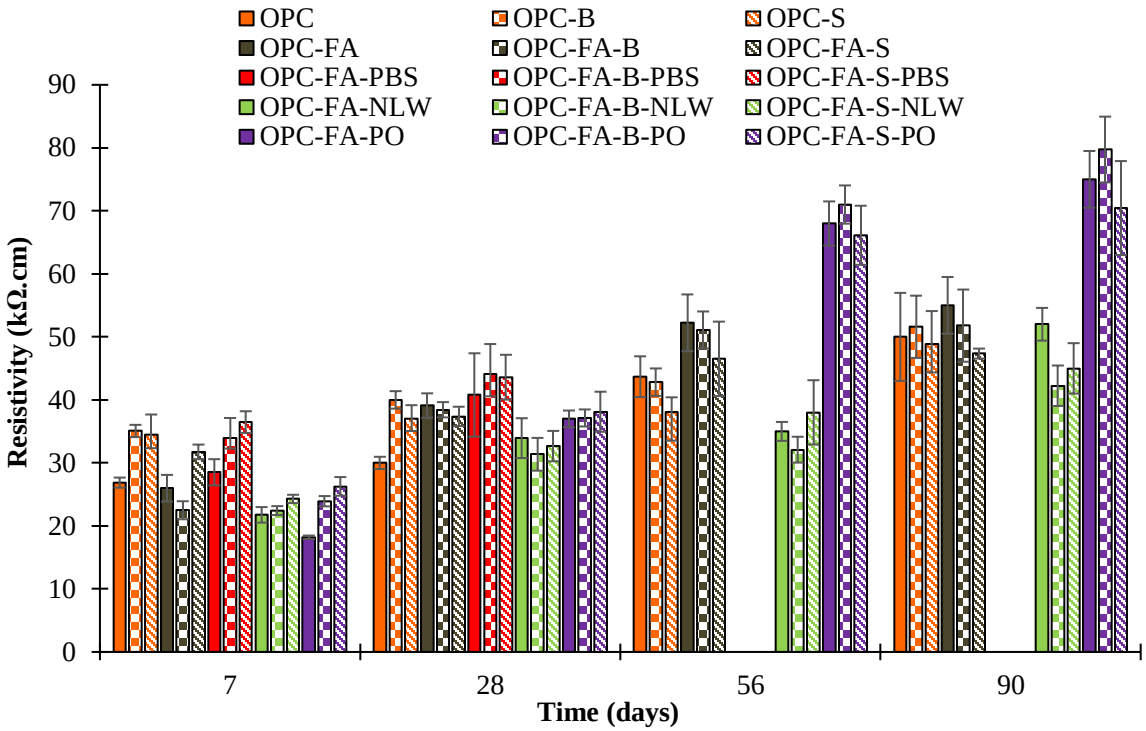

Figure 11.14 - Electrical resistivity of bacterial and non-bacterial OPC and OPC-FA mixtures with different variables.

11.3.4 Water Absorption

Figure 11.14 shows the initial and secondary water absorption results of bacterial and non-bacterial samples at 7 and 28 days. The water uptake of samples was plotted as a function of time for initial and secondary absorptions and the sorptivity was calculated from the slope. The general trend shows that i) secondary sorptivity was lower than initial sorptivity for all samples at both 7 days and 28 days since the majority of the water was absorbed in the first hours of the test and ii) both initial and secondary sorptivities decreased over time as a result of a continuous hydration. Initial sorption rate indicates the pore size between 0.42-180 µm in diameter, whereas secondary sorption, as a result of longer solution exposure times, indicates variances in internal and smaller diameter (< 0.42 µm) pores, tortuosity and the connectivity of pores (Zhang and Panesar 2018). The disconnected air voids and pores in the sample reduce the difference between the initial and secondary absorptions, leading to more durable concrete. Sample having high initial sorptivity and low secondary sorptivity result in fully-saturated sample in a short time, increasing the risk of

freeze-thaw damage (Zhang and Panesar 2018).

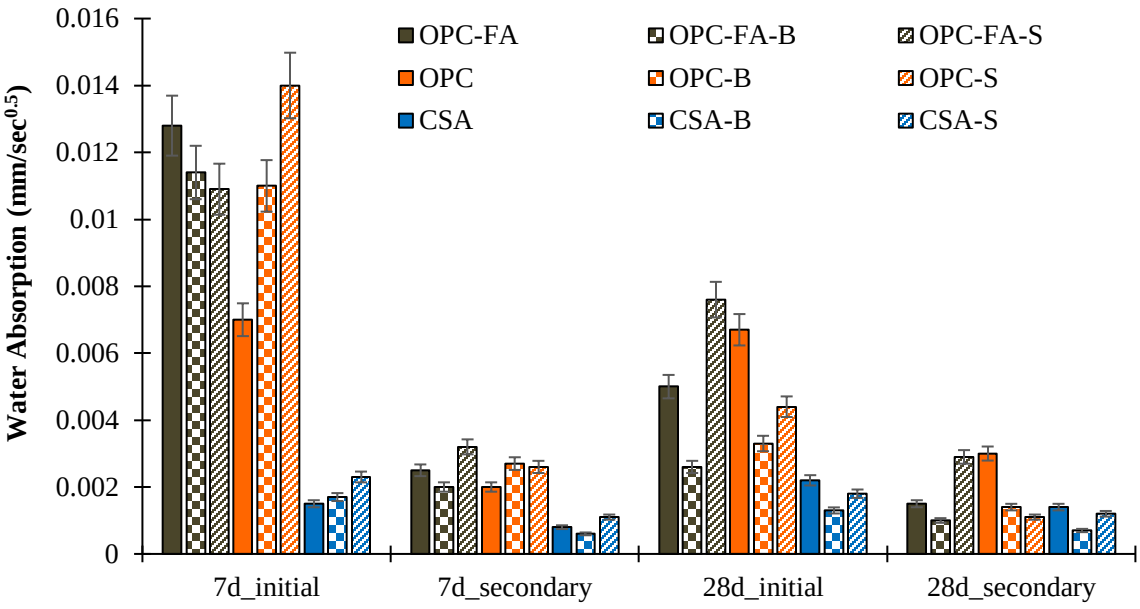

Figure 11.15 - Initial and secondary water absorption of bacterial and non-bacterial OPC, OPC FA and CSA mortars at 7 and 28 days.

7-day results of OPC samples displayed greater amount of initial and secondary sorptivities for both bacterial samples in comparison with the control samples, but both initial and secondary sorptivities of bacterial samples were reduced compared to the control at 28-days. Additionally, use of soil bacteria in OPC samples led to a big decrease in the secondary sorptivity compared to other OPC samples on 7 days (reduced by 210%) and 28 days (reduced by 136%), perhaps indicating that greater effect of soil bacteria on filling smaller pores. OPC-FA-B samples resulted in lower initial and secondary absorptions as compared to control samples (OPC-FA) on both days. Even though OPC-FA-S sample had higher bacteria concentrations up to 28 days, its secondary sorptivity was higher than the control samples at 7 days. Similarly, OPC-FA-S sample led to greater initial and secondary water absorptions at 28 days compared to the control sample. The increase in the water absorption with use of bacteria can be explained by that increased absorption does not necessarily result from greater porosity in the samples, samples can have more water uptake due to increased interconnectivity of pores even if less pore space is available. At early ages (7 days) use of fly ash in the control mixture resulted in an increased initial and secondary sorptivities but decreased at 28 days compared to OPC only mixtures, indicating the slower reactivity of fly ash when compared to OPC.

CSA samples had lower sorptivity at all ages when compared to OPC and OPC- FA samples due to the faster reactivity and faster hydration rates of CSA cement than OPC. The effect of bacteria on the water absorption was not clear within the CSA samples since some of the bacterial CSA samples had higher initial and secondary sorptivity at 7 days than the control CSA sample, despite the higher cell viability in the CSA samples.

Figure 11.15 shows the initial and secondary water absorption results of samples at 7 and 28 days

of OPC-FA samples with PBS, without LWA and when ponding was used as a curing method. In general, PBS samples had lower water absorption than OPC-FA samples at 7 days and similar water absorption at 28 days. Their 7-day results showed lower initial and secondary sorptivities with the bacterial samples when compared to control samples, similar to significantly higher strength obtainment with the use of both bacteria types. However, PBS sample with soil bacteria at 28 days resulted in higher water absorption than in the control. The same trend occurred in the spray-cured OPC-FA samples at 28 days (greater sorptivity occurred in the bacterial samples).

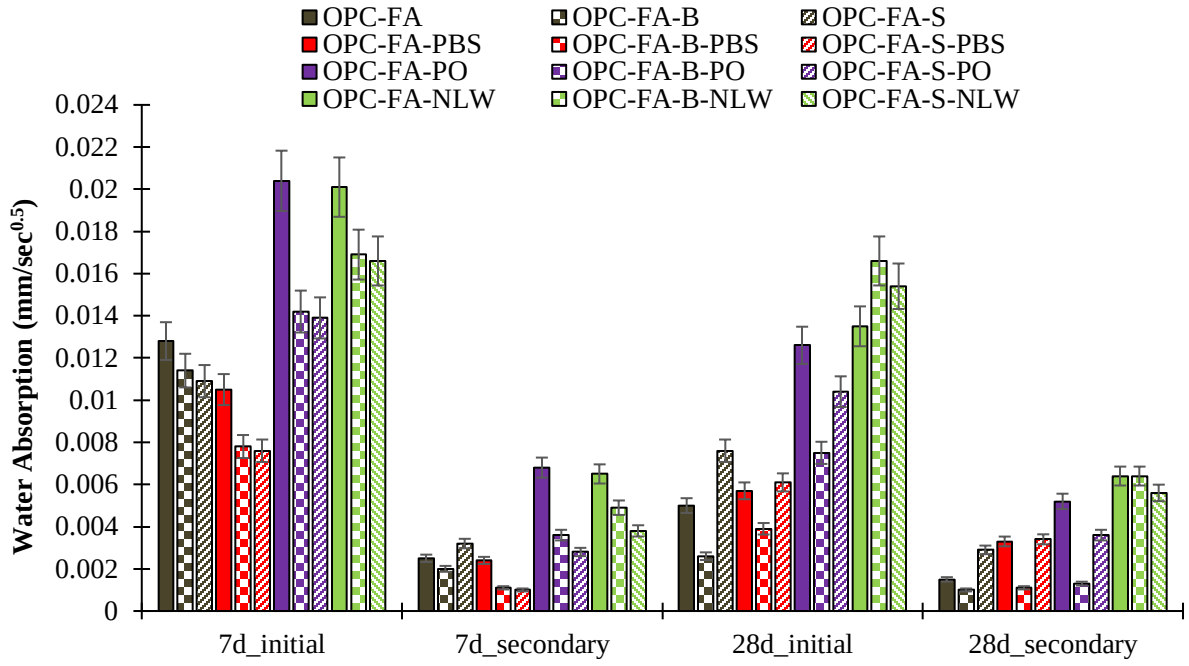

Figure 11.16 - Initial and secondary water absorption of bacterial and non-bacterial OPC FA mortars with different variables at 7 and 28 days.

Ponding samples (OPC-FA-PO) resulted in higher initial and secondary sorptivities for both bacterial and non-bacterial samples when compared to spraying (OPC- FA) at both ages. However, no significant difference was apparent between strength results of spraying and ponding. Use of LWA in the mixture (OPC-FA) led to lower initial and secondary water uptakes than samples without LWA (OPC-FA-NLW). Higher absorption of NLW samples was expected due to the lower strength and lower bacteria viability of these samples (Figures 11.7, 11.8 and 11.11). Additionally, sorptivity of bacterial NLW samples increased from 7 to 28 days. This was distinct from all other samples tested, and is attributed to the degredation of the bacteria in the sand particles leading to increased porosity and lowered strength when compared to degradation of the bacteria in LWA particles.

11.4 Impact of Biomineralization on Self-healing of Cracks

11.4.1 Visual Crack Healing Evaluation

Images of the cracked beams were taken weekly to evaluate the crack healing of the cured (CC)

beams. Cracked and not cured (NC) beams were also evaluated for 6 weeks but are not shown since they did not result in any crack healing. For all samples, visual crack evaluation was conducted on triplicates and one representative image from one set is shown. Figure 11.16 shows the cracked OPC samples before and after crack healing. Average crack size for the samples was measured as 0.4 ± 0.05 mm but crack size was not constant throughout the beam cross-section, ranging from 0.6 mm to 0.25 mm. No crack healing was obtained in control samples without bacteria cells. Crack closure was observed in both bacterial OPC-B and OPC-S samples sprayed with NBUC solution in 4 weeks. However, the closure amount was limited to crack width 0.35 mm. Additional 2 weeks of curing did not result in additional complete healing, although, densification around the edges of wider cracks were visible, leading to reduction in crack width.

Crack images of bacterial and control OPC-FA samples are shown in Figure 11.17. These samples were cured for 8 weeks due to the insignificant crack closure in 6 weeks. OPC-FA-B showed slightly better crack closure than OPC-B, almost full crack closure and greater densification the unhealed part obtained with OPC-FA-B sample. Similarly, healing of OPC-FA-S was similar to OPC-S, resulting in crack healing only on the tip of the crack (0.3 mm). However, densification was still observed on larger portions of the crack (0.5 mm), which may have demonstrated internal healing.

The average crack size for CSA samples was measured as 0.38 ± 0.03 mm and images are shown in Figure 11.18. As OPC-FA samples, CSA samples were investigated for 8 weeks to observe healing of cracks. Full crack closure by precipitation was observed in both bacterial CSA samples after 8 weeks of curing, which was aligned with the higher bacteria viability in these samples. There was not any crack healing observed in non-bacterial CSA sample. The precipitate on the CSA samples seemed denser when compared to OPC samples which may be attributed to different morphology of precipitated calcium carbonate.

Crack healing ability of the bacterial samples subject to pond curing was also investigated, images are shown in Figure 11.19. Curing samples by ponding did not lead to any significant crack closure, although *B. subtilis* bacteria samples showed a slight densification around the cracks. No densification was observed in the soil bacteria samples. All ponded samples had low bacteria viability, which likely prevented healing in these samples.

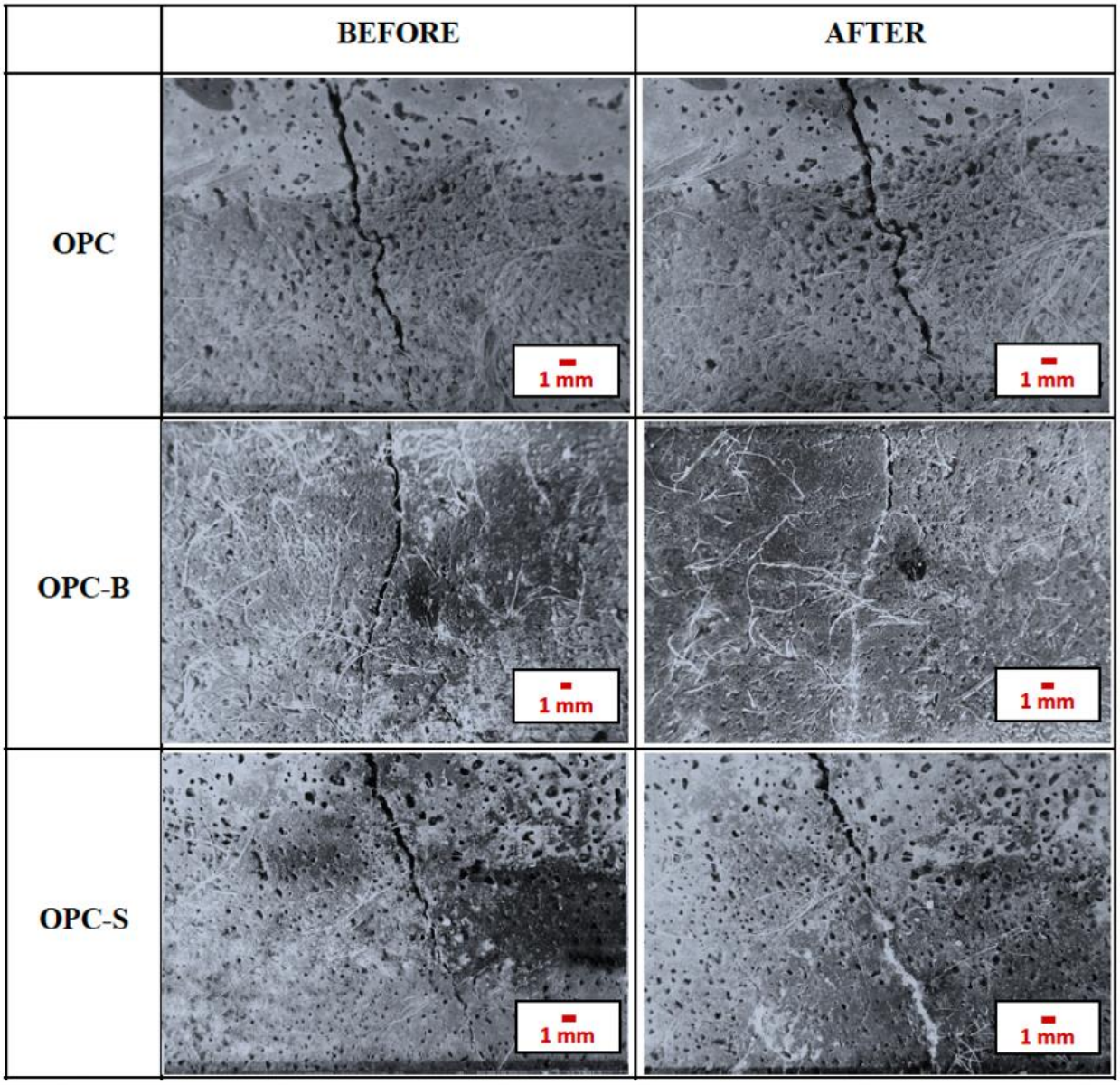

Figure 11.17 - Crack images of bacterial and non-bacterial OPC samples cracked at 14 days. Images on the left show samples right immediately after cracking and on the right are after 6 weeks of spray curing.

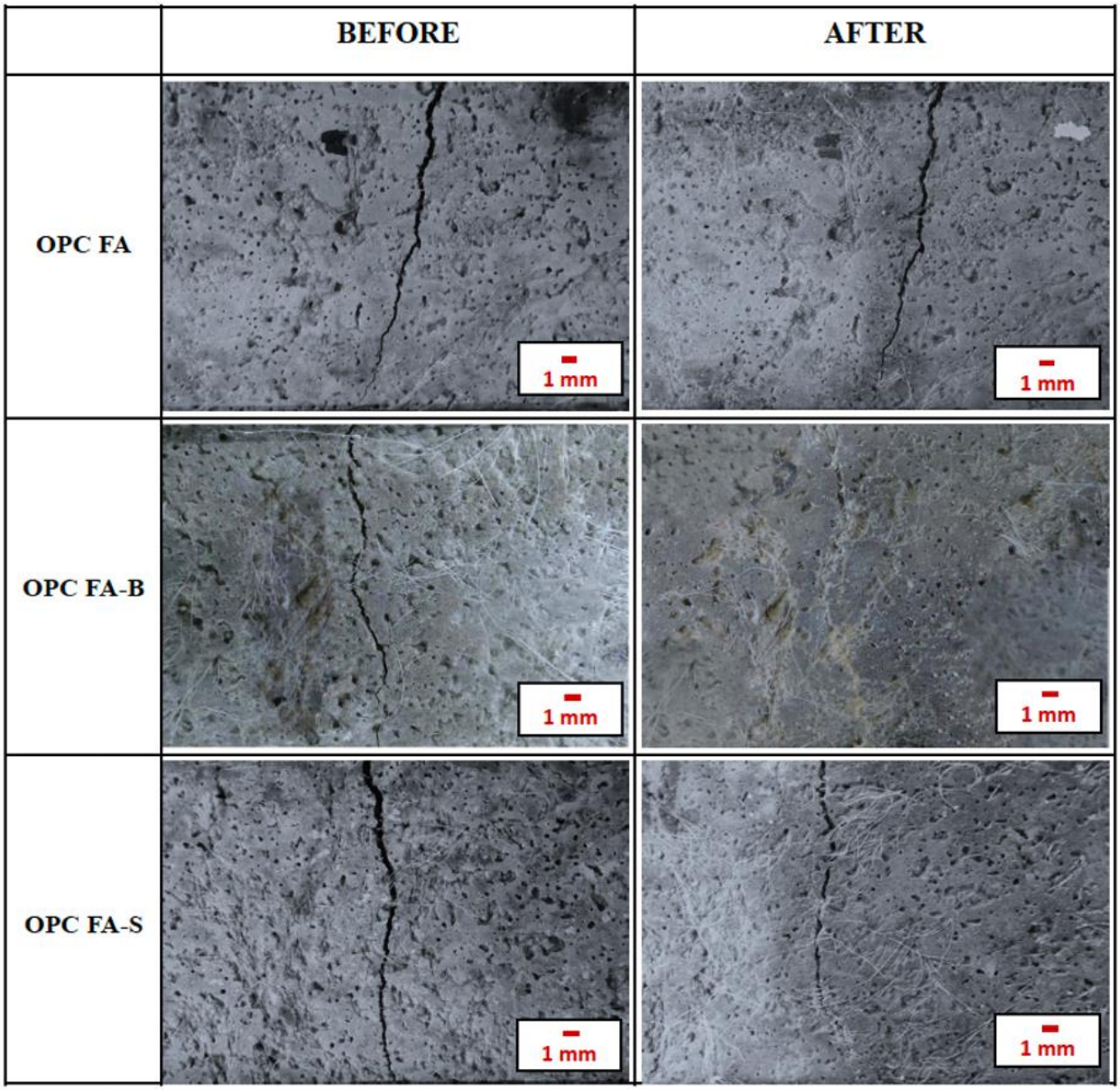

Figure 11.18 - Crack images of bacterial and non-bacterial OPC FA samples cracked at 14 days. Images on the right show samples right after cracking and left after 6 weeks of spray curing.

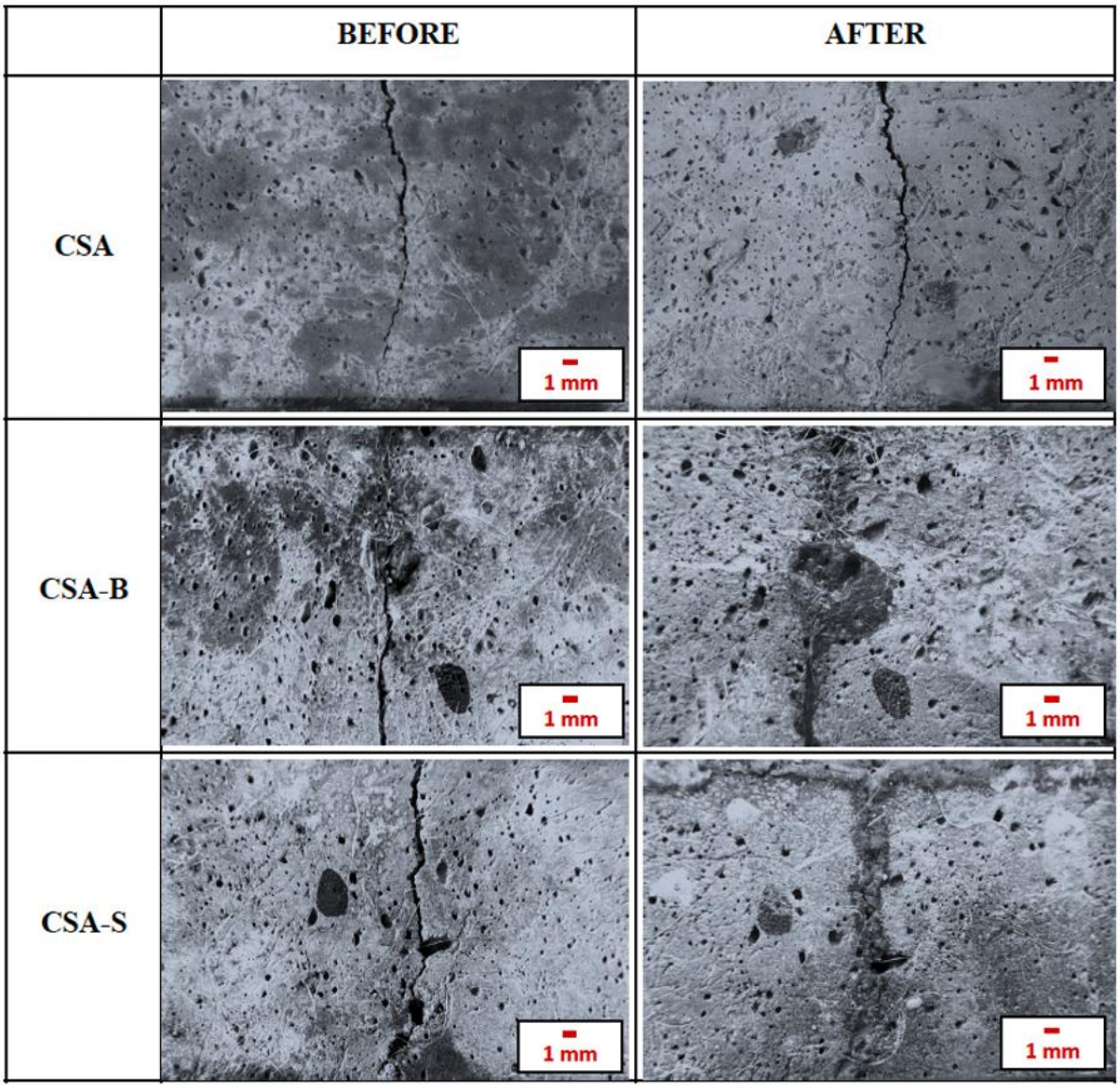

Figure 11.19 - Crack images of bacterial and non-bacterial CSA samples cracked at 14 days. Images on the left show samples right immediately after cracking and on the right are after 8 weeks of spray curing.

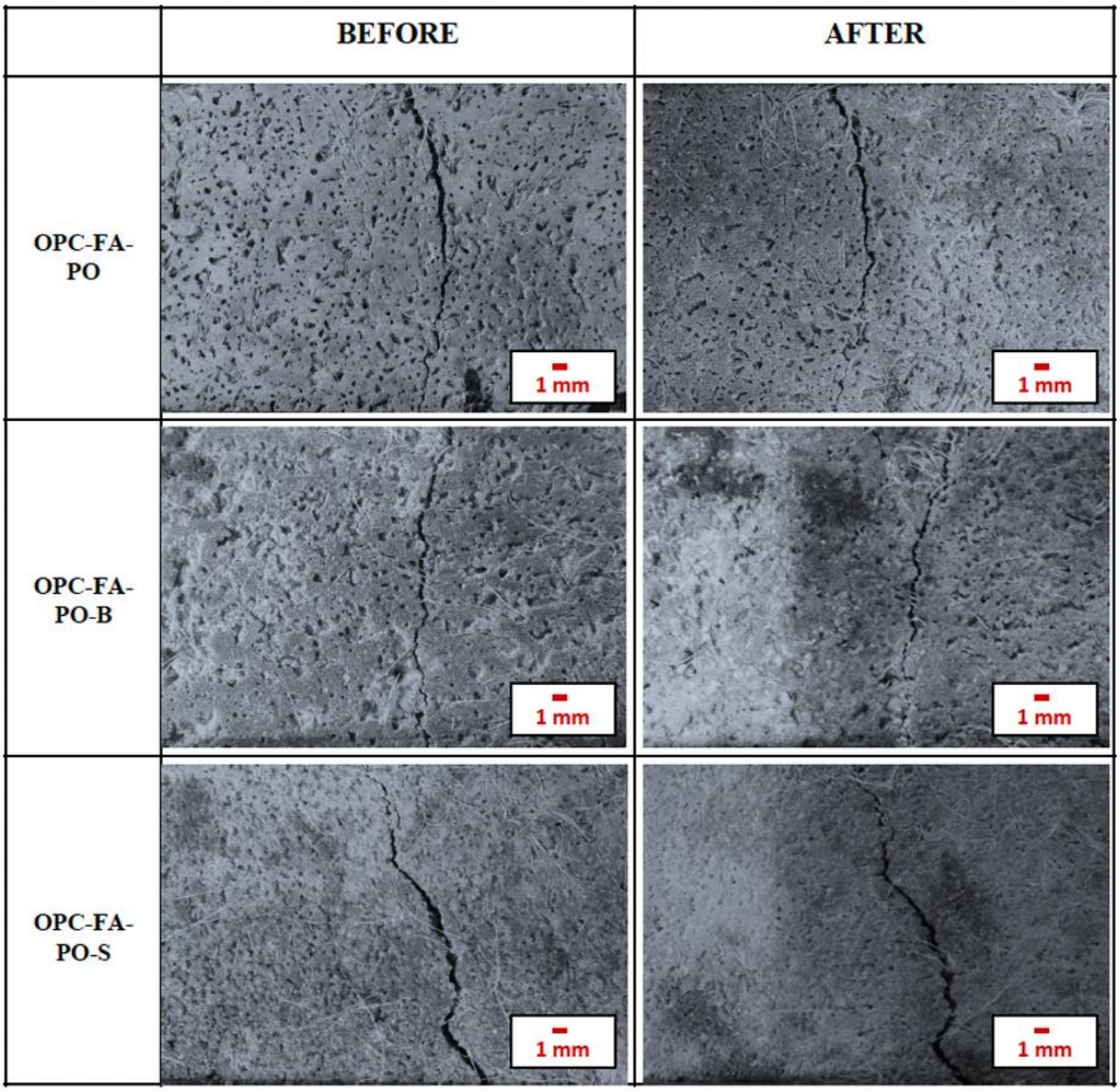

Figure 11.20 - Crack images of bacterial and non-bacterial OPC FA samples cracked at 14 days. Images on the right represent samples right after cracking and left after 6 weeks of pond curing.

11.4.2 UPV Analysis

UPV testing was conducted to assess the crack healing capacity of the samples. UPV measurements provide assessment of crack healing through the depth of the sample, whereas it is unclear from the crack-healing pictures (Figures 11.16-11.19) whether healing was occurring just as the surface of the sample, or throughout the sample depth. Figure 11.20 shows the UPV readings obtained through 6 weeks of following cracking for bacterial and non-bacterial OPC samples cracked at 14 days after mixing. Cracked and cured (CC), cracked and not cured (NC), and uncracked and cured (U) samples are shown.

Uncracked bacterial samples (U) had the highest velocity values among all three sets (NC, CC and

UC) at the end of the healing period. Cracked and cured bacterial OPC samples (OPC-B-CC and OPC-S-CC) reached higher velocities than the non- bacterial samples, coherent with the visual crack closure observations. Moreover, CC samples were able to reach the UPV values measured prior to cracking at the end of the 6-week healing period. Velocity results suggest high quality of the U and CC samples since high velocities (4000 m/s) indicate good quality concrete (Neville and Brooks 1987). However, larger density of the concrete when compared to mortar could lead to an increase in the UPV result by approximately 400 m/s (Kurtulus et al. 2010).

OPC-CC sample had a very similar velocity value to NC samples, demonstrating that even though curing was applied to these samples, internal remediation of internal pores was not attained. Additionally, bacterial CC sample pulse velocities reached the same velocity range as the uncracked samples. This may indicate that in addition to visual crack healing bacteria are densifying the microstructure of the mortars by calcium carbonate precipitation. Cracked and not cured samples had the lowest velocities. Velocity of the control sample (OPC-NC) was lower than the bacterial NC samples. Not-cured samples were tested both to determine the effect of application of curing solutions independent of the addition of bacteria as well as to determine if addition of curing solution is necessary to achieve crack healing in bacteria samples. The results indicate that crack recovery was not obtained when samples were not cured with NBUC solution.

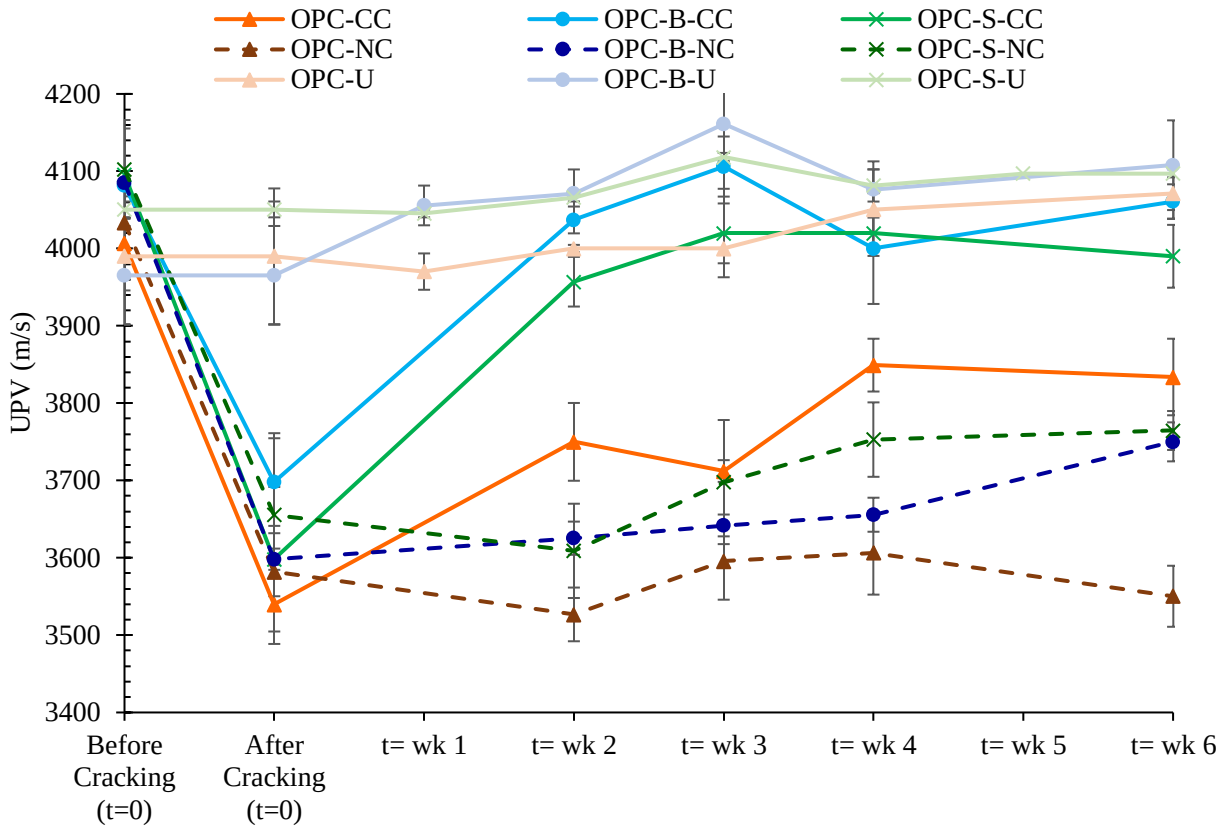

Figure 11.21 - UPV readings of bacterial and non-bacterial cracked and cured (CC), cracked and not cured (NC), and uncracked and cured (U) OPC mortar beams.

Figure 11.21 shows the UPV readings obtained through 8 weeks of observation for OPC-FA

samples cracked at 14 days after mixing. OPC-FA samples generated similar results to the OPC samples. Like OPC samples, uncracked bacterial samples (U) had the highest velocity values in between all three sets (NC, CC and UC) and at the end of the healing period, and bacterial CC samples had significantly higher velocity than the control CC sample. Cracked and not cured samples had the lowest velocity as expected, suggesting that these samples did not fully heal and were of poor quality (UPV ≤ 3600 m/s) (Neville and Brooks 1987).

UPV results of OPC-FA-B-CC are in line with the visual crack closure images. Higher velocity values support the crack closure observed with the *B. subtilis* bacteria. Likewise, visual crack healing of soil bacteria samples (OPC-FA-S-CC) is coherent with the UPV results. The soil bacteria sample did not have obvious visual crack healing and similarly, had lower pulse velocity compared to *B. subtilis* sample. However, its velocity remained higher than the control sample, suggesting that crack closure may have been observed through the depth of the crack rather than only crack mouth.

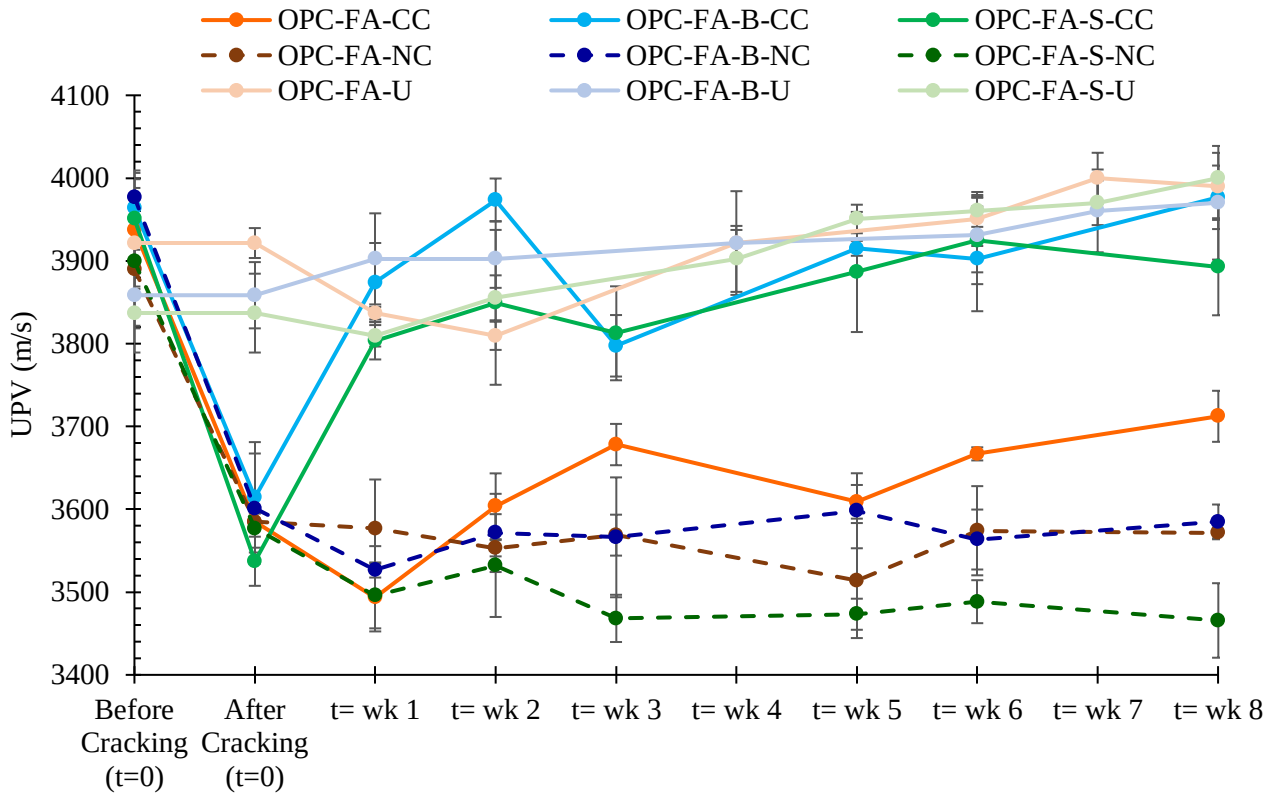

Figure 11.22 - UPV readings of bacterial and non-bacterial cracked and cured (CC), cracked and not cured (NC), and uncracked and cured (U) OPC FA mortar beams.

Crack healing efficiency was examined for CSA samples using UPV testing and Figure 11.22 shows the velocity change of cracked and cured (CC), and cracked and not cured (NC) samples from initial cracking to 8 weeks. The highest velocity, among cracked and cured samples, was observed in the uncracked and cured samples. The uncracked CSA samples with bacteria generated slightly higher pulse velocities than the uncracked non-bacterial samples, indicating creation of a

slightly densified microstructure. In cracked and cured samples no significant difference occurred in bacteria samples compared to the control sample. A more significant change in UPV was expected with use of bacteria since full crack closure was observed with these samples. However, all cracked and cured samples were able to recover most of the velocity loss that occurred due to the crack formation at the end of the 8-week crack healing investigation, indicating that they returned to good quality after the curing period. As the non-bacterial sample also regained most of its original pulse velocity it is unclear that the improvements resulted from bacterial biomineralization, and may instead be linked with continued hydration and curing in the CSA samples. However, the non-bacterial CSA-CC sample had 15% lower velocity change in 8 weeks than the both bacterial samples, perhaps suggesting slight improvements through use of bacteria. Among NC and U sets, no significant difference was found in between bacterial and non-bacterial samples. Similar to the OPC samples, not cured samples (NC) had the lowest pulse velocities, again showing that continued curing was helpful to obtain internal crack healing even without visual observations of healing at the crack mouth.

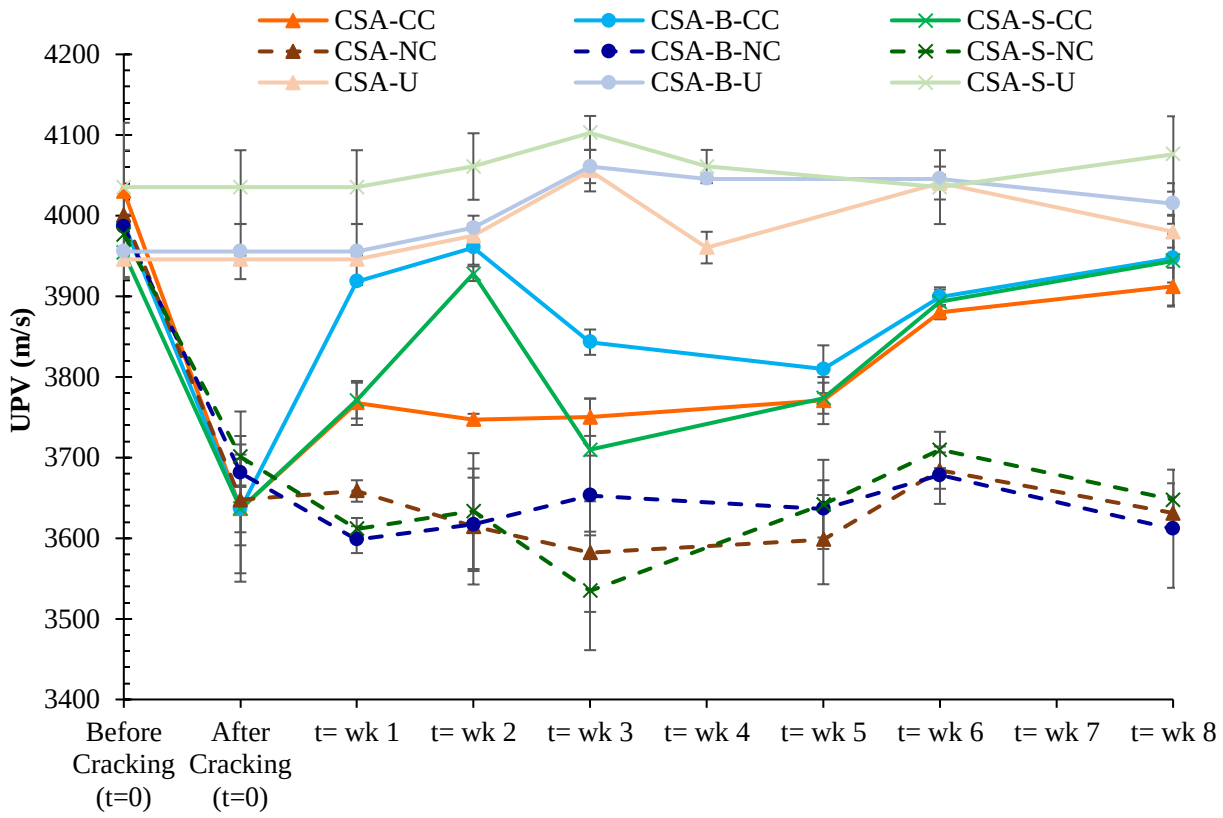

Figure 11.23 - UPV readings of bacterial and non-bacterial cracked and cured (CC), cracked and not cured (NC), and uncracked and cured (U) CSA mortar beams.

Figure 11.23 shows the UPV readings obtained through 8 weeks of observation for cracked at 14 days and curing with ponding. Unlike all other samples, the ponded bacterial CC samples did not generate any visually observable crack healing which can also be observed from UPV results. UPV results of bacterial and non-bacterial CC samples demonstrated very similar velocity values and bacterial and non-bacterial uncracked samples (U) had higher velocity compared to CC samples.

These results indicate that use of ponding as a curing method was not efficient to induce crack healing. NC samples had lower velocity in comparison with CC samples, showing that curing did improve the internal porosity despite the lack of crack healing. However, difference between CC and NC samples were lower than other sets of samples shown in Figure 11.19 suggesting that the ponding curing method provided less continued hydration compared to use of the spray curing method.

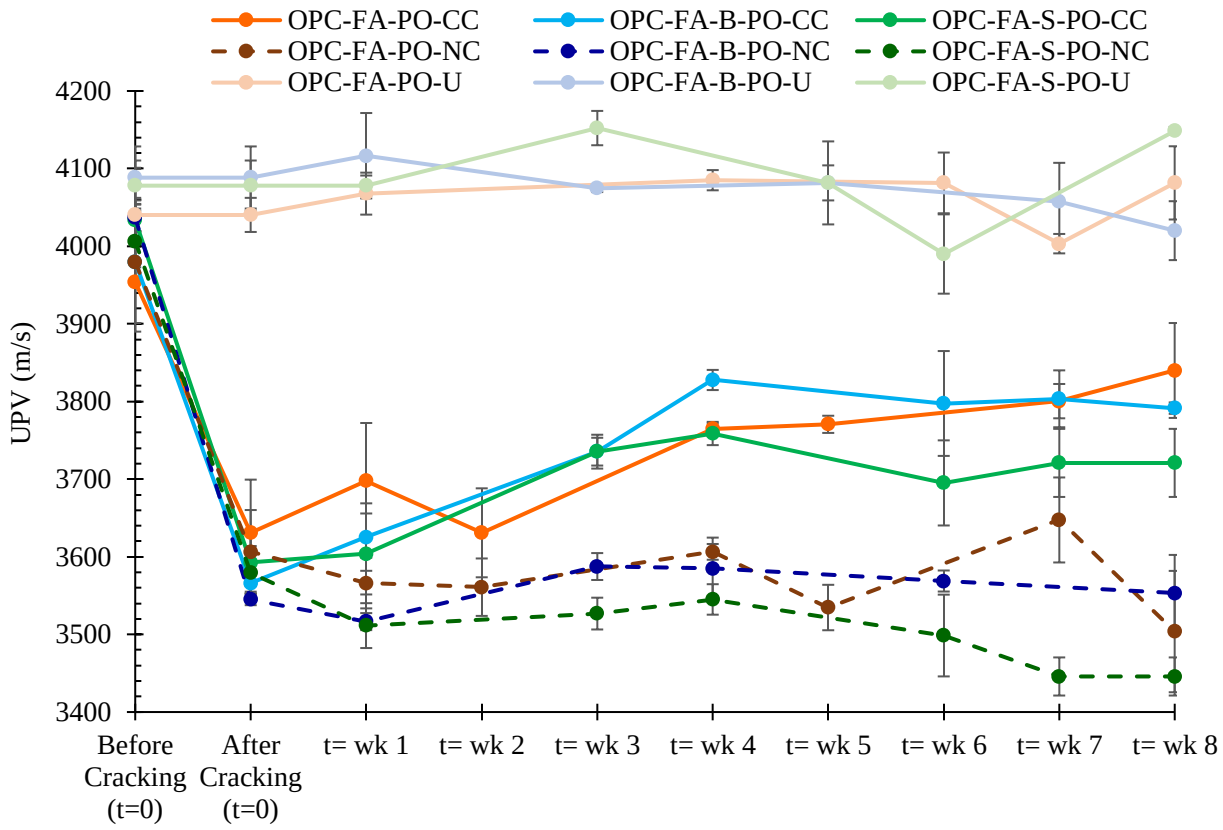

Figure 11.24 - UPV readings of bacterial and non-bacterial cracked and cured (CC), cracked and not cured (NC), and uncracked and cured (U) OPC + FA mortar beams.

Change in UPV was calculated for all cracked and cured (CC) samples to evaluate the change in UPV between right after samples cracked at 14 days and after the completion of the healing process and shown in Figure 11.24. Note that this measurement takes into account the starting UPV and change in velocity over time of each sample, rather than assessing actual UPV value. Results for the OPC and OPC + FA samples are in line with the visual crack healing observations and UPV results. OPC-FA sample with *B. subtilis* OPC-FA with soil bacteria resulted in the highest change, indicating the highest ability of crack healing. OPC-FA-S and OPC with *B. subtilis* and soil bacteria had all similar values and a little lower change than OPC-FA with *B. subtilis*. However, all four of these bacterial samples generated higher change than their controls, showing the efficiency of healing. CSA sample pulse velocity changes were not significantly increased through use of bacteria and improvements in the pulse velocity were lower in all CSA samples compared to OPC and OPC + FA samples. Lastly, as OPC-FA-PO samples did not lead to any crack healing, and expectedly change in UPV for these bacterial samples is the lowest.

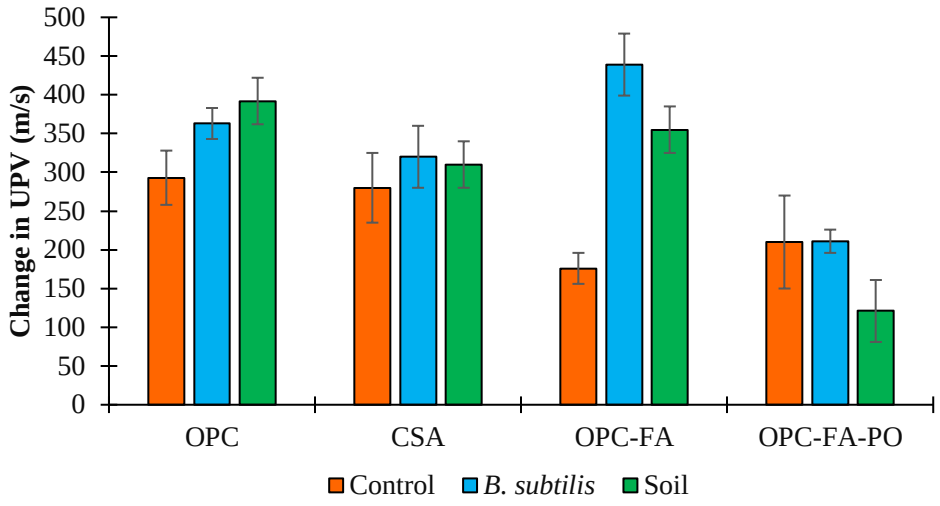

Figure 11.25 - Comparison of UPV change of bacterial and non-bacterial cracked and cured (CC) samples before and at the end of the healing process.

11.4.3 Water Absorption

Water absorption of beams after healing period was tested to quantify the degree of crack closure. The water absorption capacity of samples after 6-week or 8-week curing times was plotted as a function of time. OPC- CC control sample had higher slope for both initial and secondary sorptivities when compared to bacterial samples, indicating that bacteria in the cracked and healed samples had lower water absorption.

For OPC-CC samples, the calculated initial and secondary water absorptions are shown in Figure 11.25. All samples showed same trends for initial and secondary sorptivities, control samples had the highest initial and secondary values and bacterial samples had lower sorptivity values than the control, with 57% and 62% decreases in initial water absorption coefficient in samples with *B.subtilis* and soil, respectively, compared to the non-bacterial sample. The differences were even larger for secondary sorptivity with 73% reductions for *B.subtilis* and 75% reductions for soil samples compared to the control mixture. Water absorption results were aligned with the visual inspection and UPV test results.

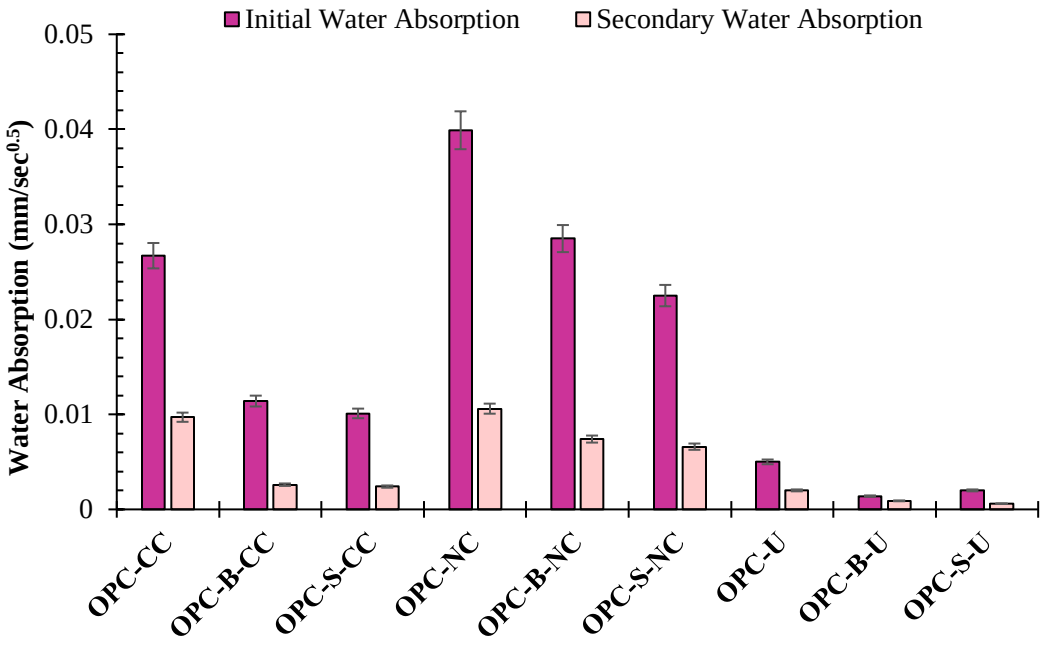

Figure 11.26 - Initial and secondary water absorptions of bacterial and non-bacterial OPC mortar beams after the healing process by spray curing. CC: cracked and cured, NC: cracked and not cured, U: uncracked and cured.

Similar observations were obtained for cracked and not cured (NC) samples, such that control samples without bacteria had higher initial (29% and 43% increase relative to *B. subtilis* and soil, respectively) and secondary sorptivities (30% and 38% increase relative to *B. subtilis* and soil bacteria, respectively). Lower water absorption of the bacterial samples compared to the control samples may indicate internal crack healing occurrence in bacterial samples, which is also consistent with the UPV results. However, although bacterial samples showed evidence of ability in crack healing, they still absorbed more water than the uncracked samples (OPC-B-U and OPC-S-U), suggesting that cracks were not returned to equal quality as in uncracked samples.

Figure 11.26 displays the water absorption capacity of OPC-FA samples cracked at 14 and days after mixing and cured for 8 weeks. Bacterial CC samples led to lower water absorption than the control CC sample, similar to the OPC set. OPC-FA-B sample showed a consistent behavior in terms of relating the change in water absorption to visual crack healing and UPV results. Such that cracks were almost completely healed and there was a more significant change in velocity in the OPC-FA-B sample when compared to control. This corresponded to 67% reduction in initial water absorption of *B. subtilis* sample when cured in NBUC, and 60% reduction in secondary sorptivity.

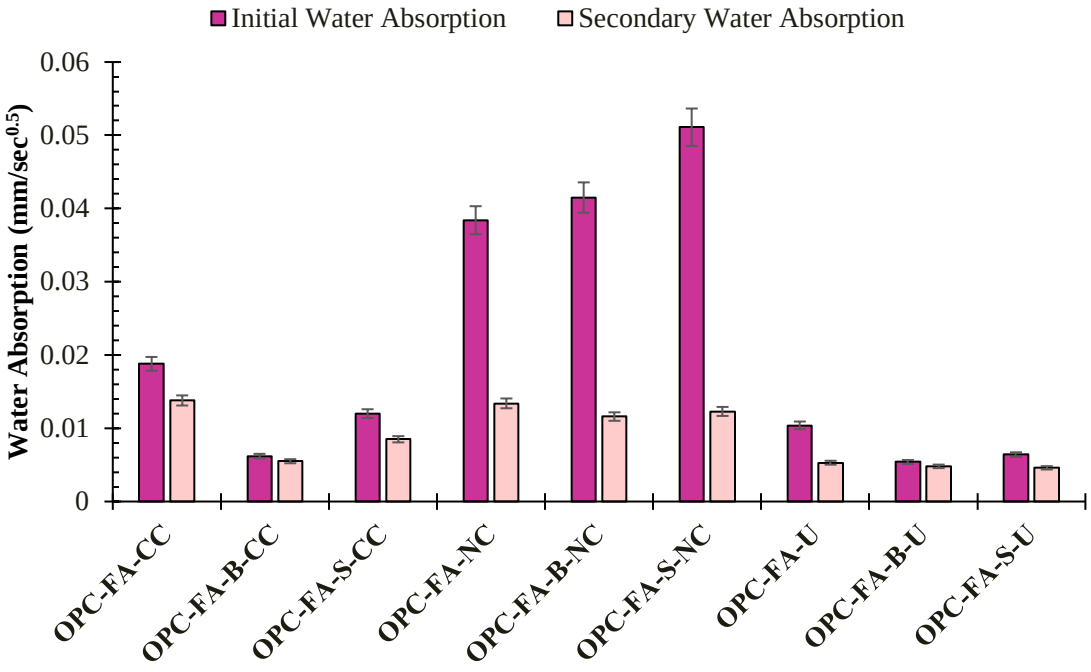

Figure 11.27 - Initial and secondary water absorptions of bacterial and non-bacterial OPC-fly ash mortar beams after the healing process by spray curing. CC: cracked and cured, NC: cracked and not cured, U: uncracked and cured.

However, for the soil bacteria sample the reduction in both initial and secondary water absorptions are 37%. This reduction was in line with the crack closure analysis since there was no obvious crack closure obtained with OPC-FA-S samples, and its velocity change was 20% lower than the *B. subtilis* sample. Therefore, it can be assumed that although use of *B. subtilis* or soil bacteria did not result in noteworthy change in OPC and CSA samples, use of *B. subtilis* in OPC-FA mixture led to more effective healing than soil. On the other hand, bacterial OPC-FA-NC samples did not result in decreased water absorption as compared to control, similar to what was shown in the UPV results. Use of *B. subtilis* with OPC-FA resulted in no difference between absorption of CC and U samples, whereas use of soil bacteria in the CC sample had slightly higher water absorption than the U sample.

Initial and secondary water absorptions for CSA samples are shown in Figure 11.27. Although there was only small amount of visual crack closure obtained and no clear distinction was found between CSA-CC and CSA-Bacterial-CC from UPV results, both bacterial samples generated significantly lower absorption compared to the control sample, with 63% and 52% reductions in the both initial and secondary sorptivity values in CSA-B-CC and CSA-S-CC samples, respectively, compared to the non-bacterial CSA-CC sample also cured with NBUC. This may be due to the precipitation of different calcium carbonate polymorphs, such as precipitation of stable calcite rather than less stable vaterite and may result in denser precipitate to induce internal crack healing and greater reduction in water absorption (Rao et al. 2013; Xu and Wang 2018). In addition, the reduction in water absorption with NC bacterial samples was less than in the CC samples, suggesting that changes in water absorption in the cracked samples are likely due, at least in part, to increased curing. Similar to OPC samples, uncracked CSA samples had lower sorptivity

when compared to cracked and cured samples. However, there was less difference between CSA-B-CC and CSA-B-U samples and CSA-S-CC and CSA-S-U samples when compared to difference between CC and U control samples, showing that healed bacterial CSA beams would perform as better as uncracked beams.

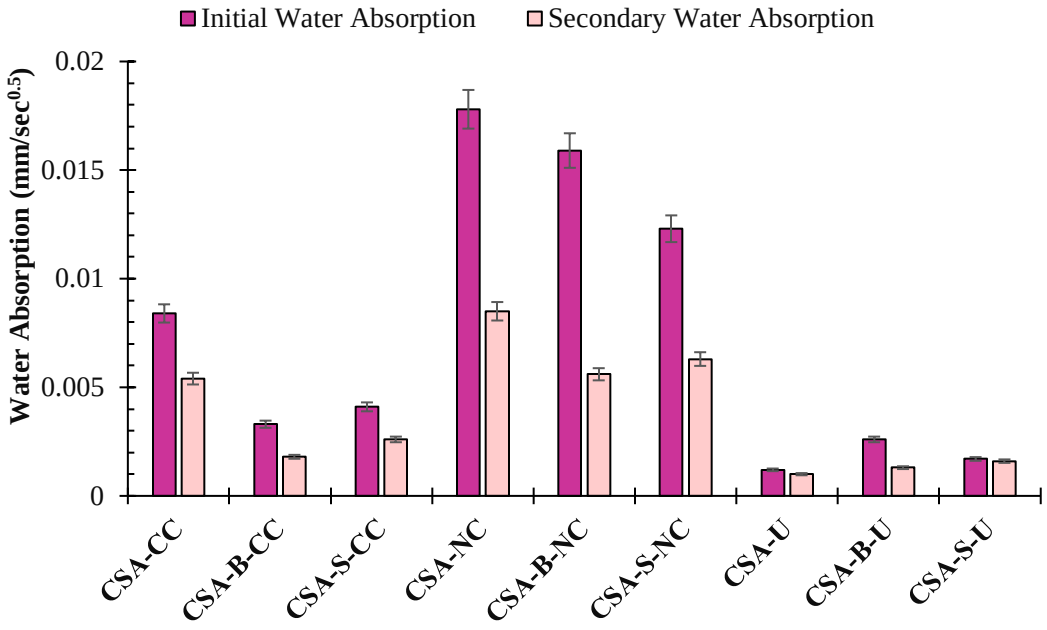

Figure 11.28 - Initial and secondary water absorptions of bacterial and non-bacterial CSA mortar beams after the healing process by spray curing. CC: cracked and cured, NC: cracked and not cured.

Lastly, water absorption results for the ponded samples were shown in Figure 11.28. In agreement with the visual crack healing and UPV results, curing samples with ponding was inefficient in terms of decreasing the sorptivity for bacterial samples. Bacterial CC samples showed an increase in the water absorption when compared to the control sample and no obvious change was obtained in the water absorption between bacterial and non-bacterial NC beams.

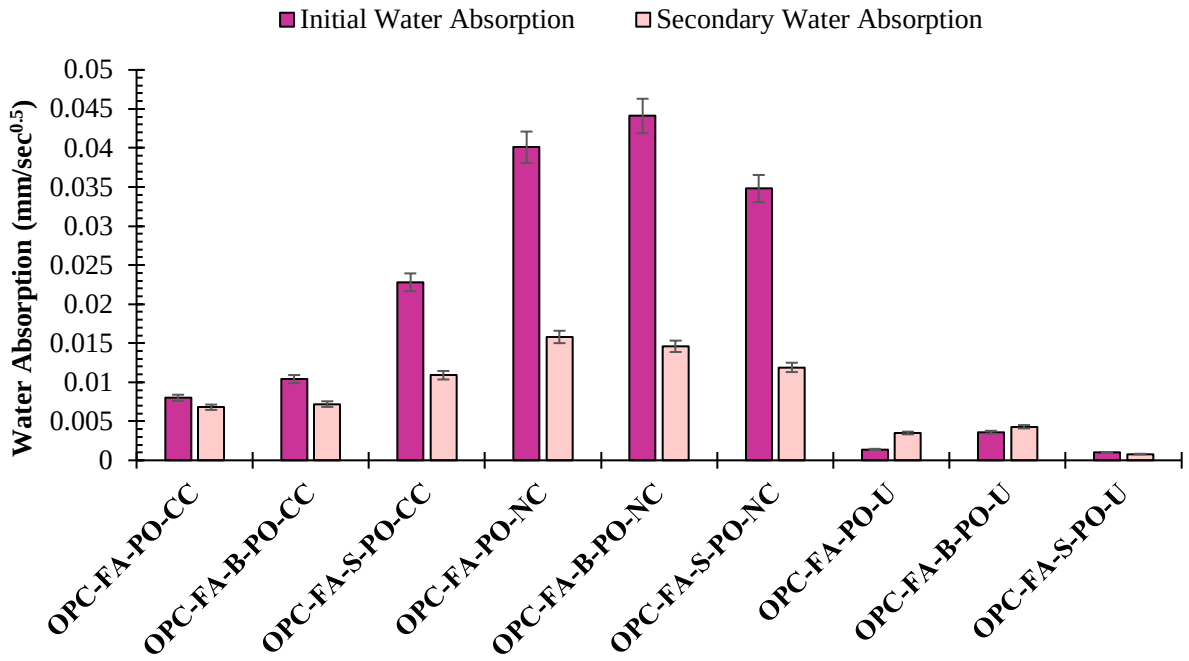

Figure 11.29 - Initial and secondary water absorptions of bacterial and non-bacterial OPC FA mortar beams after the healing process by pond curing. CC: cracked and cured, NC: cracked and not cured.

Comparison of initial and secondary sorptivities of OPC, CSA and OPC FA samples are shown in Figure 11.29. In general, CSA cement resulted in lower sorptivity when compared to OPC and OPC-FA mixtures due to its smaller pore size than OPC and higher rate of reaction (Burris and Kurtis 2018). However, no general trend was observed when fly ash was used in the mixture when compared to OPC only mixture, it reduced initial sorptivity with *B. subtilis* and increased with soil bacteria compared to OPC. Although use of *B. subtilis* in CSA led to the lowest initial and secondary water sorptivity values, it cannot be considered as the most efficient sample combination due to the minimal visualized crack healing and small changes in UPV results. Based on the combined crack healing, UPV, and sorptivity results the OPC-FA mixture using *B. subtilis* results in better crack healing ability. Use of the OPC-FA-B resulted in similar water absorption and visual crack closure results, but greater velocity improvements. With the soil bacteria, use of the OPC only mixture led to the most efficient crack healing in terms of water absorption results and visual crack closure.

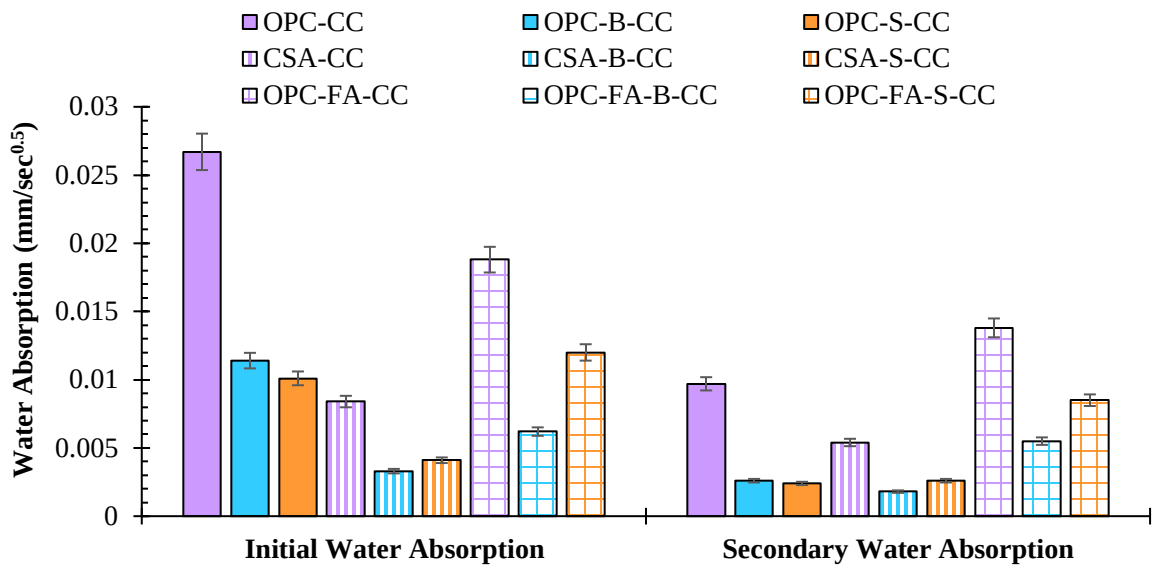

Figure 11.30 - Comparison of initial and secondary water absorptions of bacterial and non-bacterial cracked and cured (CC) OPC, OPC-FA, and CSA mortar beams after the healing process.

11.4.4 Characterization of the Healing Product Using SEM imaging

Images of bacterial OPC samples are shown in Figures 11.30 and 11.31 for OPC- B and OPC-S, respectively. Similar calcium carbonate morphologies, rhombohedral calcite, were observed in both *B. subtilis* and soil bacteria samples (shown as Cc). Additionally, evidence of bacteria was seen from the SEM images (shown with red circles). Bacteria has previously been shown to appear as 1-3 µm rod-shaped particles or 0.5-1 µm diameter round hole (Wu et al. 2019; Wang et al. 2011). Differently than OPC-B samples, OPC-S sample showed layer-by-layer calcite precipitation. The spherical crystals in Figures 11.30-right and 11.31-left may indicate formation of spherical calcite or vaterite, which can result from use of calcium acetate in the curing solution. It has been shown that the morphology of the calcite crystals can be impacted by calcium source used (De Muynck et al. 2008). Consistent with the visual observations, UPV and sorptivity, these images demonstrated that both microorganisms were able to precipitate calcite within the crack area.

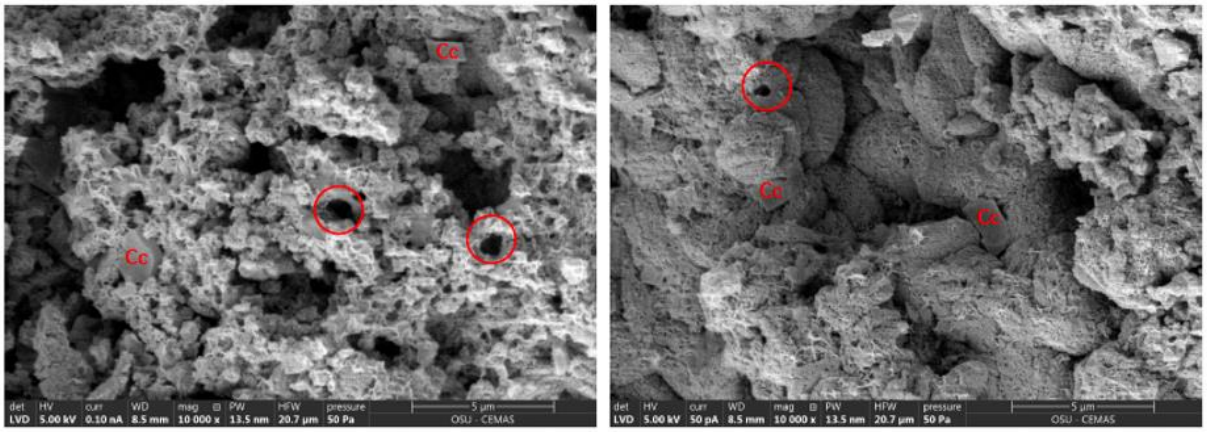

Figure 11.31 - SEM images of the crack surface obtained from OPC samples with *B. subtilis* bacteria cured with spraying for 6 weeks. Circles indicate presence of bacteria, CC: calcium carbonate.

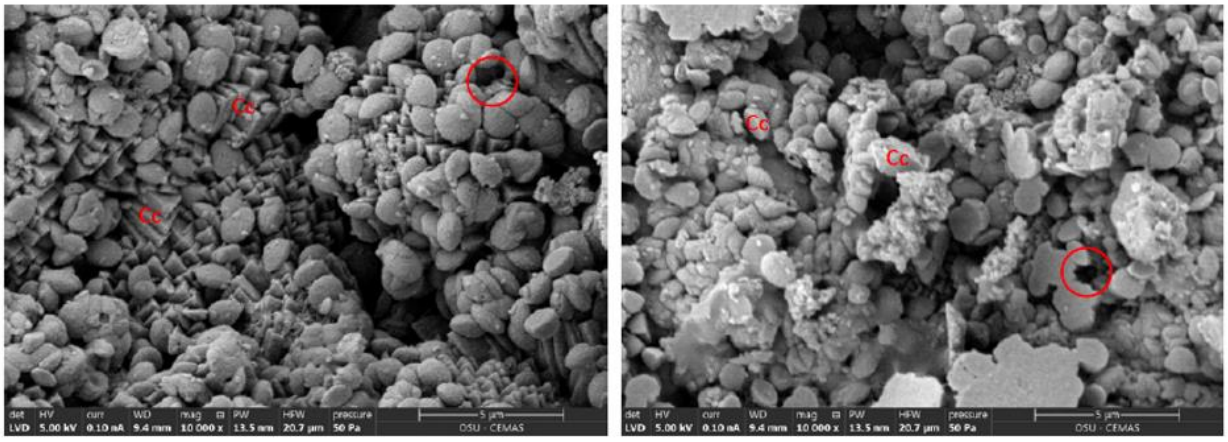

Figure 11.32 - SEM images of the crack surface obtained from OPC samples with soil bacteria cured with spraying for 6 weeks. Circles indicate presence of bacteria, Cc: calcium carbonate.

Similar to OPC *B. subtilis* samples, images of OPC-FA-B showed indication of 2 µm rod-shaped bacteria and calcite crystals (Figure 11.32). Additionally, OPC-FA-S indicated rhombohedral calcite crystals and indication of 1.5 and 3 µm of bacteria cells (Figure 11.33). The shape of the two bacteria cells observed were different than each other. Soil bacteria being an axenic (i.e. non-pure) source of bacteria, can consist of different types of bacteria rather than single strain. Therefore, their shapes and lengths can be different. OPC-FA-S showed greater and denser calcite precipitation, correlating with the lower water absorption and higher UPV obtained measured in the OPC-FA-S samples. However, although better crack healing was observed with OPC-FA-B sample, it resulted in less dense microstructure when compared to OPC- FA-S.

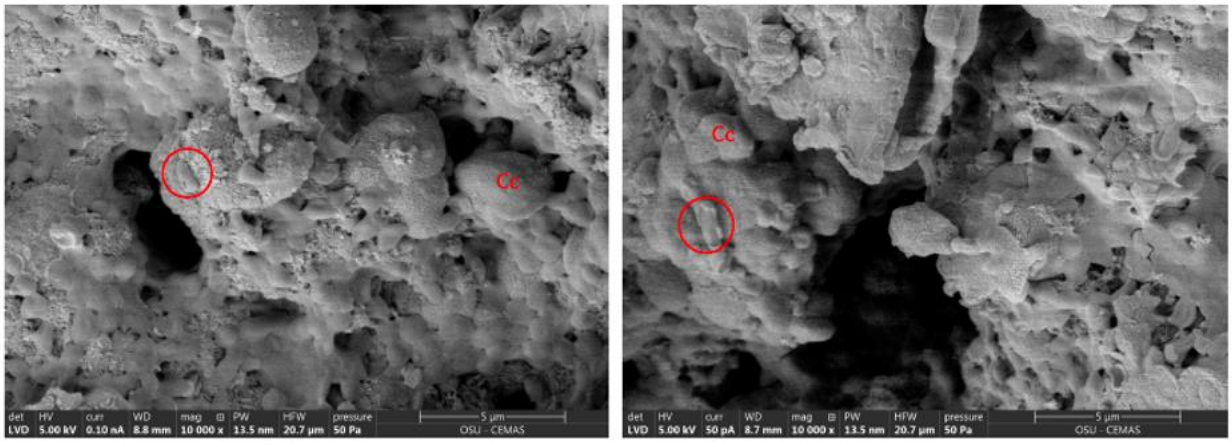

Figure 11.33 - SEM images of the crack surface obtained from OPC FA samples with *B. subtilis* bacteria cured with spraying for 8 weeks. Circles indicate presence of bacteria, CC: calcium carbonate.

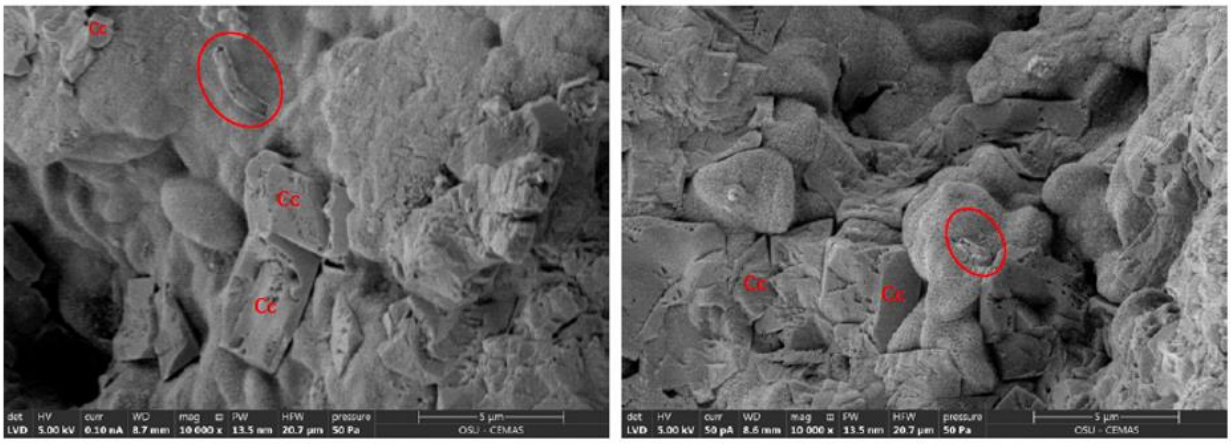

Figure 11.34 - SEM images of the crack surface obtained from OPC FA samples with soil bacteria cured with spraying for 8 weeks. Circles indicate presence of bacteria, Cc: calcium carbonate.

SEM images of the CSA-B samples showed precipitation of calcite crystals and indications of bacteria in rod-shaped (with length of 2 µm) and round holes (Figure 11.34). However, although calcite precipitates could be seen in the CSA-S samples in Figure 7.36, no clear indication of bacterial cells was found. The red circled area in Figure 11.35-right, may have been an indication of rod-shaped bacteria, but it is not obvious evidence. In addition to calcite crystals, ettringite formation was observed in CSA-S samples (shown as "AFt"). Even though indication of bacteria was not observed in CSA-S sample, it can be assumed the presence of calcite, a phase not typically found in significant proportion in hydrated CSA systems, resulted in self-healing of cracks and decreased water absorption.

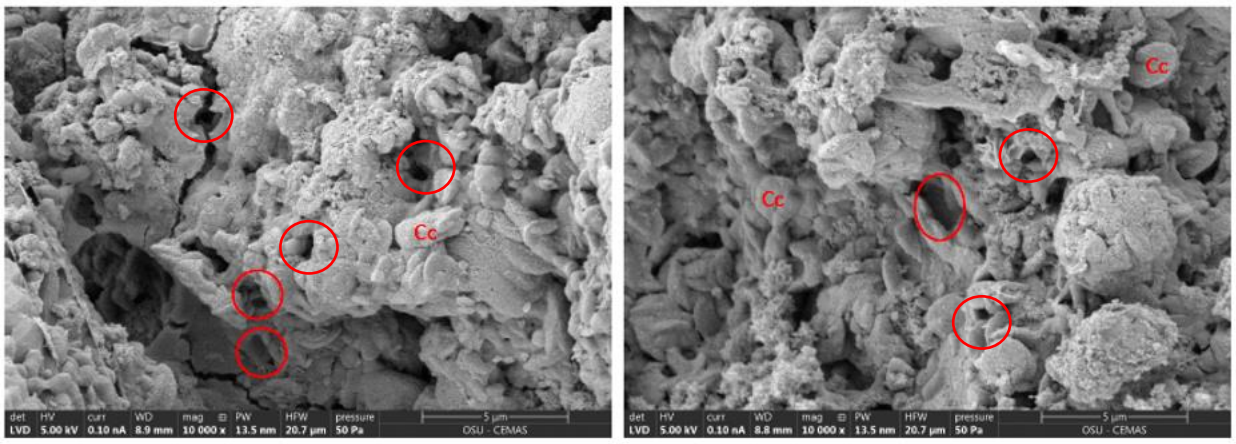

Figure 11.35 - SEM images of the crack surface obtained from CSA samples with *B. subtilis* bacteria cured with spraying for 8 weeks. Circles indicate presence of bacteria, CC: calcium carbonate.

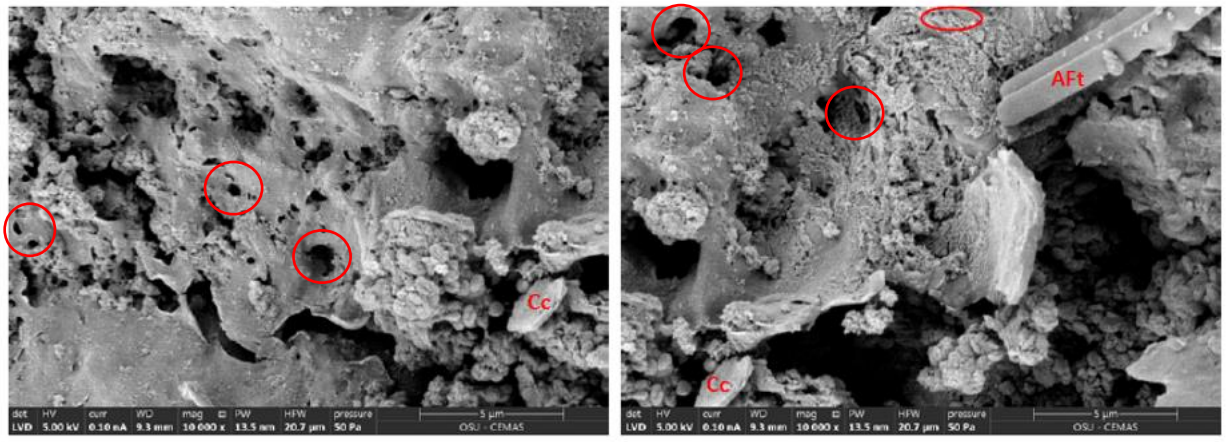

Figure 11.36 - SEM images of the crack surface obtained from CSA samples with soil bacteria cured with spraying for 8 weeks. Circles indicate presence of bacteria, Cc: calcium carbonate. AFt: ettringite.

11.4.5 TGA Testing - Amount of the Precipitated Calcite

TGA was conducted to quantify precipitated calcite in the mortar samples. The differential mass loss curves for OPC, OPC-FA, and CSA samples from 400 °C temperature to 900 °C are shown in Figures 11.36-11.38. Mass loss curve consists of one main peak for each sample, corresponding to the decomposition of calcium carbonate phase (centered around 750 °C) (Snellings 2016). The area under the peak represents the quantity of the calcite, showing that, with the exception of the CSA-S, sample bacterial samples had greater quantities of calcium carbonate when compared to their controls.

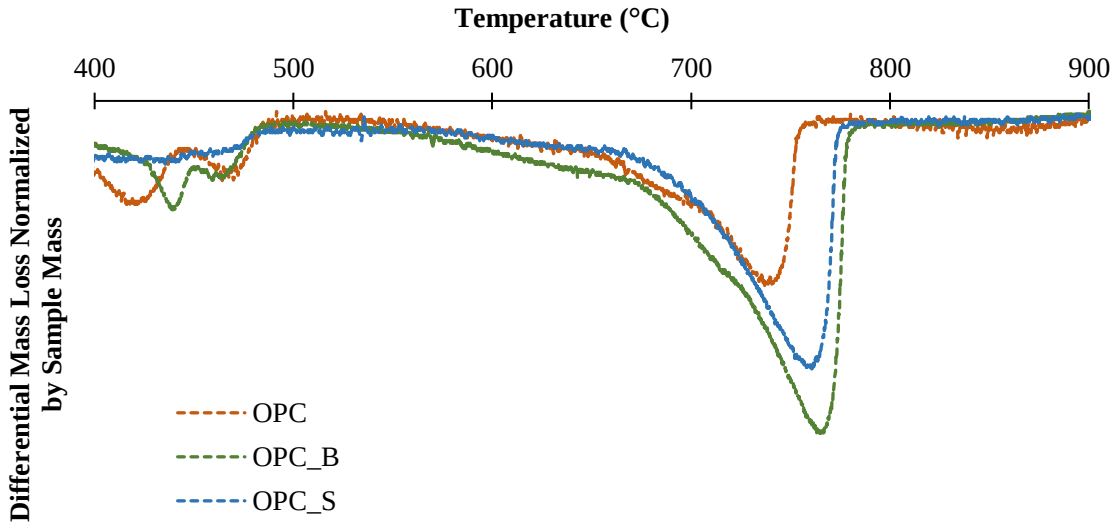

Figure 11.37 - Differential thermogravimetric mass loss curves for bacterial and non-bacterial OPC samples obtained from the crack surface.

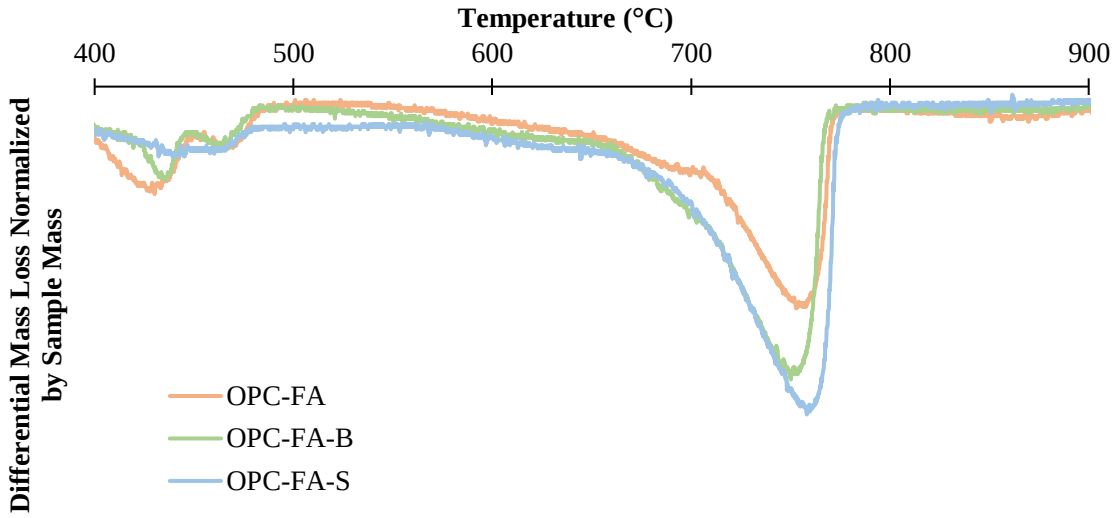

Figure 11.38 - Differential thermogravimetric mass loss curves for bacterial and non-bacterial OPC-FA samples obtained from the crack surface.

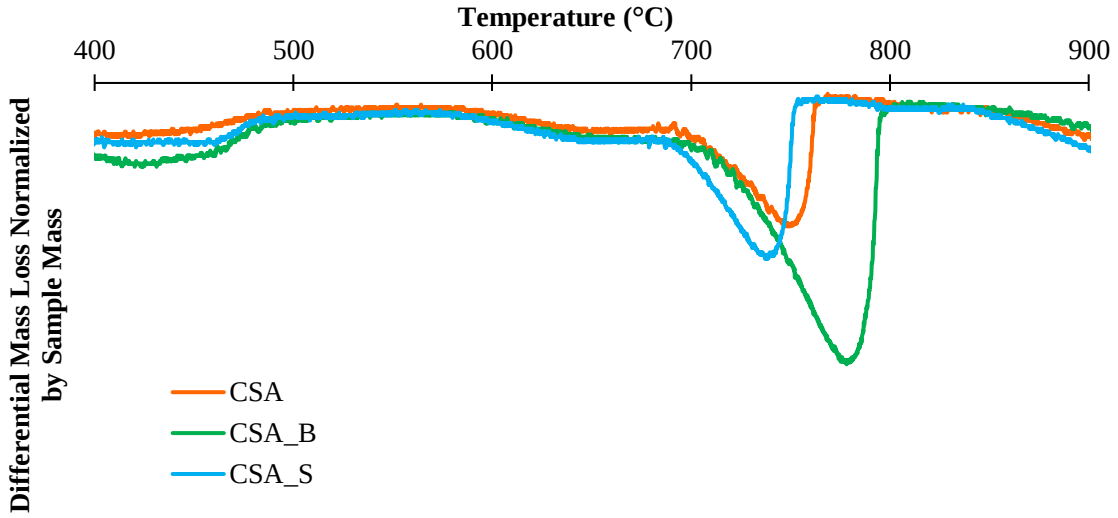

Figure 11.39 - Differential thermogravimetric mass loss curves for bacterial and non-bacterial OPC samples obtained from the crack surface.

The amount of calcium carbonate (mainly calcite) calculated in each sample from mass loss between 600 °C and 800 °C is shown in Figure 11.39. All bacterial samples had significantly higher amounts of calcium carbonate than control samples. In general, *B. subtilis* samples had greater amount of calcium carbonate than soil samples. Compared to their controls, OPC-B, CSA-B and OPC-FA-B resulted in 112%, 108% and 43% higher calcite precipitation, respectively, indicating that use of OPC led to the highest precipitation. For soil samples, highest precipitation occurred in the OPC-FA sample resulting in 63% higher calcite than in the OPC-FA control. OPC-S and CSA-S resulted in 48% and 46% higher calcite than their controls.

Although CSA samples had full crack healing when either *B. subtilis* or soil bacteria were used, they did not generate the highest amount of calcium carbonate, perhaps due to the precipitation of different polymorphs of calcium carbonate rather than calcite. While decomposition of calcite can be obtained by TGA from the mass loss between 600-800 °C. Aragonite, vaterite and other crystalline polymorphs, recrystallize without weight change at 450 °C and amorphous calcium carbonate decarbonates between 400 and 600 °C (Snellings 2016). Other cement hydrates, including calcium hydroxide, also loss mass in this range, complicating quantification of calcium carbonate phases.

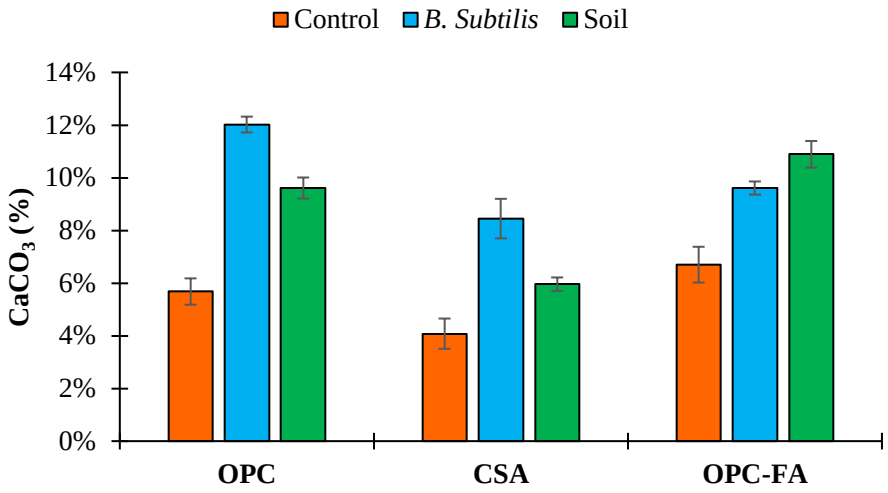

Figure 11.40 - Amount of calcium carbonate in bacterial and non-bacterial OPC, CSA and OPC FA samples after the healing process.

11.5 Effect of Environmental Conditions – Temperature and Salt Exposure on Bacterial Mortars

11.5.1 Effect of Low and High Temperatures on Bacterial Mortars

Figure 11.40 shows the bacterial viability of *B. subtilis* and soil bacteria cells in mortars with various variables to compare curing temperatures including low temperature (LT)-10 °C, high temperature (HT)-40 °C and room temperature-25 °C. Both low and hot temperatures curing resulted in a decrease in the bacterial viability compared to room temperature samples. Low temperature samples showed a slightly lower bacteria counts than high temperature samples which is attributed to the faster growth of cells at higher temperatures leading to faster cell death. *B. subtilis* samples at low temperature had higher bacteria viability compared to soil bacteria samples after 56 days, demonstrating the better resilience of B. subtilis bacteria to high temperatures.

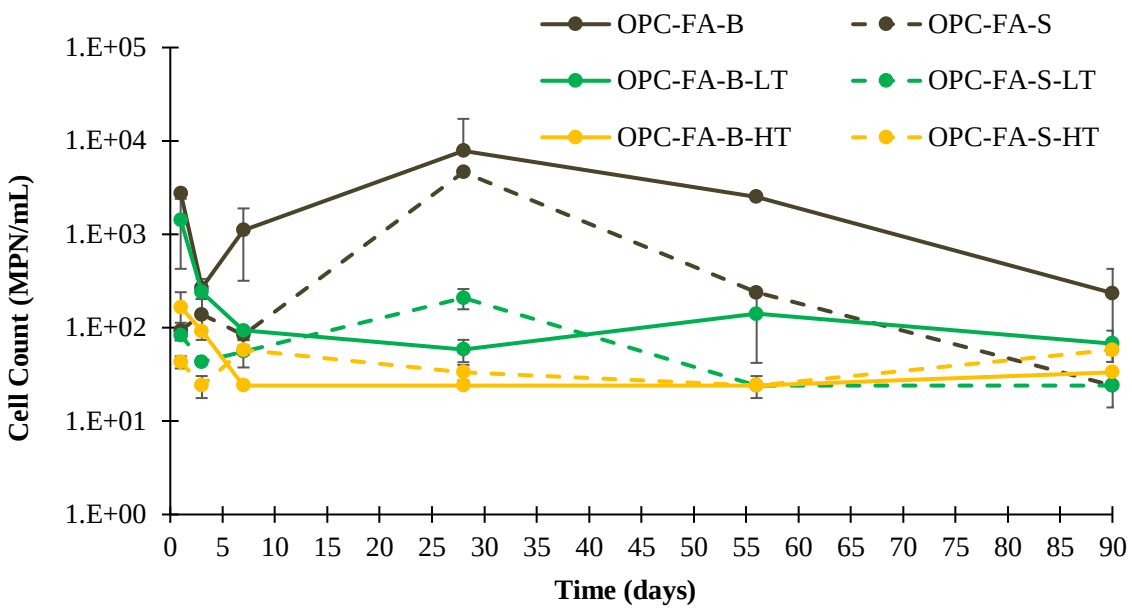

Figure 11.41 - Viability of B. subtilis and soil bacteria temperatures in mortar cubes cured at low, high and room temperatures over 90 days.

The compressive strength results of the control, *B. subtilis* and soil bacteria mortar cubes cured at room temperature, low, and high temperatures are shown in Figure 11.41. Little difference occurred between any of the samples, although at 90 days the LT bacterial cubes had achieved strengths approximately 500 psi greater than their non-bacterial counterpart. Conversely, at 90 days the HT bacterial cube strength was approximately 500 psi less than the non-bacterial HT cubes.

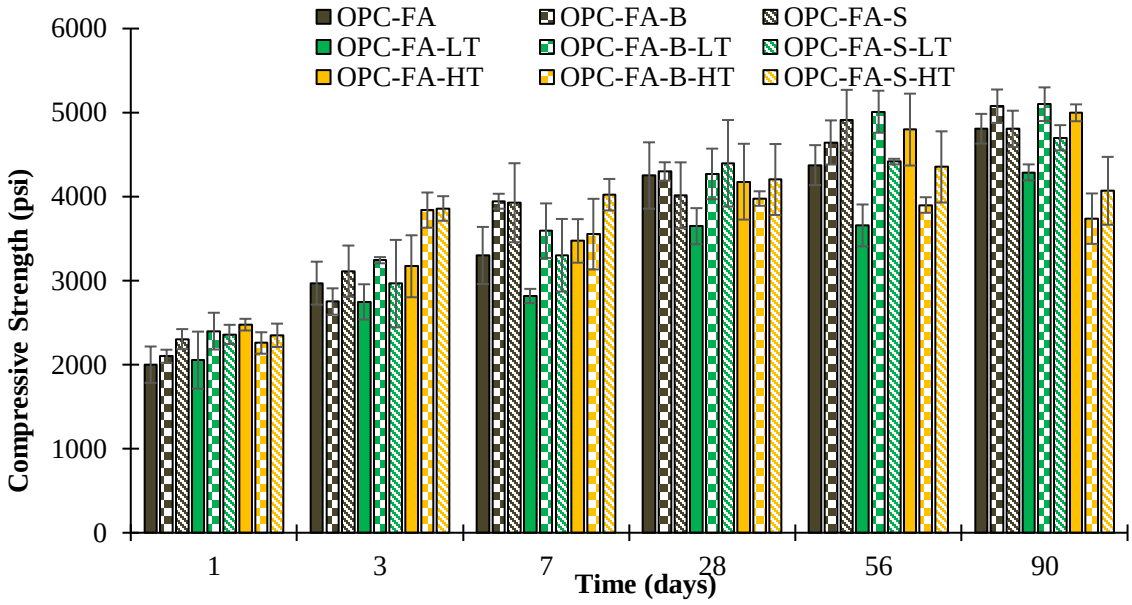

Figure 11.42 - Compressive strength development of B. subtilis and soil bacteria temperatures in mortar cubes cured at low, high and room temperatures over 90 days.

Water absorption capacities of the samples are shown in Figure 11.42. The initial sorptivity is indicated as 'i', and the secondary results are indicated as 's.' After 28-days, low temperature curing had resulted in slightly higher initial sorptivity than in the room temperature-cured samples, and similar secondary sorptivity. High temperature curing resulted in increases in both initial and secondary sorptivity. Increases in porosity resulting from faster initial hydration resulting from exposure to high temperatures is a known phenomenon (Shen and Xu 2019; Gao et al. 2021), but incorporation of bacteria in the mixture appeared to worsen the effect.

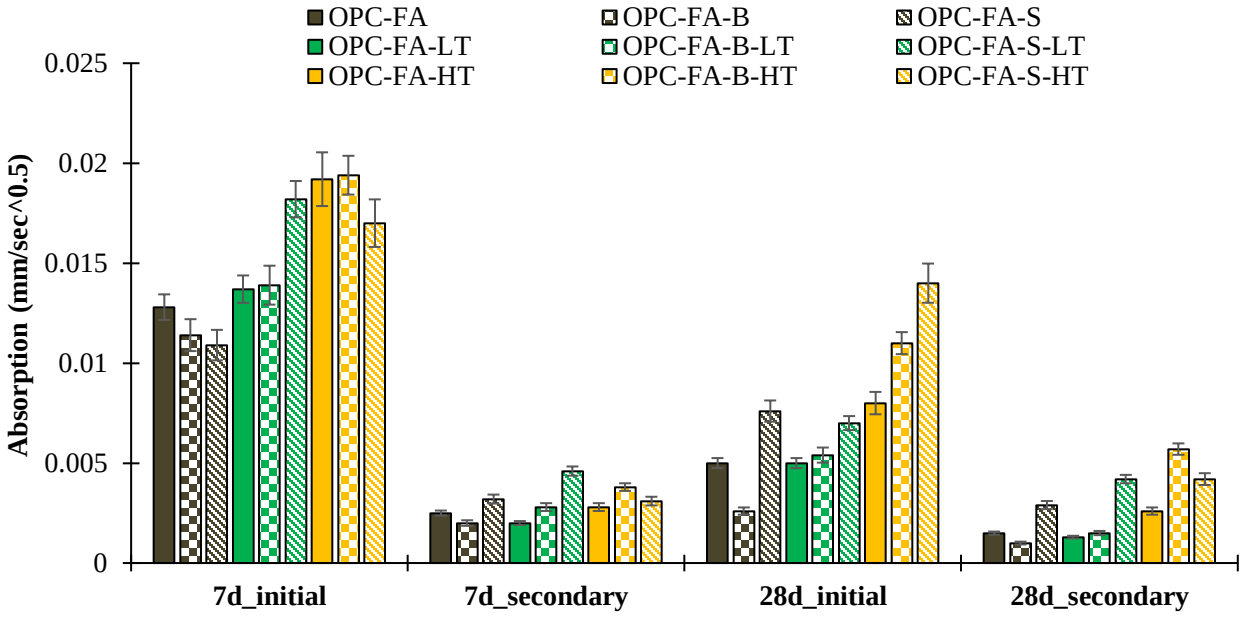

Figure 11.43 – Initial and secondary sorption in B. subtilis and soil bacteria mortars exposed to high temperatures (HT), low temperatures (LT) and room temperatures over 28 days.

Crack healing ability of the bacterial samples subjected to low and high temperature curing were investigated and images are shown in Figure 11.43 and 11.44. Samples cured at low temperatures (Figure 11.43) were unable to generate any significant crack closure, although soil bacteria samples showed a slight densification around the tip of the cracks. No densification was observed in the *B. subtilis* bacteria LT samples. Similarly, no significant crack closure observed in both bacterial and control samples when samples were cured at high temperature (Figure 11.44), which was expected due to the low viable cell counts.

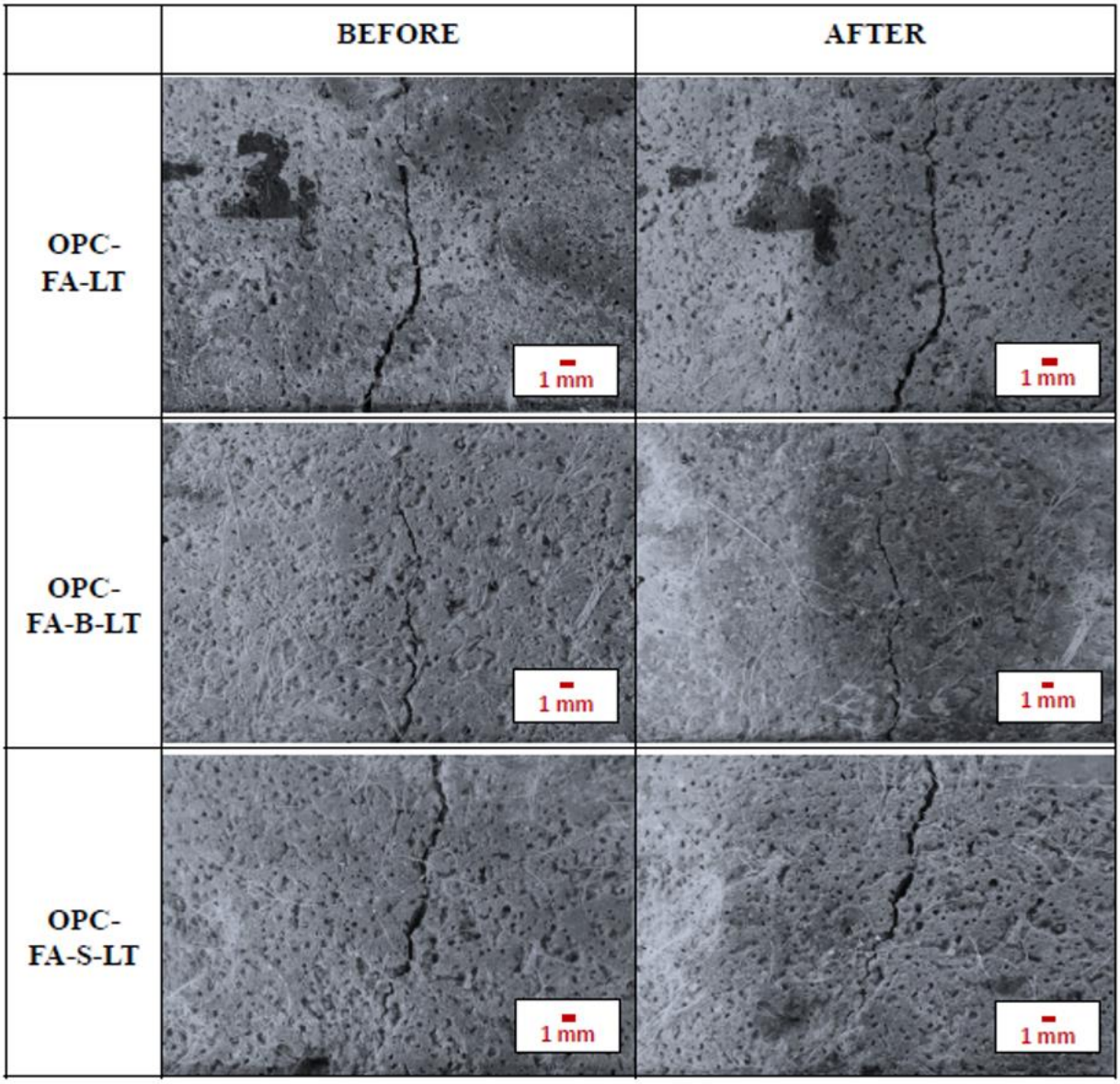

Figure 11.44 - Crack images of low temperature cured bacterial and non-bacterial OPC-FA samples cracked at 14 days. Images on the right represent samples right after cracking and left after 8 weeks of spray curing.

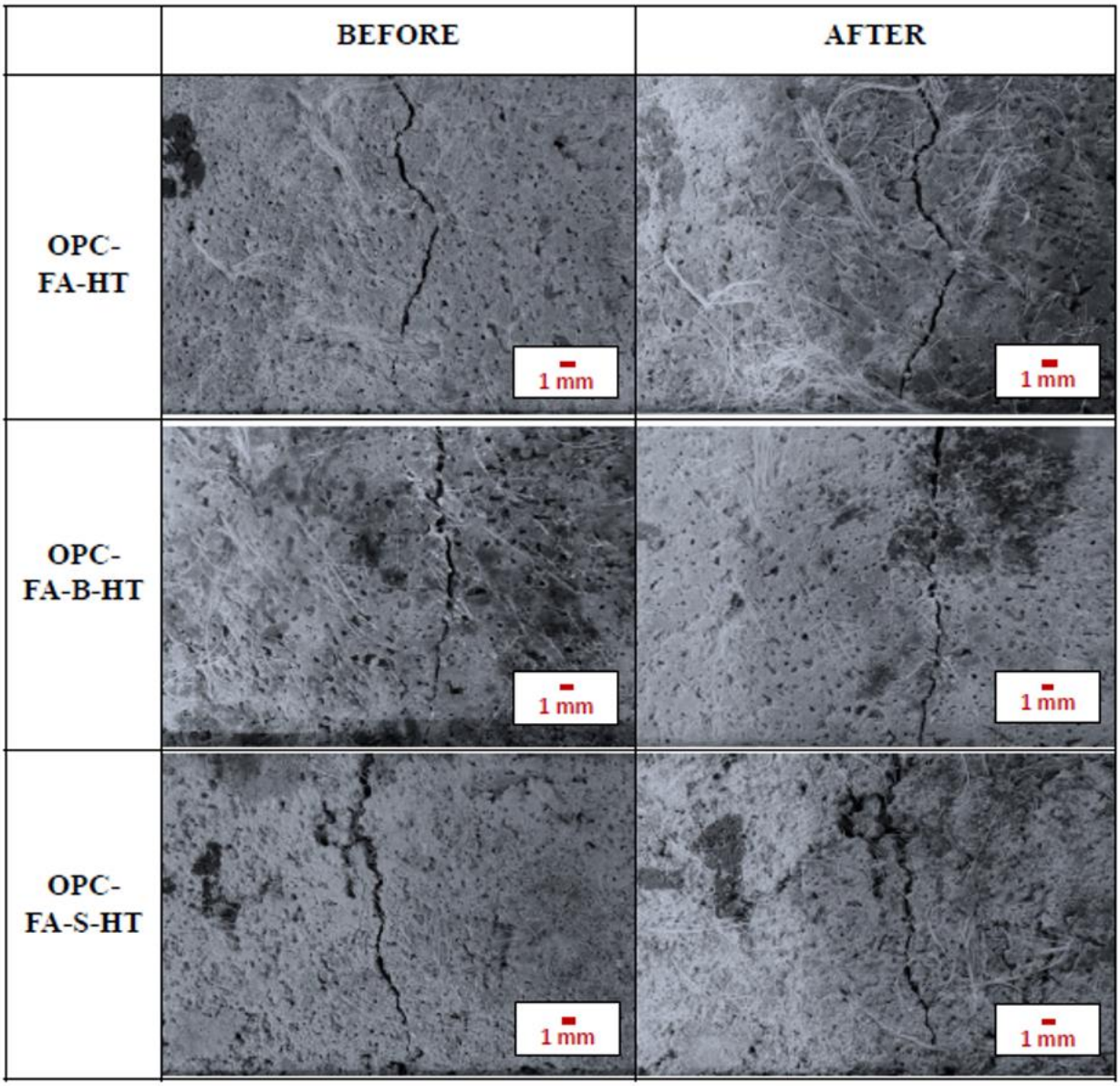

Figure 11.45 - Crack images of high temperature cured bacterial and non-bacterial OPC-FA samples cracked at 14 days. Images on the right represent samples right after cracking and left after 8 weeks of spray curing.

Figure 11.45 shows the UPV readings obtained through 8 weeks of observation for samples cracked at 14 days and cured at low temperature. The low temperature bacterial CC samples did not generate any visually observable crack healing, and similarly did not lead to improved UPV values compared to control and not-cured (NC) samples.

UPV readings for samples cracked at 14 days and cured at high temperature are shown in Figure 11.46. Although bacterial samples cured at high temperatures had low bacterial viability, and no visible crack healing was observed, the *B. subtilis* CC sample did show improved UPV when compared to its control and NC samples. The HT-cured soil bacteria CC sample did not result in a higher velocity than its control sample and resulted in similar velocity to the NC sample.

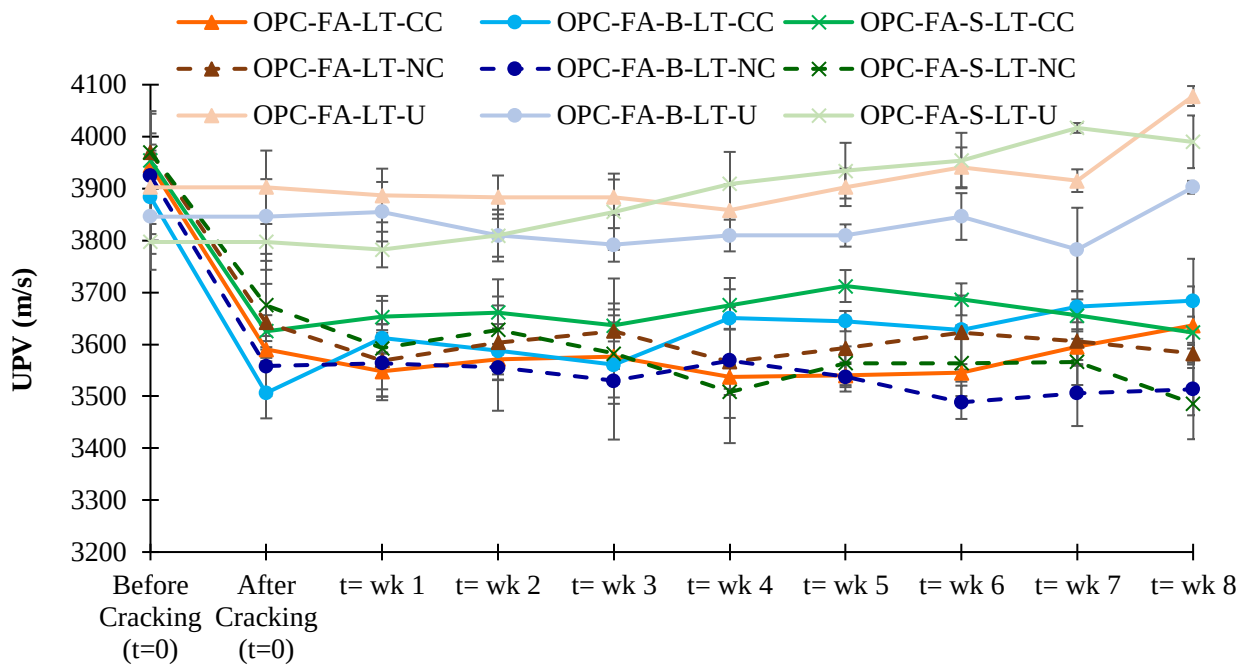

Figure 11.46 - UPV readings of low temperature cured bacterial and non-bacterial cracked and cured (CC), cracked and not cured (NC), and uncracked and cured (U) OPC-FA mortar beams.

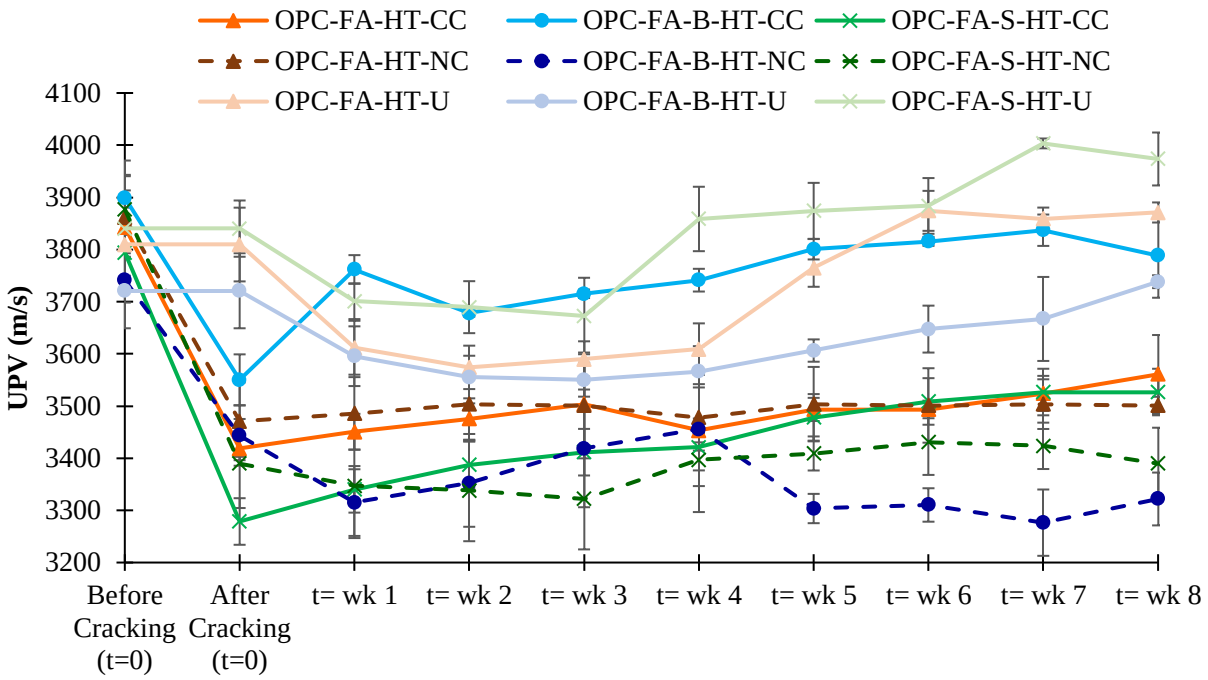

Figure 11.47 - UPV readings of high temperature cured bacterial and non-bacterial cracked and cured (CC), cracked and not cured (NC), and uncracked and cured (U) OPC-FA mortar beams.

Water absorption results for the low and high temperature-cured samples are shown in Figure 11.47 and 11.48, respectively. Although there was no clear distinction was found between low temperature control-CC and bacterial-CC from UPV and visual crack healing results, both bacterial samples generated significantly lower initial water absorption compared to the control sample, with 31% and 51% reductions in LT-B-CC and LT-S-CC samples, respectively (Figure 11.47). In addition, the reduction in the initial water absorption with NC bacterial samples was less than in the CC samples, suggesting that changes in water absorption in the cracked samples are likely due, at least in part, to forces other than increased curing. Uncracked samples had lower initial sorptivity when compared to cracked and cured samples. However, all bacterial and control samples including CC, NC and U had very similar secondary sorptivity values.

Curing bacterial samples at high temperatures led to lower initial water absorption compared to the control sample, with 20% and 62% reductions in HT-B-CC and HT-S-CC samples, respectively (Figure 11.48). However, secondary water absorptions of soil bacteria and *B. subtilis* samples were slightly greater than the control sample. The initial water absorption of NC bacterial and control samples was higher than in the CC samples. Uncracked soil and control samples had lower water absorption compared to cracked and cured control samples but *B. subtilis* had slightly higher absorption. Lower water absorption in the cracked and cured (CC) *B. subtilis* sample than the uncracked samples may indicate internal crack healing of the B. subtilis sample.

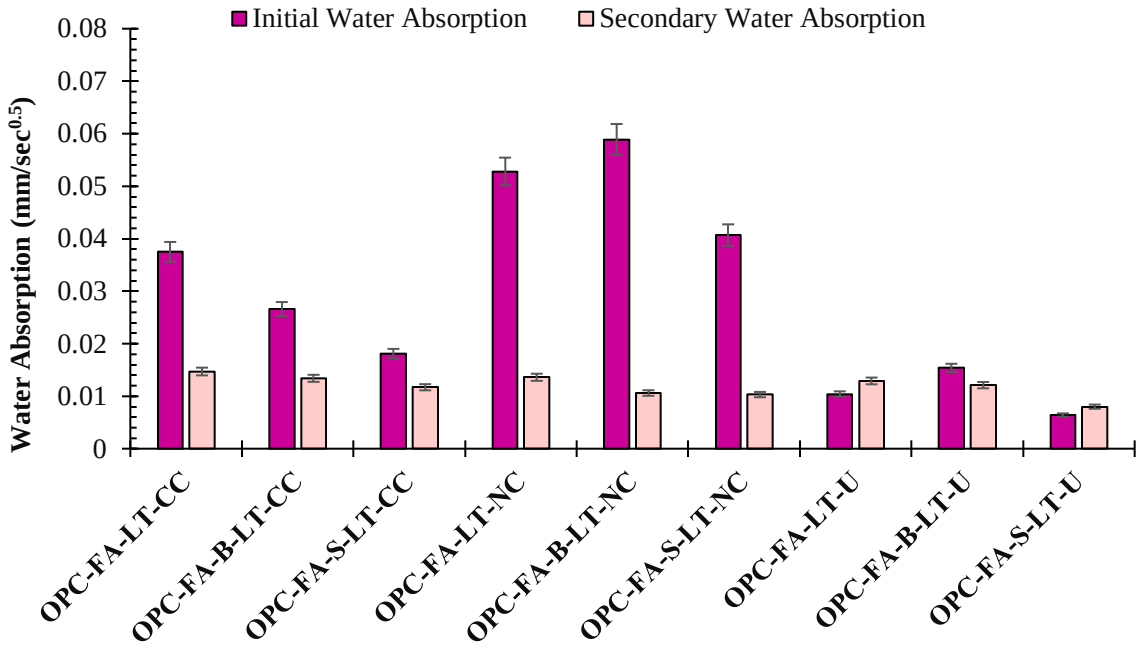

Figure 11.48 - Initial and secondary water absorptions of bacterial and non-bacterial OPC-FA mortar beams after the healing process by low temperature curing. CC: cracked and cured, NC: cracked and not cured.

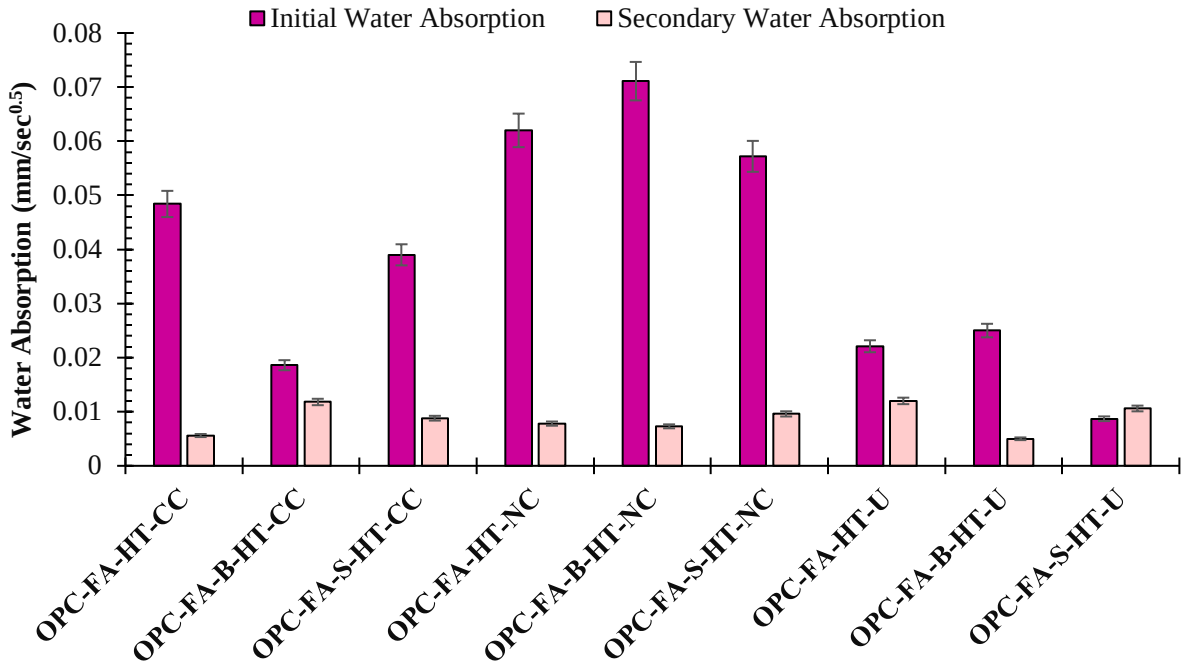

Figure 11.49 - Initial and secondary water absorptions of bacterial and non-bacterial OPC-FA mortar beams after the healing process by high temperature curing. CC: cracked and cured, NC: cracked and not cured.

11.5.2 Effect of Salt Exposure

OPC-FA mixtures with *B. subtilis*, soil bacteria and without bacteria were cured for 28 days with spray curing. Samples were then immersed for 7 days into 23% NaCl solution to evaluate the effect of salt exposure on bacteria viability, and self-healing ability. After 7 days of the exposure, samples were removed from the salt solution and spray curing was applied through the end of 63 days.

Figure 11.49 shows the bacterial viability of *B. subtilis* and soil bacteria cells in OPC-FA mortars exposed to salt solution (SA) or non-exposed. Exposing bacterial samples to salt after 28 days of hydration resulted in lower bacterial quantities compared to samples subjected to no exposure.

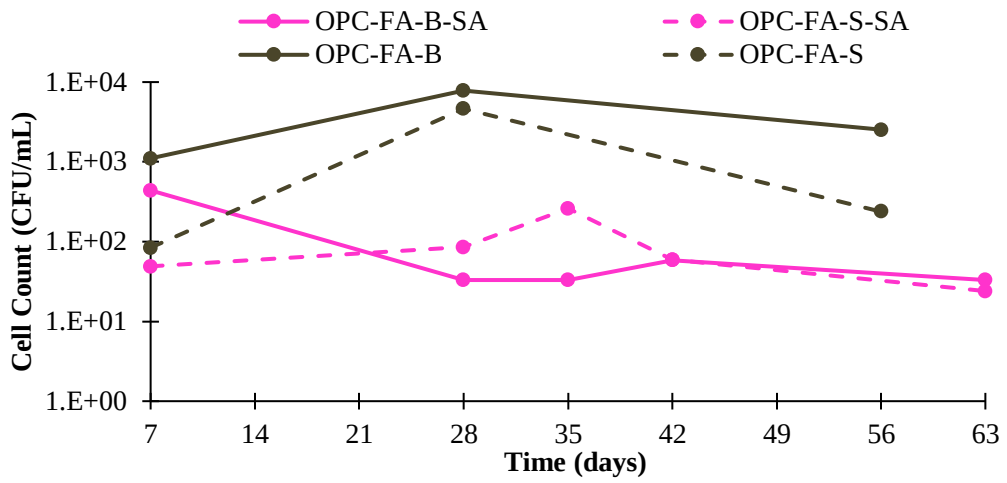

Figure 11.50 - Bacterial numbers present in salt-exposed samples through 60 days following salt exposure.

The compressive strengths of the control, *B. subtilis*, and soil bacteria mortar cubes with OPC and fly ash (OPC-FA) mixtures subjected to salt exposure are shown in Figure 11.50. No significant difference was found between the control and bacterial samples up to 35 days of the testing. However, after salt exposure the *B. subtilis* bacterial samples had significant reductions in strength. The strength of the soil sample did not appear to be affected by the salt exposure.

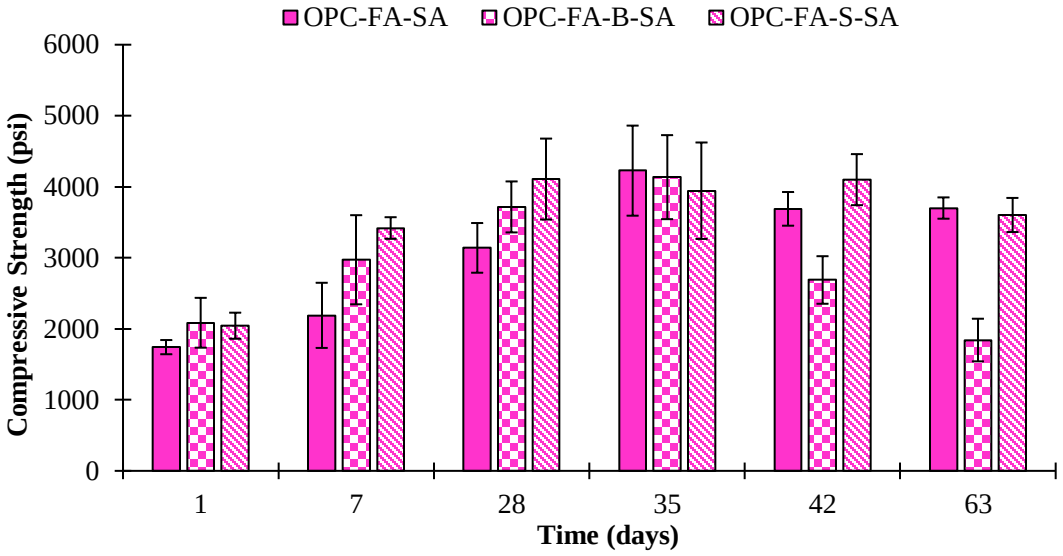

Figure 11.51 - Compressive strengths of salt-exposed samples up to 60 days following exposure.

Water absorption capacities of the samples exposed to salt are shown in Figure 11.51. The initial sorptivity is indicated as ‘i’, and the secondary results are indicated as ‘s’. OPC-FA-SA samples represent the 7d and 28d after the completion of the salt exposure, demonstrating 42 and 63 days of the hydration and OPC-FA samples represent the 7 and 28 days of the hydration.

Salt samples initial sorptivities were significantly lower than that of the control, non-salt-exposed samples at 7 and 28 days, likely at least in part due to the difference in total hydration time (7 days

represents 28 days of curing followed by 7 days of salt exposure, followed by another 7 days before testing). Soil bacteria samples' initial and secondary water absorption was significantly lower than the *B. subtilis* and control samples at all times. The *B. subtilis* sample had similar initial, but higher secondary sorptivity compared to the salt-exposed control.

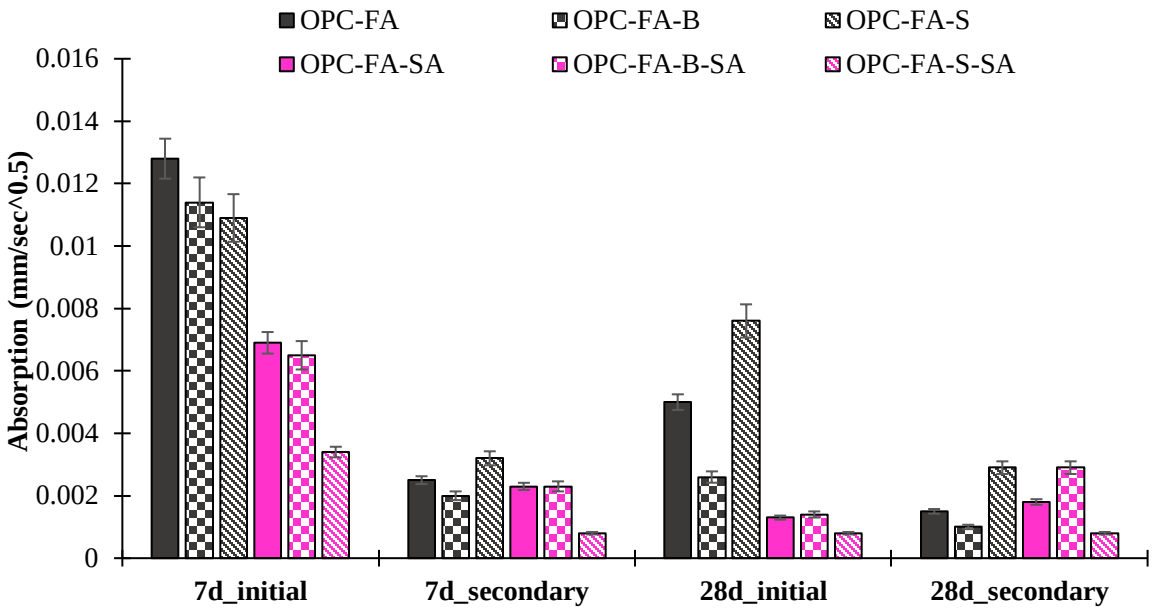

Figure 11.52 - Initial and secondary water sorption of salt exposed samples following exposure.

Crack healing ability of the bacterial samples subjected to salt exposure was investigated and the images of bacterial and control samples are shown in Figure 11.52. All samples had the same amount of partial crack healing on the tip of the cracks including the control sample which may be due to the precipitation of the salt on the cracks rather than the precipitation of the calcium carbonate.

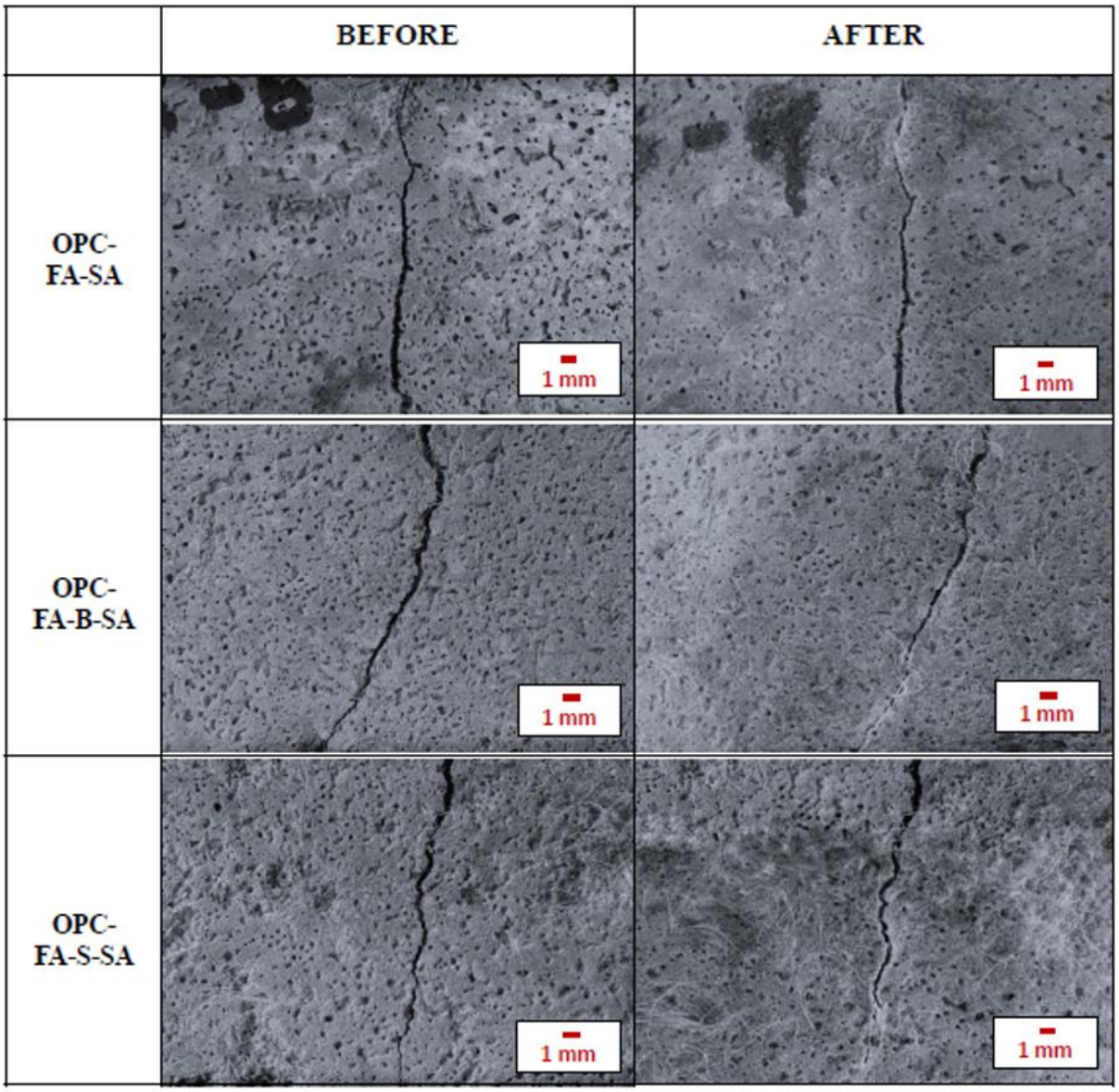

Figure 11.53 - Crack images of salt-exposed cured bacterial and non-bacterial OPC-FA samples. Images on the right represent samples right after cracking and left after 8 weeks of spray curing.

Figure 11.53 shows the UPV readings obtained through 8 weeks of observation for samples cracked at 14 days and exposed to salt. The salt exposed bacterial CC samples did not generate any improvements in the UPV results. UPV results of bacterial and non-bacterial CC samples resulted in very similar velocity values and bacterial and non-bacterial uncracked samples (U) had higher velocity compared to CC samples. These results indicate that healing ability of the samples was prevented when samples were exposed to salt. NC samples had slightly lower velocity in comparison with CC samples, showing that curing did improve the internal porosity despite the lack of crack healing.

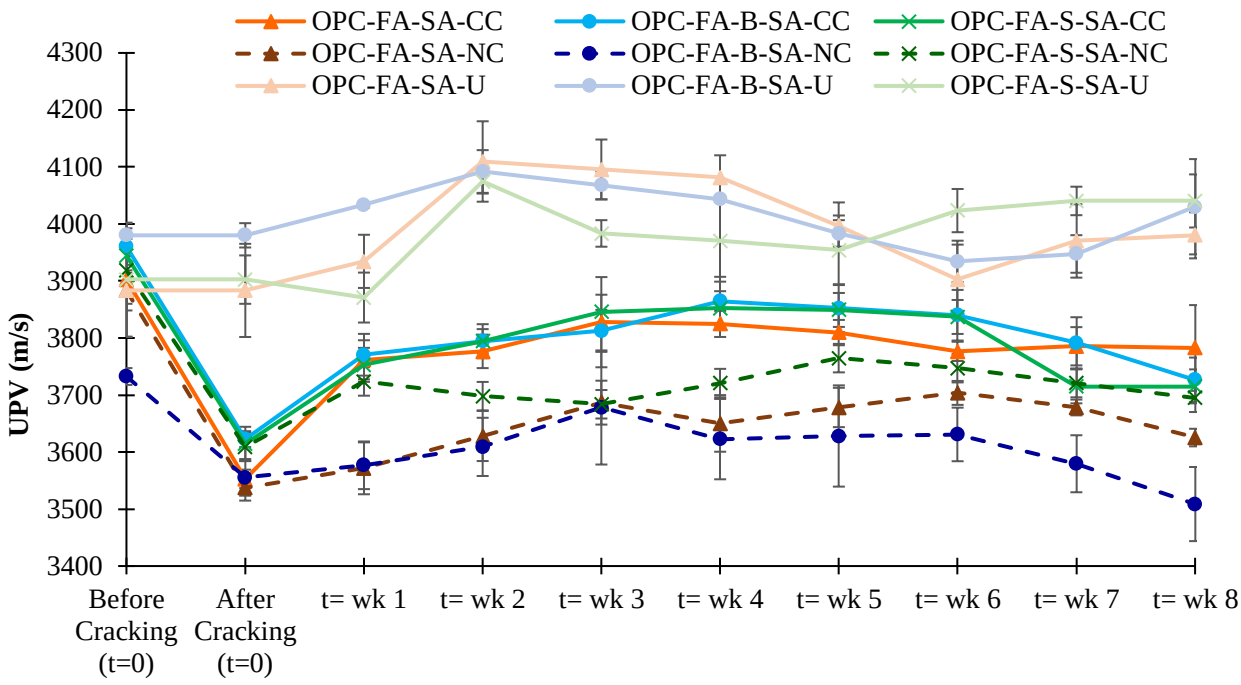

Figure 11.54 - UPV readings of salt-exposed cured bacterial and non-bacterial cracked and cured (CC), cracked and not cured (NC), and uncracked and cured (U) OPC-FA mortar beams.

Water absorption results for the samples exposed to salt are shown in Figure 11.54. In agreement with the visual crack healing and UPV results, exposing samples to salt was inefficient in terms of decreasing the sorptivity for bacterial samples. Bacterial CC samples had slightly lower initial water absorption than the control samples and the same secondary water absorption as the control samples. Both bacterial and control NC samples had higher initial absorption than the CC samples, but no obvious change was obtained in the water absorption between bacterial and non-bacterial samples.

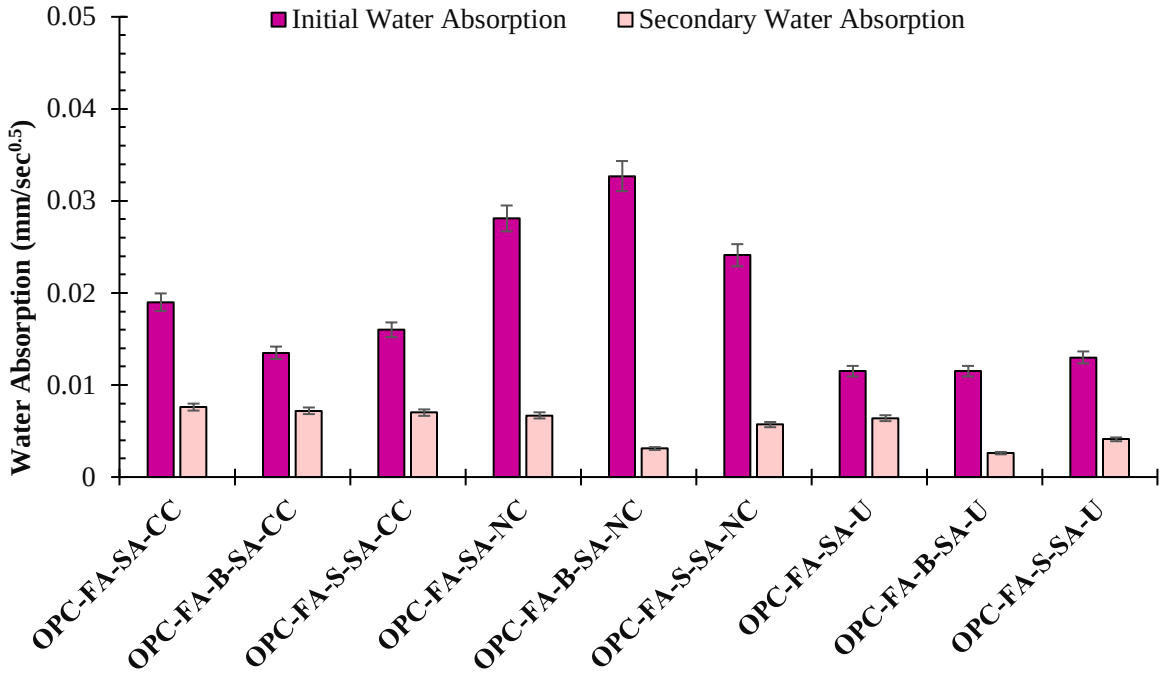

Figure 11.55 - Initial and secondary sorption in B. subtilis and soil bacteria mortars exposed salt, following curing.

11.6 Conclusions

In order to evaluate the performance and the self-healing ability of the bacteria used in cementitious systems, the performance of mixtures of OPC cement, fly ash, CSA cement, lightweight aggregate, and varying mixing solution compositions and different curing methods were evaluated using compressive strengths, sorptivity, thermogravimetric analysis and visual observations. The main findings can be summarized as:

- In general, very little effect was seen in the compressive strength and resistivity of mixtures using bacteria or incorporating fly ash, LWA, or PBS compared to the control OPC mixture. However, use of bacteria and fly ash both resulted in reductions in sorptivity, evidencing greater hydration or refinement of pores through biomineralization (in bacterial samples) and pozzolanic reaction (in the fly ash samples).

- The effect of bacteria on hydration rates varied depending on cement type and presence of fly ash. OPC cement pastes and mortars were retarded by use of bacterial LWA, with this effect observed in both isothermal calorimetry measurements and in changes in initial and final setting time. However, initial set was accelerated through use of LWA and bacteria in OPC-FA mixtures. Bacteria slightly decreased initial set in CSA mixtures, while retarding final set.

- In general, spray-curing was much more effective at stimulating improvements in crack-healing than was ponding, and also resulted in greater viability of bacteria in samples over time.

- Use of LWA as a method of integrating bacteria into the concrete resulted in considerable improvements in bacterial survivability when compared to samples without LWA. LWA represents additional concrete mixture cost, but is essential for protecting bacteria and ensuring extended crack-healing ability.

- Use of PBS in lieu of mixing water did not result in higher bacteria viability in mortar samples when compared to samples with dechlorinated tap water. Use of dechlorinated tap water is sufficient production of bacterial concrete mixtures.

- Partial crack healing occurred in bacterial OPC beams using both *B. subtilis* and soil bacteria. Crack healing was accompanied by increases in UPV, lower water absorption, and greater calcium carbonate precipitate levels compared to the control samples indicating internal crack healing.

- Fly ash did not affect the viability of bacteria in mortar samples up to 90 days following casting. Use of *B. subtilis* with the OPC-fly ash binder resulted in almost full crack closure and the most significant improvement in UPV values and water absorption out of the tested mortar mixtures. Use of the OPC-fly ash binder with soil bacteria led to the greatest densification in the (uncracked mortar) microstructure. However, full crack closure was not observed with these samples, which may suggest that use of soil bacteria with OPC-fly mixtures ash resulted in remediation of internal cracks and pores rather than the crack mouth.

- The highest *B. subtilis* and soil bacteria viability was obtained through use of CSA cement and may enable greater later age crack healing potential than mixtures using portland cement. Complete crack healing was observed in bacterial CSA cement samples, with accompanying improvements in UPV results, water absorption, and calcium carbonate contents. However, CSA crack healing required more time (8 weeks vs. 6 weeks) and more application of nutrient solution, compared to the OPC mixtures.

- The effect of exposure of bacterial mortars to non-standard (high and low) temperatures is unclear. Both low and high temperature curing resulted in a decrease in the bacterial viability compared to room temperature samples, very little difference was observed in compressive strengths among the samples, and no visual evidence of crack healing occurred. However, slight increases (suggesting further microstructural densification or crack healing) were measured using UPV in HT-cured samples and water absorption was reduced in both high- and low-temperature cured samples relative to control samples. More testing is needed to fully understand the effect of environmental temperatures on bacterial concrete and mortar performance.

- Exposure of samples to salt resulted in a reduction in the number of living bacteria in the sample and significantly reduced the compressive strength of the *B. subtilis* samples. Although the exposure to salt did not negatively affect strength development in the soil bacteria sample, and resulted in improvements (reductions) in initial and secondary sorptivity relative to the non-salt-exposed soil bacteria samples, no evidence of crack healing was obtained from visual observations, UPV measurements, or cracked-region sorptivity measurements. Exposure to

salt appeared to have negated the crack-healing ability of the bacterial mortars.

12 Appendix F: Task 3 In-situ Concrete Monitoring Research Findings and Conclusions

Quantification of numbers of bacteria living in the concrete slabs was attempted throughout the first 28 days following placement of the slabs. Contamination of samples was not a significant issue throughout the project period during optimization of growth processes, nor in testing of paste and mortar samples using the MPN method before and after placement of the concrete pads. However, significant contamination occurred in MPN sample testing of the concrete slabs, with testing revealing the presence of a greater number of bacteria in the control slabs than in the *B. subtilis* or soil bacteria concrete slabs within the first week following placement. This phenomenon is attributed to the uncontrolled conditions at the site, where the slabs were subject to foot traffic, rain water and water from nearby grass and gardens, and proximity to soil, but prevent reliable analysis of site conditions with regards to viability of bacteria within the concrete samples.

Figures 12.1 shows the bacterial and control slabs after 1 year of the placement. Slabs were observed visually to investigate the occurrence of the cracks. However, no cracking occurred on any of the slabs through the first year of the placement of the concrete. Therefore, the efficiency of the bacteria to heal cracks could not be determined.


B
S

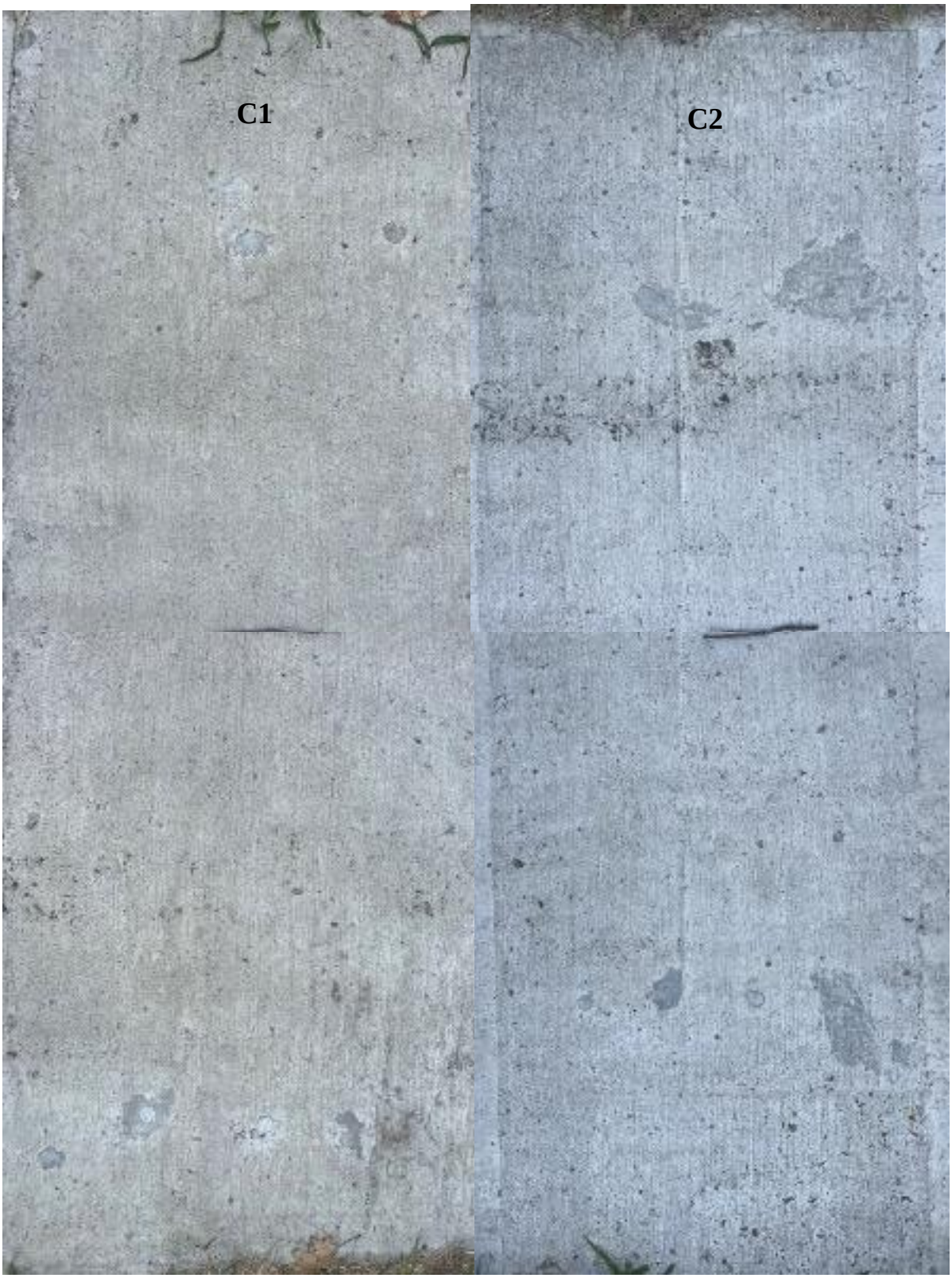
C1
C2

Figure 12.1: Concrete slabs after 1 year of the placement. B: *B. subtilis*, S: soil bacteria , C1: control-cured, C2: control-not cured.

Compressive strength development for the four mixtures tested are shown in Figure 12.2. Similar compressive strength development occurred in all mixtures across all testing days. The presence of the *B. subtilis* and soil bacteria did not have a significant impact on compressive strengths of the concrete. Although control-cured and control-not cured (Control-NC) samples had similar strength results, the control sample resulted in a slightly higher strength, showing the efficiency of the curing.

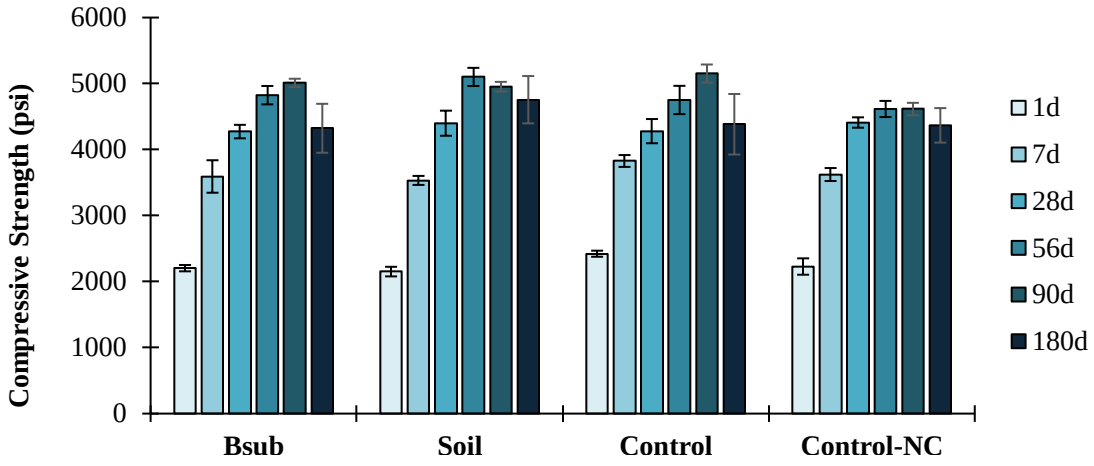

Figure 12.2 - Compressive strength development of in-situ slab concrete, tracked using cylinders cast alongside the slabs. Cylinders were cured on-site for 24 hours then moved to a temperature and humidity-controlled fog room.

Resistivity results of bacterial and control concrete samples are shown in Figure 12.3. Similar to the compressive strength results, no significant difference in the resistivity was found among the bacterial and the control samples and the effect of the bacteria on the resistivity was not clear. When compared to control-cured and control-not cured sample, it was found that the resistivity of the control-not-cured sample at 90 days was 27% lower than the resistivity of the control-cured sample, again evidencing the effects of continued curing on microstructural development.

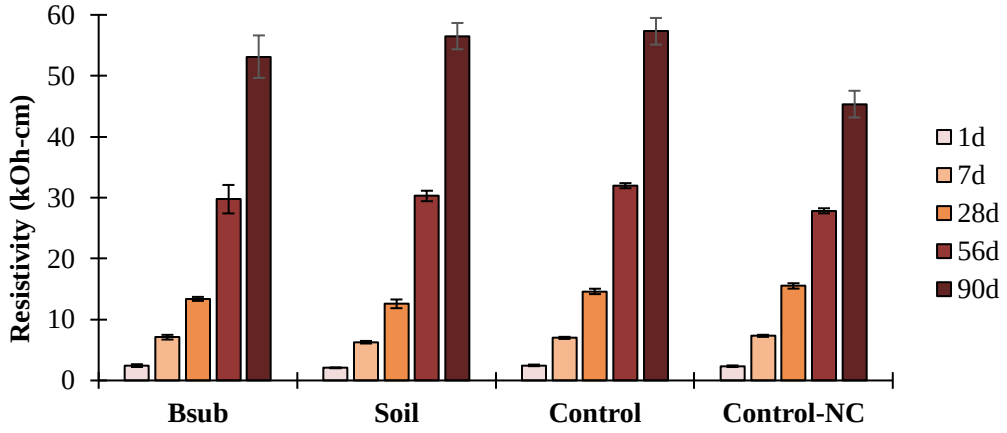

Figure 12.3 - Surface resistivity of the slab concrete mixtures.

Figure 12.4 shows the drying shrinkage changes of bacterial and control concrete samples over 180 days. The cured-Control and soil bacteria samples had the highest shrinkage through the end of measurements at 180 days. Both B. subtilis and soil bacteria samples shrank initially more slowly than the cured-Control sample, and at 180 days the *B. subtilis* sample showed overall reduced shrinkage. The not cured control sample ended testing with the lowest shrinkage, likely resulting from reduced overall hydration due to lack of curing.

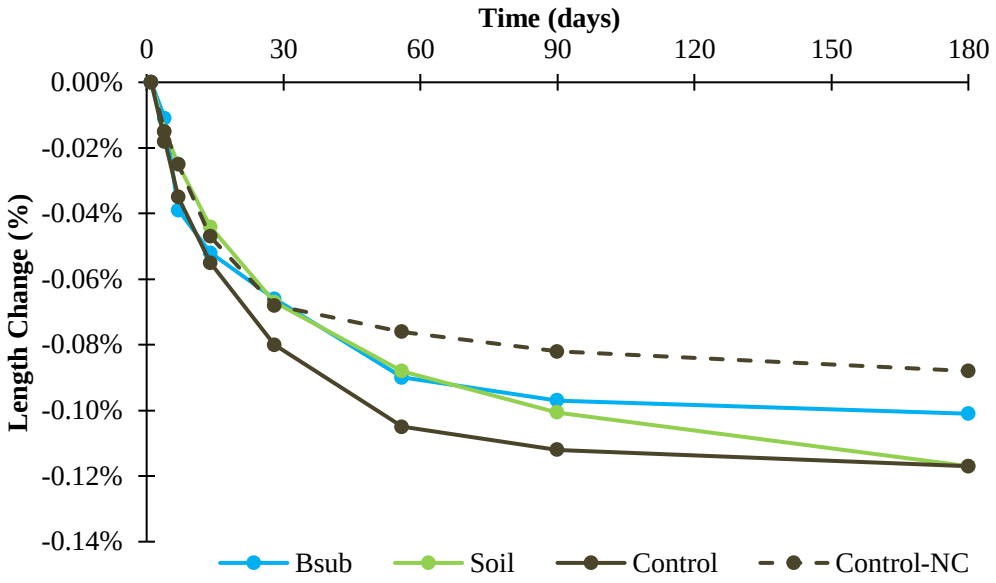

Figure 12.4 - Shrinkage of the slab concrete mixtures, stored under idealized 50% RH lab conditions.

Bacterial and control freeze and thaw beams (3" x 4" x 16") were cast and analyzed to understand the effect of bacteria on the freeze and thaw durability of the concrete samples (Figure 12.5). Dynamic modulus of samples was tested weekly (36-40 cycles per week) until samples reached 500 cycles. No significant difference was observed among *B. subtilis* and both control samples (cured and not cured) and these samples did not demonstrate any loss in the dynamic modulus through the end of 500 cycles. However, soil bacteria sample generated the lowest dynamic modulus and its dynamic modulus decreased to 95% after 500 cycles (Legg Jr 1956).

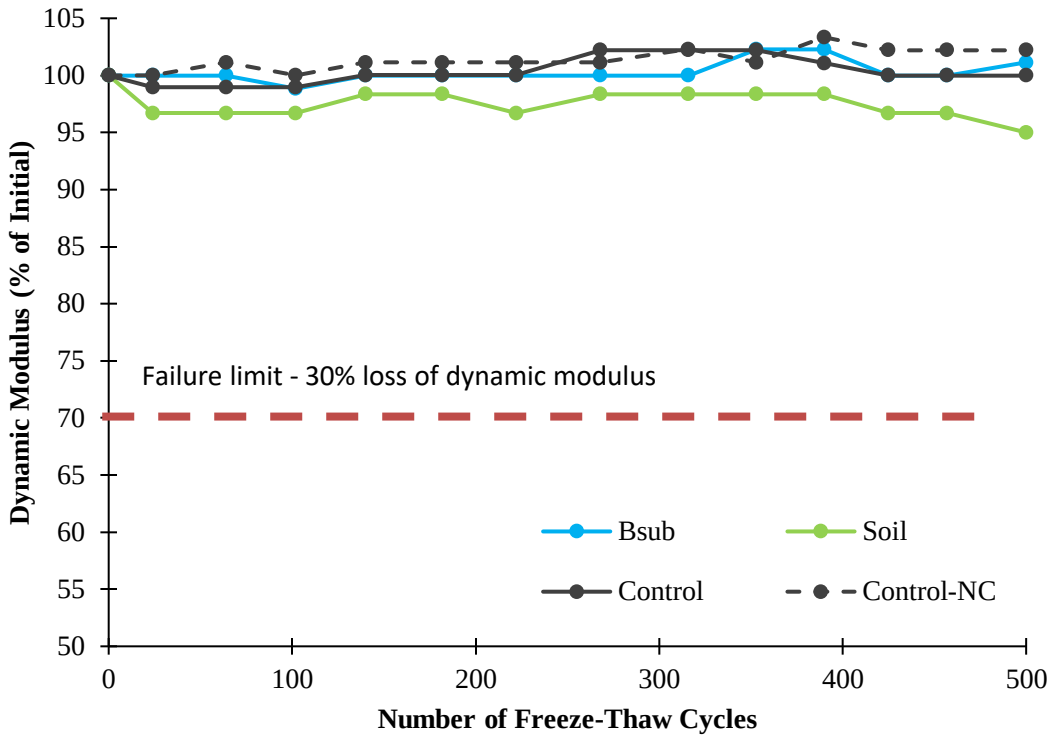

Figure 12.5 - Change in dynamic modulus of the slab concrete mixtures when exposed to cyclical freezing and thawing.

12.1 Conclusions

The main findings can be summarized as:

- No cracking occurred on any of the slabs through the first year of the placement of the concrete. LWA is known to provide internal curing and reduce the prevalence of shrinkage cracks, and may have contributed to prevention of shrinkage cracking in the concrete slabs.

- All bacterial and control samples resulted in similar compressive strengths development across the testing period. Similarly, no significant difference in the resistivity was found between the bacterial and the control samples and bacteria did not appear to have a significant effect on drying shrinkage.

- Soil bacteria resulted in the largest reduction in dynamic modulus among the samples exposed to freezing and thawing. However, the soil bacteria sample merely decreased to 95% of its initial value after 500 cycles, which is well above the minimum limit of 70% of the initial sample dynamic modulus. The *B. subtilis* and control samples did not demonstrate any loss in the dynamic modulus through the end of 500 cycles.

13 Appendix G: Task 4 Life Cycle and Cost Analysis Research Findings and Conclusions

13.1 Cost and Lifecycle Analysis Methodology and Results

This analysis provides a rough estimate of the costs of producing bacterial concrete mixtures, and the relative changes in life expectancy resulting from changes in the concrete microstructure as a result of bacterial biomineralization.

Bacterial solutions costs were obtained from Fisher Scientific, Sigma-Aldrich, and VWR chemical and biological suppliers in May 2022. Production of the solutions requires standard biological laboratory equipment, such as various sizes of beakers, pipettes, vortexer, autoclave, beaker shaker, centrifuge, oven, and an incubator or environmental chamber. The cost of obtaining these items has not been factored into the bacterial solution production costs, as most items are reusable, translating to reduced cost relative to each liter of bacterial solution produced over time with scaled production of the solutions. In addition, many sizes and varieties of each piece of equipment are available to suit the specific production quantity needs and budget of the producer. Bacterial solution production costs are instead calculated based on the cost of chemicals comprising the liquid solutions and electricity associated with the shaking and incubation equipment. All values are based on current costs and energy rates.

Concrete materials costs were obtained on July 2022 from a Columbus concrete producer. Costs do not factor in fuel or delivery costs associated with transporting the concrete to the site.

Table 13.1 shows the cost of the four variation of cell growth media tested in this study: 2xSG, and varying concentrations of nutrient broth (half, standard, and double concentration). Other variables included in the growth optimization work, which also affect overall solution cost are: incubation temperature, and growth time. The cost of electricity was calculated relative to the use of the beaker shaker and incubator (required for incubation of samples at 37 °C) at current Columbus, Ohio electricity rates of 10.01 cents/kWh.

Dried spore counts, which are used to determine the quantity of growth solution required to reach the standard 10^6 CFU/mL bacteria dosage in the concrete mixing water were experimentally tested for only the most promising bacterial mixtures. A ratio was created to predict spore counts for other mixtures in order to compare production costs. The percent difference between the spore counts in the growth solutions of mixtures for which “after drying” spore counts were available (shown in blue in Table 13.1) was calculated and predicted spore counts for mixtures without “after drying” spore counts were then determined by applying that ratio to the known samples’ after drying spore count. Predicted spore counts were used to calculate required volumes of growth solution and cost of that solution per cubic yard of concrete. The mixtures shown in blue were used to produce the in-situ concrete slabs discussed in Task 3 and were generally the most cost effective of the mixtures.

Little trend was apparent in the likelihood of one time or temperature to provide better growth, and lower cost bacterial production solutions. The most efficient mixtures were the *B. subtilis* mixture utilizing the 0.5NB solution, incubated at 37 °C for 24 hours, the soil bacteria mixture using the

0.5NB solution incubated at 25 °C for 48 hours, and the soil bacteria mixture using the 1NB solution incubated at 37 °C for 48 hours.

Table 13.1 - Materials and Electricity Costs. Blue cells indicate the mixtures selected for use in the in-situ concrete placed in Task 3.

	Growth Media	Growth Solution ($/L)	Incubation Temp (°C)	Growth Time (hrs)	Electricity Cost ($/L of growth solution)	Growth Solution Spores (CFU/mL)	Change relative to 0.5NB at similar growth time	Spores After Drying (CFU/mL)	Predicted Spore Count after Drying (CFU/mL)	Growth Solution Required (L/CY concrete)	Materials and Electricity Cost ($/CY concrete)
B. subtilis bacteria	2xSG	$5.81	25	24	0.02	0	-		-	-	-
	2xSG	$5.81	25	48	0.05	7.0E+05	0.79		2.7E+05	514	$3,009
	0.5NB	$1.36	25	24	0.02	2.1E+04	-0.99		2.1E+04	6588	$9,109
	0.5NB	$1.36	25	48	0.05	1.1E+04	-0.97	4.7E+04	4.2E+03	32700	$45,956
	0.5NB	$1.36	37	24	0.48	2.3E+06	0.00	2.3E+06	2.3E+06	60	$111
	0.5NB	$1.36	37	48	0.96	3.9E+05	0.00	1.5E+05	1.5E+05	922	$2,141
	1NB	$2.73	25	24	0.02	1.1E+04	-1.00		1.1E+04	12243	$33,701
	1NB	$2.73	25	48	0.05	6.0E+03	-0.98		2.3E+03	59950	$166,383
	1NB	$2.73	37	24	0.48	4.3E+04	-0.98	9.3E+04	4.3E+04	3217	$10,329
	1NB	$2.73	37	48	0.96	5.2E+04	-0.87	2.6E+04	2.0E+04	6917	$25,531
	2NB	$5.46	25	24	0.02	1.1E+04	-1.00		1.1E+04	12577	$68,955
	2NB	$5.46	25	48	0.05	5.3E+03	-0.99		2.1E+03	67486	$371,534
Soil bacteria	2NB	$5.81	25	48	0.05	5.3E+03	-0.999		1.2E+03	114206	$668,722
	0.5NB	$1.36	25	24	0.02	6.6E+04	0.00	3.0E+04	3.0E+04	4612	$6,376
	0.5NB	$1.36	25	48	0.05	6.6E+06	0.00	1.5E+06	1.5E+06	92	$130
	1NB	$2.73	25	24	0.02	9.3E+04	0.41		4.2E+04	3273	$9,009
	1NB	$2.73	25	48	0.05	4.3E+05	-0.94		9.7E+04	1429	$3,966
	1NB	$2.73	37	24	0.48	5.1E+05	6.73		2.3E+05	597	$1,916
	1NB	$2.73	37	48	0.96	1.9E+07	1.82		4.2E+06	33	$121
	2NB	$5.46	25	24	0.02	2.2E+04	-0.67		1.0E+04	13835	$75,851
	2NB	$5.46	25	48	0.05	1.0E+05	-0.98		2.3E+04	5968	$32,855

Tables 13.2 shows the materials costs associated with producing a bacterial and non-bacterial standard OPC concrete, OPC concrete with a 20% substitution of fly ash for OPC, and a CSA concrete. These costs do not consider costs associated with production of the bacterial solutions.

The use of fly ash reduced costs by approximately 10.5%, while the use of CSA cement in lieu of OPC cement increased mixture cost by 10%. In general, the cost of producing the non-bacterial concrete was slightly less (7-8% less) than producing bacterial concrete due to the costs water dichlorination, and substitution of a portion of the fine aggregate with lightweight aggregate (LWA) in bacterial concrete mixtures. LWA is approximately 5x the cost of other fine aggregate sources, but other research has suggested that it can provide substantial gains in curing and reduced shrinkage due to its ability to provide internal curing to the concrete mixture (Weiss et al. 2012) and so may warrant the additional cost. Table 13.3 shows the overall cost to produce a cubic yard of concrete for each mixture type and bacteria type. Including both the costs of producing the concrete and bacterial solutions, bacterial concrete was between 2 – 2.5x the cost of the non-bacterial concrete mixtures. Additional nutrient curing solution is required to induce biomineralization in the concrete mixtures. Crack healing occurred in 6 weeks for the OPC and OPC – FA mixtures, but required an additional 2 weeks (8 weeks total) of solution application for the CSA mixture. Curing solution was applied daily at a rate of 0.028 liters per square foot of concrete surface area (or 36 ft^2 per liter of solution). Total solution required for healing and the costs associated with production of 0.5 NB curing solution for these rates and application times are shown in Table 13.4.

Table 13.2 - Concrete Mixture Costs for A. OPC concrete, B. OPC concrete with a 20% substitution of class F fly ash for portland cement, and C. CSA concrete. Bacteria production costs are not included in the totals.

A.

	Component Cost		OPC Concrete		Bacterial Concrete	
	$/ton	$/100 lbs	lbs	$/cy	lbs	$/cy
Water	0.39	0.02	305	0.06	305	0.06
Water De-chlorination	-	1920	-	-	0.06	1.17
Portland Cement	190	9.50	678	64.39	678	64.39
Class F Fly Ash	0	0.00	0	0.00	0	0.00
Coarse Agg	30	1.50	1236	18.54	1236	18.54
Fine Agg	25	1.25	1366	17.08	1243	15.54
Lightweight Agg	130	6.50	0	0.00	123	8.01
Total				100.07		107.71

B.

	Component Cost		OPC + FA Concrete		OPC + FA - Bacterial Concrete	
	$/ton	$/100 lbs	lbs	$/cy	lbs	$/cy
Water	0.39	0.02	305	0.06	305	0.06
Water De-chlorination	-	1920	-	-	0.06	1.17
Portland Cement	190	9.50	508	48.29	508	48.29
Class F Fly Ash	65	3.25	169	5.51	169	5.51
Coarse Agg	30	1.50	1236	18.54	1236	18.54
Fine Agg	25	1.25	1366	17.08	1243	15.54
Lightweight Agg	130	6.50	0	0.00	123	8.01

Total				89.48		97.12

C.

	Component Cost		CSA Concrete		CSA - Bacterial Concrete	
	$/ton	$/100 lbs	lbs	$/cy	lbs	$/cy
Water	0.39	0.02	305	0.06	305	0.06
Water De-chlorination	-	1920	-	-	0.06	1.17
CSA Cement	220	11.00	678	74.56	678	74.56
Class F Fly Ash	65	3.25	0	0.00	0	0.00
Coarse Agg	30	1.50	1236	18.54	1236	18.54
Fine Agg	25	1.25	1366	17.08	1243	15.54
Lightweight Agg	130	6.50	0	0.00	123	8.01
Total				110.24		117.88

Table 13.3 - Concrete Costs including bacteria for most efficient mixtures.

Concrete Mixture		Cost ($/CY)		
		Concrete Materials Costs	Bacteria Production Costs	Total
OPC	No bacteria	100.07	0.00	100.07
	BSx0.5NBx37Cx24hrs	107.71	110.71	218.42
	Sx0.5NB, BSx25Cx48hrs	107.71	129.62	237.33
	Sx1NB, BSx37Cx48hrs	107.71	120.79	228.50
OPC+FA	No bacteria	89.48	0.00	89.48
	BSx0.5NBx37Cx24hrs	97.12	110.71	207.82
	Sx0.5NB, BSx25Cx48hrs	97.12	129.62	226.74
	Sx1NB, BSx37Cx48hrs	97.12	120.79	217.91
CSA	No bacteria	110.24	0.00	110.24
	BSx0.5NBx37Cx24hrs	117.88	110.71	228.58
	Sx0.5NB, BSx25Cx48hrs	117.88	129.62	247.50
	Sx1NB, BSx37Cx48hrs	117.88	120.79	238.67

Table 13.4 - Costs of additional curing solution application to induce biomineralization and crack healing.

	Curing Time required for Crack Healing (days)	Nutrient solution quantity (liters/ft^2)	Total solution Required (liters)	Solution Cost, using 0.5NB ($/liter)	Total Cost for Crack Healing Solution Application ($/ft^2)
OPC	42	0.028	1.167	$1.36	$1.59
OPC-FA	42	0.028	1.167	$1.36	$1.59
CSA	56	0.028	1.556	$1.36	$2.12

Improvements in sorptivity, compressive strengths, and ultrasonic pulse velocity discussed in Appendix E (Paste and Mortar Laboratory Testing), suggest that incorporation of bacteria into the cementitious mixtures could provide improvements in concrete durability and service life. In order to quantify the effect of cement microstructure improvements resulting from bacterial biomineralization 28-day secondary absorption coefficients were converted to mixture diffusion coefficients using the relationship established in Siad et al. (2014). Predicted diffusion coefficients for the OPC, OPC-FA, and CSA mixtures with and without bacteria are shown in Table 13.5.

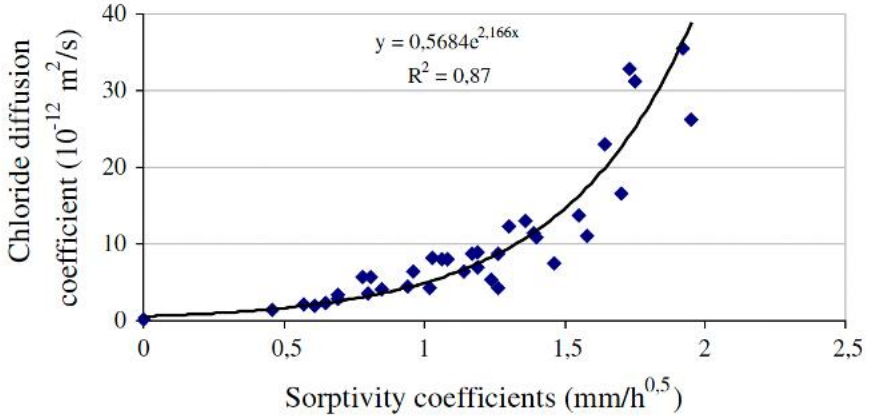

Figure 13.1 - Relationship between sorptivity and diffusivity coefficients (Siad et al. 2014).

Table 13.5 - Predicted mortar diffusivity based on secondary sorptivity rates.

		28d Secondary Absorption ($mm/s^{1/2}$)	D_{a-28} (m^2/s)
OPC	**No bacteria**	3.00E-03	5.98E-13
	B. subtilis	1.40E-03	5.82E-13
	Soil bacteria	1.10E-03	5.79E-13
OPC-FA	**No bacteria**	1.50E-03	5.83E-13
	B. subtilis	1.00E-03	5.78E-13
	Soil bacteria	2.90E-03	5.97E-13
CSA	**No bacteria**	1.40E-03	5.82E-13
	B. subtilis	7.00E-04	5.75E-13
	Soil bacteria	1.20E-03	5.80E-13

Predicted diffusion coefficients and concrete production costs were incorporated into the Life-365 service life modeling software (Bentz and Thomas, 2018) to assess the effect of the changes on chloride diffusion, concrete service life, and system costs. The Life-365 model used a 200 mm concrete bridge deck located in Columbus, Ohio. The deck was designed with 25 mm of concrete cover over the top reinforcement layer. This cover depth is less than typical for most bridge decks, but was chosen to allow for comparison of performance of the mixtures within a 100 year service life. Diffusion coefficients on the order of 10^{-13} m^2/s are extremely low diffusivity and result in extremely long service lives in structures with two or more inches of concrete cover.

All OPC mixtures were assumed to continue hydrating and decreasing in diffusivity for 25 years following placement, while the CSA mixture was assumed to hydrate for 10 years due to its known faster hydration rate. Standard decay coefficients recommended by the Life365 software were used

for the evaluation – 0.2 for OPC and CSA mixtures, 0.36 for mixtures utilizing fly ash. Larger decay coefficients suggest that a mixture is undergoing greater microstructural densification and reduction in diffusion coefficient over time. It is unclear how biomineralization will change the cement microstructure over time with or without additional curing, so bacterial mixtures were assumed to have decay coefficients and hydration times equal to their control mixture counterparts. Similarly, CSA cement was assumed to have equal decay coefficients to OPC cement. More research is needed to determine if these decay coefficients are appropriate for use with CSA mixtures and bacterial mixtures but this testing was outside the scope of this project.

Table 13.6 shows that changes in diffusion coefficients predicted from absorption measurements were generally insignificant, resulting in typically not more than a half year increase in time to corrosion initiation. However, as repair costs comprised the bulk of the costs associated with maintaining the bridge deck over the 100-year life, the increased construction costs translated only to increases in total bridge cost of between +6-9%. Note that the Life-365 model does not compare cracked structures, and so is unable to account for benefits associated with reduced sorptivity of cracked surfaces after healing by biomineralization. This benefit may further improve the value associated with use of bacteria concrete and offsetting initial cost increases.

Table 13.6 - Diffusion prediction parameters and predicted time to corrosion and total cost for bacterial and non-bacterial concrete slabs.

		Life 365 Predicted Time to Corrosion Initiation (yrs)	Predicted Construction Cost ($/ft^2)	Increased Construction Cost relative to Non-Bacterial Control	Repair Cost over 100 yrs ($/ft^2)	Total Cost ($/ft^2)	Change relative to Non-Bacterial Control	Change relative to Non-Bacterial OPC
OPC	**No bacteria**	23.3	3.59	-	56.93	60.53	-	-
	B. subtilis	23.7	5.79	+161%	58.52	64.32	+6.3%	+6.3%
	Soil bacteri	23.8	6.14	+171%	58.52	$64.67	+6.8%	+6.8%
OPC-FA	**No bacteria**	51.4	3.4	-	39.78	43.18	-	-28.7%
	B. subtilis	51.7	5.6	+165%	41.37	46.97	+8.8%	-22.4%
	Soil bacteria	50.2	5.95	+175%	40.98	46.93	+8.7%	-22.5%
CSA	**No bacteria**	28.5	3.78	-	56.38	60.16	-	-0.6%
	B. subtilis	28.7	5.98	+158%	58.50	64.48	+7.2%	+6.5%
	Soil bacteria	28.6	6.33	+167%	58.50	64.84	+7.8%	+7.1%

13.2 Conclusions

Benefits associated with production and use of bacterial concrete come at a significant cost. Altered concrete mixture designs to utilize lightweight aggregate and dechlorinated water resulted in increases in concrete costs of approximately 7-8%, but bacterial production methods pushed concrete costs to at least 100% of non-bacterial concrete mixtures. Cost increases were primarily driven by the large volumes of bacterial growth solution required to achieve adequate

concentrations of bacterial spores. If alternate production methods, such as utilization of a bacterial reactor system such as in Silva (2015) can increase bacterial spore concentrations in solution the costs of producing bacterial concrete will be significantly reduced.

Although bacterial mortars and concrete generally outperformed or performed similarly to their non-bacterial counterparts in terms of absorption, compressive strength development, ultrasonic pulse velocity changes, crack healing ability, and resistance to freezing and thawing, these improvements did not lead to significant increases in service life, at least according to the approximate methods utilized in this study. Further work is needed to more precisely assess changes in diffusivity over time in bacterial samples due to biomineralization, and to further assess the ability of the bacteria to heal cracks and prevent water intrusion relative to the associated increases in cost to produce these mixtures.